

CARDIFF UNIVERSITY

**Molecular mechanism of highly potent
NS5A inhibitors**

by

Elizabeth Melissa Navarro Garcia

A thesis submitted for the
degree of Doctor of Philosophy

in the
Medicinal Chemistry
School of Pharmacy and Pharmaceutical Sciences

June 2019

Declaration of Authorship

Statement 1 This thesis is being submitted in partial fulfillment of the requirements for the degree of PhD.

Signed (candidate)

Date

Statement 2 This work has not been submitted in substance for any other degree or award at this or any other university or place of learning, nor is it being submitted concurrently for any other degree or award (outside of any formal collaboration agreement between the University and a partner organisation)

Signed (candidate)

Date

Statement 3 I hereby give consent for my thesis, if accepted, to be available in the University's Open Access repository (or, where approved, to be available in the University's library and for inter-library loan), and for the title and summary to be made available to outside organisations, subject to the expiry of a University-approved bar on access if applicable.

Signed (candidate)

Date

Declaration This thesis is the result of my own independent work, except where otherwise stated, and the views expressed are my own. Other sources are acknowledged by explicit references. The thesis has not been edited by a third party beyond what is permitted by Cardiff University's Use of Third Party Editors by Research Degree Students Procedure.

Signed (candidate)

Date

Word count: 33040

CARDIFF UNIVERSITY

Abstract

Medicinal Chemistry
School of Pharmacy and Pharmaceutical Sciences

Doctor of Philosophy

by [Elizabeth Melissa Navarro Garcia](#)

Abstract

Hepatitis C is responsible for causing chronic infections in over 170 million people all over the world who are at a risk of developing into liver cirrhosis and hepatocellular carcinoma, locating HCV in a major public health burden. Until recently, the standard-of-care treatment consisted of Interferon-alpha and ribavirin, in addition to non-structural protein 3/4 (NS3) protease inhibitors, but due to the undesired side-effects, researchers developed more efficient therapies. Nowadays, small molecules targeting non-structural viral proteins: NS3/4 protease, NS5A D1 and NS5B polymerase activities can clear the infection in 98% of the cases. These direct acting antivirals (DAAs) are widely used, however, despite advances in recently approved potent DAAs the world-wide application of these therapies remains limited due to the expensive cost and potential drug resistance. NS5A is a nonstructural multifunctional protein. Mainly composed by an amphipatic helix, which is the major membrane anchor, Domain I, which is involved in RNA binding and assembly, and Domain II and III which are intrinsically unfolded domains and are known to interact with host factors. DAA targeting NS5A DI, Daclatasvir (DCV), has a picomolar range activity and it is used in combination therapy to combat HCV infection. Given the enormous medical relevance of NS5A inhibitors, the aim of this study was to decipher the mode of action of Daclatasvir, together with more insights to the role of NS5A structural elements. In the present study, experiments showed that DCV can block the envelopment of viral particles. Furthermore, targeting the assembly of HCV particles, this fact serve as evidence of the dual mode of action of DCV. Furthermore, we investigated the role of very conserved Proline residues in the structure of NS5A, identifying key Proline residues which are critically involved in RNA replication, and have an impact in HCV infection. This fact, also suggests that the some of these Prolines might be essential for the DCV binding, as we prove that they have a direct role in keeping the binding site of DCV. Lastly, we set up a molecular model which includes the intracellular membrane giving the full picture of how DCV works in the context of an intracellular membrane and its important interactions. Together our data, prove the dual mode of action of DCV targeting HCV replication and assembly. And importantly, we constructed a molecular model that can be use in the future to study structure-function of developing NS5A inhibitors.

Acknowledgements

The research work described in the present study was sponsored by Marie Curie Fellowship program: ANTIVIRALS Horizon 2020 EU. Experiments were performed in Heidelberg University and Cardiff University.

First of all I would like to thank my supervisor Prof Andrea Brancale at Cardiff University for believing in my work, for his motivation, supervision and support during the present work as well as all the laboratory members in the Medicinal Chemistry Department at Cardiff University. Specially to Salvatore Ferla, for all the supervision and advises. I would like to thank also Prof Ralf Bartenschlager for the advises and supervision, also all the laboratory members in the Molecular Virology Department at Heidelberg University. Specially to Margarita Zayas, Vanesa Madan, Stephanie Kallis, Marie Bartenschlager and Ulrike Herian.

I am very thankful to the ANTIVIRALS program, supervisors in the program, coordinators, and my fellow ANTIVIRAL students. Specially to Roberto Manganaro and Birgit Zoonics who helped me with my work in Cardiff University and all the other fellows for the unconditional support and the fun while the PhD time.

I want to thank all my friends that during this time were my support and motivation (specially to my awesome girls). A todos mis amigos en México por el apoyo a distancia, el amor y la motivación (a las Morras, en especial a Lilo, a Alfredo y a Gus por el apoyo con el LateX y a Nayla por el apoyo moral).

Finalmente, quiero agradecer a mi familia en México, a mi abuela, a mis tias y tío. A todos mis primos, especialmente a Diego y Tanya. A mi madre ser el apoyo, el amor y por estar a pesar de la distancia. A mi padre que en el transcurso de este trabajo se fue al cielo y quien es mi motor. Y hoy, a mi pequeña familia Manuel y Emilio, por todo el amor incondicional y el esfuerzo en equipo.

Contents

Declaration of Authorship	i
Abstract	ii
Acknowledgements	iv
List of Figures	ix
List of Tables	xii
I Introduction	1
1 Hepatitis C Virus identification and classification	2
2 HCV genome and viral proteins	4
2.1 HCV genome	4
2.2 5' and 3' Non-translated region	4
2.3 HCV viral proteins	5
2.4 Core	6
2.5 Envelopment proteins	6
2.6 Viroporin protein p7	7
2.7 Non-structural proteins	7
2.7.1 Non-structural protein 2 (NS2, 23kDa)	7
2.7.2 Non-structural protein 3 (NS3, 70kDa)	7
2.7.3 Non-structural protein 4A (NS4A, 16kDa)	8
2.7.4 Non-structural protein 4B (NS4B, 27kDa)	8
2.7.5 Non-structural protein 5A, (NS5A, 56kDa)	9
2.7.5.1 NS5A organization	9
2.7.5.2 Amphipatic helix	10
2.7.5.3 Domain I	12
2.7.5.4 Domain II and domain III	15
2.7.5.5 NS5A phosphorylation	15
2.7.5.6 NS5A functions	16
2.7.5.7 NS5A oligomerization	16

2.7.6	Non-structural protein 5B (NS5B, 68kDa)	18
3	HCV replication cycle	20
4	HCV experimental studies	23
5	HCV and host immune response	26
6	HCV antiviral therapy	28
6.1	Inhibitors	29
6.1.1	Protease NS3-4A inhibitors	29
6.1.2	RNA-dependent RNA polymerase NS5B inhibitors	30
6.1.3	Non-structural protein 5A inhibitors	32
6.1.3.1	Daclatasvir	32
6.1.3.2	Discovery and development	33
6.1.3.3	Resistance mutations	34
6.1.3.4	Mechanism of action	35
7	HCV and cellular membrane interactions	37
7.1	Molecular Dynamics as a tool for membrane studies	39
8	Objectives of the study	40
II	Materials and Methods	41
9	Materials	42
9.1	Antibodies and dyes	42
9.1.1	Bacteria and cell culture	42
9.1.2	Media	43
9.1.3	Compounds	43
9.1.4	Plasmid constructs	44
9.1.5	DNA oligonucleotides	46
9.1.6	Chemicals and manufacturers	46
9.1.7	Buffers and solutions	46
10	Methods	50
10.1	Preparation of plasmid DNA from <i>E. coli</i> cultures	50
10.2	Digestion of DNA with restriction enzymes	51
10.3	Ligation of DNA fragments	51
10.4	Generation and transformation of competent bacteria	51
10.5	Sequence analysis of DNA	52
10.5.1	PCR and site directed mutagenesis	52
10.6	In vitro transcription and RNA purification	53
10.7	Cell culture and virological methods	54
10.7.1	Culture of cell lines	54
10.7.2	Cell line for trans-complementation assay	55
10.7.3	Lentivirs transduction of cells for new cell line production	55
10.7.4	Electroporation	56

10.7.5	TCDI ₅₀ by VIRAPUR (Virus Purification)	56
10.7.6	Determination of virus titres in cell culture supernatants and cell lysates	57
10.7.7	Luciferase viral reporter assays	58
10.7.8	Transcomplementation assay	58
10.8	Drug addition experiments	59
10.8.1	Dose-response assay using stable replicon cell lines and JCR2a reporter virus	59
10.8.2	Full-length reporter virus JCR2a kinetics after DCV or SOF treatment	59
10.8.3	Full-length reporter virus JCR2a kinetics and DCV pre-treatment	60
10.9	Protein analysis	60
10.9.1	Proteinase K Protection Assay	60
10.9.2	SDS-Polyacrylamide-Gel-Electrophoresis (SDS-PAGE)	60
10.9.3	Western Blot	61
10.9.4	Paraformaldehyde oligomerization	61
10.9.5	BRET assay	62
10.10	Imaging	62
10.10.1	Immunofluorescence	62
10.11	Computational models and simulations	63
10.11.1	Proline analysis in NS5A structure	63
10.11.2	Proline analysis in NS5A structure and DCV interaction	63
10.11.2.1	Analysis of interaction with DCV	64
	<i>Docking with GLIDE®</i>	64
	<i>Molecular Dynamics</i>	64
10.11.3	Amphipathic helix studies on POPE membrane	64
10.11.4	Molecular dynamics on Amphipathic Helix (AH) and membrane studies	65
III	Results	66
11	Experimental Results	67
11.1	Key role of NS5A Proline residues	68
11.1.1	Proline residues in linker structures are key for HCV replication and infection	69
11.2	Effect of Sofosbuvir and Daclatasvir treatment	76
11.3	Daclatasvir and Sofosbuvir kinetics	77
11.4	Daclatasvir has an inhibitory effect on envelopment of viral particles	83
11.4.1	Proteinase K Assay	84
11.4.2	Rate Zonal Centrifugation Assay	85
11.4.3	Immunofluorescence Assay	87
11.4.4	Transcomplementation Assay	90
11.5	NS5A oligomerization state	93
11.5.1	PFA cross-linking	93
11.5.2	BRET assay	96
12	Computational Results	99

12.1 Proline residues in linker structures are key for DCV binding	99
12.1.1 P29A	102
12.1.2 P29G	103
12.1.3 P29V	105
12.1.4 P32A	106
12.1.5 P32G	108
12.1.6 P32V	110
12.1.7 P35A	112
12.1.8 P35G	113
12.2 DCV structural properties	115
12.2.1 DCV binding pocket	116
12.3 Amphipatic helix and membrane simulations	118
12.3.1 Amphipatic helix orientation in cellular membrane	119
12.3.2 Amphipatic helix and membrane association	120
13 Discussion	124
13.1 HCV assembly impaired by DCV activity	124
13.2 Proline mutations impact on HCV replication, infection and DCV binding	126
13.3 AH and membrane dynamics	129
A Appendix	133
A.1 Proline mutations impact on HCV replication, infection and DCV binding	133
A.2 HCV assembly impaired by DCV activity	134
A.3 Drug titration	134
Bibliography	137

List of Figures

1.1	HCV global distribution and genome types	3
2.1	HCV genome and protein structure	5
2.2	NS3-4A protease and NS3 full length structure	8
2.3	NS5A organization	9
2.4	NS5A domains	10
2.5	Amphipatic helix	11
2.6	Domain I of NS5A with linker connections	12
2.7	NS5A dimer conformations	14
2.8	NS5A oligomer model	18
2.9	NS5B	19
3.1	HCV replication cycle	22
4.1	HCV subgenomic replicons	24
4.2	Structure of Jc1 based reporter genomes	24
4.3	Table including Animal model for studying HCV infection	25
6.1	Table including DAA inhibitors	29
6.2	NS3/4 protease structure and docked DAA simeprevir	30
6.3	NS5B structure and docked DAA sofosbuvir and beclabuvir	31
6.4	NS5B inhibitor, SOF chemical formula	31
6.5	NS5A inhibitor, Daclatasvir in NS5A protein	34
6.6	Daclatasvir chemical formula	34
9.1	Buffers, solutions and composition	49
10.1	Cell Line	55
10.2	BRET calculation method	62
11.1	Domain I of NS5A with linker connections	70
11.2	Proline mutations on linker AH-DI effects on HCV life cycle	72
11.3	Proline mutations on linker DIa-DIb effects on HCV life cycle	73
11.4	Proline mutations on linker DI-DII effects on HCV life cycle	74
11.5	Established EC_{50} values for NS5A inhibitor, Daclatasvir (DCV)	77
11.6	Established EC_{50} values for NS5B inhibitor, Sofosbuvir (SOF)	78
11.7	Daclatasvir dose-response effects on HCV life cycle	79
11.8	Sofosbuvir dose-response effects on HCV life cycle	80
11.9	DCV drug addition at different time points	81
11.10	SOF Drug addition at different time points	82

11.11SOF and DCV effect on replication and reinfection processes	84
11.12Envelopment assay experiment	85
11.13DCV treatment gradients show no Core envelopment particles	86
11.14NS5A and E2 localisation	88
11.15NS5A and E2 localisation	88
11.16NS5A and Core protein localisation	89
11.17NS5A and Core protein localisation	89
11.18Trans-complementation constructs and cell lines	90
11.19Transcomplementation assay hypothetical results	91
11.20Trans-complementation of constructs on time line.	92
11.21PFA cross-linking assay principle	94
11.22NS5A oligomerization state detected at 2% PFA concentration	95
11.23NS5A oligomerization state detected at 2% PFA concentration	95
11.24BRET constructs containing RLuc or YFP	96
11.25Principle of BRET experiment	97
11.26BRET combination of RLuc constructs	97
12.1 Example Proline 29 and 35 mutations	100
12.2 NS5A dimer with highlighted Proline residues	101
12.3 P29A	103
12.4 P29G	104
12.5 P29V	106
12.6 P32A	108
12.7 P32G	109
12.8 P32V	111
12.9 P35A	113
12.10P35G	114
12.11Daclatasvir interaction map generated in MOE [®] , showing important interacting residues. Symbols are characterizing the properties of the amino acids in the proximity of DCV.	116
12.12NS5A dimer plus DCV binding pocket. A. DCV molecule is in yellow, its binding site is in green and NS5A dimer in magenta and orange. Proline mutations are marked in cyan.	117
12.13NS5A dimer plus DCV binding pocket. B. Different angle, DCV molecule is in yellow, its binding site is in green and NS5A dimer in magenta and orange. Proline mutations are marked in cyan.	117
12.14NS5A dimer containing AH and linker on cellular membrane.	118
12.15NS5A dimer with Proline-rich linker. AH-linker homology based on PxxPxxP. Taken from Nettles et al 2014, [1].	119
12.16Amphipatic helix orientation	120
12.17Amphipatic helix and membrane	120
12.18Molecular Dynamics of AH-Proline rich linker (AH-DI linker)	121
12.19Molecular Dynamics of AH-Proline rich linker (AH-DI)	122
12.20Molecular Dynamics of AH-Proline rich linker (AH-DI)	123
A.1 Conserved Proline residues	133
A.2 Diagram of experimental design	134
A.3 DCV and SOF titration	134

A.4 DCV titration	135
A.5 SOF titration	136

List of Tables

9.1	Antibodies	42
9.2	Compounds	43
9.3	BRET constructs for each one of NS5A linkers	45
9.4	Primer sequences	46
9.5	47
10.1	PCR ingredients	53
11.1	Site directed mutagenesis of conserved Prolines to Alanine (Ala), Glycine (Gly) or a Valine (Val)	69

List of Abbreviations

Apo	apolipoprotein
AH	amphipatic helix
ATP	adenosine-5'-triphosphate
BSA	bovine serum albumin
cc	cell culture
CC50	50% cytotoxicity concentration
cDNA	complementary DNA
CMV	cytomegalovirus
CRE	cis-acting RNA element
D	domain
DAA	direct acting antiviral
DAPI	4',6'-diamidino-2'-phenylindole dihydrochloride
DCV	daclatasvir
DMEM	Dulbecco's modified eagle medium
DMSO	dimethylsulfoxide
DMV	double membrane vesicle
DNA	deoxyribunocleic acid
DTT	dithiothreitol
e.g.	exempli gratia
EC50	50% effective concentration
E.coli	Escherichia coli
ELISA	enzyme-linked immunosorbent assay
EMCV	encephalomyocarditis virus
FCS	fetal calf serum

FDA	Food and Drug Administration
FLuc	Firefly-Luciferase
GAG	glycosaminoglycan
GFP	green fluorescent protein
gt	genotype
h	hour
HA	hemagglutinin
HAV	hepatitis A virus
HBV	hepatitis B virus
HCC	hepatocellular carcinoma
HCV	hepatitis C virus
HIV	human immunodeficiency virus
HRP	horse radish peroxidase
IF	immunofluorescence
IFN	interferon
IP	immunoprecipitation
IRES	internal ribosome entry site
ISG	interferon stimulated gene
JFH1	japanese fulminant hepatitis-1
LCS	low complexity sequence
LD	lipid droplet
LDL	low density lipoproteins
Luc	luciferase
MOA	mode of action
MW	membranous web

NS	non-structural
NT	non-targeting
NTR	non-translated region
o/n	overnight
ORF	open reading frame
PAGE	polyacrilamide gel electroforesis
p.e.	post electroporation
p.i.	post infection
p.t.	post transfection
RBV	Ribavirin
RC	replication complex
RdRp	RNA-dependent RNA polymerase
R Luc	Renilla- Luciferase
rpm	revolution per minute
RT	room temperature
sg	subgenomic
TCID50	tissue culture infectious dose 50
TLR	Toll-like receptor
UTR	untranslated region
VLDL	ver-low-density lipoprotein
vol	volume
wt	wild type

Dedicated to my dad

Part I

Introduction

Chapter 1

Hepatitis C Virus identification and classification

Hepatitis is an inflammation of the liver, this can be self-limiting or can continue to develop fibrosis, cirrhosis or liver cancer. According to the World Health Organization (WHO), hepatitis viruses are the common cause of hepatitis, together with toxic substances (e.g. alcohol, drugs) and autoimmune diseases which can also cause hepatitis. There are 5 main hepatitis viruses, A, B, C, D and E. Typically A and E are caused by contaminated food or water, while B, C, and D usually as a result of parental contact with infected body fluids as blood or contaminated medical equipment such as needles, sexual contact or in case of hepatitis B, from mother to baby at birth [2].

In the early 1960s, hepatitis types A and B were recognized and the treatment was corticosteroid treatment. Shortly after the discovery of hepatitis B, research of drug treatments began, among these interferon (IFN) appeared as most effective. In the 1970s a non-A non-B hepatitis was discovered too. Originally, it was not considered to contribute to cirrhosis or cancer. Non-A non-B hepatitis was formerly identified as putative viral hepatitis occurring after transfusion of blood or intravenous drug use. The evidence that non-A non-B hepatitis could lead to persistent infection in a high number of patients lead to discover that indeed it can progress into chronic liver disease, cirrhosis and hepatocellular carcinoma (HCC) [3]. Hepatitis C virus was discovered to be the cause of non-A non-B hepatitis in 1989 and now is still one of the main causes of chronic liver diseases [4].

Hepatitis C has been classified in the genus *Hepacivirus* within the family *Flaviviridae*. The *Flaviviridae* family including three genera: flavivirus, pestivirus and hepacivirus, mostly infecting mammals and birds. Many flaviviruses are host-specific and pathogenic, such as hepatitis C virus [5]. Flaviviruses include hepatitis C, yellow fever virus, dengue

fever virus, Japanese encephalitis virus and tick-borne encephalitis virus. The majority of known members in the genus *Flavivirus* are arthropod borne, and many are important human and veterinary pathogens [6]. Members of this family share a number of basic structural and virological characteristics, enveloped in a lipid bilayer, which is surrounded by a nucleocapsid, mainly composed by the core (C) protein and inside it contains the RNA genome [7]. However, HCV differs in a number of virological and epidemiological aspects, as the fact that HCV has a narrow host specificity and tissue tropism. It can be only transmitted by blood-to-blood contact between humans, instead of mosquitoes or ticks.

There are 7 HCV genotypes currently classified and each of them are divided into several subtypes (a,b,c, etc.) according to the geographical distribution. According to literature genotype 1 is the prevalent worldwide, continued by genotype 3, comprising 83.4 million cases (46.2% of all HCV cases) and 54.3 million (30.1%) approximately one-third of which are in East Asia. Genotypes 2, 4, and 6 are responsible for a total 22.8% of all cases; genotype 5 comprises the remaining less than 1%. While genotypes 1 and 3 dominate in most countries irrespective of economic status, the largest proportions of genotypes 4 and 5 are in lower-income countries [8].

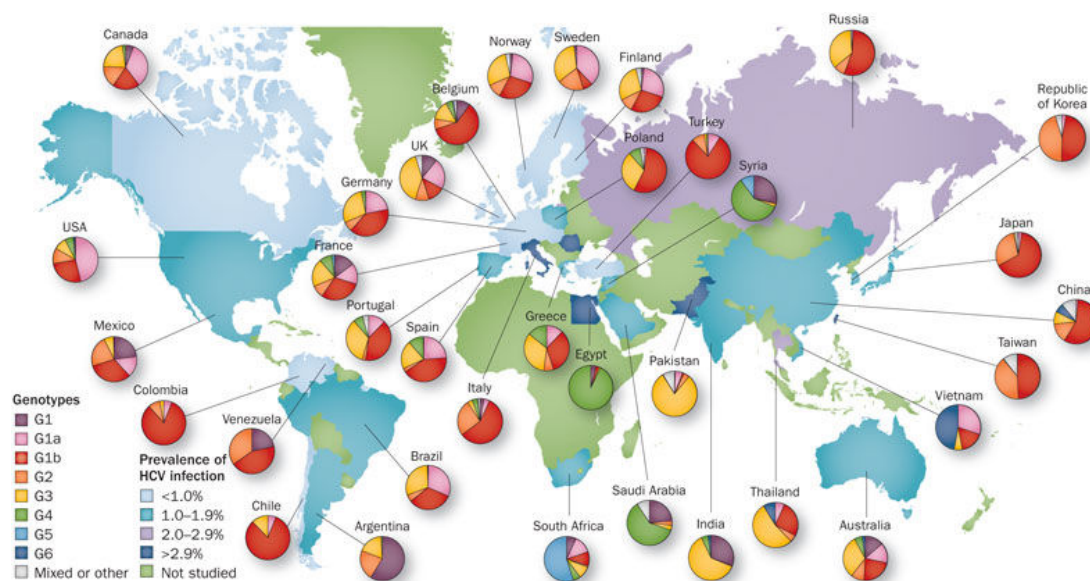


FIGURE 1.1: HCV global distribution and genome types

An estimated 130 to 170 million people have HCV infection. HCV prevalence is highest in Egypt at >10% of the general population and China has the most people with HCV (29.8 million). Around 25% of patients with acute HCV infection undergo spontaneous clearance, remaining 75% of patients progress to chronic HCV infection and are subsequently at risk of progression to hepatic fibrosis, cirrhosis and hepatocellular carcinoma (HCC). Taken from [9].

Chapter 2

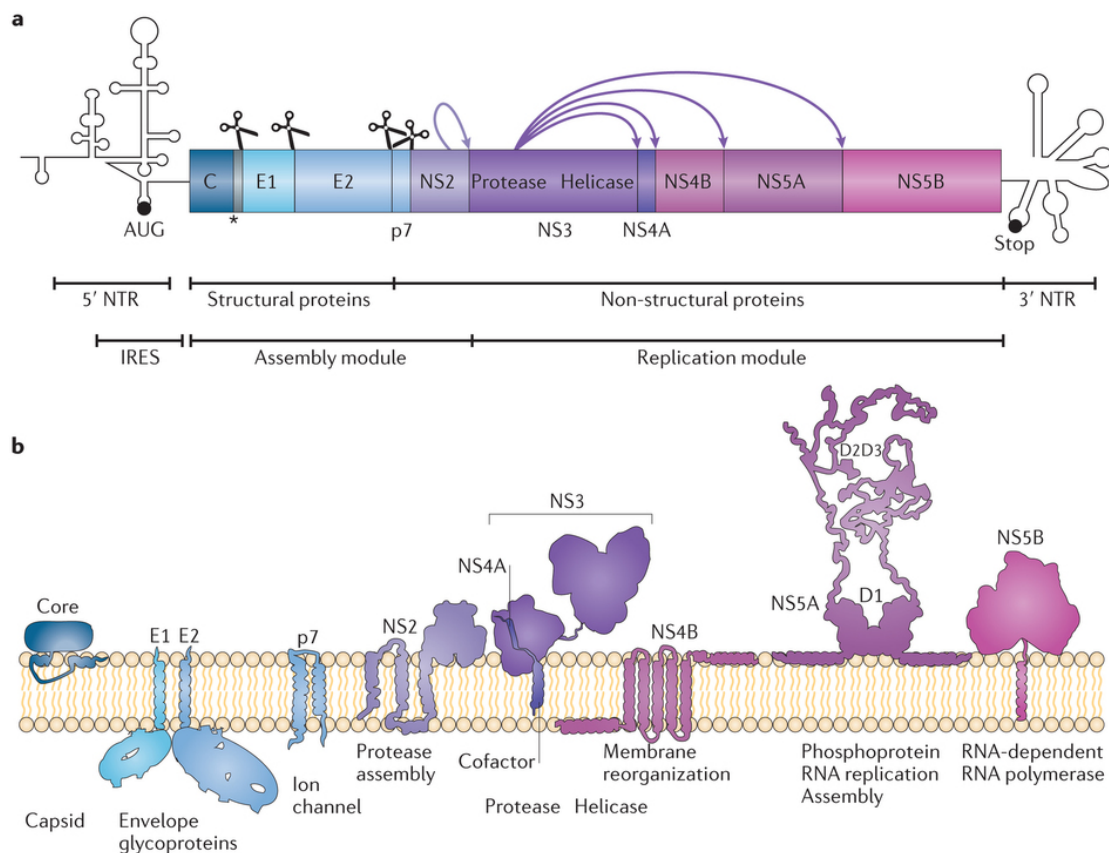
HCV genome and viral proteins

2.1 HCV genome

The HCV genome encodes 10 viral proteins, divided into two modules: assembly module (core to NS2) and replication (NS3-NS5B) module (Figure 2.1). The HCV genome is single-stranded RNA molecule that has a positive polarity and a length of 9600 nucleotides. The open reading frame (ORF) is flanked by a 5' and 3' non-translated regions (NTR) of 341 and 230 nucleotides length respectively, both containing conserved RNA structures essential for translation and replication processes. The HCV internal ribosome entry site (IRES) is located in the 5' NTR has the capacity to form a stable pre-initiation complex by directly binding to the 40S ribosomal subunit without canonical translation initiation factors. The IRES directs the cap-independent translation of the single ORF [10]. Therefore, HCV exists in its hosts as a pool of genetically distinct but closely related variants called quasispecies [11].

2.2 5' and 3' Non-translated region

The 5' NTR of HCV contains 341 nucleotides upstream of the ORF translation initiation codon and it is the most conserved region in the genome. This region contains 4 highly conserved structural domains (I- IV) containing stem-loops and a pseudoknot [12]. The domains II, III and IV together with the first 12-30 nucleotides conform the IRES. The 3' non translated region contains 225 nucleotides and it is divided in three regions a variable region 30-40 nucleotides, a long poly(U)- poly(U/UC) tract and a very conserved 3'terminal stretch of about 98 nucleotides (3'X region). The 3'NTR interacts with NS5B, RNA-dependent, RNA polymerase.



Nature Reviews | Microbiology

FIGURE 2.1: HCV genome and protein structure

HCV genome and viral proteins. a) One single open reading frame (ORF) within the viral RNA genome encodes for the HCV polyprotein it is flanked by the 3' and 5' non-translated regions (NTR). The genome is arranged into two modules, the replication module, which contains the nonstructural (NS) proteins which are required for the RNA replication and the assembly module, which contains the core (C) protein and the two envelope glycoproteins (E1 and E2), p7 and NS2 which are required for the assembly of the virus. The scissors indicate the polyprotein cleavage by the cellular signal peptidase, this cleavage removes the carboxyl-terminal indicated by an asterisk as the arrows are indicating the viral proteases cleavage. b) Membrane topologies and major functions of HCV proteins. Each protein is tethered to intracellular membranes, NS5A protein is anchored by amphipathic α -helices, also note NS5A is shown as a dimer, but almost all proteins can form homo or heterodimers. Taken from [13].

2.3 HCV viral proteins

The ORF is encoding a single polyprotein, approximately of 3000 amino acid long, which is co and post-translationally cleaved by cellular and viral proteases into 10 proteins from the amino-terminal region. As previously mentioned, the structural module, includes the structural proteins which help building the virus particle: core (C), envelope glycoproteins 1 (E1) and (E2), or support assembly but not being part of it: p7, a viroporin,

ion channel crucial for viral production [14] and the non structural protein NS2. The rest of the non structural proteins are the result of the polyprotein cleavage: NS3, NS4A, NS4B, NS5A, NS5B [15], and can sustain viral RNA replication (Figure 2.1). In addition the so-called "F" protein which results from a frameshift in the core coding region. The HCV viral proteins have been extensively studied and in the following sections the main structure and function aspects are described.

2.4 Core

Core Protein, 21kDa (mature)

During the translation of the HCV polyprotein the polypeptide is targeted to the endoplasmic reticulum (ER) membrane for translocation of the Envelope glycoprotein 1 (E1) ectodomain into the ER lumen a process mediated by the internal signal sequence between core and E1. The polyprotein cleavage yields the immature form of the core protein which contains the E1 signals sequence at the carboxyl-terminal. Furthermore this is recognized by the host peptidase giving rise to the mature core protein, most of core protein is found in the cytosol, where is bound to the ER membranes and located at the surface of lipid droplets (LD) [16–18].

The core protein is a highly basic RNA-binding protein that forms the viral capsid. It exists in a precursor of 23kDa and it is release as a mature protein in 21kDa. Its length is around 177 amino acids and is a dimeric membrane protein consisting of two domains stabilized by disulfide bonds. The hydrophilic domain is within the first 120 N-terminal amino acids of the protein, where there are several characteristics of unfolded proteins. This conformation allows plasticity which is why core protein can interact with different cellular partners. The C-terminal is hydrophobic, responsible for core association to lipid droplets (LD) and it predicted to fold into α -helices rich in glycine which can attribute to an oligomerization motif [18].

2.5 Envelopment proteins

Envelopment protein 1 (E1, 35kDa) and envelopment protein 2 (E2, 65kDa)

These proteins are both transmembrane proteins type I, where the ectodomain is in the N-terminal 160 and 334 amino acids, it is located in the ER lumen where glycosilation and folding processes take place. While the C-terminal contains the 30 amino acids long transmembrane domain, this is the membrane anchor for ER retention [19].

These proteins assemble in non-covalent heterodimers. The transmembrane domain is composed of two short stretches of hydrophobic amino acids separated by a short polar segment containing fully charged residues, the second one is acting as a signal peptide for downstream protein [20]. E1 and E2 might also be involved in fusion between the viral envelope and the host cell membrane.

2.6 Viroporin protein p7

p7, 63 amino acids

Small, intrinsic membrane protein p7, is composed by two transmembrane domains that are connected via a cytoplasmic loop [14]. The N- and C-terminal are facing the ER lumen, with predicted α -helices. The protein can undergo oligomerization and can also be used as an ion channel. These structural and membrane-permeability properties suggest that p7 belongs to the viroporin family [21].

2.7 Non-structural proteins

2.7.1 Non-structural protein 2 (NS2, 23kDa)

Non-structural protein 2 is an integral membrane protein, non-glycosylated that does not seem essential for formation of the replication complex [22]. Its main role is in the proteolytic cleavage at the NS2-NS3 junction of the HCV polyprotein and it is required for the zinc-dependent NS2-NS3 proteinase function. However, NS2 is not necessary for RNA replication but for infectious particles production in cell culture [23].

2.7.2 Non-structural protein 3 (NS3, 70kDa)

NS3 consists of two domains, the serine protease domain, 1-189 amino acids in the N-terminal, while helicase-NTPase domain, 181-631 amino acids at the C-terminal. The NS3 associates with the non-structural cofactor 4A of approx. 54 amino acids, which gives stability to the protein as it activates it to perform the cleavage in 4A/4B, 4B/5A and 5A/5B [18]. The N-terminal part appears to form a transmembrane structure which might be important for its ER membrane localisation. The protease domain is being targeted efficiently by antiviral drugs. The structure of NS3 composes a chymotrypsin-like fold composed two six-stranded β -barrel subdomains. The catalytic triad is formed by residues from the same loops of the two β -barrel. The helicase domain on the other

hand has not been successfully targeted by any drugs. It contains two structurally related subdomains folded with $\beta - \alpha - \beta$ subdomain topology. In addition NS3 interacts directly with NS5B, NS4B and NS5A via NS4A within the replication complex [24, 25] (Figure 2.2).

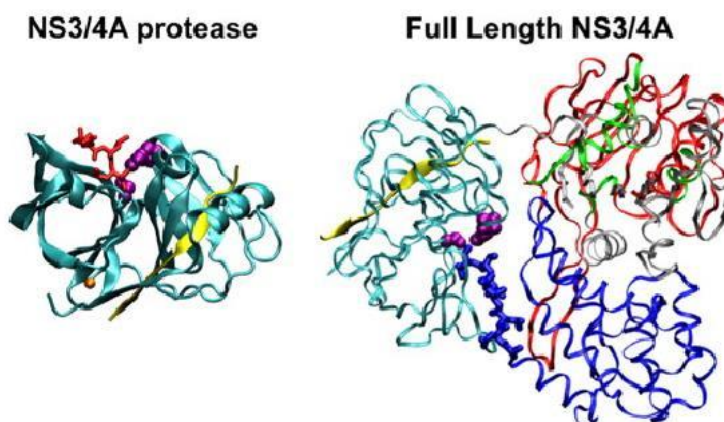


FIGURE 2.2: NS3-4A protease and NS3 full length structure
NS3-4A protease and full length structure of NS3. Modified from [26]. As it is described in the text the structure contains a protease domain together with the cofactor 4A and the full NS3 is shown.

2.7.3 Non-structural protein 4A (NS4A, 16kDa)

As mentioned before, NS4A is a cofactor responsible for several cleavage sites. Because of this interaction with other non-structural proteins, NS4A contributes to HCV RNA replication and virus particles assembly. Additionally NS3/4 protease plays a key role in blocking host antiviral signalling response (see Chapter 5), it is involved in the cleavage of CARDIF (caspase recruitment domain adaptor inducing IFN- β) [27] and TRIF (Toll/interleukin-1 receptor domain containing adaptor inducing IFN- β) [28], this results in the inhibition of RIG-I (Retinoic-acid inducible gene I) which is the main mediator of antiviral signalling in the cell [29], more detailed information is given in Chapter 5.

2.7.4 Non-structural protein 4B (NS4B, 27kDa)

NS4B is a hydrophobic transmembrane protein that co-translationally associates with the ER membrane [10]. It is predicted to be formed by an N-terminal amphipathic α -helix, which is followed by transmembrane domains [30]. Further NS4B was found to induce the formation of seemingly ER-derived membranous web that harbours all HCV structural and non-structural proteins and also allows RNA replication [31]. Thus, NS4B function provides a scaffold for the assembly of HCV replication complex (RC). In addition NS4B

has been suggested as a key participant during viral assembly, as it interacts with other proteins in the replication module [32].

2.7.5 Non-structural protein 5A, (NS5A, 56kDa)

NS5A is a multifunctional phosphoprotein associated to membranes. It is found to be phosphorylated and hyperphosphorylated. It has been described extensively as it is now one of the main targets for antiviral drugs. NS5A has been described to be involved in membranous web formation, RNA replication, viral particle assembly and host cell interactions. Thus NS5A is described extensively because it is the main protein of study.

2.7.5.1 NS5A organization

NS5A N-terminal contains three domains (D1, D2, and D3) and a very conserved amphipathic helix (AH) (Figure 2.3). The AH is located at the N-terminal and it is mainly involved in targeting NS5A to the cytosolic leaflet of the ER membrane in an in-plane manner [33]. DI (amino acid 36-214), Domain II (amino acid 250-342), implicated in RNA replication, and Domain III (356-447) involved in core interactions and viral particle assembly [34]. The domains are separated by a two low complexity sequences (LCS I and LCS II). The following paragraphs are dedicated to a more detailed description of NS5A organization for the further understanding of the results.



FIGURE 2.3: NS5A organization

HCV non-structural protein 5A organization. AH, amphipathic helix, domain I (DI) involved in RNA replication, domain II and III (DII and DIII) intrinsically unfolded involved in interactions with host proteins. Low complexity sequence I and II (LCSI and LCSII) are separating each domain. LCS regions are predicted to be interdomain connecting loops. The region believed to comprise domain I (amino acids 1-213) contains the N-terminal membrane-anchoring helix, as well as a potential metal ion coordination motif. Modified from [34]

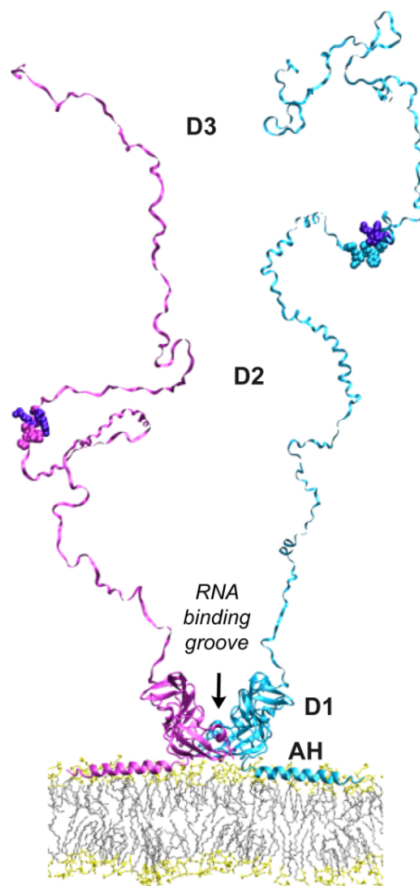


FIGURE 2.4: NS5A domains

Ribbon diagram of a model of the full-length NS5A dimer associated with a phospholipid membrane. Each subunit (lilac and cyan, respectively) consists of the amino terminal amphipathic α -helix (PDB: 1R7G), the highly structured domain 1 (D1, PDB: 1ZH1) which is shown in position relative to a 1-palmitoyl-2-oleoyl-3-sn-glycerol-3-phosphocholine membrane bilayer. In Domain II, in stick representation, the binding site for Cyclophilin A (host factor that interacts with NS5A protein) is shown. DII and DIII are intrinsically unfolded. Modified from [15].

2.7.5.2 Amphipathic helix

The AH is located at the N-terminal in 30 amino acid residues and it serves as a membrane anchor for NS5A. This domain is completely necessary and sufficient to target NS5A to the ER, which results in an integral membrane association; this association can occur by a post-translational mechanism [35]. NS5A AH (1-31 aa) was determined by NMR [33], and it is reported to form an in-plane amphipathic α -helix embedded in the cytosolic leaflet of the membrane bilayer. Polar residues present in the membrane surface provide a unique environment to allow protein-protein interactions which are essential for the assembly of a functional HCV replication complex [26]. Despite the apparent variability of some amino acids, there are several fully conserved and specific

charged amino acids with a hydrophatic character in most of HCV genotypes. For example, secondary structure predictions have predicted a conserved and consensus α -helix in the 3-26 amino acid segment. Amino acids from 29-32 including the very conserved Pro-29, is predicted to form a turned conformation, and segment 36-48 is predicted as extended [35]. In addition to other amino acid conservation, Prolines are very conserved residues in the linker connecting the AH with Domain I, as Proline 29, 32 and 35, which are studied in the present work and are shown in Figure 11.1.

Additionally, due to the natural conformation of AH it has a high propensity to bind to lipids. However, protein-protein interactions between cytosolic domains within the HCV replication complex might be weak when compared to membrane association of the proteins, this will give flexibility to fulfill the polyprotein functions [33]. On the other hand, the interactions among this proteins might be using the membrane domains within the bilayer to interact. On this regard, there are still many open questions. Although there is a NMR structure for AH, there is no information of the linker between the AH and the Domain I, where most of the resistance mutations appear to be located. The most prominent mutation affects Tyr 93, which is positioned on the dimer interface in both X-ray crystallographic structures. Importantly, mutations at this site confer cross-resistance to several NS5A inhibitors and, in the case of Daclatasvir genotype 1b subgenomic replicons and approx. 1,800 fold for genotype 1a subgenomic replicons [36].

Furthermore, conserved amino acid sequences on each linker connecting the AH with Domain I, linker connecting Domain I subdomain *a* and *b*, and finally linker connecting Domain I to Domain II, which are key for NS5A activities, shown in Figure 11.1, which are subject of the present study due to the importance in maintaining the functionality of the protein.



FIGURE 2.5: Amphipathic helix

Amphipathic helix structure created in MOE. The NMR structure is taken from the PDB entry: 1R7G. From [33]. Colour coded by secondary structure. The linker connecting AH to Domain I is a Proline rich region, which has not been yet crystallised, so in this case it has been predicted and shown as: **29-PKLPGLP-35** (prediction made by collaborator Cristophe Combet, in white end), as also shown in Figure 11.1.

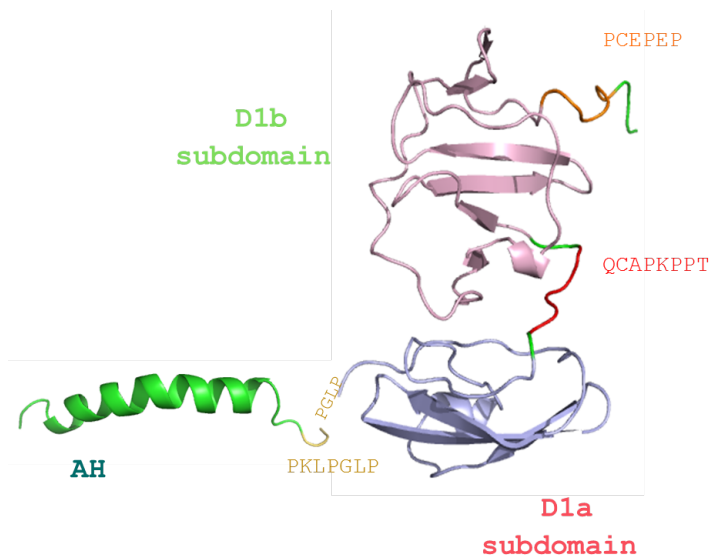


FIGURE 2.6: Domain I of NS5A with linker connections Amphipathic helix (AH), Domain I subdomains *a* and *b*. Sequences containing Proline residues are also shown, in line with the linker structure dividing each part. Courtesy by Critoph Combet. Linker sequences are also shown in [11.1](#)

2.7.5.3 Domain I

The structure of domain I (DI) has been solved by three independent groups using X-ray crystallography. These studies describe a four different dimeric forms of DI from genotypes 1a and 1b with the same monomeric unit, but different dimeric arrangement [37–39], when compared by primary sequence, DI of NS5A shares a high sequence homology to the hepaciviruses, suggesting that it has been well conserved and its critical functions are common to hepaciviruses, whereas the functions of the other two domains (domain II and III) maybe specific to each virus. In this regard, generally, DI mainly functions exclusively for genome replication [37]. Finally, it was recently published that domain I also plays a key role in assembly of infectious viral particles, identification of key sites might be important for the production of infectious virus. Additionally, this publication also describes mutations on P35A, V67A and P145A to be important for the recruitment of NS5A to lipid droplets (LD), which they also impair dimerisation of the DI and enhance the binding of DI to the HCV 3'UTR RNA, revealing a role of these NS5A in assembly of viral particles [29].

For a clearer explanation regarding the differences in the structure of DI, Tellinghuisen *et al.*, described the Domain I subdomains A and B. The subdomain A, is at the N-terminal loop, next to a three-stranded anti-parallel β -sheet, and an α -helix at the C-terminus of the third β -strand. All together, form the scaffold for a four-cysteine zinc atom coordination. This zinc atom has a structural role in the maintenance of NS5A fold. To connect subdomain A and B there is a Proline-rich region. Subdomain B,

contains four-strand anti-parallel β -sheet and other two small ones near the C-terminus surrounded by coil structures [37]. The N-terminal subdomain A has a very basic surface meanwhile in the subdomain B there is a more acidic character, this is a unusual charge distribution and has an impact in the dimerisation of the protein. The crystal structure of domain I region provided strong data for the study of NS5A. The crystal structure described by Tellinghuisen *et al*, Figure 2.7 is known as the "claw-like" structure PDB entry 1ZH1 [37].

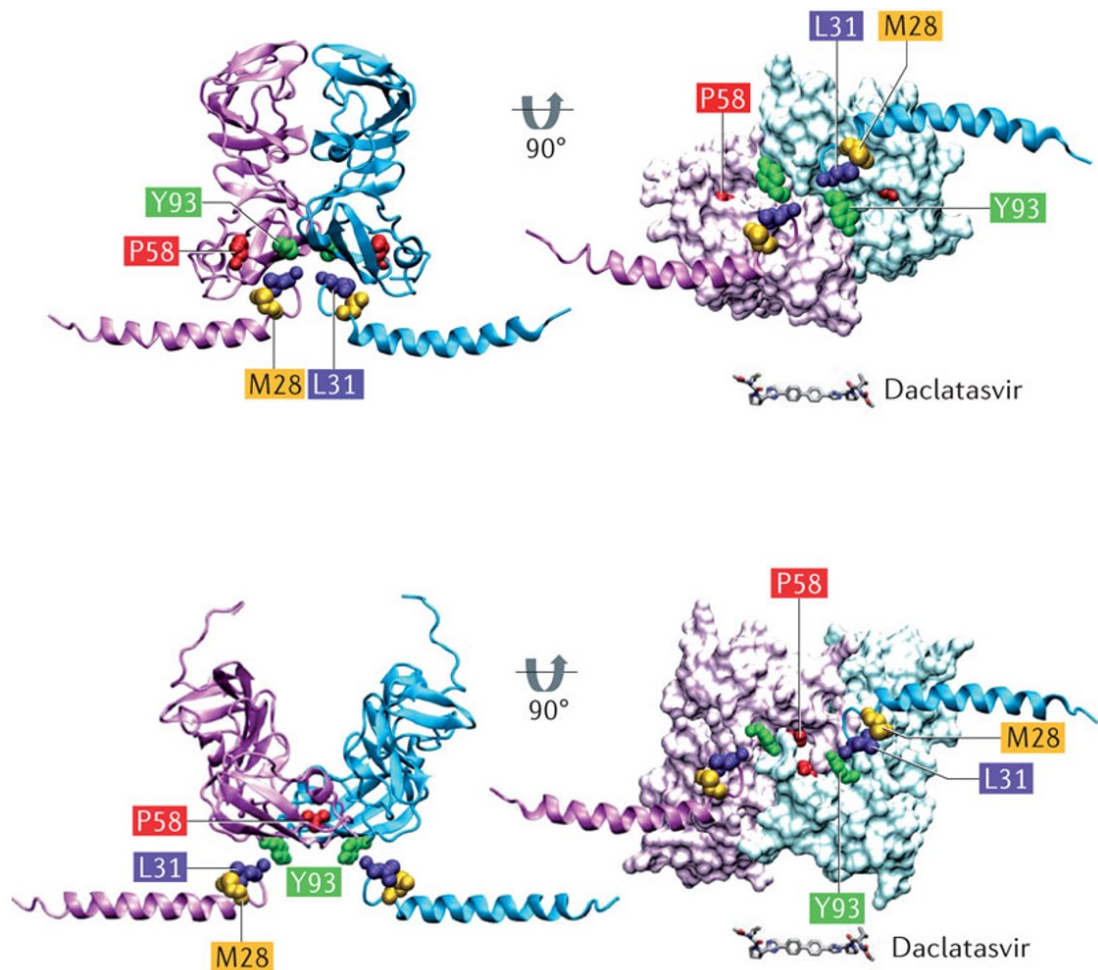
The anchoring helix AH previously described in section 2.7.5.2, is only five residues from the N-terminal of DI, suggesting it is very close to the membrane [37]. The basic surface close to the anchor is consistent and it makes it probable that the protein is in close contact with the negative charged head groups of the membrane, where it could interact with RNA. As mentioned before NS5A interacts with RNA via domain I via an RNA-binding groove located at DI [40]. Additionally, the conjunction between AH and DI is involved in lipid droplet (LD) targeting.

The second crystal structure described by Love *et al*, describes the association significantly different from the "claw-like" structure Figure 2.7. The crystal structure which PDB entry is 3FQM and it is known as "back-to-back". This describes the long axes of the monomers are nearly parallel, with numerous interactions along the entire side of each one of the monomers, which makes a cylinder appearance. The two N-termini are found on the same end of the dimer, implying that the two AH are colocalizing, which is a common feature with the Tellinghuisen structure. There is no overlap between the surfaces of the monomers, this tells that the monomers have no simple rearrangement, but rather undergo a transformation that requires a complete separation of the monomers and translocation of one monomer to the other side of its initial partner and then it is followed by a slight tilt of each monomer long the axis [38].

The last crystal structure described by Lambert *et al*, describes a very similar structure as the one from Love *et al*, where the monomers are related by a two fold axis perpendicular to their length. Additionally, it is shown that the binding cleft between the head-to-head dimer could accommodate NS5A inhibitor (Daclatasvir, DCV) in a such a fashion that the key resistance mutations (M28, L31, P58, and Y93, as shown in Figure 2.7), which are shown in close proximity to the inhibitor [39]. NS5A inhibitors confer resistance, mainly on the sites mentioned and shown in Figure 2.7, however the resistance continues to be a main problem when developing new antivirals, which is one of the reasons studying in detail the mechanism of action of DCV, can elucidate a way of avoiding resistance to new NS5A inhibitors.

More recently, it was proposed that domain I of NS5A plays multiple roles in assembly, binding nascent genomic RNA and transporting it to lipid droplets where it is transferred

to Core. Domain I also contributes to a change in lipid droplet morphology, increasing their size [42].



Nature Reviews | Microbiology

FIGURE 2.7: NS5A dimer conformations

NS5A dimer structures from two different PDB entries: The "claw-like", belonging to the 1ZH1 and the "back-to-back" structure to the 3FQM. In coloured boxes, the resistance mutations that confer resistance to NS5A inhibitors. Note that the position of the amphipathic α -helix relative to DI is arbitrary and assumes that resistance mutations observed in DI and the amphipathic α -helix would be close to each other. Also note the supposed membrane-proximal positions of the resistance mutations in both dimer structures. Mutation of Pro58 has been associated with secondary resistance to DCV but does not confer resistance by itself, this residue is shown to highlight the alternative orientations of the monomers in the different dimer structures [41]. Daclatasvir molecule is also shown in stick representation. Modified from [15]

2.7.5.4 Domain II and domain III

Domain II is required for RNA replication [26] and interactions with host and viral proteins [43]. Domain II plays a key role in HCV genome replication but has no impact on assembly or release of viral particles [7]. Domain II has a very conserved sequence and a large segment within DII can be deleted with no significant effect on RNA replication and virus production in cultured cell lines. Unlike it, domain III is essential for the assembly of infectious viral particles. These domains are less conserved than domain I. The DII and DIII of NS5A are both intrinsically unfolded monomers and because of this the exact position relative to DI is unclear, see Figure 2.4. The structural flexibility allows different interactions with cellular proteins [44]. However, just Cylophylin A (CYPA) and Phosphatidylinositol 4-kinase III α (PI4KIII α) [45, 46] have been shown to be essential for HCV replication and have been also targeted as antiviral drugs. CYPA probably interacts directly with NS5A to exert its effect, through its peptidyl-prolyl isomerase activity, on maintaining the proper structure and function of the HCV replicase. The major proline substrates are located in DII of NS5A, centered around a DY dipeptide motif that regulates CYPA dependence and Cyclosporine A (CsA) resistance. Importantly, Cyclosporine A derivatives that lack immunosuppressive function efficiently block the CyPA-NS5A interaction and inhibit HCV in cell culture, an animal model, and human trials [47].

2.7.5.5 NS5A phosphorylation

There are two phosphorylated forms of NS5A, p56 and p58, phosphorylated and hyperphosphorylated protein respectively [48]. Basal phosphorylation results in expression of the protein at 56kDa and when hyperphosphorylated it results in 58kDa and it depends on sequences from the C-terminal region of the LCSI up to the end of NS5A. The phosphorylation sites are mainly in serines [49] located at the C-terminal and to a less extent threonines and tyrosines. Phosphorylation is a very well conserved feature among other viruses related to HCV, such as Bovine Viral Diarrhoea Virus (BVDV) and Yellow Fever Virus (YFV), which suggests it is a critical step for the *Flavivirus* life cycle. The enzymes that are involved in the phosphorylation have not been completely identified, regardless some include: casein kinase I and II (CKI and CKII)[50–52], mitogen-activated protein kinases (MAPKs) [53], polo-like kinase 1 (PIK1) [54] and glycogen synthase kinase 3 (GSK-3).

2.7.5.6 NS5A functions

As mentioned already, as a multifunctional protein NS5A has a role during RNA replication and assembly of the viral particles. NS5A interacts with other non-structural proteins such as NS5B, this is key for RNA replication. In order to trigger replication and switch on HCV life cycle, NS5A binds to the 3'UTR of positive and negative strands of HCV RNA (preferentially on U/G rich single stranded RNA regions), which is absolutely required [55].

The structure of NS5A previously described gives an overview of what are the functions of NS5A. Additional interactions with other host factors such as protein kinase R (PKR), p53, TATA-binding protein (TBP), Snf2 related CREBBP activator protein SRCAP protein, vesicle associated membrane protein (VAPA) have been described [56–59]. Phosphorylation of the protein also modulates the functions of it, for instance, VAPA can bridge NS5A p56 with NS5B favouring replication complex formation, meanwhile hyperphosphorylation of NS5A interrupts the interaction allowing viral particle assembly [60].

Perhaps the multifunctionality of NS5A is also due to the dimerization and further multimerization of the protein, that can give rise to different conformations.

2.7.5.7 NS5A oligomerization

Domain I of NS5A indeed can form dimers and it is critical for this process. However, detection of high molecular forms of NS5A is whether representing a nonspecific aggregation complex or these are true higher order NS5A complexes [61]. Importantly, Love *et al*, observed an oligomeric state of NS5A and modelled possible NS5A oligomers based on the crystal structure known [38]. These studies strongly suggest the oligomerisation state of NS5A. On the other hand, dimeric structures are important for the antiviral activities of NS5A inhibitors. Binding experiments have shown that these inhibitors bind to NS5A directly and that mutations conferring resistance are mapped in the N-terminal region. Interestingly, when tested NS5A inhibitor DCV also known as BMS-790052, did not affect NS5A dimerisation, but the blockage of disulphide bridge forming cysteines in DI can reduced interaction upon treatment [61].

However, experiments measuring ratio of NS5A to NS5A inhibitor DCV present in cells, suggest that a small amount of inhibitor molecules can impact the function of a large number of NS5A protein molecules, based on these observations Sun *et al* developed a working model for NS5A inhibitors action, in which NS5A proteins interact with each other and a single bound inhibitor perturbs the function of an NS5A oligomer, thus,

resulting in the disruption of replication complex formation or NS5A normal function and this in turn, results in an amplified inhibitory effect. Together with the crystallographic data of DI and the NMR structure of amphipathic helix, hypothetically assembling in a polymer network alternating the interfaces, they built up a working model. Under this structure, DCV is docked across the dimer interface as previously reported [37]. Thereafter, when Sun *et al*, added a second inhibitor to determine whether it could, compete with DCV for binding and have no impact or to bind adjacent to NS5A inducing a conformational change by DCV binding and resulting in enhancement of its potency [62] see Figure 2.8. The complementary effect of DCV and the second inhibitor called SYN-395, after its synergistic effect, requires communication within the binding sites, more detail information on the MOA of the syn compounds is in section 6. However in this case, the polymer model proposed would suggest that the induced inhibition affects the NS5A dimer in which DCV is bound and it is also transmitted to the proteins along the helical axis through P29-P35 loop interactions (which as mentioned before, includes very conserved Proline residues 29, 32 and 35 and it is located in the linker connecting the AH to DI) to inhibit multiple NS5A proteins [62]. This study highlights not only the importance to investigate further the role of Proline residues in the structure of NS5A, but additionally NS5A oligomer formation. Thus, due to the high conservation of these Proline residues, we decided to look into their role in HCV infection and DCV binding, as shown in the Results section III and we also investigated on the oligomerization process of NS5A protein. For more information given on NS5A inhibitors and other HCV inhibitors, see section 6.

The results in this publication by Sun *et al*, suggested a formation of an extended multimeric network of NS5A that may occur through the different dimer interfaces. The combination of two genotype 1b NS5A-D1 dimers allowed the formation of a superhelical array which can give support to a model for the oligomerization of NS5A and NS5A-D1 constructs observed *in vitro* shown by Lambert *et al* [39]. However, the formation of these higher order oligomer complexes into a non-planar, superhelical array precludes its association with a lipid bilayer [38]. Different conformations of DI dimers can suggest an array of NS5A molecules that form an extended network that could interact with the membranous web. The NMR data also shows that the protein can aggregate reversibly in a concentration dependent manner, possibly into ordered oligomeric states [39]. However, more studies are needed to determine the oligomerization state of NS5A, favouring monomeric, dimeric or oligomer. In the present study we try to address this problem and investigate further to determine the oligomerization state of NS5A protein.

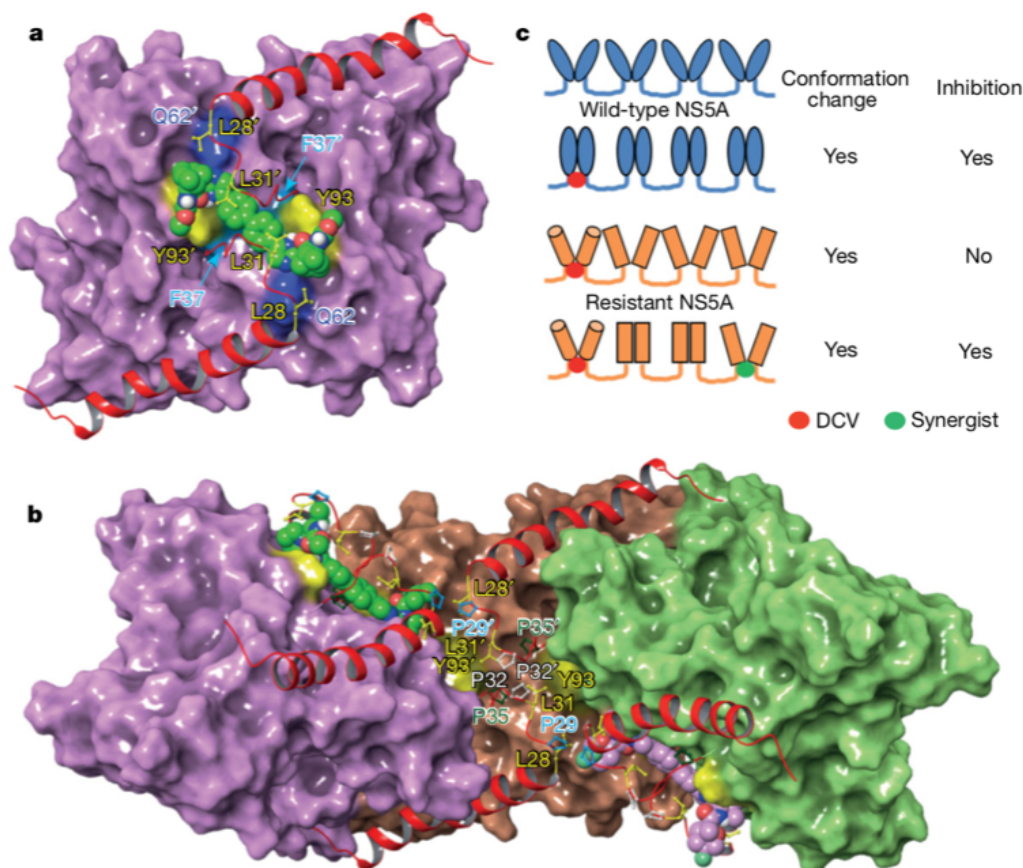


FIGURE 2.8: NS5A oligomer model

NS5A oligomer model where Daclatasvir (DCV) and Syn-395 are bound to NS5A dimer and polymer. a, DCV is docked across the NS5A dimer interface stick representation shown in green, the amphipatic helix shown in red. Some of resistance mutations to DCV are pointed (L28, L31, Y93), as well as the highly conserved Proline residues in the AH-DI linker P29, and P35. b, NS5A helical hexamer is composed of three PDB: 1ZH1, (same colour) and two PDB 3FQM dimer (alternate colours). c, Graphical representation of conformational changes that can affect inhibition and further recovery of inhibition by the synergistic effect of SYN-395 compound. Modified from [62]

2.7.6 Non-structural protein 5B (NS5B, 68kDa)

NS5B, is the RNA-dependent RNA polymerase (RdRp). It is a phosphoprotein anchored to the membrane via its C-terminal 21 amino acids. As a RdRp has a typical shape: palm, finger and thumb subdomain structure and the hallmark GDD sequence as it is shown in Figure 2.9. It forms the catalytic center of HCV replication machinery and is responsible for synthesis of negative-strand RNA intermediate from the positive-strand viral genome see next section 3.

The active site is highly conserved and located in the palm subdomain. The catalytic site domain contains a C-terminal membrane insertion sequence which is essential for RNA

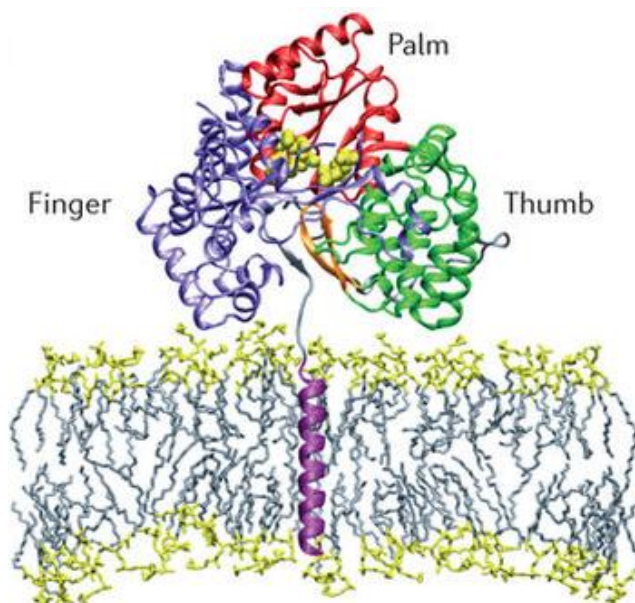


FIGURE 2.9: NS5B

NS5B structure, containing palm, fingers and thumb. Taken from [15]. Ribbon diagram of full-length NS5B (Protein Data Bank (PDB: 1GX6) and the association with the membrane via the NS5B carboxy-terminal transmembrane tail. The finger, thumb and palm subdomains are indicated, and the so-called β -loop is shown in orange. The C-terminal linker sequence (grey) connects the core of the enzyme with the membrane insertion sequence (magenta). The structure indicates the proposed membrane topology of NS5B in the so-called closed conformation, on the basis of available X-ray crystallographic structures, and this is believed to represent the initiation state of the polymerase. The active site is highlighted by two priming nucleotides (yellow). In this conformation, the RNA-binding groove is hidden by the NS5B ectodomain that stacks to the membrane. Modified from [13].

replication in cell culture and for *in vitro* enzymatic activity. When compared to other RdRp, NS5B has a closed conformation of the active center, where the C-terminal linker folds back into the active center involved in RNA synthesis [63–65]. Starting of initiation is represented by the polymerase closed conformation, after this, the enzyme undergoes a big conformational change that allows the opening of the structure to generate a cavity capable of binding the double stranded RNA [13]. NS5B is one of the main targets for direct acting antivirals (DAAs) together with NS3/4B and NS5A. Many other polymerases have been target of antiviral therapy and this will be discussed in section 6.

Chapter 3

HCV replication cycle

Replication of HCV RNA is a multi-step process that is orchestrated by synchronized action of viral and cellular proteins. Structural arrangements are necessary to originate the sites where HCV replication takes place. Once HCV has infected an hepatocyte (main cellular target), it associates to low-density lipoproteins (LDL), to very-low-density lipoproteins (VLDL) and to apolipoproteins: E, B, C1, C2 and C3 to form a complex lipoviroparticle [66, 67], this process is followed attachment, entry and fusion. The attachment requires the receptor of E2 glycoprotein, facilitated by heparan sulfate proteoglycans present on the hepatocyte's surface. The LDL and VLDL receptors can bind HCV and promote its entry. The main cellular receptors and entry factors for HCV are scavenger receptor class B type I (SRBI), [68], CD81 [69] as well as some tight junction proteins such as claudin-1 (CLDN1) [70] and occludin (OCLN) [71, 72]. Among other receptors recently identified which are also entry factors to mention: receptor tyrosine kinases (RTK), epidermal growth factor receptor (EGFR), ephrin receptor A2 (EphA2) and the Niemann-Pick C1 like cholesterol adsorption receptor (NPC1L1). All together these receptors are key for attachment and entry which give the essential venue for HCV to enter the cell and establish infection. At the fusion step, HCV enters the cell via clathrin-mediated endocytosis and is internalized into target cell via pH-dependent in the endosome which triggers the viral envelope and endosomal membrane to release the nucleocapsid to the cytoplasm, where the RNA is released [73–75]. See Figure 3.1.

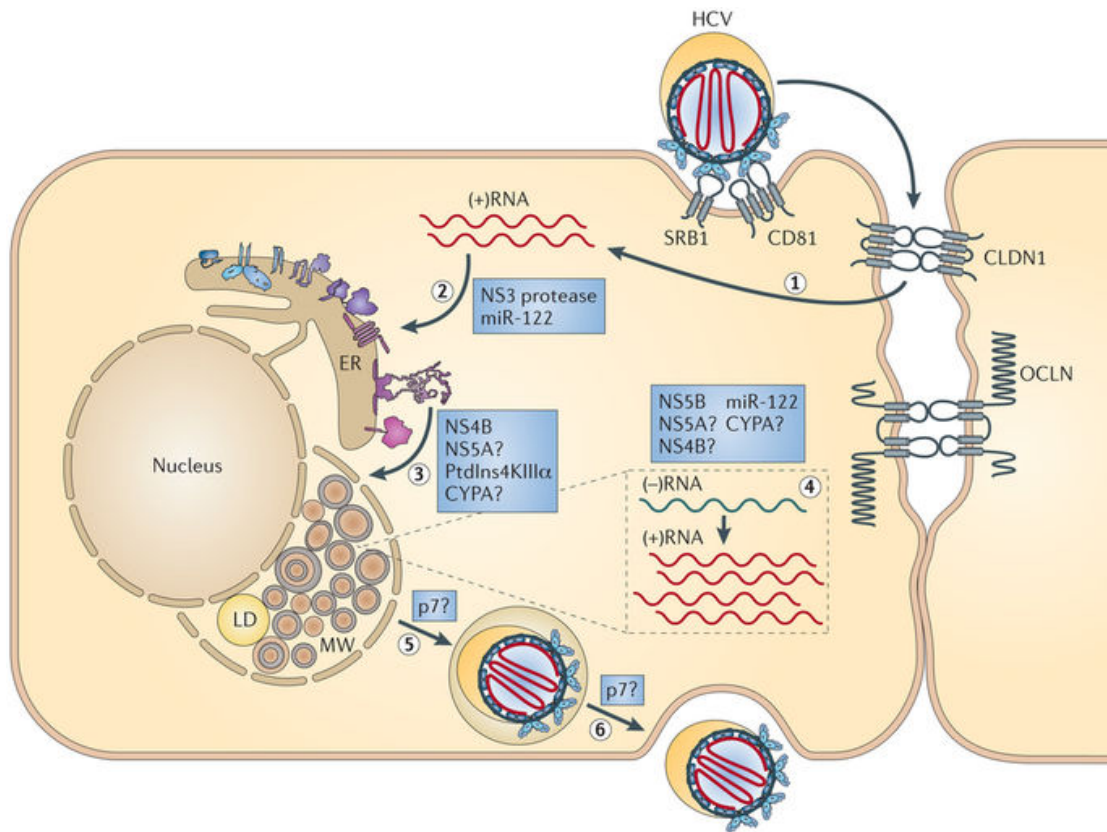
Once the RNA genome enters the cytoplasm, the HCV polyprotein is translated in the rough ER with the positive strand as a template. Translation is initiated in a cap-independent manner using the IRES at the 5'NTR. The HCV single polyprotein precursor is then processed by cellular (signal peptidases) and viral proteases (NS2, NS3/4A) to give rise to the 10 viral structural and non-structural proteins as previously described on section 2.3 [76].

Like other positive-strand RNA viruses, HCV can remodel intracellular membranes, generating organelle-like membranous structures, which can be called replication factories or membranous web. The main functions of the replication factories (vRFs) are: increase local concentration of factors required in RNA replication, spatial coordination in the replication cycle process (RNA translation, replication and assembly), and protect the viral proteins and RNA from antiviral defenses [13, 77].

There are two types of membrane rearrangements: invaginated vesicles or double membrane vesicles (DMV) [78]. HCV non-structural proteins are associated with the membranous web which includes DMVs containing nonstructural proteins, ER membranes, HCV RNA, and lipid droplets. As mentioned before, this membranous web or replication factories are the sites where RNA replication takes place, viral RNA is amplified by NS5B, (RdRp), together with most of the NS proteins and some host cell factors such as cyclophilin A (which can modulate NS5B RNA-binding capacity and interact with NS5A) [79] and PI4KIII α (recruited to membranous web by NS5A and required for HCV replication providing integrity to the membranous viral replication complex) [46].

As the positive strand is copied into negative strand RNA via replicative form is used for synthesis of excess amounts of positive strand RNAs viral replicative intermediate. Starting of RNA synthesis requires highly structured RNA elements in the 3'NTR of the template, the new synthesized RNA genomes are translated, then RNA replication takes place, finalizing with the assembly of the virions [80].

The viral RNA is thought to be delivered to the replication sites to the core protein on LDs by the viral replicase, alternatively, NS5A which can bind RNA may be released from the replicase complex to move onto the LD surface. The capsids are finally budding to the ER lumen in a process tightly linked to VLDL synthesis, which is why assembly then is dependent on (V)LDL synthesis and requires several enzymes and apoE [15, 67, 77]. Infectious HCV particles are pleomorphic, lack discernible surface features and have broad size range 40-80 nm diameter [81]. More recently, NS5A was identified as a major determinant in HCV assembly. Domain III, was found to be a key element to ensure the production of infectious viral particles [26].



Nature Reviews | Microbiology

FIGURE 3.1: HCV replication cycle

HCV replication cycle starts when binding of HCV lipoparticle to the SRB1 and CD81 receptors, further interactions with CLDN1 and OCLN are necessary. Once the virus enters the cell via receptor-mediated endocytosis (step 1), the positive-sense single stranded viral RNA is released into the cytoplasm and translated at the rough ER, giving rise to a single polyprotein cleaved in 10 mature proteins (step 2). Together viral proteins and host factors induce the formation of the membranous web (MW) located in close proximity to LD (step 3). RNA replication proceeds via negative-sense copy which is the template for the production of excess amounts of positive-sense RNAs (step 4). Assembly of HCV particles supposedly taking place close to the ER and LDs, where core and vRNA accumulate. Viral envelope is acquired by budding through the ER membrane (step 5). Finally HCV particles, are thought to leave via constitutive secretory pathway (step 6). The blue boxes represent the viral and host factors which are known or suspected to be essential for the viral life cycle, thus, potential drug targets. (CYPA: cyclophilin A, PtdIns4KIII α : phosphatidylinositol 4-kinase III α). Taken from [13].

Chapter 4

HCV experimental studies

This chapter is dedicated to describe the HCV experimental tools available for studying HCV infection. Until 1989, the lack of a cell culture system and the small animal models to propagate HCV was a major issue for HCV research. In 1997, the only model to study HCV was the chimpanzees (*Pan troglodytes*), which could be injected with HCV, this allowed to study HCV genome and its encoded proteins. However, bioethical and high costs could not allow a certain number of experiments, other attempts involved xenotransplantation system of human liver into mice (*Mus musculus domesticus*). Thus, there was not much data regarding HCV molecular biology research, finally in 1999 a major step for HCV investigation was made by the establishment of the subgenomic system [82], see Figure 4.1. To generate this tool, a full-length clones consensus genome of the genotype (called Con1); the region encoding p7 and NS2 proteins was replaced by elements which do not belong to HCV, a selectable marker neomycin (neo) gene for drug selection G418, the second is the IRES element of encephalomyocarditis virus (EMCV), which ensures translation of HCV polyprotein NS3-5B. To ensure IRES full activity the replicon contains 48 nucleotides of core coding sequence at the 3' end of the HCV IRES. Thus, this changes made a bicistronic construct that can replicate autonomously within human hepatoma cell line Huh-7 upon transfection of *in vitro* transcribed RNA [82]. This tool was then used to generate replicon cell lines with high RNA replication level that can be selected by treatment. Continuous analysis of these cell clones and replicons showed increased replication capacity caused by adaptive mutations and increased host cell permissiveness. Some of these mutations identified have been included to make a highly adapted replicon, Con1/ET, containing two point mutations NS3 (E1202G, T1280I) and one in NS4B (K1846T) [82–84].

The neo marker can be also substituted by firefly luciferase (FLuc) bicistronic, or renilla luciferase (RLuc) monocistronic which can also work as a reporter, additionally other

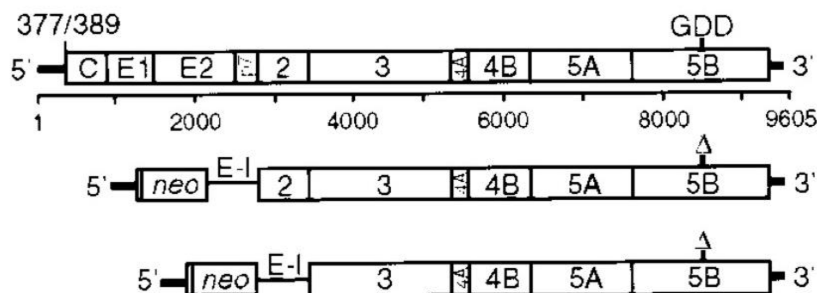


FIGURE 4.1: HCV subgenomic replicons

Structure of the HCV subgenomic replicons created by [82]. Indication of the cleavage location products and the 5' and 3' NTRs. HCV-IRES selected for the construction and a GDD active site of the NS5B. The selection of subgenomic replicons contain a 5'HCV-IRES, the neo gene, the EMCV-IRES and the HCV non-structural proteins NS2or NS3 to the 3' end δ is representing the deletion in the position of the 10-amino acid in the NS5B polymerase. Normally, GDD stands for an NS5B polymerase-defective replicon in which the critical GDD motif in the polymerase active site is replaced by AAG (referred to as GDD). Modified from [82].

reporters have been inserted in the NS5A region such as green fluorescent protein (GFP), to allow monitor cells by immunofluorescence or western blot [85, 86] as shown in Figure 4.2.

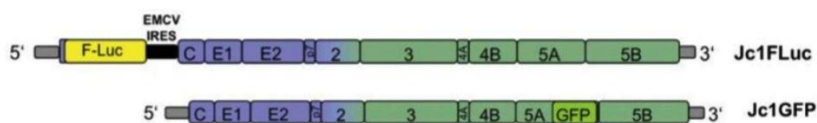


FIGURE 4.2: Structure of Jc1 based reporter genomes

Reporter genomes containing (blue) structural proteins, (green) non-structural HCV proteins. Jc1FLuc, containing Firefly Luciferase and EMCV IRES. Jc1GFP containing green fluorescent protein (GFP) before NS5B. Modified from doctoral thesis of Margarita Zayas.

In the recent years, other breakthroughs have been made in HCV research, the cloning of subgenomic replicon of the genotype 2a consensus genome from a Japanese patient with fulminant hepatitis (JFH1) which has high levels of replication in Huh7 cells without any cell culture adaptive mutations and also when JFH1 was discovered to be able to produce infectious virus particles upon transfection of the full length genome *in vitro* transcripts into Huh7 cells [87, 88].

Furthermore, the full-length JFH1 genome supports the production of culture-derived particles (HCVcc), which are infectious *in vitro* and *in vivo* [88]. This particles are around 60-75nm in diameter and spherical and are have high specificity infecting at a peak buoyant density of approximately 1.10g/ml like serum produced particles. To improve the system virus chimeras were generated consisting of the JFH1 replicase (NS3-NS5B) fused to the core to NS2 region of different HCV isolates. Another tool to study

HCV are HCV pseudo particles (HCVpp) system, this are retroviral nucleocapsids surrounded by lipid envelope which contains authentic HCV glycoprotein complexes this system allowed a robust infection system in Huh7 cells and in primary human hepatocytes to study the early stages of infection with HCV such as entry and receptor binding [89, 90].

Nevertheless, the research continues to be improved by trying to develop small animal models by humanized mice, which can be infected with HCVcc or HCV patient sera. More reliable experimental set-ups with an authentic and physiological condition present in the infection with HCV are yet to develop [91, 92]. The following Figure 4.3, contains the most recent advances in animal models to study HCV infection [93].

Animal model	Complete viral life cycle	Viremia	Liver disease	DAA testing	Passive immunization	Vaccine development	Availability
Non-rodent models							
Chimpanzee	Yes	High	Acute, chronic ^a	Yes	Yes	Yes	Very low
Tree shrew	Yes	Low	Fibrosis, cirrhosis	No	Yes	No	Low
Zebrafish	Replication	Not relevant	Virus–host interaction	Yes	No	No	High
Viral protein transgenic mouse models							
Inducible transgene expression	Not relevant	Not relevant	Virus–host interaction	Not relevant	Not relevant	No	High
Full HCV genome	Not relevant	Not relevant	Fibrosis, HCC	Not relevant	Not relevant	No	High
Immunocompromised human liver xenograft mouse models							
Trimera mouse	Yes	Low	No	Yes	Yes	No	Low
Alb-uPA-SCID mouse with humanized liver	Yes	High	No	Yes	Yes	No	Low
FRG mouse	Yes	High	No	Yes	Yes	No	Low
Immunocompetent xenograft mouse models							
Tolerized rat	Yes	Very low	No	Yes	Yes	Yes	Very low
AFC8-hu HSC/Hep mouse	Yes	Only in liver	Inflammation, fibrosis	No	No	Yes	Very low
HIL mouse	Yes	Very low	Inflammation, fibrosis	No	No	Yes	Very low
Viral adaptation							
	Entry	No	No	No	Yes	No	High
Genetically humanized mouse models							
Rosa26-Fluc mouse	Yes	Persistent viremia	No	Yes	Yes	Yes	High
ICR-C/OTg mouse	Yes	Persistent viremia	Fibrosis	Yes	Yes	Yes	High
HCV homologs in natural host							
GB-virus	Yes	Acute	No	Yes ^b	Yes ^b	Yes ^b	Low
NPHV in horses	Yes	Persistent viremia, acute	Inflammation	Yes ^b	Yes ^b	Yes ^b	Low
NrHV in rats	Yes	Acute, chronic	Inflammation	Yes ^b	Yes ^b	Yes ^b	High

FIGURE 4.3: Table including Animal model for studying HCV infection Studies using animal models where the complete viral life cycle has been performed (or parts), viremia levels, liver disease, DAA testing, passive immunization, vaccine development and availability are shown for each. Details on the advantages and disadvantages are reviewed in citation. Taken from [93].

Chapter 5

HCV and host immune response

As mentioned earlier, HCV can cause persistent infections, this can cause that the host defenses initially sense HCV by the antiviral innate immune response which is triggered by pattern recognition receptors (PRRs), these are responsible for a downstream signaling that can activate immunity. Approximately 20-30% infected people can resolve the infection but 70-80% develop a chronic infection. HCV is among the most successful of persistent human viruses, it persists in 70% of those infected [94].

The innate immune response against RNA viruses is mainly composed by three classes of PRRs: retinoic acid-inducible gene I (RIG-I)-like receptors (RLRs), toll-like receptors (TLRs), the nucleotide oligomerization domain-like receptors (NLRs) [95] or double-stranded RNA sensing proteins such as protein kinase R (PKR), which are in charge of recognizing pathogen-associated molecular patterns (PAMPs) present during viral infection. The HCV IRES is recognized by RNA-dependent PKR while the HCV 3'poly-U/UC, 5' triphosphate of the uncapped HCV RNA and the short double-stranded RNA region sequences are recognized by the RIG-I. A sequence of downstream signaling proceeds to activate various genes and cytokines such as interferon I and III and IL-1 β , which in turn activate paracrine or autocrine pathways to establish full antiviral state.

The best described detector of HCV infection is RIG-I, which is a cytosolic RNA sensor and together with MDA5 (melanoma differentiation-associated protein 5) and LGP2 (laboratory of genetics and physiology 2) can regulate HCV infection. These pathways converge on the activation of the key transcription factors NF- κ B and the interferon regulatory factor (IRF) 3 and 7. Activated IRF3 and NF- κ B bind to response elements in the promoters of type I and III IFN genes, which are essential for antiviral defence [96].

Innate immune responses rely on interferons (IFNs) to activate and regulate the cellular components for the antiviral response such as the natural killer (NK) cells. Type I IFN comprising several IFN- α and one IFN- β and type III IFN- γ 1, IFN- γ 2 and IFN- γ 3 also called IL29, IL28A and IL28B which are produced by the infected cell and by macrophages and dendritic cells (DCs). Type II IFN (IFN- γ) is produced by NK and T cells from antigen specific T cells (CD4+ and CD8+ cytotoxic lymphocytes) [96]. Subsequent activation of IFNs induced transcription of multiple interferon-stimulated genes (ISGs) through the activation of the JAK/STAT signaling pathway results in the recruitment of effector immune cells that can trigger the adaptive immune response [97, 98].

When adaptive immune responses fail to neutralize the infection, chronic infection is established. Despite the global failure of the immune reaction against HCV, T cell exhaustion and emergence of viral escape mutations are the main cause of T cell failure, which causes the establishment of HCV life cycle [99].

Furthermore, HCV supports a reaction against the host cell immune responses. The viral NS3-4A protease is central in the HCV host immune evasion strategy [100], it can block RIG-I signaling, because in addition to proteolytically processing of the HCV polyprotein it targets and cleaves mitochondrial antiviral-signaling protein (MAVS) from intracellular membranes preventing the subsequent signaling transduction. The cleavage prevents activation of RIG-I pathway and during acute infection abrogates IFN induction which supports the progression to a chronic infection [101, 102]. In addition, HCV can control PKR-mediated translation suppression of host mRNAs during HCV infection and IFN therapy can inhibit translation of host factors require for HCV replication (PKR works as an antiviral molecule) but it can also inhibit ISGs and IFN (PKR as a proviral molecule) [98]. More recently, NS4B was found to degrade TRIF in order to avoid the activation of TLR3 mediated interferon signaling pathway as part of HCV host immune system evasion [29].

Further studies on how HCV evades the immune responses of the host can give more insights into antiviral drug development.

Chapter 6

HCV antiviral therapy

An estimated of 130 million are vulnerable to chronic infections around the world whom can develop liver cirrhosis ($\approx 27\%$) and hepatocellular carcinoma ($\approx 25\%$) as mentioned in section 1. This has made HCV infection a global medical problem which has drawn the attention and efforts to develop drugs and new antiviral treatments. Unfortunately, prophylactic treatment for HCV has not been very successful, having no vaccine development. Many limitations in HCV vaccine development as genomic variability and worldwide different genotype distribution see Figure 1.1, which causes poor cross-genotype immunity [99].

The majority of infections are treated with a combination of pegylated interferon- α (PEG-IFN α) and ribavirin, as many other viral infections are treated. In some of the cases this therapy can eliminate HCV infection with this treatment but it depends on the stage of the disease, genotype and some polymorphisms (for example IL28-B gene). However, the rest of the cases are unresolved, in the recent years the development of direct acting antivirals (DAAs) has lead to a big step in HCV antiviral development[13].

Every step of HCV life cycle can be a potential drug target for antiviral therapy, however the successful inhibitors at the moment are just made for the non-structural proteins NS3/4A, NS5A and NS5B, which are use in combination, and together they can clear around 98% of infection, yet resistance mutations and high cost of this inhibitors promotes new development of antiviral treatments. This chapter will describe the DAAs available, a summary of the DAA inhibitors for the non-structural proteins of HCV are described in Figure 6.1. We described more in detail NS5A inhibitors due to the purpose of the present study, in the following subsection 6.1.3.

Table 2
Antiviral activity of FDA-approved compounds in HCV cell culture.

Protein	Compound	In vitro activity (EC ₅₀ , nM)								Ref.
		GT-1a	GT-1b	GT-2a	GT-2b	GT-3a	GT-4a	GT-5a	GT-6a	
NS3/4A	Boceprevir (SCH503034)	196 ± 56	251 ± 71	283 ± 36	315 ± 30	159 ± 5	–	–	–	Silva et al., 2013
	Telaprevir (VX-950)	395 ± 16	285 ± 60	252 ± 54	402 ± 52	953 ± 103	–	–	–	Silva et al., 2013
	Paritaprevir (ABT-450)	1.0 ± 0.33	0.21 ± 0.07	5.3 ± 1.2	–	19 ± 5.2	0.09 ± 0.03	–	0.69 ± 0.09	Pilot-Matias et al., 2015
	Grazoprevir (MK-5172)	0.4 ± 0.2	0.5 ± 0.3	2.3 ± 1.2	3.7 ± 1.1	2.1 ± 1	0.3 ± 0.2	6.6 ± 0.6	0.9 ± 0.1	Lahser et al., 2016
	Simeprevir (TMC435)	28.4 (19–39.7)	8.1 (4.5–11.9)	–	–	–	–	–	–	Lin et al., 2009
NS5A	Daclatasvir (BMS-790052)	0.05 ± 0.013	0.009 ± 0.004	0.071 ± 0.017	–	0.146 ± 0.034	0.012 ± 0.004	0.033 ± 0.01	–	Gao et al., 2010
	Ledipasvir (GS-5885)	0.031	0.004	21	16	168	0.39	0.15	1.1	Cheng et al., 2016
	Ombitasvir (ABT-267)	0.0141 ± 0.0068	0.005 ± 0.0019	0.0124 ± 0.0027	0.0043 ± 0.0012	0.0193 ± 0.0058	0.00171 ± 0.00088	0.0043 ± 0.0009	0.415 ± 0.097	DeGoeij et al., 2014
	Elbasvir (MK-8742)	0.004 ± 0.002	0.003 ± 0.001	0.003 ± 0.001	3.4 ± 2.6	0.14 ± 0.09	0.0003 ± 0.0001	0.001 ± 0.001	0.009 ± 0.006	Lahser et al., 2016
	Velpatasvir (GS-5816)	0.013	0.015	0.009	0.01	0.013	0.009	0.059	0.007	Cheng et al., 2013
NS5B	Sofosbuvir (GS-7977)	44 ± 4.7	48 ± 13	37 ± 3.6	20 ± 4.4	16 ± 3.4	–	–	–	Lam et al., 2012
	Dasabuvir (ABT-333)	7.7 ± 3.8	1.8 ± 0.98	–	–	–	–	–	–	Kati et al., 2015

–: Unavailable data. Information of HCV strains and experimental settings is available in the literature.

FIGURE 6.1: Table including DAA inhibitors

Summary of FDA-approved antivirals against HCV infection. Table contains targeted protein, name of the compound, EC₅₀ values in nM for each of HCV genotypes and the corresponding reference. Taken from [103].

6.1 Inhibitors

6.1.1 Protease NS3-4A inhibitors

NS3 is a multifunctional protein and together with NS4A cofactor constitute the serine-type protease that HCV uses for cleavage of viral and cellular (MAVS, CARDIF, VISA and IPS1) proteins while the C-terminal contains the NTPase activity, see section 2.7.2, both activities have been pursued as drug targets. However, the NS3 protease was the target for DAAs, by exploiting the fact that after NS3-4A mediated cleavage the product derived from the N-terminal fragment remains bound to the active site and thus blocks the enzyme, which gives this DAA a high potency [104–106], see Figure 6.2. These compounds belong to the first class of compounds and they bind to the active site Serine, being called 'Ser-trap'. These inhibitors antagonize the enzyme by forming enzyme-inhibitor adduct that dissociates with very slow kinetics. Three classes of these compounds have been developed: first class linear peptidomimetics are forming a covalent but reversible link, adducts with enzyme (telaprevir and boceprevir), the second class are linear peptidomimetics and third class are macrocyclic inhibitors on the basis of their structure. Unfortunately, these last ones do not target all the HCV genotypes to the same extent. Furthermore, the barrier to select for resistance against these first-generation inhibitors is low and cross-resistance has been identified [107]. Consequently, overcoming these limitations are the goal of the second generation of NS3-4A inhibitors

like MK-5172 and ACH2684 which are macrocycles that have a pan-genotypic activity with improved resistance profiles [108, 109]. It is worth mentioning that the NS3/4A inhibitor simeprevir, as shown in Figure 6.2, in the combination with the NS5B inhibitor sofosbuvir (NS5B inhibitor, see Figure 6.3, is considered to efficiently inhibit different stages of HCV life cycle [103].

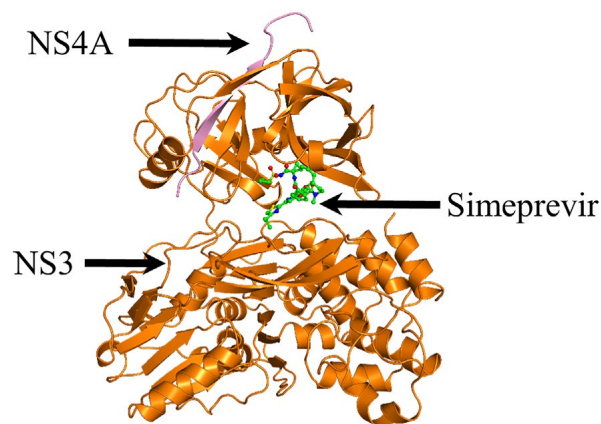


FIGURE 6.2: NS3/4 protease structure and docked DAA simeprevir
Tertiary structure of HCV NS3/4A protease. The tertiary structure of NS3/4A protease in complex with simeprevir (PDB codes: 3KEE and 4B76). HCV NS3 and NS4A proteins are displayed in orange and pink, respectively [110]. Modified from [111].

6.1.2 RNA-dependent RNA polymerase NS5B inhibitors

As already described in section 2.7.6, NS5B is a key enzyme for HCV life cycle, it mediates RNA synthesis by using its catalytic core with a typical structure of a polymerase (right hand: fingers, palm and thumb), see Figure 6.3 and 6.4. There are two groups of drugs, according to their mode of action which target NS5B protein: nucleoside and nucleotide inhibitors (NIs) and non-nucleoside inhibitors (NNIs). The first group of NIs, mimic the natural substrates of the polymerase and act at the active site of the enzyme, while the NNIs bind to different allosteric states and inhibit conformational changes in the polymerase. Due to the high degree of conservation NIs are usually more effective towards resistance than NNIs [112], examples are shown in Figure 6.3

NIs are derivatives of ribonucleosides or ribonucleotides and compete for the natural active site of the polymerase, they require high intracellular concentrations. Usually have a low-micromolar range and are typically delivered as prodrugs, where the non-phosphorylated chemical modifications are cleaved off and the liberated nucleoside is converted to 5'-triphosphate by cellular enzymes. Once phosphorylation occurs, the active drug can compete for the natural site and incorporate into the growing RNA.

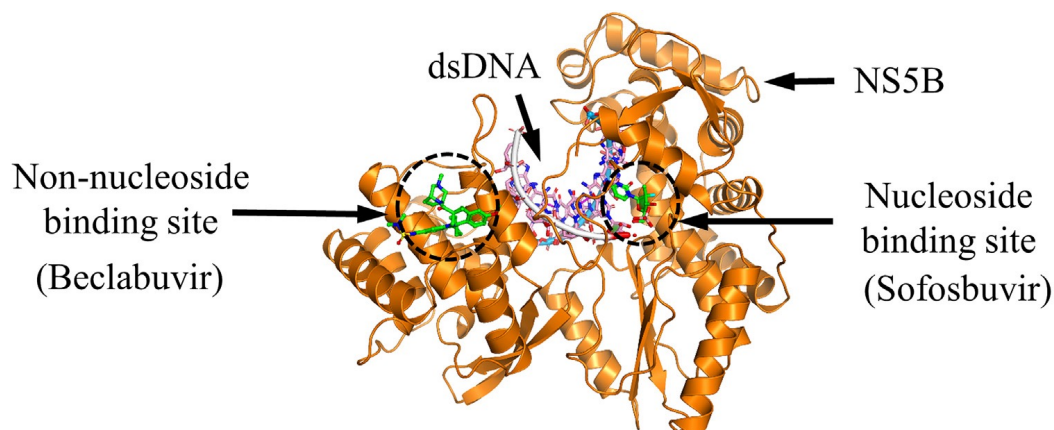
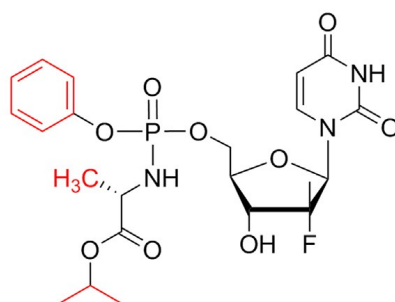


FIGURE 6.3: NS5B structure and docked DAA sofosbuvir and beclabuvir
Tertiary structure of HCV NS5B and structural formulas of approved or experimental nucleoside inhibitors. NS5B structure in complex with beclabuvir and sofosbuvir diphosphate (PDB codes: 4NLD and 4WTG) is visualized on top. Modified from [111].



(39) Sofosbuvir

FIGURE 6.4: NS5B inhibitor, SOF chemical formula

Sofosbuvir chemical formula. The discovery of sofosbuvir undertaking path from 20-C-methylcytidine to 20-F, 20-C-methyluridine 5-phosphoramidate [113]. Modified from [111].

Another way to inhibition NS5B is to use 3'-deoxy modified nucleosides that are classical chain terminators, but due to phosphorylation are poorly active in cell culture [114]. Additionally another drawback from ribonucleoside analogues is their interference with human mitochondrial RNA polymerase, which can inhibit mitochondrial gene expression, which might be the explanation to the serious side effects of several drugs (Valopicitabine, Balapiravir, and others). On the other hand, NNIs are commonly more diverse and are grouped into 4-5 classes depending on their allosteric binding, even though they can be highly active, resistance can be rapidly selected [115].

Advanced nucleoside analogue, Mericitabine, has been shown to be active in genotype 1 and genotype 4, and the most advanced nucleotide analogue is Sofosbuvir (SOF) structure shown in Figure 6.4, which has high efficacy against genotypes 1-6 in combination with PEG-IFN α and ribavirin [113, 116].

Furthermore, there are alternative viral drug targets which can interfere with HCV life cycle, NS4B and p7 proteins are now under development as antiviral drugs. As an alternative host cell target, cyclophilins and mir-122 have been extensively studied [103].

6.1.3 Non-structural protein 5A inhibitors

NS5A inhibitors have several effects on HCV life cycle. They might affect formation of the replication complex at the ER and sequester NS5A in lipid droplets to inhibit virus formation and release [1] or directly affect the assembly of viral particles [117]. Henceforth, the FDA has approved the following drugs: Daclatasvir (BMS-790052), ledipasvir (GS-5885), ombitasvir (ABT-267), elbasvir (MK-8742), velpatasvir (GS-5816), and on clinical tests: Pibrentasvir (ABT-530), ravidasvir (PPI-668), GSK2336805, ruzasvir (MK-8408), EDP-239, samatasvir (IDX719). It is known, that NS5A inhibitors do not affect stability or dimerisation of NS5A but block HCV RNA synthesis at the stage of membranous web formation [118]. Recently, it was discovered that DCV, can impair viral assembly by inhibiting the delivery of HCV genomes to the assembly sites [117]. NS5A inhibitors slowly inhibit HCV RNA synthesis when compared to HCV protease or polymerase inhibitors [119]. Furthermore, NS5A inhibitors can enhance drug resistance barrier and restore antiviral activity against NS5A resistance variants [62]. Notably, the crystallographic structures have been very useful in the development of NS5A inhibitors and further studies will elucidate the whole picture under the high potency, see Figure 6.5 and 6.6. In the following subsections we describe a more detailed information on NS5A inhibitor, Daclatasvir (DCV), as main subject of the present study.

6.1.3.1 Daclatasvir

DCV inhibits NS5A at DI and it is a food and drug administration (FDA) approved for the treatment of HCV infection, see Figures 6.5 and 6.6. DCV has been administered together with PEG-IFN and RBV as well as IFN free options [120], it can be administered together in combination with other DAAs including asunaprevir (NS3 protease inhibitor) (ASV) and sofosbuvir (SOF) (NS5B inhibitor). Normally, DCV plus SOF is given for 12 weeks [121] to have a high treatment efficiency. DCV has high rates of sustained virological response (SVR) >90%, which has a clinical relevance regarding the clearance of HCV infection in most patients. Interestingly, studies with DCV in replicon cells

showed that double or triple inhibitor combination of DAAs can produce resistance which can be different from when using mono-therapy. Indeed, onset of resistance may lead to cross-resistance among DAAs or to other NS5A inhibitors, while DCV-variants remained completely sensitive to other classes of DAAs [122–124].

Importantly, resistance-associated substitutions (RASs) in NS5A have a major impact clinically. As previously mentioned, RASs at key positions (28, 30, 31, and 93) in HCV genotype 1a result in broad cross-resistance to early generation NS5A inhibitors, except L31M RAS on ombitasvir and of the M28V RAS on elbasvir or ledipasvir. Next-generation NS5A inhibitors pibrentasvir (ABT-530) and ruzasvir (MK-8408) show a retain activity against all of the key single-position NS5A RASs in HCV genotypes 1a and 1b and, therefore, may retain activity despite resistance to current NS5A inhibitors [125].

Alternatively, mathematical models have been proposed to study and predict the possible mode of action of the inhibitors [126], many other attempts in medicinal chemistry are undergoing forward to develop new and better antiviral therapies. HCV resistant associated variants can occur naturally and usually after virological failure,, DCV resistant variants tend to persist even after discontinuation of the treatment and cross-resistance can be observed to all NS5A inhibitors. This remarks the importance of understanding fully the mechanism of action of NS5A inhibitors can elucidate insights into new drug development or improvement of existent drugs.

6.1.3.2 Discovery and development

At the beginning it was believed NS5A was not druggable mainly because of its lack of enzymatic activities. But in 2009, a high throughput screening showed pico to nano antiviral efficacy of leading compounds [36, 127]. One of these compounds was Daclatasvir, which has been widely studied and available against HCV infection. DCV displayed a therapeutic index (CC_{50}/EC_{50}) of at least 100,000 *in vitro* fold and works on genotype 1a, 1b, 2a and 3. Symmetry of this compound defined its antiviral activity having an EC_{50} of 5 picomolar (pm) and 9 pm (for genotype 1a and 1b, respectively). Then, clinical development increased towards NS5A inhibitors, initially mono-therapy was tried using DCV single dose, which showed dropping on HCV plasma RNA levels and it was well-tolerated treatment with few side-effects. Unfortunately, mono-therapy showed rapid resistance mutation emergence, which is why nowadays is taken in combination with other DAAs or traditional standard of care (SOC) therapy [36]. In general, HCV drug development has advanced in several aspects: interferon-free regimens, genotype specific drugs, therapies based upon one pill per day, drug potency increased, treatment

duration were shortened, therapies can be administered orally, despite all, HCV drug discovery challenges remain to identify and treat difficult-to-treat patients [111].

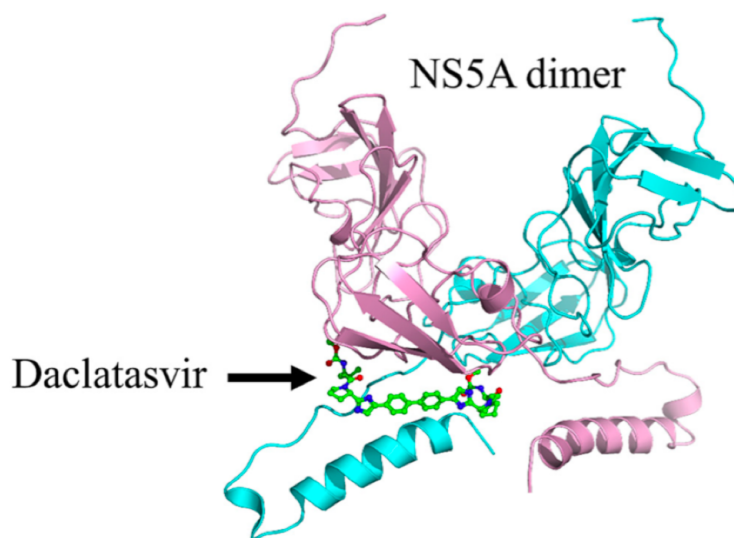


FIGURE 6.5: NS5A inhibitor, Daclatasvir in NS5A protein
Tertiary structure of HCV NS5A and structural formula of approved DCV docked into the two units of an NS5A, shown as a dimer, which are coloured by pink and cyan, respectively. Modified from [111].

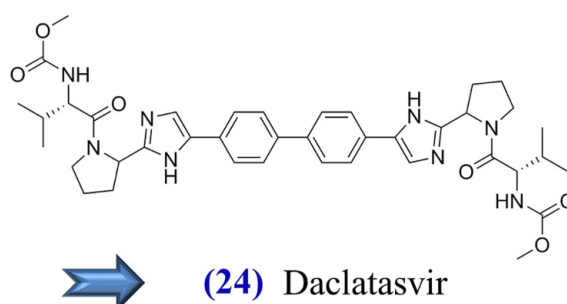


FIGURE 6.6: Daclatasvir chemical formula
NS5A inhibitor Daclatasvir is also illustrated. FDA-approved compound Daclatasvir [128]. Taken from [111].

6.1.3.3 Resistance mutations

The downside of using DCV as antiviral therapy is that it comes with selective mutation resistance. Most of the mutations have been found in NS5A between the amphipatic helix and domain I linker, specifically in amino acids 28-31 and around amino acid 93 of NS5A, which is one of the most described mutations, Y93H. The role of the amino acids in linker AH-DI is crucial for NS5A protein to fulfill its functions. This is one of the main reasons in the present study we aimed to understand the mode of action of DCV in relation of the structure of the linkers present in NS5A protein.

It has been identified in several genotypes, which points out a conserved inhibitor-binding site [129]. Substitutions at L31 and Y93 have the greatest ability to confer resistance to DCV. These substitutions can also confer resistance to first-generation NS5A inhibitors, double or triple combinations of NS5A inhibitors with other DAAs, can generate resistance in replicon systems [122], see Figure 2.7. Resistance mutations at amino acids M28, L31, P58 and Y93, are also found in DI under DCV treatment [13]. Another relevant aspect of DCV resistance is the existence of HCV quasispecies, which are variants that can replicate at low levels and usually cannot be detected by current techniques. However, quasispecies can be selected if any NS5A inhibitor, including DCV is administered and their expression levels can increase. Additionally, escape pattern can also confer resistance whereby viral replication returns to pre-treatment levels and the dominant virus harbours amino acid substitutions which can increase the drug resistance without impairing the fitness of the virus [130].

6.1.3.4 Mechanism of action

Many questions remain unanswered about the molecular mechanism of action of NS5A inhibitors, fortunately, some elucidating insights have described a major part of what these inhibitors can be targeting. Due to NS5A critical role in replication and assembly, NS5A is an attractive antiviral, which is why it has been widely studied. In HCV replicon cells, inhibition of NS5A resulted in its redistribution from ER to LD, thus, the targeting molecules have a dramatic effect on the phenotypic localization of NS5A [131]. On the same study, kinetic compound analysis showed that the redistribution was concomitant with the onset of inhibition [1]. As previously mentioned, NS5A inhibitors were found to block HCV replication by preventing the formation of the MW, which was not linked to an inhibition of PIP4KIII α [118].

Recently, Boson *et al*, showed that short exposure of HCV-infected cells to DCV reduced viral assembly and induced clustering of structural proteins with non-structural proteins (Core, E2, NS4B and NS5A), where they appear to be inactive. Daclatasvir reduced the delivery of viral genomes to these core clustered structures. However, when using the resistant mutant, NS5A-Y93H, DCV showed no induced clustered structures nor inhibition of HCV assembly, indicating that DCV targets a mutual specific function of NS5A inhibiting both processes [117]. This dual mode of action described by Boson *et al*, was also observed in our experiments, see section Results III, which conclude that DCV indeed targets NS5A not only during HCV replication but has an additional effect during assembly of the viral particles.

Moreover when considering the sub-stoichiometric antiviral activity it was suggested that not only DCV but all NS5A inhibitors might target one NS5A molecule which communicates using conformational changes to neighbouring NS5A molecules of an NS5A oligomer [39, 62]. This hypothesis was supposed by Sun *et al*, where they discovered the synergist compounds (Syn-395 and Syn-535), as already mentioned in section 2.7.5, and in Figure 2.8. Syn compounds were found inactive alone against both wild-type and resistant variants but can greatly enhance the potency of DCV against resistant variants. Specifically, DCV exhibits an EC_{50} of 0.033 nM against wild type GT-1a, but has no activity towards a GT-1a Y93N mutant (EC_{50} 339 nM). The synergist Syn-395, is inactive towards both wild type and Y93N (EC_{50} 214 nM and 215 nM, respectively). However, in the presence of Syn-395, the potency of DCV against the Y93N variant is greatly enhanced. For example, no inhibition of Y93N was observed at 40 nM Syn-395, but in the presence of 40 nM Syn-395 the potency of DCV against Y93N is enhanced by approximately 2,600-fold, with the EC_{50} value shifting from 339 nM to 0.13 nM [62]. This study highlights the importance of determining the oligomerization state of NS5A protein, which will clarify the conformational changes necessary for the mode of action of DCV and further NS5A inhibitors.

Lastly it was suggested that indeed NS5A is only targeted at a spatially and temporally restricted point with crucial role in the HCV RNA replication [131]. This might apply only for a subset of NS5A molecules. However Guedj *et al*, hypothesized by using a mathematical multiscale model that NS5A inhibitors not only inhibit HCV RNA synthesis, but also virion assembly and/or secretion [126]. This hypothesis was later confirmed by Boson *et al*, as already mentioned. However the present study gives a parallel importance of the dual mode of action of DCV.

Chapter 7

HCV and cellular membrane interactions

HCV and many other Flaviviruses exploit cellular resources to facilitate viral propagation, one of them is to manipulate cellular membranes. In HCV case, major rearrangements of the ER membranes take place during infection. RNA replication occurs in tight association with the ER derived membranes which are recognized as replication organelles. As already mentioned, these organelles have defined architecture and morphology but little is known about the viral or cellular factors involved in their biogenesis. The alteration of lipid composition of cellular membranes can serve as scaffold for replication changes in the biophysical properties of the membrane such as curvature, permeability and fluidity [132]. The understanding of the membrane interactions with viral proteins could help in the development of broad-spectrum antiviral drugs.

Experimental studies have been performed trying to elucidate the role of non-structural proteins of HCV in the membrane remodelling. Glycine zipper motifs within HCV NS4B transmembrane segments were found to be crucial for the protein's self-interaction. Moreover, glycine residues within NS4B transmembrane helices critically contribute to the biogenesis of functional replication organelles and, thus, efficient viral RNA replication. These results reveal how glycine zipper motifs in NS4B contribute to structural and functional integrity of the HCV replication organelles and in viral RNA replication [133]. Structural importance of NS4B has also being described through the role of a second amphipathic helix at the N-terminal (AH2), which revealed to have a key role in the remodelling events that NS4B performs in cellular membranes. The role of AH2 is to cluster negatively charged lipids within the lipid bilayer, thus reducing the strain within the bilayer and facilitates the its remodelling. Additionally, the same study describes that this negatively charged lipids are important to promote dissociation of AH2

oligomers which might be key for lipid recruitment of NS regulating protein interactions [134]. Other studies remark the importance of amphipathic helix formations in NS4B, as disrupting its nature results in abolished RNA replication as well as mislocalisation. This suggests that amphipathic helices might have a key role in membrane-targeting domain within the NS proteins [135].

Moreover, studies have revealed that not only NS4B has a structural link to membranes, NS4A, also forms a detergent-stable complex with NS4B-5A polyprotein substrate [136], which might be the reason of the requirement of 4A to the cleavage of 4B/5A.

Additional studies on NS3 have shown that it can bind spontaneously and penetrate to an ER complex membrane containing phosphatidylinositol 4,5-bisphosphate (PIP2), where an amphipathic helix has an anchoring role to keep the protein on the membrane surface. Residue R161, was found to be crucial to ensure proper orientation. PIP2-interaction determines the protein orientation at the membrane while both hydrophobic interplay and PIP2 interaction can stabilize the NS3-membrane complex [137].

Finally, NS5A, as already mentioned, contains a three dimensional structure of the membrane anchor domain, the alpha helix anchor which includes amino acid 5 to 25, which was exhibited a hydrophobic tryptophan rich side embedded in detergent micelles, while the polar charged side was opposed to the solvent side. The amphipathic helix is embedded in the cytosolic leaflet of the membrane bilayer. Importantly, mutations in this position might affect RNA replication without interfering with membrane association of NS5A [33].

Regarding NS5A and its association to membranes, it comes to one key element, the amphipathic helix, as mentioned several times, the AH is key for the membrane localisation, as it is also essential in the binding to cell-derived membranes. The mechanism of binding for AH on artificial pure lipid bilayers is different from cell-derived membranes. The difference observed is the rate of association, were in more complex cell-derived membrane bilayer more time is required for NS5A AH to fully interact with partner ligands as suggested in [138]. Cho *et al*, suggest that a cellular membrane protein component contributes to the association, which would explain how NS5A proteins are localised in ER or Golgi derived membranes, including lipid droplets but not plasma membranes or subcellular membranes as others have described [65, 139–141]. Finally, genetic disruption of AH-mediated membrane association of NS5A has been found to abrogate HCV RNA replication [142], suggesting that such a structural motif is indeed important for some essential aspect of the HCV life cycle. The relocalisation of NS5A to the nucleus after disruption of the amphipathic nature of its N-terminal helix and the strict preservation of this motif in all known HCV isolates, which suggests that disruption of the AH may have significant consequences for HCV RNA replication [142].

7.1 Molecular Dynamics as a tool for membrane studies

x By definition, Molecular dynamics is a method for simulating macromolecular motions based on an empirical force field that describes the energetics of interactions between the constituent atoms [143]. This can include atomistic simulations provide us with a detailed observation of membrane lipid-protein interactions [143–145]. Computer simulations, specifically molecular dynamics are very detailed studies on structural biology, providing key information from a crystal to a bilayer and monitor its dynamic behaviour within its native environment. Molecular dynamics is a very powerful tool to understand and characterize interactions of membrane-protein in order to elucidate mechanisms of action or conformational changes that might be key for the development of cellular processes.

In fact, most of membrane protein structures are studied without a lipid bilayer environment and at best reveal only a small number of bound lipid or detergent molecules, often incompletely resolved. Importantly, several studies have indicated that lipid molecules play active roles in modulating membrane protein structure and function [146]. Evidently, there is a need to obtain a better understanding of membrane protein interactions within a bilayer. Ultimately, there has been a growing development in refinement of computational tools to achieve this purpose. Recently, new methods can predict bilayer-spanning region of a membrane protein structure, this can already be semi automatic and are available (for example: OPM; <http://opm.phar.umich.edu/>). However, for the relevance of the present study we will use the predictions of MD to correlate experimental data.

Chapter 8

Objectives of the study

The main aim of the present study is to contribute to the studies on NS5A inhibitors and elucidate the molecular mechanism of action by some specific objectives:

1. Analysis of NS5A domain I structural linkers *in vitro* and *in silico* to understand the importance of conserved Proline residues within linker structure and their impact in HCV life cycle.
2. Investigate the role of Proline residues in the interaction with NS5A inhibitor, DCV.
3. Role of NS5A inhibitor DCV in assembly of HCV viral particles.
4. NS5A amphipatic helix role in membrane interaction and DCV interaction.

Together the present data will give experimental approaches in the recently discovered dual mode of action of NS5A inhibitor, DCV. Its participation during the inhibition of NS5A protein during HCV replication and assembly of the viral particles. Additional computational tools were used to understand *in silico* the mechanism of action involving specific conserved Proline residues in the linker structures of NS5A and their role in HCV life cycle. These key Proline residues were analyzed *in silico* to evaluate DCV binding site. Finally, we built up a comprehensive model in which NS5A inhibitors can be located in the context of membrane interaction and can be used to evaluate and test new antiviral drugs against NS5A protein.

Part II

Materials and Methods

Chapter 9

Materials

9.1 Antibodies and dyes

The following table (Table 9.1) contains the primary antibodies, secondary antibodies used during the present study. The only dye used in the study was: 4', 6'-diamidino-2-phenylindole (DAPI).

TABLE 9.1: Antibodies

Antibody	Generated in	Manufacturer	Dilution/Method
Primary			
α -NS5A	Mouse monoclonal	Austral Biologicals	1:200 IF
α -52	Rabbit polyclonal	In house	1:2000 WB
α -NS5A-9E10	Mouse monoclonal	gift from C.Rice	1:100 IF, 1:10,000 WB
α -Core C-380	Rabbit polyclonal	In house	1:200 IF, 1:2000 WB
α - β actin	Mouse monoclonal	Sigma	1:20,000 WB
α -Flag M2	Mouse monoclonal	Sigma	1:20,000 WB
Secondary			
α -mouse IgG AlexaFluor488	Goat polyclonal	Molecular Probes	1:1000 IF
α -rabbit IgG AlexaFluor546	Goat polyclonal	Molecular Probes	1:1000 IF
α -mouse IgG AlexaFLuor647	Goat polyclonal	Molecular Probes	1:1000 IF
α -mouse HRP	Goat polyclonal	Sigma	1:10,000 WB
α -mouse HRP	Goat polyclonal	Sigma	1:200 TCID50

9.1.1 Bacteria and cell culture

Bacteria

E.coli DH5 α : derived from construct F'end A1 hsR17A (rkmk) supE44 thi-recA1 gyrA (Nalr) relA1 δ (lac ZYA-argF) U169deoR (ϕ 80 dlac δ (lacZ) M15.

Eukaryotic cells

293 MCB cells: are derived from human embryonic kidney cells and later transformed with large t antigen of Simian Vacuolating Virus 40 (SV40) [147], (a gift from Birke Bartosch).

Huh7 cells: are derived from a human hepatoma cell line, [148]

Huh7 Lunet: this cells are a subclone of Huh7 cells that was generated by curing a stable replicon cell line; they support high level of RNA replication.

Huh7 Lunet T7: Huh7-Lunet cells expressing T7 RNA polymerase under selection with 2 g/ml puromycin [84].

Huh7.5: highly infectable Huh7 cell clone. This cell line was generated by curing a stable replicon cell line and has high level expression of CD81 [83].

9.1.2 Media

Bacteria:

LB:10g/l tryptone, 5g/l yeast extract, 5g/l NaCl: 1.5% agar-agar were added for solid media; ampicilin or carbenicilin were added at 100g/ml and kanamycin at 30g/ml for selection media.

Eukaryotic cells:

DMEM complete ®: cell lines were grown in Dulbecco's modified eagle medium (Invitrogen ®) supplemented with 2mM L-glutamine, non-essential amino acids, 100U/ml penicilin, 100mg/ml streptomycin, 10% fetal calf serum (FCS; seromed, inactivated at 56°C for 30 minutes). For selections antibiotics were added in the already mentioned concentratios.

OptiMEM: modification of DMEM with reduced serum (Invitrogen ®).

9.1.3 Compounds

The following compounds were used for various experiments (Table 9.2). Titration of the compounds for the present study is described in the Results section III. Structure of Daclatasvir can be found in Figure 6.6

TABLE 9.2: Compounds

Compounds		
Name	Class	Source
Daclatasvir (DCV)	NS5A inhibitors	Bristol-Meyers
Sofosbuvir (SOF)	NS5B polymerase inhibitors	Gilead Sciences

9.1.4 Plasmid constructs

Vectors for viral constructs:

pFK: low copy plasmid used as template for in vitro RNA transcription of viral constructs. Transcription is driven for T7 polymerase.

pTM: high copy plasmid containing T7 promoter that allows the transcription of viral RNA transcripts in cells stably expressing the T7 polymerase.

Consensus genomes

HCV wild type and chimeric constructs used in this study are based on the following sequence genomes:

Con1: genotype 1b, accession number GeneBank AJ238799.

JFH1: genotype 2a, accession number GeneBank AB047639.

All the viral constructs used and generated in the present study are listed here.

Con1 constructs:

pFK-Con1wt : full length Con1 wild type sequence.

pFK-Con1/S2204R: contains a mutation S2204R in NS5A [149].

pFK-Con1ET : contains mutations E1202G, T1280I and K1846T in NS3 and NS4B.

pFK-Con1/NS5A: contains a mutation in S2197P and two silent nucleotide changes (C6842T and C6926T)[150].

pFK-I389Luc/NS3-3/Con1/wt: bicistronic subgenomic replicon; the FLuc gene is expressed under the control of the Con1-IRES; the Con1 NS3 to NS5B region is expressed under the control of the EMCV- IRES. From [151].

pFK-I389Luc/NS3-3/Con1/GND: contains a deletion of previous construct [151].

JFH1 constructs:

pFK-JFH1wt-dg (JFH1wt): full length JFH1 wild type sequence [88].

pTM-NS3-3-JFH1wt (sgJFH1wt): plasmid for T7 promoter-driven expression of the NS3-3 portion of wild type JFH1 [79].

Chimeric constructs:

pFK-JFH1/J6/C-846-dg (Jc1): full length virus chimera consisting of the 5NTR of JFH1, the region encoding core to the first putative TMS in NS2 of J6 and the remaining sequence of JFH1 [152].

pFK-Luc-Jc1 (Jc1FLuc): bicistronic full length reporter virus; it carries the FLuc gene in the first cistron driven by the JFH1-IRES and the Jc1 polyprotein driven by the EMCV-IRES in the second cistron. [86].

pFK-RLuc-2A-core-Jc1 (JcR-2A): monocistronic full length reporter virus; RLuc

is fused in-frame to the N-terminal 16 aa of the core protein with the foot-and-Mouth Disease Virus (FMDV) 2A peptide between the luciferase and the following complete Jc1 open reading (from M Poenish).

pFKi389-Luc-NS3-3'-NS5A-HA-Y93H-dg-JFH1: containing a HA tag in the resistance mutation number 93 of NS5A.

Generated plasmid constructs for BRET

Constructs taken from Dr. Berger and new constructs developed using the following ones (Table 9.3), we use several in combination.

TABLE 9.3: BRET constructs for each one of NS5A linkers

pcDNA_RLucF1_NS5A	Linker 1	<i>Thr-Gly-Gly-Ser-Asp-Ile</i>
pcDNA_RLucF2_NS5A	Linker 1	<i>Thr-Gly-Gly-Ser-Asp-Ile</i>
pcDNA_YFPF1_NS5A	Linker 1	<i>Thr-Gly-Gly-Ser-Asp-Ile</i>
pcDNA_YFPF2_NS5A	Linker 1	<i>Thr-Gly-Gly-Ser-Asp-Ile</i>
pcDNA_RLucF1_NS5A	Linker 2	<i>Thr-Gly-Pro-Ala-Pro-Ala-Pro-Gly-Gly-Ser-Asp-Ile</i>
pcDNA_RLucF2_NS5A	Linker 2	<i>Thr-Gly-Pro-Ala-Pro-Ala-Pro-Gly-Gly-Ser-Asp-Ile</i>
pcDNA_YFPF1_NS5A	Linker 2	<i>Thr-Gly-Pro-Ala-Pro-Ala-Pro-Gly-Gly-Ser-Asp-Ile</i>
pcDNA_YFPF2_NS5A	Linker 2	<i>Thr-Gly-Pro-Ala-Pro-Ala-Pro-Gly-Gly-Ser-Asp-Ile</i>
pcDNA_RLucF1_NS5A	Linker 3	<i>Thr-[Gly-Gly-Gly-Gly-Ser]3-Asp-Ile</i>
pcDNA_RLucF2_NS5A	Linker 3	<i>Thr-[Gly-Gly-Gly-Gly-Ser]3-Asp-Ile</i>
pcDNA_YFPF1_NS5A	Linker 3	<i>Thr-[Gly-Gly-Gly-Gly-Ser]3-Asp-Ile</i>
pcDNA_YFPF2_NS5A	Linker 3	<i>Thr-[Gly-Gly-Gly-Gly-Ser]3-Asp-Ile</i>
pcDNA_RLucF1_NS5A	Linker 4	<i>Thr-Gly-Ala-[Glu-Ala-Ala-Ala-Lys]2-Ala-Gly-Gly-Ser-Asp-Ile</i>
pcDNA_RLucF2_NS5A	Linker 4	<i>Thr-Gly-Ala-[Glu-Ala-Ala-Ala-Lys]2-Ala-Gly-Gly-Ser-Asp-Ile</i>
pcDNA_YFPF1_NS5A	Linker 4	<i>Thr-Gly-Ala-[Glu-Ala-Ala-Ala-Lys]2-Ala-Gly-Gly-Ser-Asp-Ile</i>
pcDNA_YFPF2_NS5A	Linker 4	<i>Thr-Gly-Ala-[Glu-Ala-Ala-Ala-Lys]2-Ala-Gly-Gly-Ser-Asp-Ile</i>

9.1.5 DNA oligonucleotides

Aliquots were made and saved at -20. The following table shows the DNA oligonucleotides used to perform experiments and its respective sequences (Table 9.4).

TABLE 9.4: Primer sequences

Primer	Sequence primer (5'-3')
S/2A/6978	TCCTCAGTGAGCCAGCTATCAGCA
S/2A/6767	CATAGGTTTGCACCCACACCAAAG
S/2A/7139	GAGCCCTCAATACCATCGGAGTG
S/2A/7194	CCAGGAGCGGGTTTCCACGGGCCT
S/2A/7380	CCATATCAGAAGCCCTCCAGCAA
A/2A/3089	CGTCAGAGCTCACGCTCTGATAAG
A/2A/7759	GCCTGGAGATCCGGACCTGGAGTCTG
A/2A/7839	GTCATAATGGGCGTCGAGCACTTG

9.1.6 Chemicals and manufacturers

The following Table shows the chemicals that were used and the manufacturer which provided them, see Table 9.5. All chemicals are stored under label conditions and in the chemical room where temperature is regulated.

9.1.7 Buffers and solutions

The following Figure is a list which describes the buffers and solutions used in the present study (Figure 9.1). Conditions were all established previously in the laboratory, were most of the buffers and solutions are freshly made and distributed. All buffers and solutions are stored at the correct temperature and conditions indicated.

Chemical	Manufacturer
2-Mercaptoethanol	Roth, Karlsruhe
35 S methionine/cysteine	Perkin Elmer, Rodgau
Agarose	Invitrogen, Karlsruhe
Albumin, from bovine serum (BSA)	Sigma-Aldrich, Steinheim
Ampicillin	Roche, Mannheim
Benzonase	Merck, Darmstadt
Calf Intestinal Phosphatase (CIP)	New England Biolabs, Frankfurt/Main
Coelenterazine (native-CTZ)	PJK, Kleinblittersdorf
Complete protease inhibitor cocktail	Roche, Mannheim
CytoTox 96 Non-Radioactive Cytotoxicity Assay	Promega, Mannheim
DAPI	Molecular Probes, Karlsruhe
Digitonin	Sigma-Aldrich, Steinheim
D-Luciferin	PJK, Kleinblittersdorf
DMSO	Roth, Karlsruhe
DNaseI	Promega, Mannheim
dNTPs	Roche, Mannheim
ECL Plus Western Blot Detection System	Amersham/Perkin-Elmer
Expand Long Template PCR Kit	Roche, Mannheim
Expand Reverse Transcriptase System	Roche, Mannheim
FCS	Invitrogen, Karlsruhe; PAA, Clbe
Geneticin (G418)	Invitrogen, Karlsruhe
Glycerol	Roth, Karlsruhe
Kanamycin sulfate	Serva, Heidelberg
L-Glutamine for cell culture	Invitrogen, Karlsruhe
Lipofectamin 2000	Invitrogen, Karlsruhe
Mirus TransIT Transfection Reagent	Mirus Bio, LLC, Madison, WI
Nucleobond PC100	Macherey-Nagel, Dren
Nucleospin Extract II	Macherey-Nagel, Dren
Nucleospin Plasmid	Macherey-Nagel, Dren
Nucleospin RNA II	Macherey-Nagel, Dren
OptiMEM	Gibco, Invitrogen
PEG-8000	Applichem, Darmstadt
Penicillin	Invitrogen, Karlsruhe
PhosphoStop phosphatase inhibitor cocktail	Roche, Mannheim
Polyacrylamide : Bisacrylamide Mix (29:1)	Applichem, Darmstadt
Protein A/G sepharose beads	Biorad, Mnchen
Puromycin	Sigma-Aldrich, Steinheim
PVDF Western Blot membrane	Perkin Elmer, USA
RNasin	Promega, Mannheim
rNTPs	Roche, Mannheim
Sodium dodecylsulfate	Applichem, Darmstadt
Streptomycin	Invitrogen, Karlsruhe
Sucrose	USB, Europe
Superscript III Reverse transcriptase	Invitrogen, Karlsruhe
T4 DNA-Ligase	Fermentas, St. Leon-Rot
T7 polymerase	Promega, Mannheim
T7 RNA polymerase	Promega, Mannheim
TEMED	Applichem, Darmstadt
Triton X- 100	Merck, Darmstadt
Tween-20	Roth, Karlsruhe

TABLE 9.5

Buffer/Solution	Composition
Ampicilin	100mg/ml ampicilin in H ₂ O, filter sterilized and stored at -20°C
Blasticidin stock solution	5mg/ml in H ₂ O, sterile filtered
Bradford reagent	100mg coomassie g250 is dissolved in 50ml 100% ethanol and added to 100ml 85% phosphoric acid (final volume 1), filtered and stored at 4°C
Colenterazine	5mg colenterazine in 11.6ml methanol, store at -80°C
Cytomix	120mM KCl, 0.15mM CaCl ₂ , 10mM potassium phosphate buffer (pH7.6), 25mM HEPES (pH7.6), 2mM EGTA, 5mM MgCl ₂ , adjust the pH to 7.6 using KOH, freshly add 2mM ATP (pH 7.6 adjusted with KOH), 5mM glutathione and 1.25% DMSO
DMEM complete	Dulbecco's modified minimal essential medium (GIBCO, Invitrogen) containing 2mM L-glutamine (GIBCO, Invitrogen), 1x nonessential aminoacids (GIBCO, Invitrogen), 100U/ml streptomycin (GIBCO, Invitrogen) and 10% (v/v) fetal calf serum (heat inactivated at 56°C for 20 min).
DNA loading dye orange (10x)	45ml 50% glycerol, 1ml TAE(50x), 0.5ml EDTA (0.1M, pH 8.0), 0.13g Orange G, H ₂ O to 50ml
Firefly Luciferase assay	25mM glycine-glycine (pH7.8), 15mM potassium phosphate buffer (pH7.8), 15mM MgSO ₄ , 4mM EGTA, freshly add 1mM DTT and 2mM ATP just before use
IF blocking buffer	3-5% (w/v) BSA in PBS
LB-Agar	10g Bacto-Trypton, 5g yeast extract, 2.5g NaCl, 20g Agar in 1l H ₂ O, autoclaved
Luciferase lysis buffer	1% (w/v) triton x-100, 10% glycerol, 25mM glycine-glycine (pH7.8), 15mM MgSO ₄ , 4mM EGTA, keep at 4°C, freshly add 1mM DTT just before use
Luciferin solution	1mM luciferin in 25mM glycyl-glycyl, store at -80°C
Luria Broth (LB) medium	10g Bacto-Trypton, 5g yeast extract, 2.5g NaCl, 20g Agar in 1l H ₂ O, autoclaved
NEB buffer 1	10mM Bis Tris Propane HCl, 10mM MgCl ₂ , 50mM NaCl, 1mM DTT (pH7.9 at 25°C)
NEB buffer 2	10mM Tris-HCl, 10mM MgCl ₂ , 50mM NaCl, 1mM DTT (pH 7.9 at 25 °C)
NEB buffer 3	50mM Tris-HCl, 10mM MgCl ₂ , 100mM NaCl, 1mM DTT (pH 7.9 at 25 °C)
Paraformaldehyde 4%	4g paraformaldehyde dissolved stirring at 60°C in 100 ml PBS
PBS (10X)	400 g NaCl, 10 g KCl, 12 g KH ₂ O ₄ , 89g Na ₂ HPO ₄ x 2H ₂ O, add 5l H ₂ O

Buffer/Solution	Composition
Protein sample buffer (6x)	375mM Tris-HCl (pH 6.8), 60% Glycerol, 6% (w/v) SDS, 0.1% (w/v), Bromphenol Blue, 9% (v/v) b-Mercaptoethanol
Puromycin stock solution	1mg/mg in H ₂ O, sterile filtered
Renilla Luciferase assay	25mM glycine-glycine (pH 7.8), 15mM potassium phosphate, buffer (pH 7.8), 15mM MgSO ₄ , 4mM EGTA
Resolving gel buffer	1.5 M Tris-HCl, pH 8.8, 0.4% (w/v) SDS
Semi-dry blotting buffer	48mM Tris, 39mM Glycine, 0.00375 (w/v) SDS, 20% (v/v) Methanol in dH ₂ O
Sodium acetate (pH 4.5) 3M	3M Sodium Acetate, pH adjusted to 4.5 with Glacial Acetic acid
Sodium acetate (pH 6.8) 2M	2M Sodium Acetate, pH adjusted to 4.5 with Glacial Acetic acid
Stacking gel buffer	1M Tris-HCl (pH 6.8), 0.8% (w/v) SDS
TAE (50x)	2M Tris, 2M Acetic Acid, and 50mM EDTA, pH 8.3
TCID 50 detection substrate - solution II	75ml 0.5M NaAcetate, 30ml 0.5M acetic acid, 945ml dH ₂ O (store at 4°C)
TCID 50 detection substrate solution I	0.4g 3-amino-9-ethyl carbazolein in 125ml N,N dimethylformamide (store at 4 °C in the dark; use within 3 months)
TGS	150mM Tris, 1,92M Glycine, 1% (w/v) SDS
Transcription buffer RRL (5x)	400mM Hepes (pH 7.5), 60mM MgCl ₂ , 10mM spermidine, 200mM DTT
Trypsin solution	0.05% trypsin; 0.02% EDTA
Western Blot blocking buffer	0.5% (w/v) of Tween-20, 5% Protease free Milk Powder in PBS
Western Blot washing buffer (PBS-T)	0.5% (w/v) Tween-20 in PBS

FIGURE 9.1: Buffers, solutions and composition

Chapter 10

Methods

All centrifugation steps in Eppendorf tubes[®] were performed in table top centrifuges, Biofuge pico (Heraeus instruments[®]) or 5417R (Eppendorf[®]) for RT or 4°C, respectively. Fifty ml polypropylene conical tubes (Falcon[®]) were centrifuged in a Sorvall Centrifuge RC5C Plus d with a F15-S FiberLite rotor[®]. Cell suspensions were centrifuged in a Multifuge 3 S-R, rotor 75006441 (M&S Laborgerete[®]). All centrifugation steps were performed at RT, if not stated otherwise. Experiments with infectious HCV were done in a BSL3 laboratory.

10.1 Preparation of plasmid DNA from *E. coli* cultures

Small scale preparation of plasmid DNA (miniprep) Minipreps of plasmid DNA were performed with 2 ml o/n *E. coli* culture which were centrifuged in 2 ml Eppendorf tubes step wise for 30 s at 11,000 g. Plasmid DNA purification was obtained by using the NucleoSpin[®] Plasmid Kit according to the manufacturer's protocol. The kit provides all buffers for an alkaline based cell lysis and uses a silica membrane based spin column to further purify the plasmid DNA. The DNA was eluted in either 50 μ l H₂O or 5mM Tris-HCl (pH 7.5).

Middle scale preparation of plasmid DNA (midiprep) For larger plasmid preparations of low copy vectors 100 ml o/n *E. coli* cultures were pelleted in 50 ml tubes. For plasmid preparation the NucleoSpin[®] Plasmid Kit was used with all buffer amounts multiplied by 16. The DNA plasmid elution was divided onto four columns in 75 μ l H₂O or 5mM Tris-HCl (pH 7.5) per column.

10.2 Digestion of DNA with restriction enzymes

Separation of linear DNA fragments by their length was done using agarose gel electrophoresis. The percentage of the gel depended on the size of the DNA fragment. Typically a 1% (w/v) gel was used to separate DNA fragments with a size between 700 and 8,000 bp. For higher fragments a 0.8% and for smaller fragments a 1.2% gel was used, respectively. The agarose was dissolved and boiled in 1X TAE buffer. Ethidium bromide was added to a final concentration of 1 μ g/ml. DNA samples with 10% DNA loading buffer as well as a molecular weight marker (λ -DNA digested with Eco130I/Sty1I) were loaded on the agarose gel which was run horizontally in 1X TAE buffer at 100-200 V for 15 to 45 min. DNA was visualized by UV light and the DNA band of interest was cut out of the gel. Agarose extraction and DNA purification from the band was done by using the NucleoSpin[®] Extract II Kit according to the manufacturer's protocol. Usually DNA was eluted in 30 μ l H₂O or 5mM Tris-HCl (pH 7.5).

10.3 Ligation of DNA fragments

For ligation reactions the linearised and dephosphorylated plasmid as well as one or two DNA fragments of interest (either a plasmid-derived DNA fragment or a PCR product) were mixed in a ratio of 1:1 with 5U T4 DNA ligase and 1/10 ligase buffer in a total reaction volume of 10 μ l. After incubation for 2h at RT or o/n at 16°C the complete reaction was used to transform competent bacteria.

10.4 Generation and transformation of competent bacteria

Competent bacteria DH5 α were generated by using the CaCl₂ method. Bacteria of an overnight culture were diluted 1:50 with LB-medium and incubated at 37°C until the bacterial growth reached its logarithmic phase (OD 600 of 0.8 to 1). The culture was centrifuged at 4°C for 10 min at 6000 rpm and the pellet was resuspended in ice-cold 0.1M CaCl₂ and kept for 30 min on ice. After centrifugation at 4°C for 5 min at 6000 rpm the pellet was resuspended in a ratio of 1:10 in 0.1M CaCl₂ with 15% glycerol, aliquoted, frozen in liquid nitrogen and stored at -70°C. For transformation, 100 μ l of competent bacteria and 10 μ l ligation reaction (or approx. 0.1 μ g plasmid DNA) were mixed and incubated for 20 min on ice. After a heat shock at 42°C for 2 min the reaction was incubated for 5 min on ice, supplemented with 800 μ l of LB medium and incubated for 30 min at 37°C in a shaker. Finally, bacteria were pelleted (2 min, 6000 rpm) and the supernatant was discarded except for approx. 50 μ l. The pellet was resuspended in the

remaining medium and plated on LB agar plates containing the appropriate antibiotic (ampicillin, 100 μ g/ml; kanamycin, 30 μ g/ml). Colonies were grown o/n at 37°C.

10.5 Sequence analysis of DNA

For sequencing, an ABI 310 sequencer (Applied Biosystems[®]) was used according to the manufacturer's instruction with slight modifications. Approx. 300ng of plasmid DNA were mixed with 2 μ l big dye (containing buffer, polymerase, deoxy- and dideoxynucleotides), 1 μ l primer (5 pmol/ μ l), 1 μ l 5X sequencing buffer and water to a final volume of 10 μ l. The following program was used for the cycle sequencing reaction:

1. 95 °C for 10 sec
2. 55 °C for 30 sec
3. 60 °C for 4 min (30 cycles step 1. 3.)
4. 10 °C until stop

PCR sample was denatured by addition of 2% SDS in a total volume of 100 μ l and incubation at 98°C for 5 min. After cooling down to RT, DNA fragments were precipitated with 1/10 vol 3M sodium acetate and 2.5 vol ethanol by centrifugation for 20 min at 13000 rpm. Finally, the pellet was washed once with freshly prepared 70% ethanol (3 min, 13,000 rpm), air-dried briefly, dissolved in 20 μ l Hi-Di-formamide and sequenced with the ABI PRISM 31.

10.5.1 PCR and site directed mutagenesis

PCR was performed to selectively amplify a defined DNA sequence from a DNA template using Taq (thermostable DNA polymerase named after the thermophilic bacterium *Thermus aquaticus*) as polymerase according to the manufacturer's protocol. Two oligonucleotide primers that are complementary to approx. 25 bp upstream and downstream (sense, S and antisense, A) of the region of interest had to be designed. Depending on the following cloning strategy, restriction enzyme recognition sites were added to the primer sequences. A PCR contained the following reagents:

TABLE 10.1: PCR ingredients

Reagent	Volume
10x PCV buffer	5 μ l
dNTPs mix (10mM each)	1 μ l
sense primer (100pmol/ μ l)	0.5 μ l
antisense primer (100pmol/l)	0.5 μ l
DNA template	<500ng
Taq (5U/ μ l)	0.25 μ l
water	add 50 μ l

PCR was performed with the standard program:

1. 95 °C for 1 min
2. 55 °C for 30 sec (denaturation)
3. 50 °C for 1 min (annealing)
4. 68 °C for 1 min (elongation, 8 cycles)
5. 68 °C for 5 min
6. 4 °C until stop

For the site-directed mutagenesis PCR was performed. Two overlapping mutagenesis primers (sense and antisense) were designed to anneal to the mutation target and have at least 18 nucleotide overlap. The flanking primers (forward and reverse) are designed to carry restriction sites for cloning. The products generated from the two first round PCR involving each flanking primer along with matching fusion primer are purified and used as template in the subsequent PCR reaction, where the priming is done with the flanking primers. The products generated are treated with restriction endonucleases and cloned into target plasmid. For mutagenesis PCR generally a non-proofreading Taq polymerase was used.

10.6 In vitro transcription and RNA purification

Ten μ g of DNA was linearized to prepare run off transcripts of the correct length. Constructs carrying the genomic ribozyme of hepatitis δ (δ g) downstream of the 5' end of the RNA were additionally digested with MluI, which cuts directly after the ribozyme sequence, in a reaction volume of 100 μ l. All full-length Con1 constructs had to be linearized with AseI and subsequently with ScaI. For purification, plasmid DNA was mixed with 20 μ l 3M sodium acetate (pH 6.0) in a total volume of 200 μ l extracted

twice with 200 μ l TE saturated phenol and once with 200 μ l chloroform. At each step, the sample was first mixed with a vortex and then centrifuged (5 min, 13,000 rpm) for proper separation of the organic and aqueous phases and the upper aqueous phase was transferred to a new Eppendorf tube. To precipitate the DNA, 2.5 vol 100% ethanol were added and the sample was left at -20°C for at least 30 min. After centrifugation for 20 min at 13,000 rpm at 4°C, the pellet was washed once with 200 μ l 70% ethanol (3 min, 13,000 rpm), air-dried briefly and dissolved in 60 μ l RNase-free H₂O. For in vitro transcription, 20 μ l 5 x RRL transcription buffer, 12.5 μ l 25 mM rNTPs, 2.5 μ l RNasin (40 U/ μ l) and 4 μ l T7 RNA polymerase (19 U/ μ l) were added to the purified DNA. After incubation for 2 h at 37°C, again 2 μ l of T7 RNA polymerase were added, followed by another 2 h incubation at 37°C. Transcription was terminated by addition of 6 μ l of RNase-free DNase (1 U/ml) for 30 min at 37 °C. For purification of the RNA, 60 μ l (1/10) 2 M sodium acetate (pH 4.5), 440 μ l H₂O and 400 μ l water-saturated phenol were added. The sample was mixed with a vortex, left on ice for 10 min and centrifuged at 4 °C for 10 min at 13,000 rpm. The upper phase was transferred to a new Eppendorf tube and extracted again with 1 vol chloroform (vortex, 5 min at 13,000 rpm). RNA was subsequently precipitated with 0.7 vol isopropanol (15 min at 13,000 rpm), washed once with 70% ethanol (3 min at 13,000 rpm) and dissolved in 50 μ l RNase-free H₂O. Agarose gel electrophoresis was used to determine the RNA integrity and the concentration was calculated by measurement of the optical at 260 nm.

10.7 Cell culture and virological methods

10.7.1 Culture of cell lines

All cell lines used in this work were cultured as monolayers on cell culture dishes or flasks, using DMEM complete and the respective selection drug, if needed (see Materials section 9). In general, cells were split twice a week 1:4 to 1:6, depending on the cell line and the momentary growth. To this end, cells were washed with PBS, detached by incubation in trypsin solution (2 min at 37°C), sheared by pipetting up and down through a 1000 μ l tip to yield a single cell suspension and a fraction of the cells was transferred to a new dish. For long-term storage cells were frozen in liquid nitrogen. Therefore, usually cells of a confluent 15 cm dish were washed with PBS, trypsinized, resuspended in 10ml DMEM complete and centrifuged for 5 min at 700 rpm. Cells were then resuspended in 9 ml ice-cold DMEM supplemented with 20% FCS and 10% DMSO and frozen in five 1.8 ml aliquots in pre-chilled tubes for 24 or 48 h at -70°C before storage in liquid nitrogen. For thawing, cells of one aliquot were incubated at 37°C, washed with 10 ml DMEM complete (5 min at 700 rpm), resuspended in 5ml

and seeded into a T25 flask. Selection marker(s) were added immediately or 24 h after seeding.

10.7.2 Cell line for trans-complementation assay

Huh-7 cells were cotransfected by electroporation as previously described with 5 μ g of a neo-replicon as helper RNA and 1 μ g of a replication-deficient luciferase reporter replicon. After addition of 12ml of complete DMEM, 1ml aliquots of the cell suspension were seeded into a 10 cm² culture dish and harvested at the time points given in Results. For determination of luciferase activity, cells were washed three times with phosphate-buffered saline and scraped off the plate into 350 μ l of ice-cold lysis buffer (1% Triton X-100, 25mM glycylglycine, 15mM MgSO₄, 4mM EGTA, and 1mM DTT). One hundred microliters of lysate was mixed with 360 μ l of assay buffer (25mM glycylglycine, 15mM MgSO₄, 4mM EGTA, 1mM DTT, 2mM ATP, and 15mM K₂PO₄ [pH 7.8]) and, after addition of 200 μ l of a 200 μ M luciferin stock solution, measured in a luminometer (Lumat LB9507; Berthold, Freiburg, Germany) for 20 seconds. Values obtained with cells harvested 4h after electroporation were used to determine the transfection efficiency.

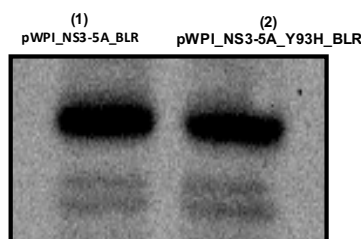


FIGURE 10.1: Cell Line
Western Blot showing NS5A for the cell line generated. (1) Assembly mutant: pWPI-NS3-5A-BLR and (2) Resistant mutant: pWPI-NS3-5A-Y93H-BLR.

10.7.3 Lentiviruses transduction of cells for new cell line production

293T cells 6X(1.2X10⁶) were seeded in a 6 cm dish in a volume of 4 ml DMEM complete, 24 h after seeding cells were replaced with 4 ml of fresh medium and transfected with the CalPhos mammalian transfection kit (Becton Dickinson ®). All transfection solutions were calibrated at RT. For transfection, 6.4 μ g packaging plasmid (psPAX2), 6.4 μ g transfer vector encoding the respective shRNAmir and puromycin resistance (pAPM) and 2.1 μ g VSV envelope glycoprotein (pMD2.G) were mixed and diluted to a final volume of 438 μ l in H₂O. Then, 62 μ l 2 M CaCl₂ and 500 μ l 2X HBS buffer were added and mixed well by pipetting up and down. The mixture was immediately added to the cell culture dish in a drop-wise fashion and the plate was gently swirled to evenly distribute

the transfection mix. After 3 to 4 h, a fine precipitate formed which could be easily confirmed under the microscope. After 6 to 24 h, the transfection mix was replaced 5 by 5 ml of fresh complete DMEM. On the next day, 2×10^6 of Huh7.5 target cells were seeded in a 6-well plate. Twenty-four hours later (48 h post transfection), the lentiviral particles containing supernatant from the 293T cells were harvested and replaced by another 4 ml fresh DMEM complete. The supernatant was filtered through a $0.45 \mu\text{m}$ filter and 1.5 ml was used to infect the target cells. After 12 h, fresh 1.5 ml infectious supernatant was used to infect the target cells a second time. On the next day, the medium from the 293T cells was harvested and filtered a second time and pooled with the infectious supernatant from the previous day. Target cells were infected a third time with 1.5 ml of infectious supernatant for 4 to 6 h and were then supplied with fresh DMEM complete containing $0.4 \mu\text{g/ml}$ puromycin. As soon as possible, cells were expanded to a T25 flask and $1 \mu\text{g/ml}$ puromycin was added. Cells were expanded and amount of selection antibiotic was increased up to $2\text{-}5 \mu\text{g/ml}$ puromycin.

10.7.4 Electroporation

Monolayer of cells were washed once with PBS, trypsinized and sheared by pipetting up and down through a 1 ml tip to get single-cell suspensions. After washing once with DMEM complete (5 min at 7, 700 rpm) and once with 50 ml PBS (5 min at 700 rpm) Huh7-Lunet cells were resuspended at 1×10^7 cells per ml in cytomix, whereas Huh7.5 cells were resuspended at 1.5×10^6 cells per ml. Unless otherwise stated, 5-10 μg of in vitro transcribed RNA were mixed with $400 \mu\text{l}$ cell suspension and electroporated with a Gene Pulser system (Bio-Rad®, Munich) in a cuvette with a gap width of 0.4 cm (Bio-Rad) at $960 \mu\text{F}$ and 270 V. Cells were immediately transferred to DMEM complete and seeded as required for the indicated experiment.

10.7.5 TCID₅₀ by VIRAPUR (Virus Purification)

The procedure is performed to determine the infectious titer of any virus which can cause cytopathic effects (CPE) in tissue culture over a reasonable period of 5 to 20 days while cells in culture remain viable. This procedure is performed to quantify how much infectious virus is in a preparation by visual inspection of cell morphology or cytopathic effect (CPE). Not all virus types cause CPE in tissue culture, and the cell line and virus must be carefully matched in order to see a cytopathic effect. The TCID₅₀ is determined in replicate cultures of serial dilutions of the virus sample. The titer of the virus stock is expressed as the TCID₅₀ which can be calculated using a statistical Excel program and is more accurate than a negative end-point. Previous to infection,

prepare 48-well dishes by seeding each well with 710^4 cells in 0.5ml DMEM plus 7.5% fetal bovine serum, 4mM glutamine, antibiotics. Alternatively another cell density may be required, based on the cell line required for viral growth. On the day of infection, make dilutions of virus sample in PBS. Make a series of dilutions at 1:10 of the original virus sample. Fill first tube in series with 2 ml of PBS, fill the remaining 6 tubes in series with 1.8 ml of PBS. Vortex virus sample, transfer $20\mu\text{l}$ of virus to first tube, vortex, discard tip. With a new tip, transfer $200\mu\text{l}$ of first dilution to next tube. Vortex, discard tip. Repeat series of dilutions through the last tube. Calculate the TCID₅₀ titer using the Excel spreadsheet available for download from Yale School of Medicine at the following url: www.med.yale.edu/micropath/pdf/Infectivity%20calculator.xls or in our case use Excel file by Dr. Marco Binder available for laboratory users.

10.7.6 Determination of virus titres in cell culture supernatants and cell lysates

Virus titers in cell culture supernatants were determined as described in a publication of Lindenbach and coworkers [5] with slight modifications. Huh7.5 target cells were seeded at a density of 1.110^4 cells/well in 96-well-plate in a total volume of $200\mu\text{l}$ DMEM complete. Twenty-four hours later, serial dilutions of virus supernatant were added with 8 wells per dilution. Three days later, cells were washed with PBS, fixed for 20 min with ice-cold methanol at -20°C , washed once with PBS. After three washes with PBS, NS3 was detected with $30\mu\text{l}/96$ -well of a 1:100 dilution of antibody 2E3 or NS3-49 1:1000 in PBS for 1 h at RT or o/n at 4°C . Cells were washed three times with PBS and bound primary antibodies were detected by incubation with $30\mu\text{l}/96$ -well peroxidase conjugated anti-mouse or rabbit antibody diluted 1:200/500 in PBS. After 1 h incubation at RT cells were washed three times with PBS and peroxidase activity was detected by using $30\mu\text{l}/96$ -well of a home made TCID₅₀ see 10.7.5 detection substrate (1.5 ml solution 1 plus 5 ml solution 2 and $20\mu\text{l}$ H₂O₂; see Chemicals Table at section 9). Virus titers (50% tissue culture infective dose [TCID₅₀/ml]) were calculated based on the method of Spearman and Kärber. Intracellular infectivity assays as determined with freeze-thaw lysates of transfected cells were at 48 h post transfection. Huh7-Lunet cells were extensively washed with PBS, scraped off the plate and centrifuged for 5 min at 700xg. Cell pellets were resuspended in 1 ml of DMEM containing 5% FCS and subjected to three cycles of freezing and thawing using liquid nitrogen and a thermo block set to 37°C . Samples were then centrifuged at 10,000Xg for 10 min at 4°C to remove cell debris, and cell-associated infectivity was determined by TCID50 assay. Culture supernatants from transfected cells were treated in the same way and infectivity was determined in parallel. Importantly, establishment of 4 h post electroporation comes as a result of

translation of transfected RNA and indicates transfection efficiency. This is why 4 h time point is used in the present study as a threshold for transfection efficiency.

10.7.7 Luciferase viral reporter assays

Quantification of luciferase reporter activity (Firefly or Renilla-Luciferase) was used to determine transient HCV RNA replication of subgenomic or full-length virus constructs. Transfected or infected cells were harvested at the appropriate time points (see individual experiment description) by washing once with PBS and addition of ice-cold luciferase lysis buffer (350 μ l per 6-well, 200 μ l per 12-well and 100 μ l per 24-well).

(A) **Firefly-Luciferase assay.** For measurement of cells out of 6 or 12-wells 150 or 50 μ l lysate were mixed with 360 μ l luciferase assay buffer and, after addition of 200 μ l of luciferin substrate solution, measured for 20 sec in a luminometer (Lumat LB9507®; Berthold, Freiburg, Germany).

(B) **Renilla-Luciferase assay.** For measurement of cells out of 12 or 24-wells 20 μ l lysate were mixed with 100 μ l Renilla-Luciferase substrate solution and measured for 10 sec in a luminometer (Lumat LB9507®; Berthold, Freiburg, Germany). Cells in 24-well plates measured after addition of 400 μ l Renilla-Luciferase substrate solution for 10 sec in a plate luminometer (Mithras LB 940®, Berthold Technologies, Freiburg, Germany). Each well was measured in duplicates. Kinetics of replication were determined by normalizing the relative light units (RLU) of the different time points to the respective 4 h value. Established 4 h post electroporation is the threshold for HCV infection to be stabilized in the cells, this is why we use 4 h post-electroporation as the normalizing value for every assay containing HCV electroporation. If replication of viral constructs was compared in cells treated with different siRNAs then replication was normalized to cells treated with the negative control siRNA, or with Hiperfect®(unique blend of cationic and neutral lipids that enables effective siRNA uptake and efficient release of siRNA inside cells, resulting in high gene knockdown even when using low siRNA concentrations) from QIAGEN®.

10.7.8 Transcomplementation assay

Huh7-Lunet cells were co-transfected with 5 μ g of Jc1 genomes and 0.5 μ g of helper RNAs containing a Renilla luciferase (RLuc) reporter gene (corresponding to a 1:0.1 molar ratio, respectively). Electroporated cells were resuspended in 20 ml culture medium. Two ml aliquots were seeded per well of a 6-well plate and replication was determined by measuring luciferase activity at 4, 24, 48 and 72 h post-electroporation. Transient replication of helper RNAs was determined by luciferase assay at 4, 24, 48 and 72 h after

electroporation. Values obtained 4 h post electroporation were used to determine the transfection efficiency. Supernatants were harvested 24, 48 and 72 h after electroporation and concentrated three times by using Amicon columns (Millipore®), Schwalbach) according to the instructions of the manufacturer. Release of infectious particles from co-transfected cells was determined by TCID₅₀ assay by using the concentrated culture supernatants. Replication of trans-packaged subgenomic helper RNA was determined by luciferase assay performed with lysates of Huh 7.5 cells that had been inoculated with the concentrated culture supernatants of co-transfected cells. See generated cell line 10.7.2 and Figure 10.1.

10.8 Drug addition experiments

10.8.1 Dose-response assay using stable replicon cell lines and JCR2a reporter virus

For dose-response LucUbiNeo_Con1ET, using stable replicon cells, LucUbiNeo_JFH1, were seeded into a 12-well plate at a density of 4×10^4 cells/well. One day later, Sofosbuvir (SOF) or BMS-790052 (DCV) was added at different concentrations. As mock control, DMSO was added according to the highest inhibitor concentration used in the assay. After 72h of treatment, cells were washed, lysed and analyzed by luciferase activity using Luminometer measurement. EC₅₀ and EC₉₀ values were calculated by using GraphPad Prism ®(version 5.03). For dose-response assays using reporter virus JcR2a, Huh7 cells were seeded one day prior to infection in a 12-well culture dish at a density of 4×10^4 cells/well. Eight hours post infection (five TCID₅₀/cell) cells were incubated with indicated concentrations. As mock control, DMSO was added according to the highest inhibitor concentration used in the assay. After 72h of treatment, cells were washed, lysed and analyzed by luciferase activity assay, EC₅₀ and EC₉₀ were calculated.

10.8.2 Full-length reporter virus JCR2a kinetics after DCV or SOF treatment

Huh7 cells transfected by electroporation with in vitro transcribed RNA of HCV JCR2a full-length reporter virus were seeded in 12-well culture plates. Two days later DMSO, SOF or DCV was added at a concentration of $5 \times EC_{90}$. Cell lysates were harvested after 0, 10, 24 and 48h of treatment and analyzed by luciferase activity assay. Huh7.5 FLuc cells were seeded in a 12-well culture plate at a density of 1×10^5 cells/well. One day later they were infected with JCR2a virus (1 TCID₅₀/ml) for 48h before DMSO,

SOF or DCV was added at a concentration of $5XEC_{50}$. After 6, 12, 24 and 48h cell lysates were harvested and used for luciferase activity assay. Note that in this case Renilla Luciferase activity as well as firefly luciferase activity was determined to study virus replication and cell growth, respectively.

10.8.3 Full-length reporter virus JCR2a kinetics and DCV pre-treatment

For replication kinetics of reporter virus JcR-2a (pFK_i389RLuc2A_Core-3-Jc1), Huh7.5 cells were seeded into a 12-well culture plate at a density of $1X10^4$ cells/well. One day later cells were infected with JCR2a with one $TCID_{50}$ /cell. After 48h inoculation, medium was replaced by fresh medium. In case post-treatment, cells were subsequently treated with DCV, SOF or DMSO (mock control). In case of pre-treatment, cells were additionally incubated in DCV or SOF containing medium ($50X EC_{90}$) for 2h prior to inoculation with JCR2a. Directly prior to infection, medium was replaced by fresh DMEM. Forty-eight hours post infection, inhibitor was added. After 6, 12, 24 and 48h of treatment cells were washed, fixed and analyzed by luciferase activity assay.

10.9 Protein analysis

10.9.1 Proteinase K Protection Assay

Protease digestion assay. A membrane protection assay was performed as previously indicated [153–155]. For analysis of proteins expressed in cells, transfected Huh 7.5 cells, transfected with JFH1 or Jc1 RNA. The post-nuclear supernatants or samples obtained from *in vitro* synthesis were divided into three portions. One portion received no treatment. The second portion was treated with Proteinase K $150\mu\text{g}/\text{ml}$. The third portion was solubilized with a final concentration of 1% Triton X-100 before Proteinase K treatment. After incubation on ice for 1h, samples were analyzed by SDS-PAGE followed by Western blotting.

10.9.2 SDS-Polyacrylamide-Gel-Electrophoresis (SDS-PAGE)

The cells were washed in PBS and lysed by addition of SDS-PAGE sample buffer. The viscosity of the samples was reduced by sonication in a cup-horn Sonifier (Brandson 450®), which shears the genomic DNA. The sample was then heated to 95°C for 3 min and cooled to RT. The polyacrylamide gels were prepared according to standard protocols and gel electrophoresis was carried out at constant current of 200V for 3-4h

(15x15cm gels). Pre-stained protein markers (New England Biolabs ®) were used as molecular size marker.

10.9.3 Western Blot

Following gel electrophoresis the proteins were transferred to PVDF membranes using a semidry blotter 2 (BioRad) for 90 min at a constant current of 1mA/cm . The membrane was blocked with blocking buffer (5% milk powder in PBS 0.5% Tween20 (PBST)) for 1h at RT or overnight at 4 °C. The membrane was incubated with the primary antibody diluted in blocking buffer for 1h at RT or overnight at 4 °C followed by three washes for 10 min with PBST. Similarly the secondary antibody diluted in blocking buffer was incubated for 60 minutes and washed thrice with PBST. The chemiluminescence signal was revealed using ECL Home Made Kit ® according to the instructions and detected by INTAS machine.

10.9.4 Paraformaldehyde oligomerization

Formaldehyde solution was obtained by dissolving 0.4% to 4% paraformaldehyde Fisher Scientific in PBS for 2 h at 80 °C. The solution was filtered in 0.22 µm filters, stored in the dark at RT and discarded after 4 weeks. For cross-linking, Lunet cells were pelleted in a 50 ml reaction tube, resuspended in PBS and counted. Cells were centrifuged again and resuspended to 1×10^7 cells/ml in formaldehyde solution. Cells were incubated with mild agitation for 7 min at RT and then pelleted at 1800xg and RT for 3 min, resulting in 10 minutes exposure to formaldehyde. The supernatant was removed and the reaction was quenched with 0.5 ml ice-cold 1.25 M glycine/ PBS. Cells were transferred to a smaller tube, spun, washed once in 1.25 M glycine/PBS and lysed in 1 ml RIPA buffer (50 mM Tris HCl, pH 8.0, 150 mM sodium chloride, 1% NP40, 0.5% sodium deoxycholate, 0.1% SDS, 1 mM EDTA, protease inhibitors (Complete mini, EDTA-free, Roche Diagnostics)) per 1×10^8 cells for 60 minute on ice. Incubation for 20 min at 65 °C or 99°C. Lysates were spun for 30 minutes at 20000 g and 4 °C to remove insoluble debris. The supernatant was either used directly or stored at 80 °C. Control cells were treated exactly the same way, except that they were resuspended in PBS instead of formaldehyde solution. When platelets were used for cross-linking, 1.5×10^9 cells were resuspended in 10 ml formaldehyde solution and lysed in 1 ml RIPA buffer. Protocol taken from [156].

10.9.5 BRET assay

293 T cells were seeded in a 24-well plate (1.5×10^5 cells/well). Day after, transfected with the YFP-construct (500ng) together with the Renilla Luc construct (500ng). Remove medium from cells, then added $500 \mu\text{l}$ /well of fresh DMEM at least 30 min before transfection, return cells to incubator. In the meanwhile prepare DNA mixtures: JetPEI transfection reagent PolyPlus Transfection® standard protocol was used. DNA/transfectant mixture was added to a 150mM NaCl solution for a final volume of $50 \mu\text{l}$ /transfection. The mix was vortexed and incubated for 20 minutes, then added to the wells in a drop-wise manner. The day after cells are checked for transfection efficiency (70-80% cells expresses), the cells are washed with 1X PBS. The plate then is read by a spectrometer for YFP expression before adding RLuc substrate (necessary for Saturation Curves). Add $10 \mu\text{l}$ /well of 1:20 dilution of Coelenterezine (1:200 final dilution), swirl plate gently, check for absence of visible air bubbles. Incubate in the dark for 5 min to 40 min at RT. Read the plate at Spectrometer (5 min to 40 min post-coelenterezine addition by measuring YFP emission and RLuc emission (respectively 535 and 485 nm; 0.5" each channel). Finally calculate data as follows in Figure 11.26, where long-wavelength is YFP signal and short-wavelength is RLuc signal. The background is the same ratio calculated in wells were only the RLuc-tagged protein at the same concentration was transfected.

$$\text{BRET signal (or BRET ratio)} = \frac{\text{'long-wavelength emission from interacting proteins'}}{\text{'short-wavelength emission from interacting proteins'}} - \frac{\text{'background long-wavelength emission'}}{\text{'background short-wavelength emission'}}$$

FIGURE 10.2: BRET calculation method

Taken from [157].

10.10 Imaging

10.10.1 Immunofluorescence

Transfected Huh7-Lunet cells were seeded into 24 well-plates containing glass coverslips. Seventy two hours after electroporation, cells were washed twice with PBS, fixed with 4% PFA in 150 mM sodium cacodylate buffer [pH 7.5] for 15 min at RT and permeabilized with digitonine ($50 \mu\text{g}/\text{ml}$) for 5 min at RT. Permeabilized cells were washed twice with PBS and blocked with PBS containing 5% (w/v) bovine serum albumine for 30 min at RT. Viral proteins were detected with specific primary antibodies see Table 9.1. After 1 h at RT, cells were washed three times with PBS and incubated with a 1:1,000 dilution

of Alexa 488, 546 or 647- conjugated secondary antibody (Invitrogen ®, Molecular Probes), shown in Antibodies Table 9.1 in PBS 5% BSA for 1 h in the dark.

10.11 Computational models and simulations

All proteins structures were downloaded from Protein Data Bank and completed with MOE software ®. Maestro software ® was used for Protein Preparation, System Builder and Molecular Dynamics (MD) (using Desmond tool). All proteins have energy minimised and analysis of its structure was performed previously to ensure analysis. For NS5A protein, PDB number: 1ZH1, clam like structure taken from [38].

10.11.1 Proline analysis in NS5A structure

Analysis of Proline residues located in the linker structures of NS5A protein were analysed using MOE. The missing residues connecting linker AH-DI were added and energy minimized with AMBER99 force field 0.001 gradient. This procedure was applied to all the Proline residues present in the different linkers. Following analysis using MOE was performed to measure and predict conformational changes in NS5A structure. See Table 11.1.

Linkers:

- AH-DI: 29-PKLPGLP-35
- DIa-DIb: 97-QCAPKPPT-104
- DI-DII: 189-PCEPEP-194

To explore the role of Proline residues in the linkers, we selected the residues and explore the interactions within NS5A structure by visualization with MOE. Further, we wanted to investigate whether they have a role in the binding of DCV or NS5A interactions which might be important for the drug activity. Using MOE tool, DCV interacting residues were analysed by visualisation.

10.11.2 Proline analysis in NS5A structure and DCV interaction

Prolines identified after site-directed mutagenesis of Proline residues in the linker connection between amphipathic helix and domain Ia and domain Ib were situated in NS5A structure from Nettles et al. 2014 [1]. Later, we mutated *in silico* to the corresponding

amino acid and explore the different conformation of NS5A structure itself and interaction with DCV. We used Molecular Dynamics (conditions mentioned in 10.11.2), to analyse in time, the conformational changes of DCV with the different Proline residues.

- Protein Preparation Wizard: for protein preparation
- System Builder:
 - a) Solvent model: TIP3P
 - b) Box shape: Cubic, different distances used to minimize volume for dynamics (distances, very close to the membrane a=5; angles 90 degrees all).
 - c) Minimize volume: Force filed: OPLS 2005
- Molecular dynamics:
 - a) Simulation time: 300ns;
 - b) Frames: 625, Trajectory: 320
 - c) Energy: 16Relaxation of model before simulation
Advanced: seed: random

10.11.2.1 Analysis of interaction with DCV

Docking with *GLIDE*® The analysis was performed by re-docking DCV into NS5A structure with the correspondent Proline mutation made 11.1. To select the best conformation given by the docking program, i.e minimum energy of the protein-ligand complex and maximum binding affinity should be selected for molecular dynamics study. Furthermore, MD was performed on selected poses to explore the stability of the conformation and the possible changes in the DCV interaction sites.

Molecular Dynamics After docking DCV to the selected pose into the NS5A dimer structure with the Proline mutations, we run Desmond MD, to explore the different conformations DCV might take due to the Proline mutation. The MD conditions were the same as established for all studies 10.11.2.

10.11.3 Amphipathic helix studies on POPE membrane

To start up with the analysis of the systems, protein preparation was performed using Protein Wizard in Maestro (removal of water molecules and adding hydrogen missing atoms). Considering a temperature of 300K a pH of 7 and salt concentration of 0.1M.

The energy was minimized and then proceeded with the System Builder in Maestro, where the membrane was loaded from workspace. Membrane used was large POPE bilayer with 340 lipids downloaded from the following url: <http://people.ucalgary.ca/~tieleman/download.html>.

10.11.4 Molecular dynamics on Amphipatic Helix (AH) and membrane studies

The previous set up was used to run Desmond set up of the system, then, the output file was used to run Desmond Molecular Dynamics. The structure of amphipatic helix was manually placed either horizontally or vertically from the membrane, both conformations were minimize at MOE, prepared by Protein Preparation Wizard and analysed by molecular dynamics from Desmond in MAESTRO. The following parameters were used:

- Protein Preparation Wizard: for protein preparation
- System Builder:
 - a) Solvent model: TIP3P
 - b) Box shape: Cubic, different distances used to minimize volume for dynamics (distances, very close to the membrane a=1, b=1, c=1; angles 90 degrees all).
 - c) Minimize volume: Force field: OPLS 2005
- Molecular dynamics:
 - a) Simulation time: 200 ns or 500 ns (horizontal)
 - b) Frames: 625, Trajectory: 320
 - c) Energy: 16Relaxation of model before simulation
Advanced: seed: random

Part III

Results

Chapter 11

Experimental Results

Some of the big remaining questions regarding HCV field, are the precise mode of action of the NS5A inhibitors, other types of DAAs have been widely studied and have now, a well described mechanisms of action. However, NS5A is a multifunctional protein, that is involved in many key points of HCV life cycle, as the full picture of all the activities NS5A performs is not yet finished, the mechanism behind NS5A inhibitors is not fully understood. In recent years, many and joint efforts have been made in getting a better and clearer picture of the mode of action. The present study aims to contribute to the full picture in a detail manner to elucidate the NS5A inhibitors mode of action by using the best of two approaches to research, experimentally and computationally.

Furthermore, we wanted to focus on aspects that have not been fully studied on the structure of NS5A, where important binding and interaction sites are located. Some studies have looked into this aspect trying to reveal what are the key aspects on NS5A structure that could explain the mechanism of action of the inhibitors [1, 117, 158].

First, we wanted to elucidate the importance of Proline residues located in the linker structures of NS5A and their impact in HCV replication and infection. Additionally, we evaluated the effect of this mutations in relation with DCV inhibitor *in silico*, see Computational Results section 12. Second, we evaluated the role of DCV inhibitor during the assembly process of HCV viral particles. Third, we look at the role of the Amphipathic helix of NS5A in membrane interaction and thus, the impact of DCV-membrane interaction *in silico*. We briefly look at the oligomerization state of NS5A to look further into the multifunctionality of the protein. Lastly, we put together the results to describe the mechanism of action of NS5A inhibitor DCV.

The following chapter describes the experimental results and the next chapter describes the computational results in section 12. Later in the discussion, these results are commented and discussed as one topic itself, as the purpose of this study was to use both tools to further elucidate and understand the mechanism of action of NS5A inhibitors.

11.1 Key role of NS5A Proline residues

To further understand the mode of action of DCV, we performed studies together with collaborators (Cristoph Combet, at Lyon University) on the role of Proline residues in the linker structures connecting the different domains of NS5A, see Appendix A.1. The amphipatic helix is connected to Domain I via a Proline rich linker (linker AH-DI), which promotes membrane association through an interaction of the AH with the membrane. This linker might be key, not only for the binding of NS5A protein to the cellular membrane but additionally the binding of DCV. Because as mentioned in the introduction, it contains most of the resistance mutations and we do not have structural data on this linker. Thus, we decided to study Proline residues in this linker which confer conformational changes that will allow us to know the key role of the Proline residues maintaining the structure of such linker in a functional position. The next linker is the one between Domain I subdomain *a* connecting to Domain I subdomain *b*, (DIa-DIb), the Prolines contained in this linker will maintain the structure of Domain I in position regarding the membrane and the inhibitor binding, which is why it was also chosen for mutational analysis. Finally, Domain I linker connecting Domain II (DI-DII), this linker was studied because of its relevant interactions with PKR, PI3K, as well as NS5B, which might be of importance keeping NS5A structure and function see Figure 11.1.

Domain I of NS5A is required for RNA replication, protein and membrane interaction, its crystal structure is solved by the PDB entry: 1ZH1 and 3FQQ see Figure 2.7. NMR structure is also solved for AH is solved in PDB: 1R7G, see Figure 2.5. However there is no information available for the linker connecting AH and DI, where most of the resistance mutations are clustering and where NS5A associates to the membrane [60, 129, 130]. Therefore the first thing to perform was to directly target Proline residues in the linkers via site-directed mutagenesis. The linker sequences are the following:

Linkers:

- AH-DI: 29-PKLPGLP-35
- DIa-DIb: 97-QCAPKPPT-104
- DI-DII: 189-PCEPEP-194

11.1.1 Proline residues in linker structures are key for HCV replication and infection

We performed site-directed mutagenesis to specific conserved Proline residues within the linkers as you can see in the table 11.1. Cloning strategy in this fragment Nsil/SanDI by double PCR was used to introduce the single point mutations in positions: P29, P32, P35, P100, P102, P103. The next cloning strategy was using a digest vector to generate 2 fragments vector Luc-JcR2A, together with 1) Nsil/BsiWI and 2) SanDI/BsiWI, bind together by a triple ligation, this method was used for Proline residues P189, 192, and 194; for further details see section 10. Later, the RNA from these mutants was electroporated into Lunet cells and collected at different timepoints. Furthermore the supernatant was used to infect Huh 7.5 cells and the read out was Renilla Luciferase (RLuc) as the constructs contain the reporter gene, as negative control we used Δ GDD, which is deficient in the nucleotidyl transfer reaction during HCV translation. As a positive control of transfection efficiency we used the 4 h normalization value. The following table contains the mutations made for each Proline residue within the linker structures.

TABLE 11.1: Site directed mutagenesis of conserved Prolines to Alanine (Ala), Glycine (Gly) or a Valine (Val)

AH-DI linker			
P29	Ala	Gly	Val
P32	Ala	Gly	Val
P35	Ala	Gly	Val
DIa-DIb			
P100	Ala	Gly	Val
P102	Ala	Gly	Val
P103	Ala	Gly	Val
DI-DII			
P189	Ala	Gly	Val
P192	Ala	Gly	Val
P194	Ala	Gly	Val

The site directed mutagenesis of conserved Prolines was performed to Glycine (G), to mimic the different conformations of Proline (P) *cis-trans* isomer, which would in turn have a deleterious effect that would indicate a strong structural role of that Proline residue. Mutations to Alanine (A), to mimic the *cis-trans* isomer of Proline, which if there is no *cis-trans* isomerisation would mean that such mutant is functional. At last, mutations to Valine (V) has no effect, means the Proline residue has no essential

role. The next Figure 11.1 contains the mutations made to each Proline residue in the linkers, showing the structure of Domain I of NS5A protein as a monomer. The linker connections are located in between AH-DI, DI-DII, and DII-DIII, with the correspondent sequence, where each sequence is shown in colour coding according to the correspondent linker structure dividing each of the segments in Domain I.

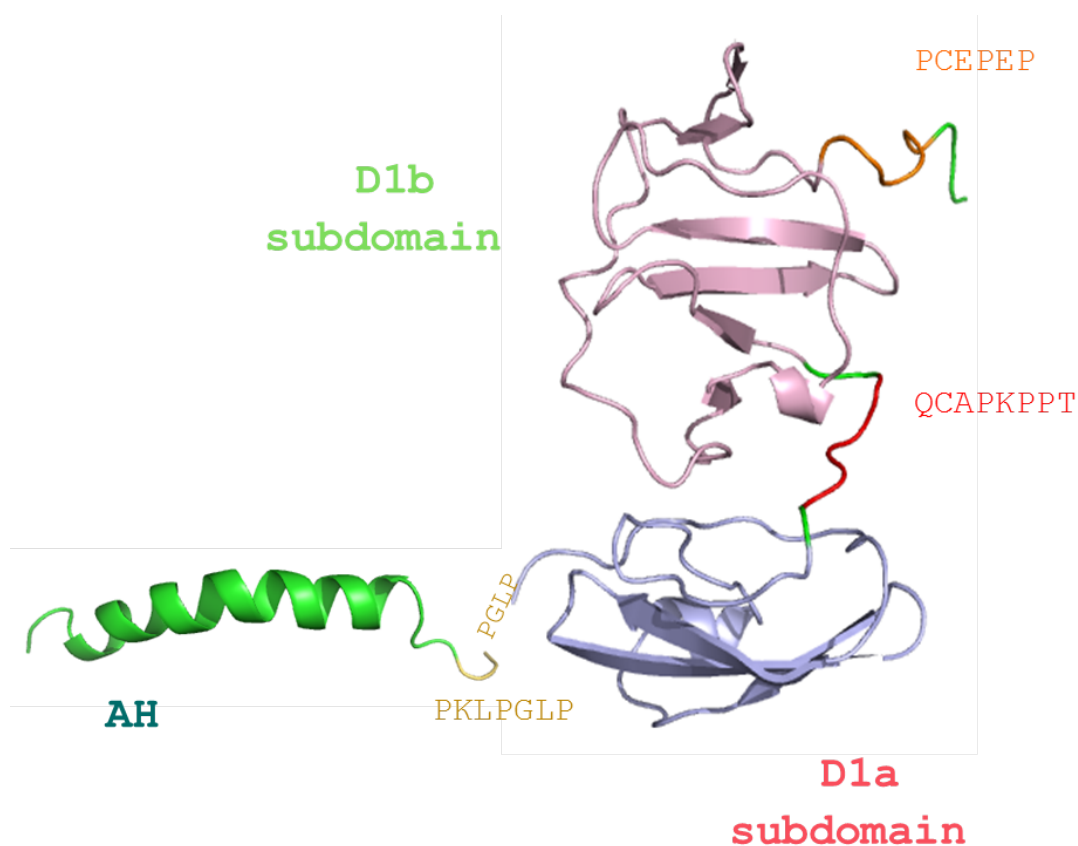


FIGURE 11.1: Domain I of NS5A with linker connections Amphipathic helix (AH), Domain I subdomains *a* and *b*. Sequences containing Proline residues are also shown, in line with the linker structure dividing each part. Courtesy by Critoph Combet.

After transfecting the HCV RNA via electroporation into the Lunet cells, we harvested the cells at 24, 48 and 72 hours post-infection (hpi), we collected the supernatant. The following Figure 11.2 shows first read out by RLuc, of the replication results of the Proline residues located at the linker AH-DI. In Figure 11.2 panel A, AH-DI linker shows a complete inhibition of replication with the exception of P29G, P35G and P35V. No inhibitory effect during replication was observed in P35A, as expected P35A mutation has a comparable effect to JCR2a wt (genotype 2a wildtype), which was used as a HCV replicon positive control. The supernatant collected from the replication samples was used to further infect Huh 7.5 cells, then RLuc was measured. In the case of Figure panel B 11.2, where the same linker is shown, where the mutations seem to have a defective phenotype during assembly/release of viral particles.

The same procedure was performed for the DIa-DIb linker and DI-DII. Where Lunet cells were transfected with the following Proline mutations to Glycine, Alanine or Valine accordingly. Mutations in linker DIa-DIb: P100A, P100G and P102A show complete inhibition of the HCV replication, as compared to the negative control (Δ GDD). As for linker DI-DII, mutations did not show any effect, as the replication and infection was as wt (JCR 2a, positive control). Mutations P194A and P194V, did not show replication or particle production, resulting in essential Proline residue at the site to achieve NS5A functionality. However, the rest of the mutations in both linkers were able to replicate as the wt values. When infection was analyzed by using the supernatant and infecting Huh 7.5 cells, the mutants showed the same pattern as HCV replication, with or without any additional effect on the viral particle production as compared to the wt, see Figures 11.3 and 11.4.

Some of these Proline residues showed a critical role when mutated to another amino acid (G, A or V), showing that their role in maintaining structure by *cis-trans* isomerisation or by changes in the conformation due to the different interaction pattern. These results give a detail perspective on how the linkers on DI of NS5A are key for the functionality of the whole protein. In addition, the changes in the conformation due to the *cis-trans* isomerisation can be critical to HCV life cycle as shown in the deleterious effect on replication and infection of viral particles. Moreover, the linker structures are known to be essential for NS5A inhibitors binding site, which makes these results key to understand how Proline residues can affect NS5A and thus, the mechanism of action of NS5A inhibitors.

Along the same lines, Proline mutations were shown to affect each of the linker structures, due to the change in the amino acid conformation and interaction pattern. In the following Figures, each linker is shown with the correspondent Proline mutations. Renilla Luciferase (RLuc) was normalized to 4 hpi in the replication assay, positive control JCR2a (wildtype HCV virus) and as negative control Δ GDD, which is the motif of HCV NS5B RNA-dependent RNA polymerase. Luciferase activity at 4 hours after electroporation correlates with the translation of input transcripts prior to onset of replication and subsequent time points were normalized to 4hpe signal to account for electroporation efficiency.

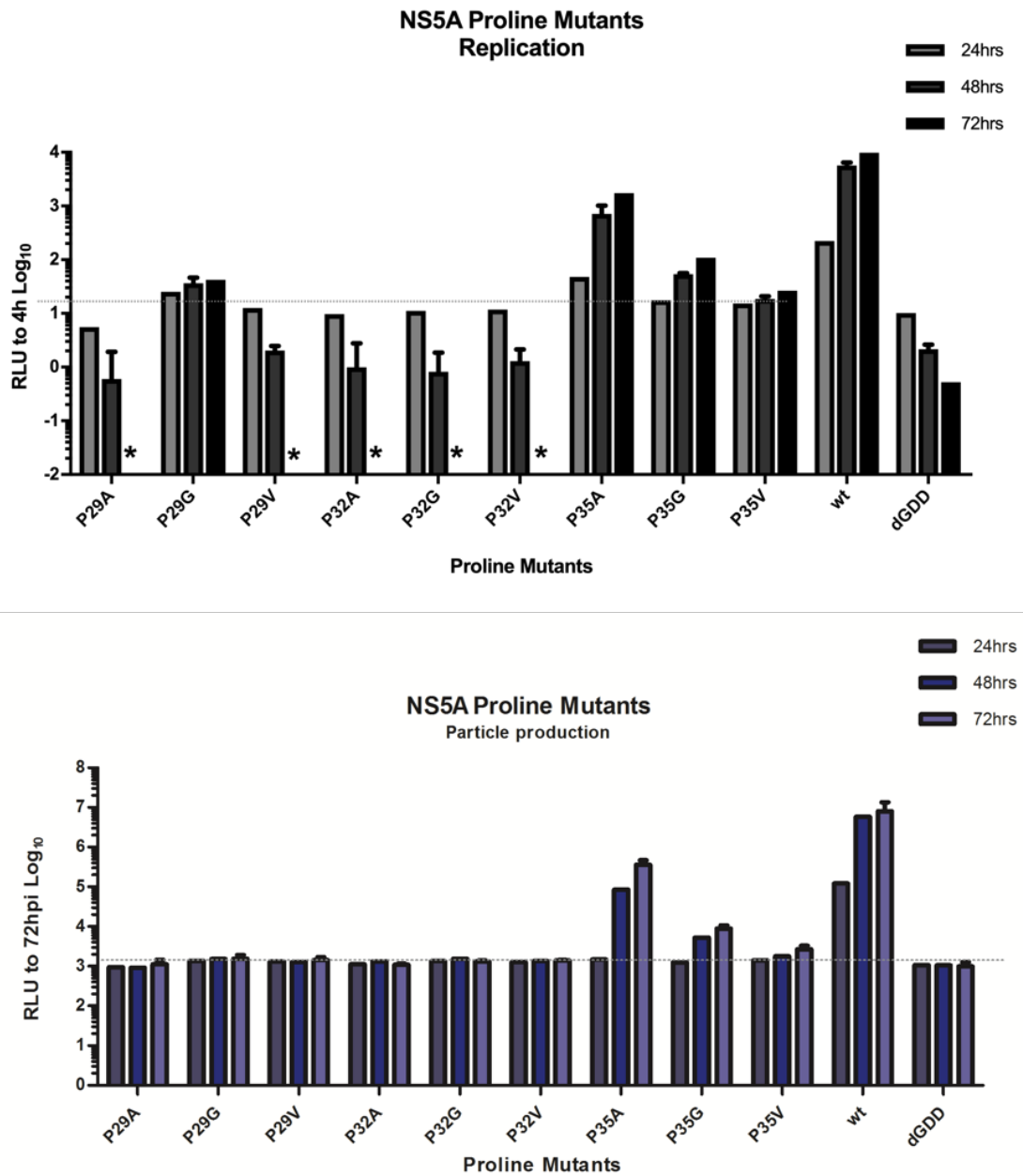


FIGURE 11.2: Proline mutations on linker AH-DI effects on HCV life cycle

P29-35V showed complete inhibition of replication, as compared to the negative control (Δ GDD, which is the motif of HCV NS5B RNA-dependent RNA polymerase). Mutations P29G, P35G, and P35V were able to replicate however their replication was strongly reduced as compared to WT. No inhibitory effect during replication was observed for P35A mutant. As expected P35A mutation had a comparable replication and particle production kinetics to WT, panels A and B, respectively. Marked with *, samples that are below detection.

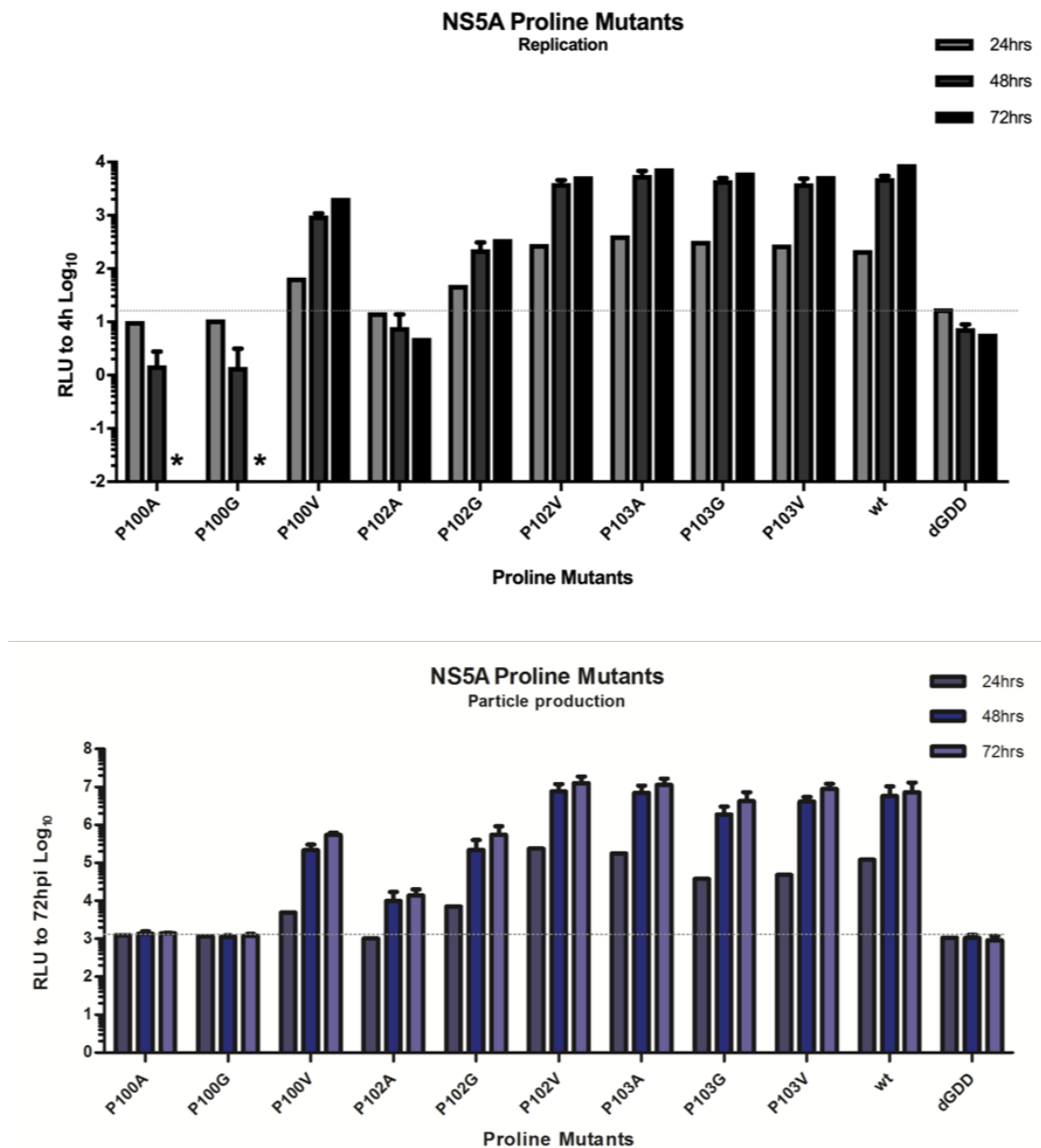


FIGURE 11.3: Proline mutations on linker DIa-DIb effects on HCV life cycle. Mutations at P100A, P100G and P102A, showed complete inhibition of replication, as compared to the negative control. Whereas the rest of the mutants in this linker were able to replicate as WT. The rest of the mutants did not show any additional effect on particle production when compared to WT. Marked with *, samples that are below detection.

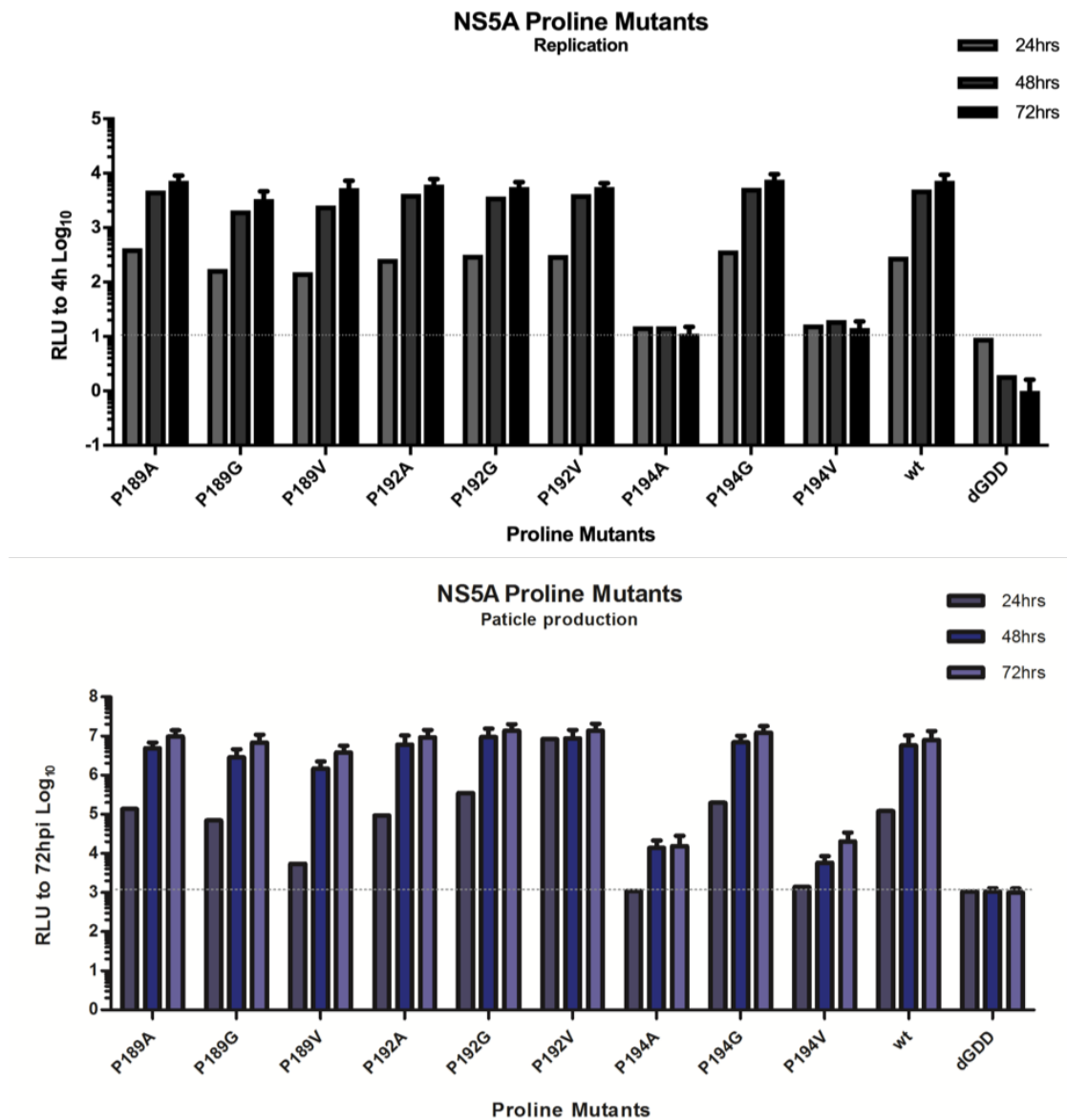


FIGURE 11.4: Proline mutations on linker DI-DII effects on HCV life cycle. Mutations within this linker did not show any effect on replication and particle production, except for P194A and P194V mutants, which did not replicate and therefore there was no particle production, when compared to negative control Δ GDD.

Results of this experiment show that in each of the 3 linkers at least one Proline is crucial for replication (P29 P32, P100 P102 and P194). Moreover, the crucial Proline residues seem to be involved in *cis-trans* isomerisation. Together, these data indicate that NS5A domain 1 changes conformation, which is needed to acquire precise conformation to be activated by isomerisation to achieve its function, the crystal structures of domain 1 are only one picture of the changes in the conformation. Other conformational changes can be taking place in:

- between AH and domain 1, which could be the most crucial, taking into account the membrane proximity, reinforced by location of resistant mutations.
- between subdomains 1a and 1b, which might involve the opening of D1a-D1b probably by domain swapping in dimers.
- between domain 1 and 2, which might be crucial for host interactions.

This leads to the involvement of *cis-trans* Proline isomerase as many have shown before [159, 160]. Hence, these results show the role of key Proline residues in the linker structures of NS5A, which might have a role maintaining not only in HCV replication or infection, but additionally the binding or interaction site with DCV. Computational studies to explore and visualize the conformational changes of the NS5A protein and the DCV binding site could elucidate the role of this key Proline residues, to further improve or develop new antiviral agents. In the section 12, we explore this possibilities and analyse the Molecular Dynamics of NS5A inhibitor DCV interactions with NS5A dimer structure.

Furthermore, inhibitors targeting NS5A affect HCV replication by inhibiting conformational changes in NS5A protein or protein complex formation that occur in the context of HCV polyprotein expression and in the replication compartment formation [161]. Others have observed the effect of DCV, blocking HCV replication by preventing formation of the membranous web, which was not linked to an inhibition of phosphatidylinositol-4 kinase III α [118].

However NS5A protein has a key role during the assembly process. As it is proposed by Zayas *et al* [162], where a highly conserved basic cluster (BC) of Domain III was found to play a key role during the assembly of viral particles. During the assembly process of HCV, NS5A plays several key roles [163, 164]:

- it interacts with core protein via NS5A DIII [26, 165].
- NS5A is recruited to cLDs where core protein accumulates [26, 165, 166].

- assembly requires the phosphorylation of a serine residue in NS5A DIII by casein kinase II α [51].
- NS5A facilitates the association of core protein with the viral RNA genome [165].
- NS5A interacts with the p7-NS2 complex that is required for the envelopment of the HCV particles [167].
- NS5A also interacts with apolipoprotein E that is incorporated into the virion and with Annexin A2, which is a host cell membrane sorting protein enhancing HCV assembly [20, 43, 168–171].

Consequently, assembly of HCV particles requires a spatio-temporally coordinated association of the replicase, NS3 helicase and NS5A together with the Core protein allow packaging of the RNA genome into the virion. To determine whether DCV, NS5A inhibitor has an effect at some point during the assembly process we first wanted to ruled out the specific effect on assembly by using another inhibitor of NS5B protein, Sofosbuvir. The results from the experiment will show the specific effect of NS5A inhibitor during assembly as an inhibition of NS5A protein activity.

11.2 Effect of Sofosbuvir and Daclatasvir treatment

We started with the titration of both drugs DCV and SOF, in order to have both EC₅₀s that could correlate to each other and have the precise drug concentration at which both drugs inhibit HCV infection. We first electroporated HCV RNA from the JCR2a (wt) genotype in Lunet cells and as a control included untransfected cells (MK cells). The drugs were added 12 hours post electroporation (hpe) and 24 hpe. We recover the supernatant at 24, 48 and 72 hours post infection (hpi), this means when we infected the cells using the supernatant of the eletroporated cells, for more details see diagram on Appendix A.2. We lysed the plates and store them at -20 °C, this plate was further used to perform a Renilla Luciferase (RLuc) assay. The supernatant was used to infect Huh7.5 cells where we also included MK cells. After 72 hpi, we harvested the cells and perform RLuc assay. The results of the plate reader were all normalised to 24 hpi. Results gave us the optimal concentration to use of SOF with comparable effect to DCV for further experiments, see Figure 11.5 and 11.6.

Figure 11.5 shows the EC₅₀ values for DCV are extremely low, which gives NS5A inhibitor its high antiviral potency. A decline in viral protein upon treatment was observed for replication and reinfection measurements, in comparison to the mock cells. When

using SOF Figure 11.6, we observed a faster effect of the drug upon infection and replication compared to Mock cells and DCV treatment. In the corresponding tables we have the data needed to calculate the IC_{50} , which is the concentration of an inhibitor where the response (or binding) is reduced by half. We continue taking the IC_{50} as EC_{50} , because EC_{50} is the concentration of a drug that gives half-maximal response, in this case both concepts give the same number. This result gave us the exact number by which both drugs act effectively on HCV infection.

	24 h	48 h	72 h
LogIC50	-2.199	-2.478	-2.346
HillSlope	-2.317	-1.577	-1.132
IC50	0.006328	0.003330	0.004508

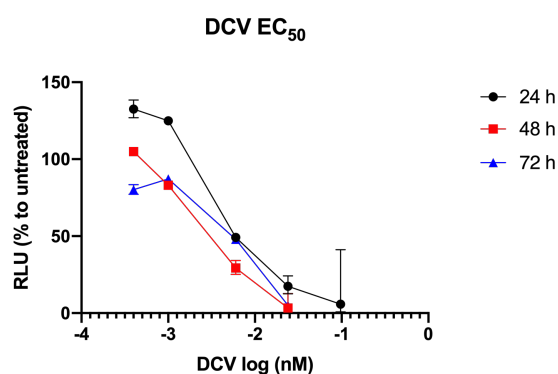


FIGURE 11.5: Established EC_{50} values for NS5A inhibitor, Daclatasvir (DCV)

Logarithmic inhibitor vs response in a variable slope graphic showing EC_{50} values for DCV titration. Table above shows logarithmic calculation of EC_{50} data on time points 24, 48 and 72 hpe.

11.3 Daclatasvir and Sofosbuvir kinetics

Once we found the EC_{50} values for both drugs, we use this to formulate a kinetic experiment with different time points of drug addition. The goal was to find the optimal concentration by which both drugs inhibit HCV replication at the same time post-infection. For this purpose we use the same conditions of previous experiment, but in a dose-response set-up. We achieved this by adding a range of concentrations around the optimal EC_{50} value, as shown in Figure 11.5 and 11.6. Thus, SOF and DCV were added to Lunet cells 12hpe and 24hpe, and the supernatants (SN) were recovered and used for infection of new Huh 7.5 cells, measuring RLU at points of 24, 48 and 72 hpi (as described in Appendix A.2). In the following, Figures 11.7 and 11.8, we show the last experiment data ($n=1$), where the concentration is related to the the percentage of untreated cells (RLU normalisation to 4hpi was set to 100% or 1%). Where we use

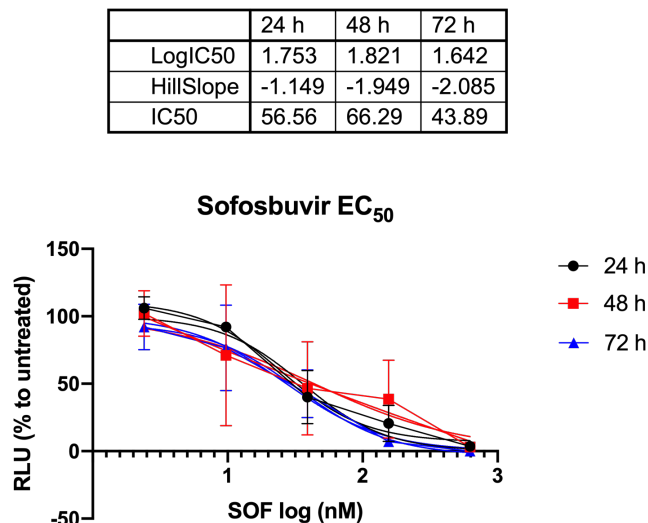


FIGURE 11.6: Established EC_{50} values for NS5B inhibitor, Sofosbuvir (SOF) Logarithmic inhibitor vs response in a variable slope graphic showing EC_{50} values for SOF titration. Table above shows logarithmic calculation of EC_{50} data on time points 24, 48 and 72 hpe.

some concentrations around the EC_{50} values (DCV **0.0062nM** and SOF **56.56nM**) to determine the concentration at which both drugs have an effect on HCV infection, observed by calculating the ratios between replication and reinfection (infection with SN). An early inhibition with a lower concentration of 0.097nM DCV can inhibit replication, an effect in assembly is shown when the EC_{50} value is reached at 0.0062nM as shown in Figure 11.7. This concentration was then used to further evaluate the effect of DCV on the assembly process, as this experiment pointed that its effect could be in addition to its effect in HCV replication. In Figure 11.8, the results of the last experiment (n=1), showed that Sofosbuvir has an effect just on replication (as expected because it is a NS5B inhibitor), using its EC_{50} concentration of 56.56nM, which is why this drug was used as a positive control of solely replication inhibition.

Additionally, we wanted to establish the time of drug addition, to rule out any other effect on the HCV cycle, but assembly. For this we used the values obtained in the experiment and did a logarithmic graph, where the shift in plotting replication or reinfection could be interpreted as a drug-related effect 11.9, as for SOF, 11.10; (see Appendix A.5, for details on n=3 of the drug titrations). We then used 24 hours post electroporation to add the drug and 24 hours after drug addition we electroporated the cells with HCV genome JCR2a. Together these experiments gave us the exact concentration and time, at which both drugs inhibit HCV infection, but more important, the ratios showed already an effect of DCV on assembly steps, which we continue to investigate.

Daclatasvir 24hpe drug addition

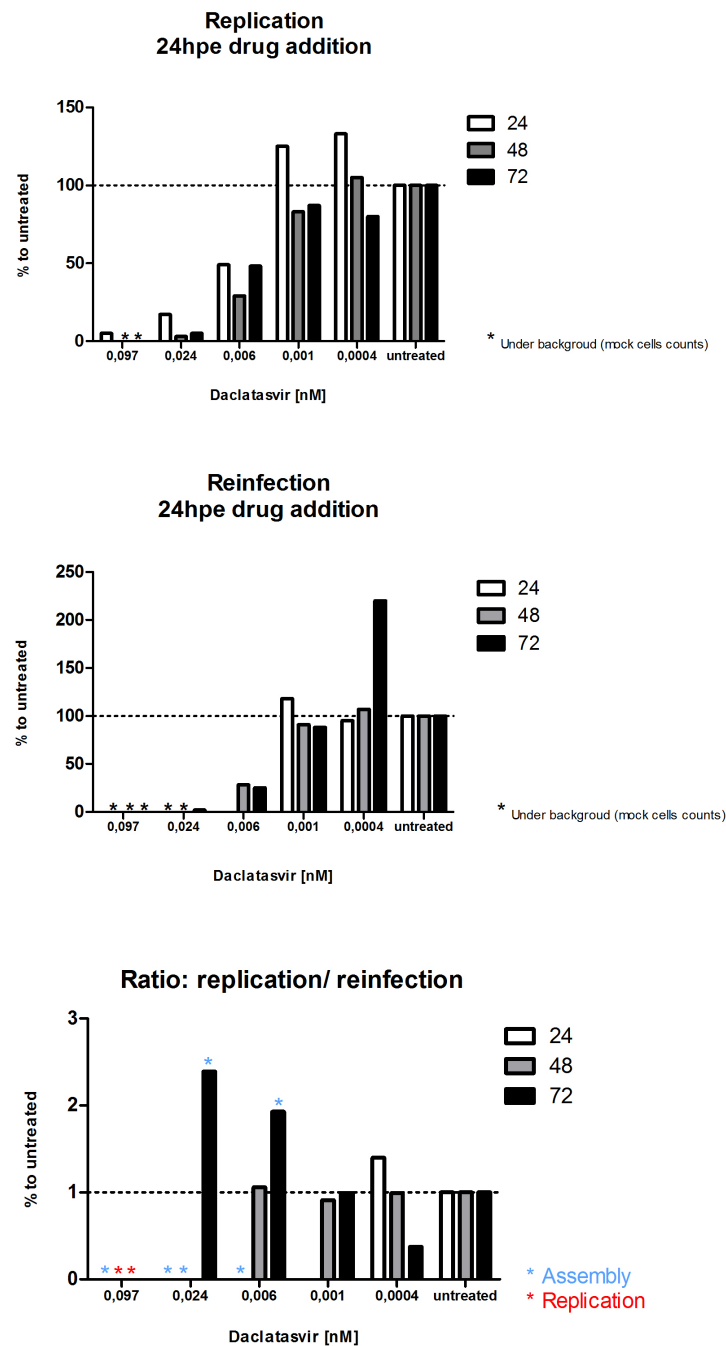


FIGURE 11.7: Daclatasvir dose-response effects on HCV life cycle

Different concentrations of DCV were chosen and normalized to untreated cells (uninfected, no electroporated HCV RNA). DCV effects on HCV replication and reinfection are shown. In addition, the ratio between the replication and the reinfection values is shown to underline DCV effect. The line shows the 100% of inhibition. Readout by RLuc measurement (n=1). All samples were treated to RLU % to untreated cells.

Sofosbuvir 24hpe drug addition

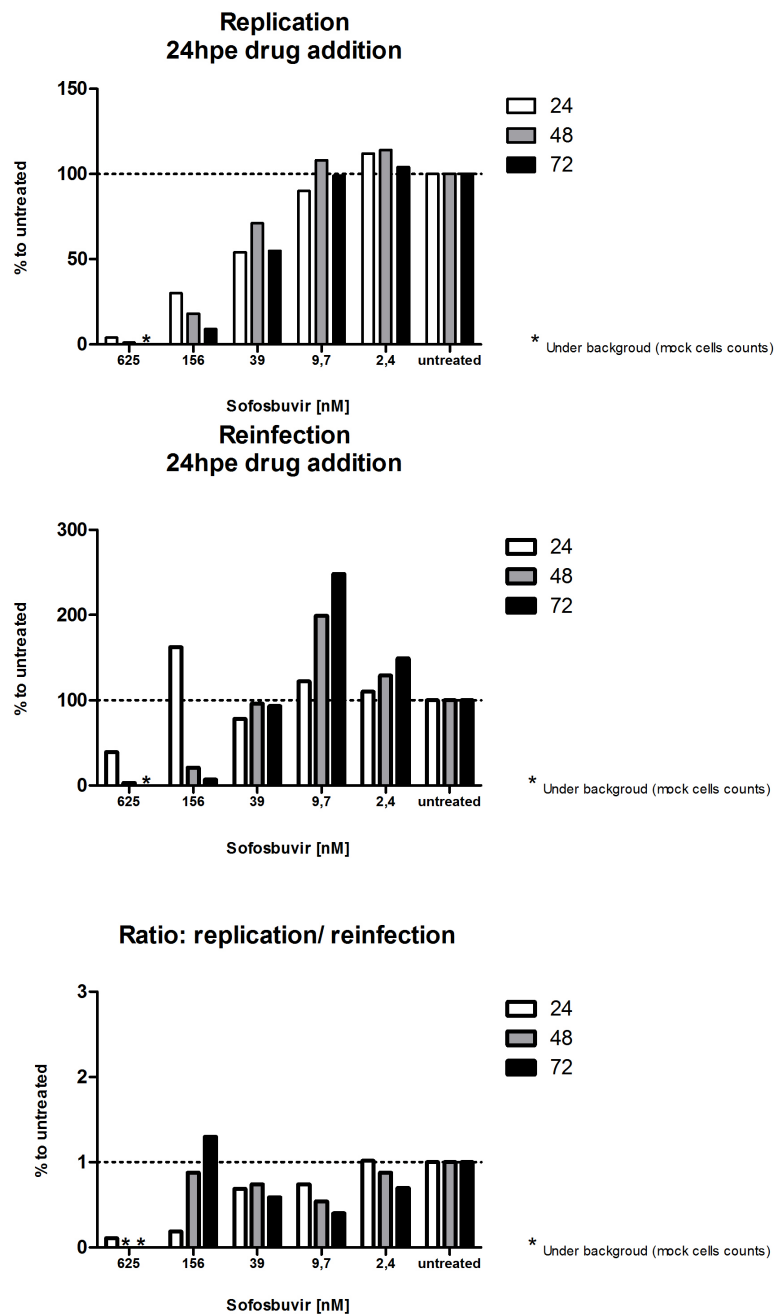
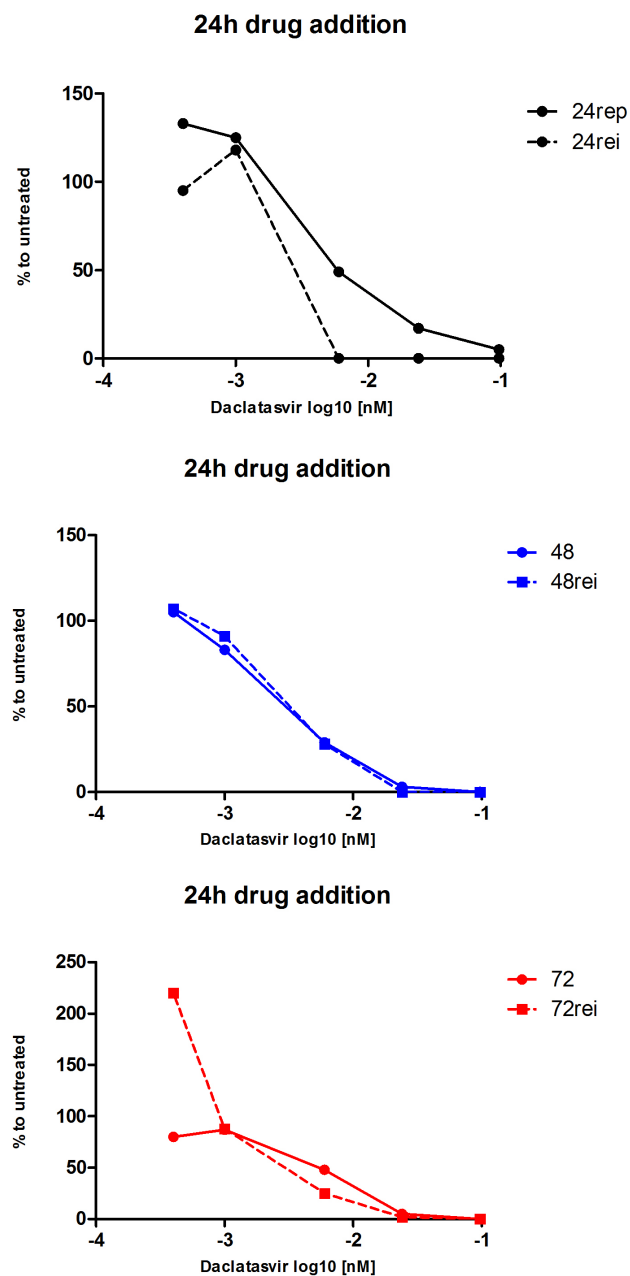


FIGURE 11.8: Sofosbuvir dose-response effects on HCV life cycle

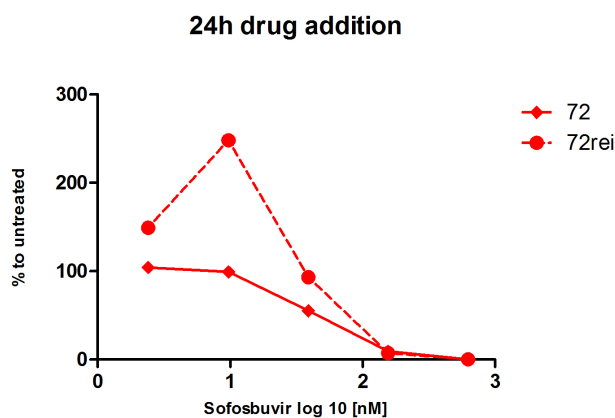
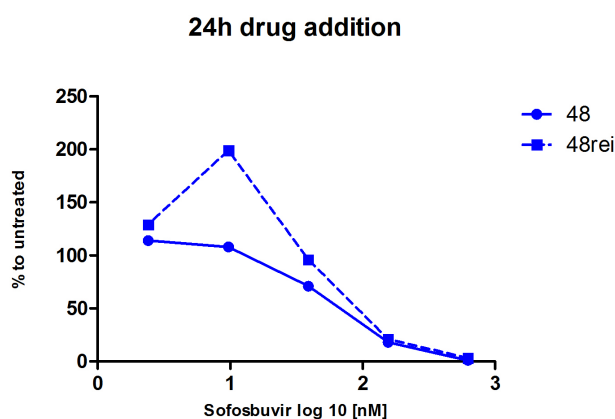
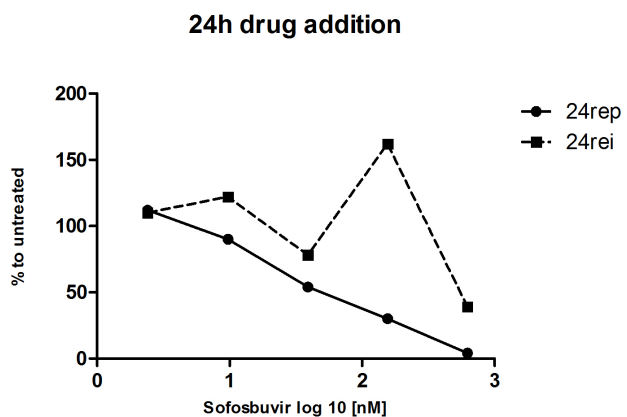
Different concentrations of SOF were chosen and normalized to untreated cells (uninfected, no electroporated HCV RNA). SOF effects on HCV replication and reinfection effects are shown. In addition, the ratio between the replication and the reinfection values are shown to underline SOF effect. The line shows the 100% of inhibition. Readout by RLU measurement (n=1). All samples were treated to RLU % to untreated cells.



	24rep	24rei	48	48rei	72	72rei
LogIC50	-2.204	~ -2.426	-2.481	-2.429	-2.348	-2.379
HillSlope	-2.397	~ -29.61	-1.589	-2.048	-1.123	-3.069
IC50	0.006247	~ 0.003746	0.003301	0.003727	0.004485	0.004181

FIGURE 11.9: DCV drug addition at different time points

Drug addition 24hpe and harvesting time points 24, 48 and 72hpi with different DCV concentrations for HCV replication (rep) and reinfection (rei) are shown. Normalized to 4hrs of untreated cells. Readout by RLU measurement(n=1). All samples were treated to RLU % to untreated cells. (see Appendix A.5, for details on n=3 of the drug titrations).



	24rep	24rei	48	48rei	72	72rei
LogIC50	1.753	~ 2.779	1.821	2.030	1.642	1.899
HillSlope	-1.149	~ -11.56	-1.949	-3.543	-2.085	-3.965
IC50	56.56	~ 601.3	66.29	107.2	43.89	79.30

FIGURE 11.10: SOF Drug addition at different time points

Drug addition 24hpe and harvesting time points 24, 48 and 72hpi with different SOF concentrations for HCV replication (rep) and reinfection (rei) are shown. Normalized to 4hrs of untreated cells. Readout by RLuc measurement (n=1). All samples were treated to RLU % to untreated cells. (see Appendix A.5, for details on n=3 of the drug titrations).

11.4 Daclatasvir has an inhibitory effect on envelopment of viral particles

Until the moment of the present experiments, direct-acting antiviral DCV mode of action was not fully understood and strong evidence from various groups have shown that this drug might have an effect in assembly of the virus [26, 126, 165].

Nonetheless, NS5A participates in various ways during assembly. It is known it regulates the coordinated packaging which is required for viral RNA to get into the nucleocapsid. Also, during assembly of infectious virus particles, NS5A appears to be colocalising with core protein in lipid droplets which seem to be required [26]. Finally, it has been suggested that NS5A is regulating the switch between replication of the viral RNA and its packaging into virions [162]. All together these experiments pointed into NS5A activities also being inhibited by NS5A inhibitor, DCV. However, the role of DCV in assembly of HCV viral particles remained unclear. To investigate further on the role of DCV in assembly and decipher the MOA, we performed the following experiments.

We use then the established conditions in the previous experiments. Lunet cell culture was treated with DCV or SOF after 24h post electroporation of JCR2a HCV genome. We added the established EC_{50} values: **0.06nM** and **56.56nM**, respectively. As we can see in Figure 11.11, the effect was observed only in the cells treated with DCV compared to SOF treated cells, which main target is NS5B and has no effect on the assembly of the viral particles. This was the first evidence that was indeed affecting the assembly process and not only the replication of HCV viral particles, as shown in Figure 11.11. This Figure represents the ratio calculated between replication values and reinfection values when samples were treated with both drugs SOF and DCV. As shown in Figure 11.9, by one time experiment, the shift was observed when samples were treated 24 after drug addition, so this effect was also observed when the ratios were calculated for reinfection values at 24 hours post drug addition.

Once we observed the effect of DCV treatment in HCV assembly, we continued to investigate at which step of the assembly process DCV is inhibiting NS5A activities. The assembly process is divided into distinct steps such as core trafficking to the lipid droplets, core oligomerization, capsid formation and finally envelopment. We first look into the envelopment of the viral particles and if it was interrupted by the drug. For this purpose, we used the same conditions in which we electroporated Lunet cells with HCV RNA, after 24 hpe, we added the different treatment of drug SOF or DCV, using EC_{50} values and use control cells as untreated without a drug. After 24, 48 and 72 hpi, we harvested the cells collecting the supernatant and the debris.

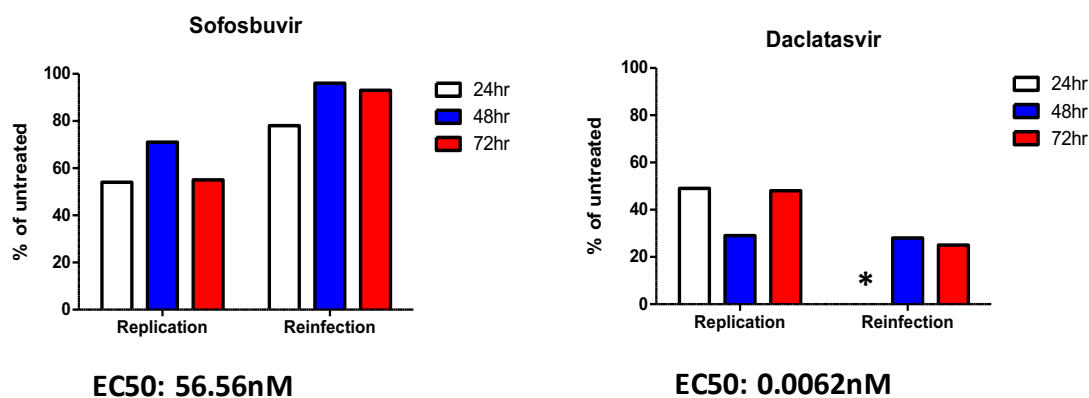


FIGURE 11.11: SOF and DCV effect on replication and reinfection processes
 DCV and SOF ratios and the effect of the drug addition after 24hpi. Underneath each drug treatment the EC50 value selected for treatment at 24 hpe is shown. Then the cells were harvested at 24, 48 and 72 hpi. Replication and reinfection values are shown. All the values were normalised to the untreated cells. Results are shown in percentage.

11.4.1 Proteinase K Assay

First, we assessed if core protein was protected against the proteolytic digestion with proteinase K, to ensure the envelopment of the protein into membranes as the assembly of HCV viral particles. The residual core protein was quantified by Western blot and the data was normalized to the amount of core protein in the untreated sample. As a control, cell lysates were pre-treated with Triton X-100 to solubilize all membranes before proteinase K digestion. Under these latter circumstances, all core proteins are expected to be sensitive to proteolytic digestion, ensuring that the proteinase K concentration was not limiting in the assay. The core amount detected under these conditions was used for background subtraction. A representative immunoblot stained for HCV core is shown in Figure 11.12. This method is also described in 10 as it was published by [162].

Accordingly, in samples treated with SOF, quantification of signal intensities revealed that all of intracellular core protein was resistant to protease digestion and thus, had already acquired a membrane envelope and proceeded to a post-budding step see Figure 11.12. In contrast, samples under the treatment with DCV showed a highly significant reduction in amount of protected core, indicating that most core species present were digested shown in Figure 11.12, the quantification shows the more evident reduction on the envelopment of viral particles. Together, these data suggest that treatment with DCV confer a defect in infectious particle production occurring at, or prior to, core envelopment. As already mentioned, assembly of infectious HCV particles requires the acquisition of a lipid membrane containing the envelope glycoproteins and as previously reported [162], this process can be monitored in a time-resolved manner by determining the sedimentation profile of core protein using rate zonal centrifugation [155].

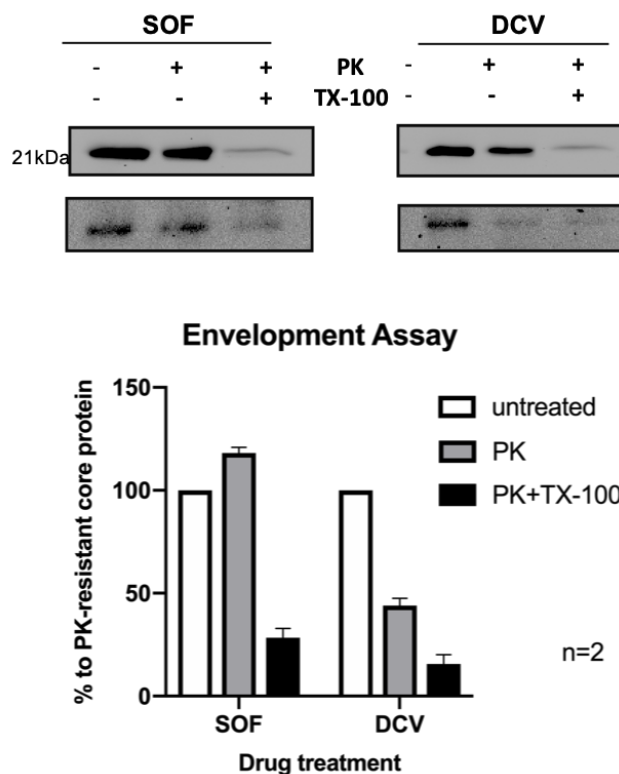


FIGURE 11.12: Envelopment assay experiment

Jc1 cell lysates were subjected to a proteolytic digestion protection assay as follows: Lysates were separated into three aliquots which received different treatments: (i) left untreated (-), (ii) treated with 150 g/ml proteinase K (PK) for 1 h on ice, or (iii) lysed in 1% Triton X-100 prior to PK treatment (condition used for background correction).

The amount of protease-resistant core was determined by Western Blot both blots stained for HCV core.

Western Blot signal intensities were quantified with LabImage 1D and values obtained for the proteinase K-treated sample were background-corrected and normalized to untreated control. Mean values and standard deviations of 3 independent experiments are shown.

11.4.2 Rate Zonal Centrifugation Assay

Secondly, we use rate zonal centrifugation which separates particles by size, using different concentrations of sucrose in different densities (gradients). Larger particles to the bottom (more viscous) and small on the top (not enough mass to go through gradient). To this end, we prepared lysates of the Lunet cells at 24h after electroporation of JC1 HCV genome into Lunet cells and 24h after drug addition (SOF and DCV) as previously. Post nuclear supernatants were loaded on top of a linear sucrose gradient (0-30%) and separated by rate zonal centrifugation [155]. Gradients were fractionated and core protein amount in each fraction was determined by CMIA (Chemiluminescent microparticle immunoassay). Fractions are collected after centrifugation, see Figure 11.13.

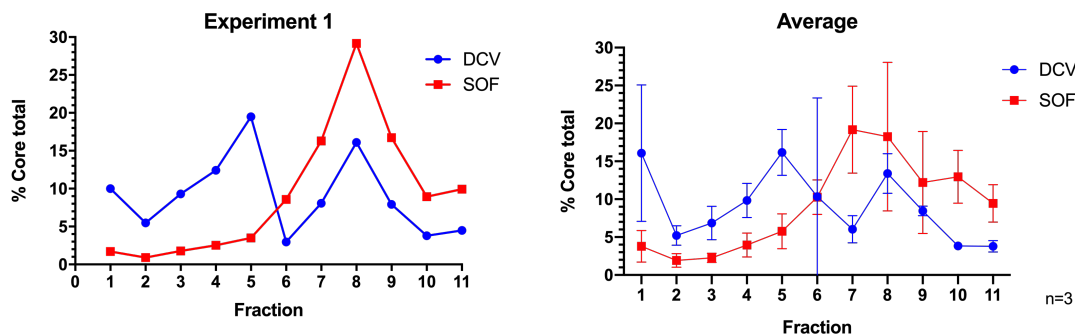


FIGURE 11.13: DCV treatment gradients show no Core envelopment particles

Rate zonal centrifugation. Post-nuclear supernatants of cell lysates obtained by repetitive cycles of freeze and thaw 48 h post-transfection were layered on top of a preformed continuous 0 to 30% sucrose density gradient and subjected to rate zonal centrifugation for 1h at 270,000xg. Core content was measured along the gradient by ELISA and normalized to the total core amount in the lysate. Experiment 1, shows one repetition and the average data come from 3 independent experiments where we performed separation by 030% linear sucrose gradient, the collected 11 fractions are shown.

At 48hrs post transfection we observed all complexes are sedimented slower in SOF treated samples than in DCV treated samples. The samples under DCV treatment showed the first peak at fraction 4-5, and a second one between 7-9, this shows the dual mode of action. Hereby, DCV shows an inhibition of the envelopment of viral particles, shown by the first peak, which refers to its effect at slow sedimenting fractions 4-5. In contrast, SOF treated samples were a large proportion of core protein has assembled into fast-sedimenting complexes that accumulated in fractions 6-9, which have no effect on the envelopment of HCV viral particles. Therefore, this experiment shows that samples treated with SOF had the Core protein fully enveloped by 48hrs after transfection mainly because the samples pass through the gradient showing highest peak at fraction 6-9. In contrast, samples with DCV, did not pass rapidly though the gradient and accumulated in first fractions 3 to 5 having a significant peak at fraction 8 to 9. This last point shows that in samples treated with DCV the Core protein appears not to be enveloped as shown in Figure 11.13. We suggest then, that DCV treatment can block the assembly at the envelopment stage.

However further experiments using different time points could be useful to determine if the process of envelopment is blocked prior to assembly of the HCV viral particle. Thus, performing the experiments prior to the 24hpe and 24 post drug addition of our settings, could elucidate this question (for example, 12h as previously reported in [162]).

11.4.3 Immunofluorescence Assay

NS5A inhibitors interfere with the assembly of infectious virions and at the same time block the membrane rearrangements that are essential to build up the viral replication factory [126]. Accordingly, we wanted to analyse the same samples by confocal microscope to determine the co-sedimentation of core protein with the HCV envelope glycoproteins, which could show a relevant effect of DCV on membrane rearrangements or on NS5A sub-cellular location. We found that HCV Core colocalizes with NS5A, this is because core protein is directed to LDs whereas RNA replication most likely is mediated by a replicase complex associated with ER or ER-derived membranes as previously reported [162].

Moreover, during virus assembly the RNA genome is transferred from the replicase complex to the core protein. This process will require the action of NS5A to mediate the interaction between the core protein and the replicase complex, giving NS5A a clear role during assembly. Using microscopy data we analysed the co-localization of core and NS5A in Huh7-Lunet cells transfected with HCV JCR2a and then treated the samples with DCV or SOF. As shown in Figure 11.14 and Figure 11.16, we observed co-localization between NS5A and core proteins and glycoprotein E2. Moreover, the ring-like staining pattern of NS5A indicates that this protein also associates with LDs. The drug treatment with SOF or DCV, did not alter the colocalisation with glycoprotein E2 or to LDs see Figure 11.15 and Figure 11.17.

This results could suggest that the differences in core-NS5A (replicase complex) interactions are not detectable for the different level of virus production. Moreover the drug addition treatment apparently did not affect the localisation of HCV Core protein or E2 glycoprotein. When treated with DCV samples show the same pattern as SOF and NS5A colocalization with LDs suggests no additional relocation of the proteins due to the drug treatment. Anyhow, additional time points could help elucidating the effect of the drug on this step of the assembly, because the effect of the drug might be in the early or late steps of the assembly process.

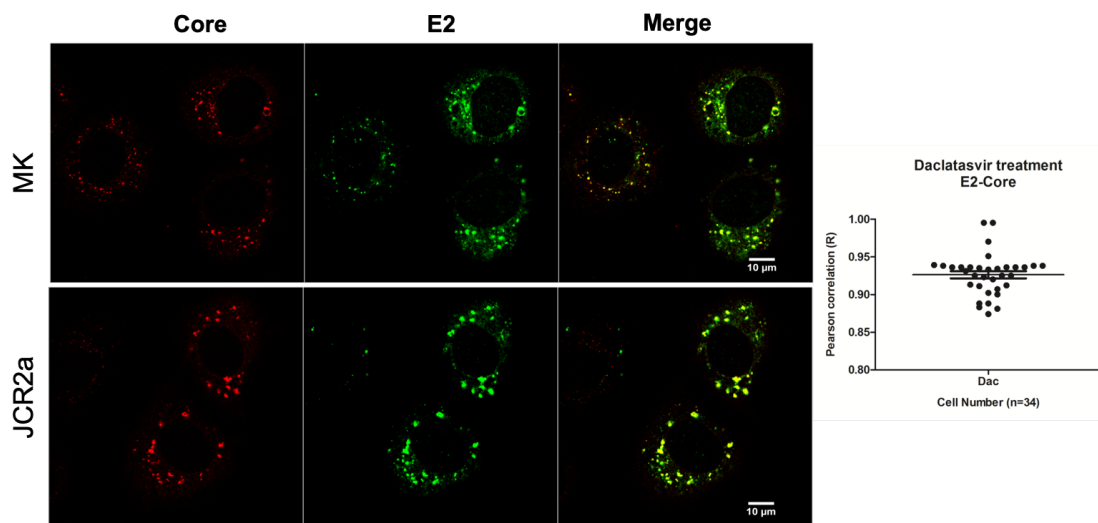


FIGURE 11.14: NS5A and E2 localisation

NS5A localisation in relation to glycoprotein E2 in samples treated with DCV. JCR2a genome was transfected into Huh7-Lunet cells which then were fixed after 48h and subjected to immunofluorescence staining of E2 (AP33, 1:300 mouse monoclonal antibody, green) and core (C830 1:200 rabbit polyclonal antibody, red). Nuclei were counterstained with DAPI (blue), not shown. Representative transfected cells were counted for each construct. To the right, a quantification of samples performed by R pearson in ImageJ.

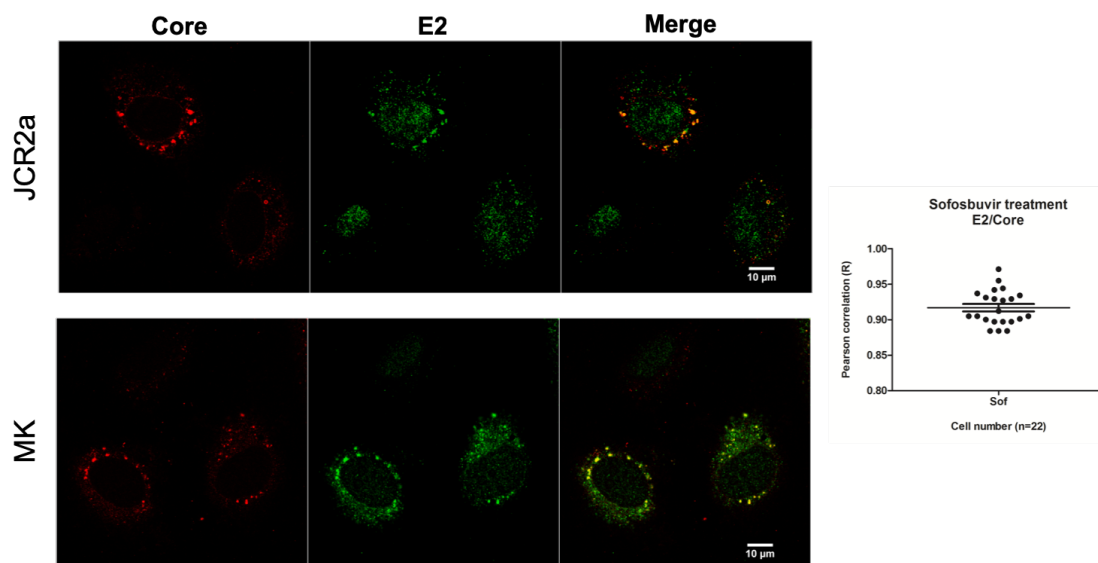


FIGURE 11.15: NS5A and E2 localisation

NS5A localisation in relation to glycoprotein E2 in samples treated with SOF. JCR2a genome was transfected into Huh7-Lunet cells which then were fixed after 48h and subjected to immunofluorescence staining of core (C830) 1:200 rabbit polyclonal antibody, red) and E2 (AP33, 1:300 mouse monoclonal antibody, green). Nuclei were counterstained with DAPI (blue), not shown. Representative transfected cells were counted for each construct. To the right, a quantification of samples performed by R pearson in ImageJ.

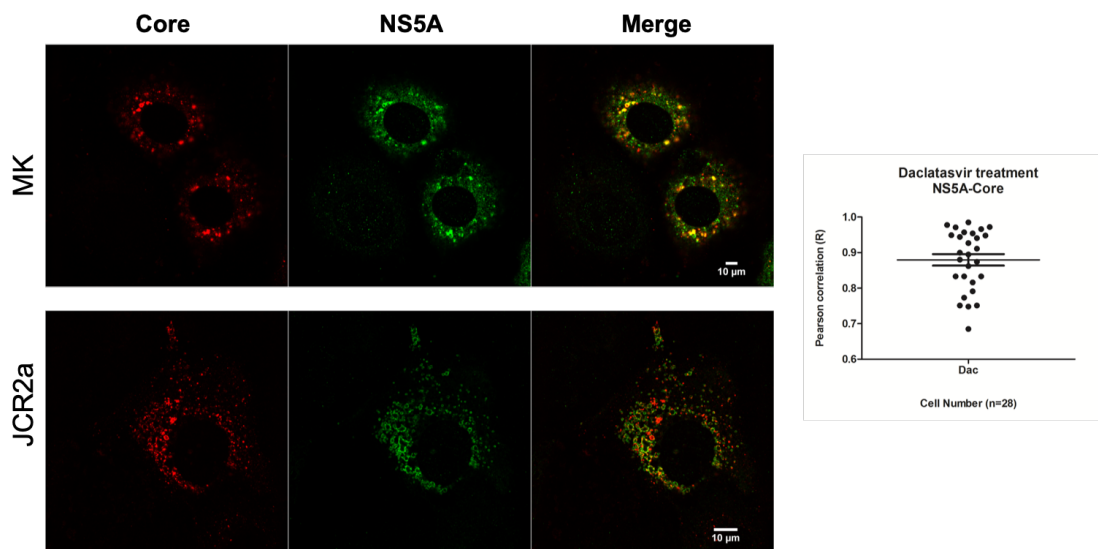


FIGURE 11.16: NS5A and Core protein localisation
NS5A localisation and Core protein in samples treated with DCV. JCR2a genome was transfected into Huh7-Lunet cells which then were fixed after 48 h and subjected to immunofluorescence staining of core (C830 1:200 rabbit polyclonal antibody, red) and NS5A (9E10 1:1000, mouse monoclonal antibody, green). Nuclei were counterstained with DAPI (blue), not shown. Representative transfected cells were counted for each construct. To the right, a quantification of samples performed by R pearson in ImageJ.

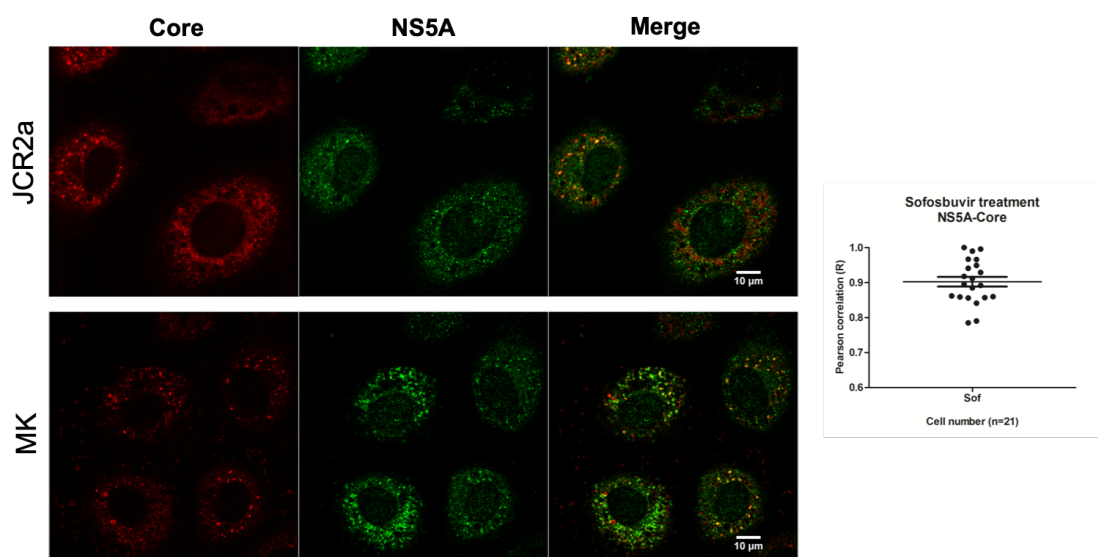


FIGURE 11.17: NS5A and Core protein localisation
NS5A localisation and Core protein in samples treated with SOF. JCR2a genome was transfected into Huh7-Lunet cells which then were fixed after 48h and subjected to immunofluorescence staining of core (C830 1:200 rabbit polyclonal antibody, red) and NS5A (9E10 1:1000, mouse monoclonal antibody, green). Nuclei were counterstained with DAPI (blue), not shown. Representative transfected cells were counted for each construct. To the right, a quantification of samples performed by R pearson in ImageJ.

11.4.4 Transcomplementation Assay

Moreover, replication-incompetent NS5A mutants could be rescued by transcomplementation assay [26], knowing now that NS5A inhibitors could interfere with the assembly of viral particles, we were interested whether this NS5A function can also be restored by trans-complementation and/or if NS5A inhibitors could interfere with the rescue of assembly. To this end we established a trans-complementation assay based on the co-transfection of a JCR2a genome carrying the deletion in domain III of NS5A (Δ 2328-2435), with or without a resistant mutant Y93H and an HA-tag, into two different cell lines containing a subgenomic luciferase-helper RNA that lacks the region encoding core to the C-terminus of NS2 and in case of the resistant mutant, contains the mutation on Y93H, as shown in Figure 11.18. Replication of this helper RNA was determined by luciferase assay. The final aim of the transcomplementation assay was to uncouple the assembly function of NS5A by deleting its DIII and treatment with or without drugs to rescue its function by transcomplementation assay. This assay utilizes the transfection of selectable replication-deficient HCV replicons into cells that harbour replicons expressing the trans-complement. We transfected the following helper RNA constructs, see 11.18 into Huh7-Lunet NS3-NS5A (wildtype) and Y93H (resistant mutant) cell lines previously prepared as described previously in section 10.7.2.

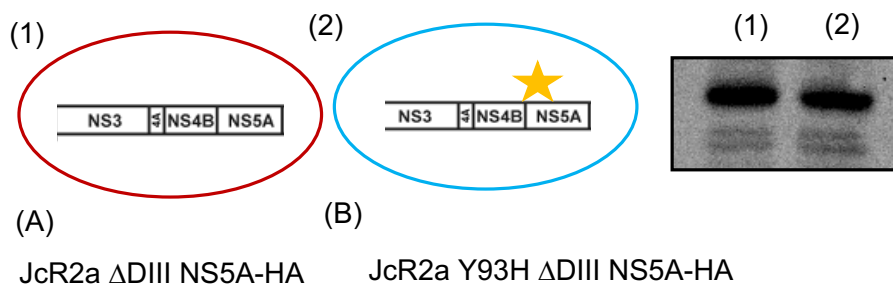


FIGURE 11.18: Trans-complementation constructs and cell lines

Constructs used for the trans-complementation assay. Cell lines (1)

pWPI-NS3-5A-BLR. (2) pWPI-NS3-5A-Y93H-BLR (yellow star marking the drug resistant mutation on NS5A). Right side panel shows the cell lines detection by WB: (1) pWPI-NS3-5A-BLR and (2) pWPI-NS3-5A-Y93H-BLR, respectively. Constructs containing JCR2a HCV genome used for assay were (A) JCR2a Δ DIII NS5A-HA and (B) JCR2a Y93H Δ DIII NS5A-HA.

Depending on the particular combination of the constructs, different outcomes were possible. Upon transfection of cells with the helper RNA constructs we expected different rescue patterns as shown in Figure 11.19. The first (A) JCR2a construct was used as a marker for assembly blockage -assembly mutant- and the second, (B) construct was used to evaluate the effect of the drug in the resistant mutation Y93H -resistant mutant-. Treatment with DCV or SOF will help or not in the recovery of the assembly of viral



FIGURE 11.19: Transcomplementation assay hypothetical results
 Expected results from different combinations of constructs and cell lines, to observe the recover effect of each trans-complementation. DCV or SOF treatment in each combination is crucial for the recovery or not of assembly.

particles. We expected that combination of both cell lines and both constructs under the treatment of SOF, would recover the assembly, because SOF treatment will not interfere with the assembly process. In contrast, using the assembly mutant construct together with either of the cell lines will result in no rescue of the assembly, due to the effect of DCV on assembly of the viral particles. However, when using the cell line with the resistant mutant (2) and constructs (A) or (B), assembly will be recover, due to the resistance phenotype, as shown in Figure 11.19.

However the experiment did not show exactly the results as we expected. The combinations of constructs (JCR2a wt, JCR2a Δ III and JCR2a Δ III-Y93H) are shown in the y axis together with cell line types: Lunet, Lunet wt (pWPI-NS3-5A-BLR), and Lunet Y93H (pWPI-NS3-5A-Y93H-BLR), on the x axis, RLuc measurement normalized to 4hrs hpe, as shown in Figure 11.20. Instead, the combinations showed the following:

- When using JCR2a (wt) construct and the three different cell lines, HCV replication showed a normal infection curve where we have 1.0×10^4 RLuc counts after 24hrs for HCV replication time-point, as this was used as positive control.

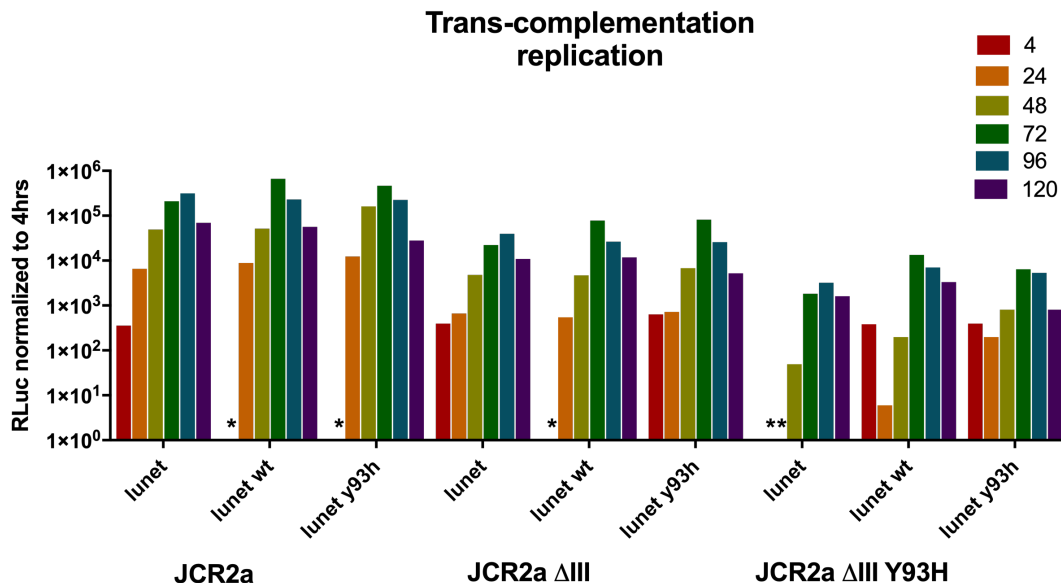


FIGURE 11.20: Trans-complementation of constructs on time line. Combinations of three different constructs (JCR2a wildtype, JCR2a Δ III and JCR2a Δ IIIY93H and three different cell lines: Lunet, Lunet (wildtype: pWPI-NS3-5A-BLR) and Lunet Y93H (resistant mutant: pWPI-NS3-5A-Y93H-BLR). RLuc measurement at different time points of HCV replication, normalized to 4hrs.

- When using JCR2a Δ III construct and the three different cell lines, resulted in a lower HCV replication. And in when using the Lunet wt cells (1) pWPI-NS3-5A-BLR, showed no detectable counts at 4hpi, which we could not develop further. When using Lunet Y93H cell line, at 24hpi, HCV replication was not yet established, but at 48hpi, HCV replication was observed, but not as wildtype.
- When using JCR2a Δ III-Y93H construct with Lunet cells, we did not detect any RLuc counts on the plates, which we account for a defect on the trans complementation assay. When using Lunet wt cells, we observed a reduction on HCV replication after 4hr infection, which showed that trans-complementation was not established and when using Lunet Y93H cell line, the construct JCR2a Δ III Y93H, the HCV replication RLuc counts could not be enough to use this combination for a established trans-complementation assay.

Unfortunately, we could not use this combination set-up as expected due to the non recovery of the trans-complementation assay between constructs and cell lines. The future plan was to recover the supernatant and infect new Huh7.5 cells with it, then further treat with DCV or SOF. Nonetheless, we could improve the set-up by addition of double mutants, addition of a antibiotic resistance, or different helper RNA constructs to have a precise *cis* or *trans* complementation of each part of the assay, as further discussed in section 13. Regardless, the results were conclusive to build the cell lines and

constructs needed for such experiments and improvements can be taken from previous reported transcomplementation assays in other studies [172–174].

11.5 NS5A oligomerization state

Among other unsolved questions regarding the multifunctionality of NS5A is the oligomerization state of the protein. Controversially, it has been reported that NS5A forms a dimer [37–39], but even these studies suggest the formation of high oligomer formation during NS5A functions. A more recent report suggests there is a higher oligomer formation [62], which is crucial for NS5A multifunctionality and so for the inhibition by NS5A drugs. It has been hypothesized that the oligomer must be present for the inhibitor to attach to the binding site. Moreover, high resolution structural studies of NS5A protein reveal that the protein forms a dimer via contacts near the N-terminus, and the Y93H resistant mutation lies at the interface between two NS5A proteins [37], which is why we used both constructs (wildtype and resistant mutant Y93H). Although other reports claim that drug treatment does not seem to affect dimerization process [161]. In the end we wanted first, to investigate whether NS5A forms high oligomers during HCV infection. Second, to investigate if this can be disrupted by the addition of NS5A inhibitors. And lastly, to see if the oligomerization state affects the efficacy and efficiency of NS5A inhibitors. To approach this matter and study the presence of higher oligomer formation of NS5A, we used PFA (Paraformaldehyde) cross-linking assay [156] and using BRET (Bioluminescence Resonance Energy Transfer) assay [118]. This last assay results are undergoing which is why results are not all shown in the present study.

11.5.1 PFA cross-linking

In order to confirm the detection of PFA cross-linked complexes. Lysates were incubated at 65°C and 99°C, respectively and analyzed by western blot using the antibody against NS5A protein (9E10), as described in 10.9.4. As seen in Figure 11.21, the assay’s principle is that at 65°C, the oligomer would continue in a oligomer conformation, whereas at 99°C, the oligomer would loose its conformation, thus, being able to detect different parts of it.

We use the following constructs to transfect Lunet-T7-puromycin cells:

- pTM-NS3-3’ JFH1
- pTM-NS3-3’-NS5A-gfp Y93H-JFH1

- pTM-NS3-3'-NS5A-gfp Δ DI-JFH1 (aa28-213) (data not shown)

Later, we prepared formaldehyde as cross-linking reagent at different concentrations 0.4% to 4%, then Lunet cells were suspended under the different PFA concentrations and incubated at different temperatures 65°C or 99°C and then lysed with RIPA buffer for later analysis by western blot, as shown in 11.22 and 11.23.

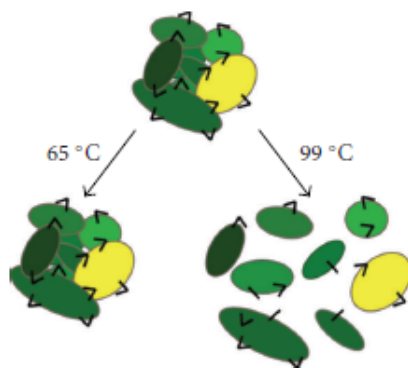


FIGURE 11.21: PFA cross-linking assay principle

Schematic model. Formaldehyde derived cross-links are preserved, if samples are only incubated at 65°C, whereas most of the cross-links are reversed at 99°C. Proteins are depicted as oval shapes, formaldehyde cross-links as black triangles. Taken from [156]

Under this circumstances we could recognize a higher molecular weight complex (a smear) containing NS5A, in samples treated for 5 min at 65°C and 99°C. In Figure 11.22, samples showed a clear band at 56 kDa using both constructs (wt and Y93H resistant mutant). PFA concentration 0.4, 0.8 and 2%, in samples including the wt construct, showed a smear and a band at around 75 kDa, which can correlate to a higher molecular weight NS5A oligomer formation. In contrast to samples with Y93H resistant mutant, a smear was lightly detected at 0.4-0.8% PFA concentration, but a clear band was detected at 2% PFA concentration. This suggested that using 2% of PFA concentration we could detect an cross-linked complex containing non-structural protein 5A. In Figure 11.23, NS5A was detected at 58 kDa using 0.2, 0.4, 0.8 and 1% PFA for the wt construct. Additionally, at 0.8, 1 and 2% PFA, we could detect three different molecular weight bands, at approx 70, 90 and 130 kDa, indicating that using 99°C, can separate the oligomer in separate molecular weight protein parts, as shown in Figure 11.21. As for the resistant mutant, we could detect NS5A at 58 kDa using 0.2, 0.4, 0.8% PFA concentration. Additional bands were observed at 70, 90 and using 1.8 and 2% bands detected at 130 kDa, indicating that the resistant mutation does not seem to affect the oligomer formation of NS5A.

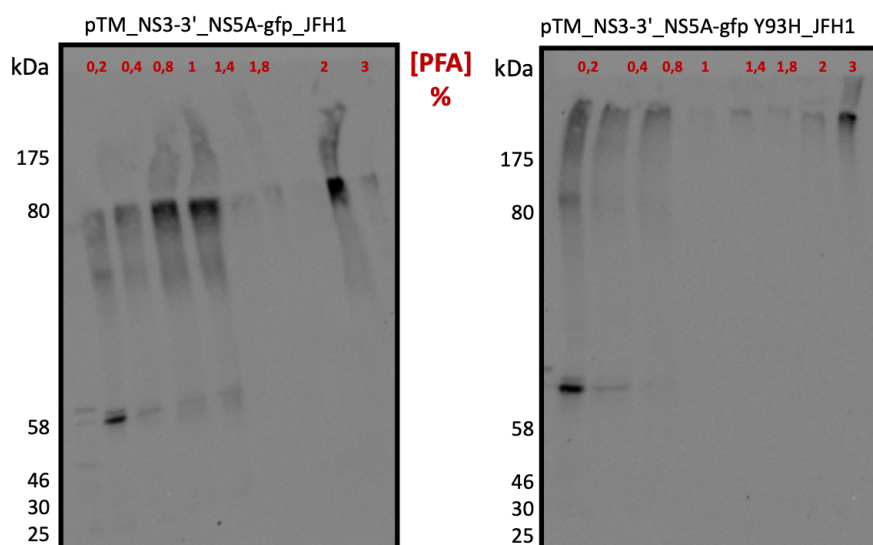


FIGURE 11.22: NS5A oligomerization state detected at 2% PFA concentration Samples incubated at 65°C for 5 minutes under different PFA concentrations. Different molecular weights are shown. Western Blot for NS5A (using 9E10 antibody).

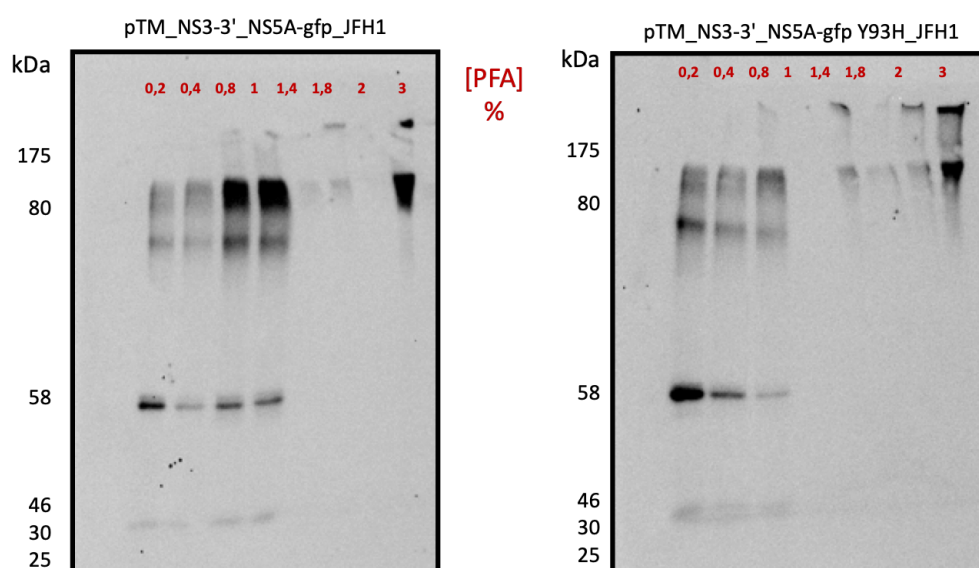


FIGURE 11.23: NS5A oligomerization state detected at 2% PFA concentration Samples incubated at 99°C for 5 minutes under different PFA concentrations. Different molecular weights are shown. Western Blot for NS5A (using 9E10 antibody).

However, NS5A was also found in the monomeric form at approximately 58 kDa after incubation at 65°C, as shown in Figure 11.22, which was detectable at different PFA concentrations treating the samples at the higher temperature, which correlates with what we were expecting from this assay. This could be due to incomplete cross-linking, as the conditions applied during formaldehyde cross-linking do not lead to a high extent of protein cross-linking, leaving a large fraction of NS5A non cross-linked. Alternatively,

incubation at 65°C may lead to partial reversal of formaldehyde cross-links and release of NS5A even at a lower temperature. Moreover, samples at 99°C show less smear than the samples treated at 65°C, this could also suggest the presence of a high oligomer formation, as shown in Figures 11.22 and 11.23. Interestingly the resistant mutant construct did not show significant differences at 99°C but at 65°C boiling temperature, samples showed a decreased in the smear, which suggests that it is less likely to form oligomers of higher molecular weight. Ultimately, repetitions of this experiment must be performed to have more conclusive data. Regardless, this experiment shows evidence for a higher order complex formation at an optimal PFA concentration for cross linking.

11.5.2 BRET assay

Another technical tool to detect oligomer formation is using BRET (Bioluminescence Resonance Energy Transfer), previously used in the laboratory. Unfortunately, the results generated in the laboratory did not work due to the construct preparation, so we improve the set constructs using RLuc or YFP label and generated newly designed constructs as shown in as shown in section 9, we use different linker lengths for each construct. Each of the constructs contain two fragments of each reporter protein (F1 or F2), that could complement each other and reconstitute the whole Renilla Luciferase or full YFP NS5A labelled, respectively. The aim was to reconstitute the BRET signal, which we could interpret as having several of this constructs in close proximity, which could strongly suggest the formation of a higher oligomers.

First, we designed 16 constructs with different linker lengths as shown in section 9, that contained as the following Figure 11.24:

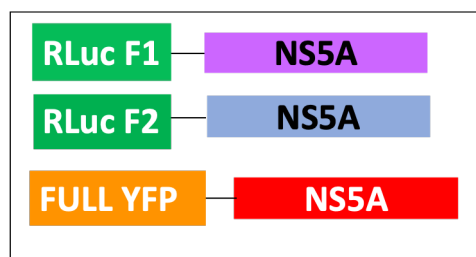


FIGURE 11.24: BRET constructs containing RLuc or YFP
Constructs and method are in detailed described in sections 9 and 10. In green, are RLuc containing constructs and in orange YFP containing constructs, that were selected. Diagram of each construct is illustrated (taken from DR. Berger data).

Second we use in combination all 16 constructs and try to combine all of them, and see which combination works best. The assay works as seen in Figure 11.25, where two dimers of NS5A, each expressing a RLuc fragment, and another expressing full YFP, we hypothesized that when this complex is in close proximity, we could recover BRET signal, as an acceptor-donor interaction. Furthermore, when NS5A inhibitors are present we would observe no BRET signal, if NS5A inhibitors are blocking the formation of a high molecular weight oligomer.

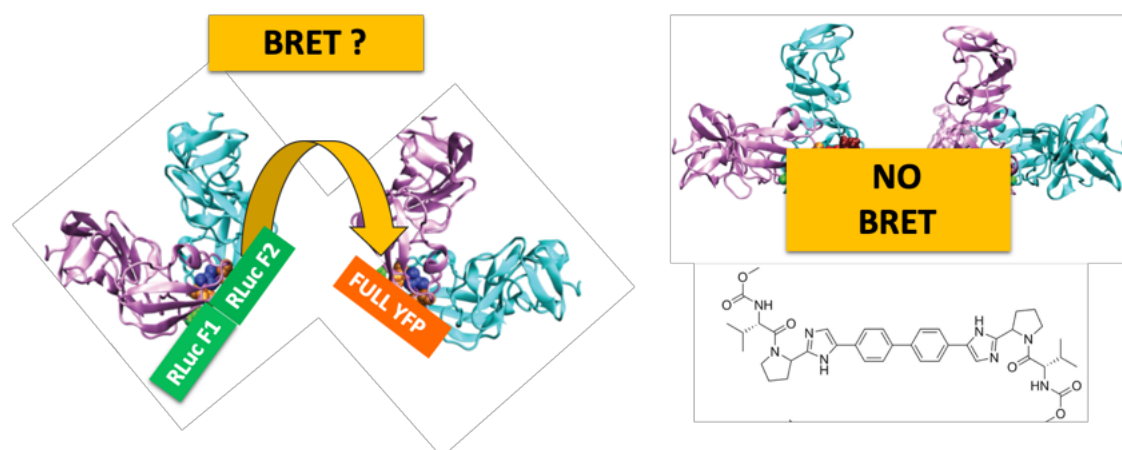


FIGURE 11.25: Principle of BRET experiment

NS5A is represented as a dimer (magenta and cyan), each containing a representative of RLuc fragments or YFP full-length. Two hypothetical scenarios are shown: left, shows a scenario where BRET signal can be recover due to the expression of each construct (RLucF1 or RLucF2 together with YFP) and thus, the formation of the oligomer. Right, shows the scenario where NS5A inhibitors interfere with this oligomer formation by a steric clash or a blockage in the interaction via the binding site. DCV chemical structure is shown.

	Rluc	Plasmid	Linker	
a	F1.1	pcDNA_RLucF1_NS5A	Linker 1	Thr-Gly-Gly-Ser-Asp-Ile
	F2.1	pcDNA_RLucF2_NS5A	Linker 1	Thr-Gly-Gly-Ser-Asp-Ile
b	F1.1	pcDNA_RLucF1_NS5A	Linker 1	Thr-Gly-Gly-Ser-Asp-Ile
	F2.2	pcDNA_RLucF2_NS5A	Linker 2	Thr-Gly-Pro-Ala-Pro-Ala-Pro-Gly-Gly-Ser-Asp-Ile
c	F1.1	pcDNA_RLucF1_NS5A	Linker 1	Thr-Gly-Gly-Ser-Asp-Ile
	F2.3	pcDNA_RLucF2_NS5A	Linker 3	Thr-[Gly-Gly-Gly-Gly-Ser]3-Asp-Ile
i	F1.3	pcDNA_RLucF1_NS5A	Linker 4	Thr-Gly-Ala-[Glu-Ala-Ala-Ala-Lys]2-Ala-Gly-Gly-Ser-Asp-Ile
	F2.1	pcDNA_RLucF2_NS5A	Linker 1	Thr-Gly-Gly-Ser-Asp-Ile
j	F1.3	pcDNA_RLucF1_NS5A	Linker 4	Thr-Gly-Ala-[Glu-Ala-Ala-Ala-Lys]2-Ala-Gly-Gly-Ser-Asp-Ile
	F2.2	pcDNA_RLucF2_NS5A	Linker 2	Thr-Gly-Pro-Ala-Pro-Ala-Pro-Gly-Gly-Ser-Asp-Ile
k	F1.3	pcDNA_RLucF1_NS5A	Linker 4	Thr-Gly-Ala-[Glu-Ala-Ala-Ala-Lys]2-Ala-Gly-Gly-Ser-Asp-Ile
	F2.3	pcDNA_RLucF2_NS5A	Linker 3	Thr-[Gly-Gly-Gly-Gly-Ser]3-Asp-Ile
l	F1.3	pcDNA_RLucF1_NS5A	Linker 4	Thr-Gly-Ala-[Glu-Ala-Ala-Ala-Lys]2-Ala-Gly-Gly-Ser-Asp-Ile
	F2.4	pcDNA_RLucF2_NS5A	Linker 4	Thr-Gly-Ala-[Glu-Ala-Ala-Ala-Lys]2-Ala-Gly-Gly-Ser-Asp-Ile

FIGURE 11.26: BRET combination of RLuc constructs

Letter code stand for each RLuc fragment needed in each combination for BRET. F1 or F2.1, stands for the linker number, although also shown. Each fragment linker number and length are shown.

Third, we transfected each construct in Huh7.5 cells, obtain and quantify protein for each one of the constructs. Later, we use this quantification numbers, to use the exact amounts of each construct using western blot (data not shown) and then protein quantification method using LabImage®. Once we calculated protein concentration we were able to express all constructs with the same amount of protein; this improved the assay's accuracy. Lastly, we use selected constructs in combination RLucF1 or RLucF2, as a test before performing BRET final assay which will include one of the RLuc fragments together with full YFP. Figure 11.26, shows the constructs which showed a significant RLuc measurement (above 4hrs post transfection normalization). The last is undergoing.

Chapter 12

Computational Results

The following section describes the computational experiments based on the experimental results in order to complement and fully understand the mechanism of action behind NS5A inhibitors and NS5A multifunctionality. First, we decided to look at the same Proline residues used in our experimental data, to compare with using a computational approach. Second, we wanted to look into DCV properties in relation to NS5A. Lastly, we wanted to elucidate the role of the NS5A amphipatic helix in the cellular membrane and its role using NS5A inhibitors. Together all these results could give us a slight picture of how the inhibitor is working and how key aspects of NS5A are relevant for DCV mechanism of action.

12.1 Proline residues in linker structures are key for DCV binding

As described in the experimental results, see [11.1](#), we use the Proline mutations on the linkers, as in [11.1](#), to investigate the impact of Proline mutations in the interaction with DCV. We use our experimental data to identify the effects of this Proline mutations on the interaction site with DCV inhibitor. For this, we use the NS5A dimer structure described in [\[1\]](#) and analyse each identified site-directed mutagenesis Proline residue in the linker connection between the amphipatic helix and domain Ia and domain Ib. We analyse each mutation on the overall structure of NS5A by visual analysis. Then we re-docked DCV inhibitor in the NS5A structure including each Proline mutation and run molecular dynamics, All together to fully understand the binding mechanism in the interaction site in addition to understand how the Proline mutations affect or promote this interaction.

Using MOE we introduce the Proline substitutions for the mutations performed experimentally, we compared the position to the wildtype Proline residue in one of the linkers as an example we used Proline residue 29 and 35, as shown in 12.1. We then performed this visual analysis with all the Proline mutations (data not shown). But to demonstrate that the mutation is having an effect on the binding with NS5A inhibitor, DCV we performed Molecular Dynamics to study this in detail.

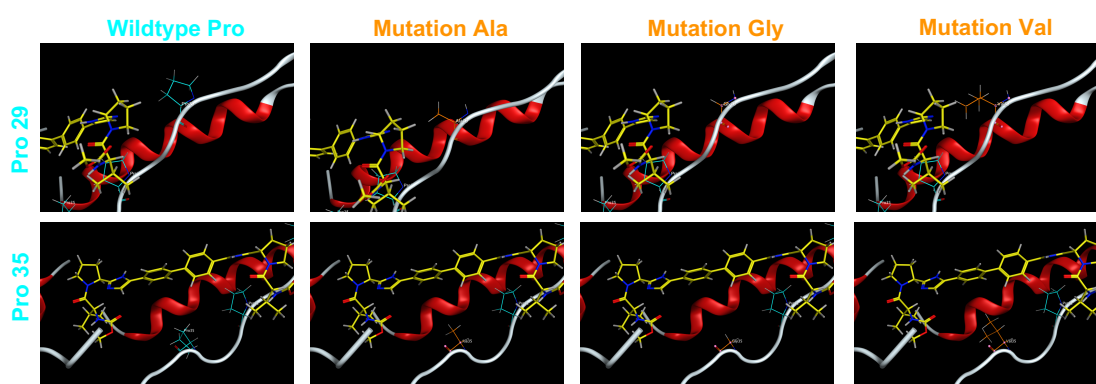


FIGURE 12.1: Example Proline 29 and 35 mutations

Site-directed mutagenesis to Proline residues mutations on linker structures of NS5A.

Visual analysis of position in comparison to wildtype in MOE. DCV is shown in yellow, Pro29 and Pro35 shown in cyan as wildtype and each of the substitutions for Ala, Gly or Val are shown in orange.

The location of the Proline residues is shown in 12.2, were each of the Proline residues found in the experimental results are colour coded to the impact they had in the HCV life cycle. The site-directed mutagenesis experiments resulted in the highlight of key Proline residues that showed an impact on HCV replication and thus on HCV infection. This Proline residues were mainly in the linker connection between subdomain Ia and Ib or in the connection with the domain II. While, the Prolines showing a more wildtype-like (shown in example Figure 12.1 in cyan) behaviour were located in the linker connecting AH and domain Ia, this might be related to the high conservation of this Proline residues. Thus, their activity might be key for the binding to the cellular membrane through their interaction with the AH. This was further investigated with molecular dynamics results in results section (see 12.3). Furthermore, as you can observe in Figure 12.2, the location of the Proline residues as wt (shown in cyan), are in close proximity to the AH, and located in the binding site of DCV, this interesting correlation might indicate that the Proline residue might have a key role in maintaining the linker structure for further stability of the protein. Hence, this conserved activity might be key for the mechanism of action of DCV.

For the next step we use the same generated Proline substitutions and re-docked the DCV inhibitor into the structure of NS5A taken from [1] as mentioned before. This resulted in the selection of a re-docked poses of DCV that best fitted to the system,

(as stated) and the major event was described in steps (bullet points). Additional MD movies are further discussed in section 13. Each monomer is shown in a different colour. We based our studies on the Proline mutation analysis of the AH-DI linker, which is of major relevance.

12.1.1 P29A

The following sequence of snapshots describe the molecular dynamics for the system containing NS5A, DCV and P29A mutation on AH-DI linker of NS5A structure. Figure 12.3 shows a representative snapshot. Molecular dynamics video is described in the following steps.

- Step 1: beginning. The model with its starting position, were all components are inserted as the previous re-docked position of DCV with NS5A.
- Step 2: 15ns, slight movement of the AH on one of NS5A dimers.
- Step 3: 30ns, the AH undergoes slight movements making DI on both dimers come closer together.
- Step 4: 97ns, DCV loses contact with AH.
- Step 5: 135ns, DCV reconnects with AH.
- Step 6: 173ns, AH reconstitutes its original position, horizontally to where membrane is located.
- Step 7: 202ns, AH and DCV are brought closer to NS5A via closed conformation of linker.
- Step 8: 262ns, DCV changes configuration drastically, changing plane and location of side chains.
- Step 9: 297ns, DCV changes conformation, in contact with AH and NS5A DI, and has a closed conformation.

In conclusion, molecular dynamics on P29A showed major changes in the position of AH. This might be due to the lack cellular membrane position, which stabilizes its position. As a result of the AH movement we can see a movement in DI on each dimer, this might also cause a disruption in important interactions between AH and DCV. In fact, this observation can explain the experimental results, where we detect a reduction on HCV replication as compared to wildtype. See Figure 11.2. In general, the structure of NS5A

remains in same position while DCV changes conformation to fit into space between AH and linker. This observation can predict that when P29A is mutated, DCV binding site can change, thus, disrupting its activity.

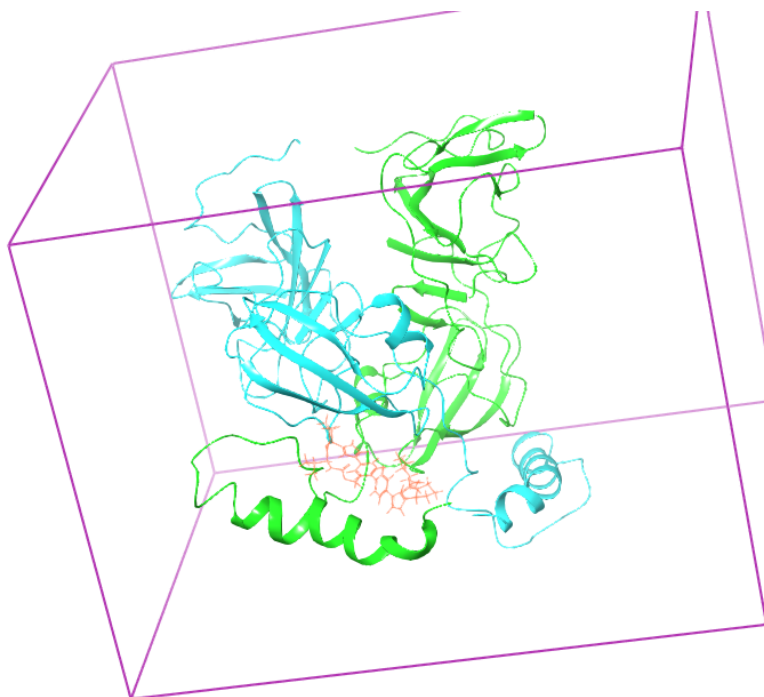


FIGURE 12.3: P29A

- Representative snapshot is shown, where as described, AH undergoes changes that provoke DI to rearrange. DCV fitting into interdomain region. Each monomer is shown in cyan and green. DCV in orange. MD total time was 300ns.

12.1.2 P29G

The following sequence of snapshots describe the molecular dynamics for the system containing NS5A, DCV and P29G mutation on AH-DI linker of NS5A structure. Figure 12.4 shows a representative snapshot. Molecular dynamics video is described in the following steps.

- Step 1: starting position where DCV is re-docked to NS5A.
- Step 2: 7ns, AH comes closer to DCV.
- Step 3: 15ns, DCV almost gets to an overlapping position with AH.
- Step 4: 60ns, DCV core rings change plane (from horizontal to vertical), side chains of DCV core are closer to the external amino acids chains of AH.
- Step 5: 109ns, AH loses contact with side chain of DCV, AH makes a turn.

- Step 6: 128ns, AH turns again facing DCV, which is closer to AH-DI linker, while DCV core rings remain in the horizontal plane.
- Step 7: 148ns, AH last loop continues changing conformation while DCV changes position relative to the AH-DI linker orientation (opening of the linker, by extension), provoking drastic conformational changes in the DI subdomains of both NS5A dimers.
- Step 8: 168ns, AH last loop continues changing conformation together with DCV, maintaining a tight interaction.
- Step 9: 273ns, AH loses last two loops, while DCV conformation changes accordingly. AH-DI linker is in the closed position bringing closer interactions between AH and DCV.
- Step 10: 291ns, AH without 2 of 5 loops, DCV changes conformation through the last ns together with AH. Mainly changing last chain, the core remains in plane, while the AH-DI linker opens and closes conformation bringing closer together the AH to DCV which maintains the interaction.

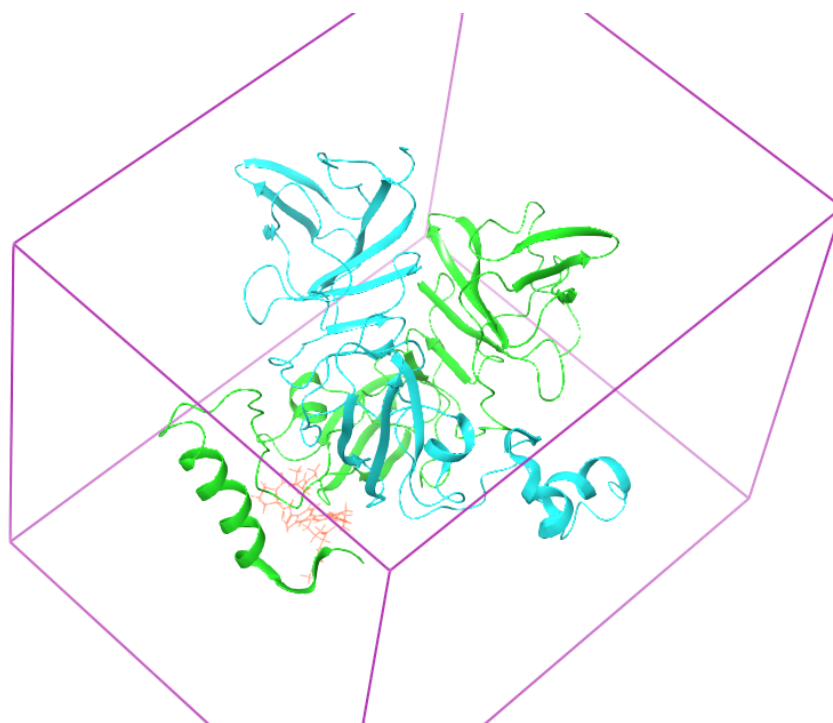


FIGURE 12.4: P29G

Representative snapshot of molecular dynamics is showing the interesting position DCV adapts after AH movement, as described. Each monomer is shown in cyan and green. DCV in orange. MD total time was 300ns.

Consequently, the MD of P29G mutation showed a major movement of the AH which impacts on the position of DCV. We observed drastic changes in the DCV position

which relate to the experimental results which show that this mutation can still have some replication at 72 hpe, in comparison to the other Proline 29 mutations, see Figure 11.2, where the values are not enough to reach wt. Additionally, the AH-DI linker main function is to bring together the AH to the space in between two NS5A dimers where the binding site of DCV is located, this happens when DCV is in a closed position, see Figure 12.4.

12.1.3 P29V

As before, the following sequence of snapshots describe the molecular dynamics for system the containing NS5A, DCV and P29V mutation on AH-DI linker of NS5A structure. Figure 12.5 shows a representative snapshot. Molecular dynamics video is described in the following steps.

- Step 1: beginning, starting position of DCV re-docked with NS5A.
- Step 2: 18ns, DCV structure is located in between the AH-DI linker and AH. Then there is a conformational change and DCV moves into the interdomain space (this term refers in this study to the area in between the DI of both NS5A dimers).
- Step 3: 28ns, DCV interacts with AH, this movement brings AH-DI linker to a closed conformation and which in turn moves the AH closer to DCV.
- Step 4: 45ns, the last loop of AH loses its conformation. DCV interacts with AH and the interdomain region, while AH-DI linker remains in a closed conformation.
- Step 5: 91ns, DCV changes conformation drastically and its position has almost no interaction with AH or the interdomain region (where binding site is located).
- Step 6: 173ns, AH reconstitutes its original position, in a horizontal relation to where cellular membrane is supposed to be located.
- Step 7: 202ns, AH plus DCV are brought closer to NS5A dimer via the closed conformation of AH-DI linker.
- Step 8: 262ns, DCV changes configuration drastically, which makes a change in its plane conformation and thus, in the location of the side chains.
- Step 9: 297ns, DCV changes conformation again, and it is in close contact with AH. NS5A DI is in a closed conformation.

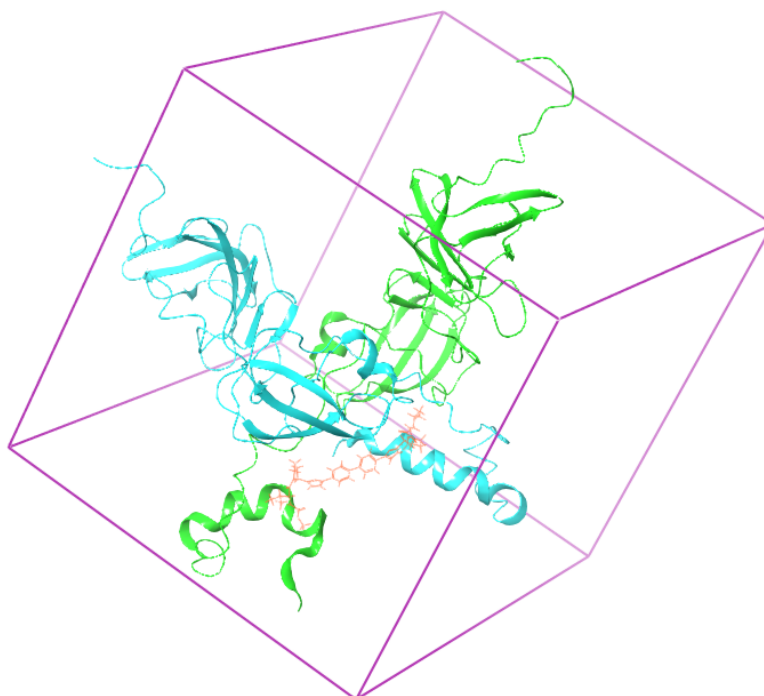


FIGURE 12.5: P29V

Representative snapshot molecular dynamics of mutation at P29V, where we observe DCV fitting into AH-DI linker and AH, as described. Each monomer is shown in cyan and green. DCV in orange. MD total time was 300ns.

As can be seen, the results on P29V molecular dynamics showed that NS5A dimer structure remains in position while DCV changes conformation to fit into space between AH and AH-DI linker. The connection with the AH changes through the MD, showing closer interactions of the compound and DI, see Figure 12.5. When using the MD to explain the experimental results, we found similarities with P29A, where both mutations showed no HCV replication or infection (compared to wt), and MD showed drastic changes of DCV, which correlates to the important role of this Proline residues in maintaining NS5A functionality, see Figure 11.2.

12.1.4 P32A

To continue, the following sequence of snapshots describe the molecular dynamics for the system containing NS5A, DCV and P32A mutation on AH-DI linker of NS5A structure. Figure 12.6 shows a representative snapshot. Molecular dynamics video is described in the following steps.

- Step 1: beginning DCV located in between linker and AH region.

-
- Step 2: 6ns, DCV side chains and core moved to a closer proximity with AH, as the AH-DI linker extends into an open conformation.
 - Step 3: 20ns, DCV in close proximity to AH, AH-DI linker keeps extended position, a side chain of DCV makes contact with the second AH (on the other NS5A monomer).
 - Step 4: 48ns, DCV in only in contact with AH, AH-DI linker is in a total open conformation, full extension. AH loses the last loop conformation, and, thus, the contact to second AH (on facing NS5A monomer) is lost.
 - Step 5: 77ns, AH-DI linker is closer to AH, DCV remains in contact with AH.
 - Step 6: 99ns, AH-DI linker in a full extension conformation, allows the opening of the AH, which leads the side chains of DCV free into the interdomain region while the core of DCV remain in contact with AH.
 - Step 7: 123ns, DCV structure is in a conformation that allows the connection between the two AH located in both dimers. AH-DI linkers are completely extended and both lost the last loop of the AH configuration, this movement brings the DI of both subunits to collapse into each other.
 - Step 8: 181ns, DCV undergoes an insertion into AH the AH-DI linker loses its conformation into a complete extension. AH loses last loop and, thus, DCV lies in AH horizontally but with no contact to the AH-DI linker.
 - Step 9: 236ns, DCV core makes contact again with the AH-DI linker but continues to lie in the AH in a horizontal position.
 - Step 10: 273ns, DCV shifts to the interdomain region between AH-DI linker and AH making contact with both structures. The last loop of AH is lost and the AH-DI linker remains in an extended configuration. DI of both subunits are collapsing into each other.

P32A mutation changes drastically the structure of the key components: AH, interdomain region and AH-DI linker, which stabilize DCV into the binding pocket. This dramatic change of the AH and the key components of the system lead to an overall change of the whole NS5A protein structure. When analysed in detail, the linker seems to be several times in close contact with the interdomain region making the whole structure shrink. This result correlates with the experimental data, where we observe no HCV replication or infection (compared to wt), which might be explained by the rearrangement of NS5A structure, see Figure 11.2.

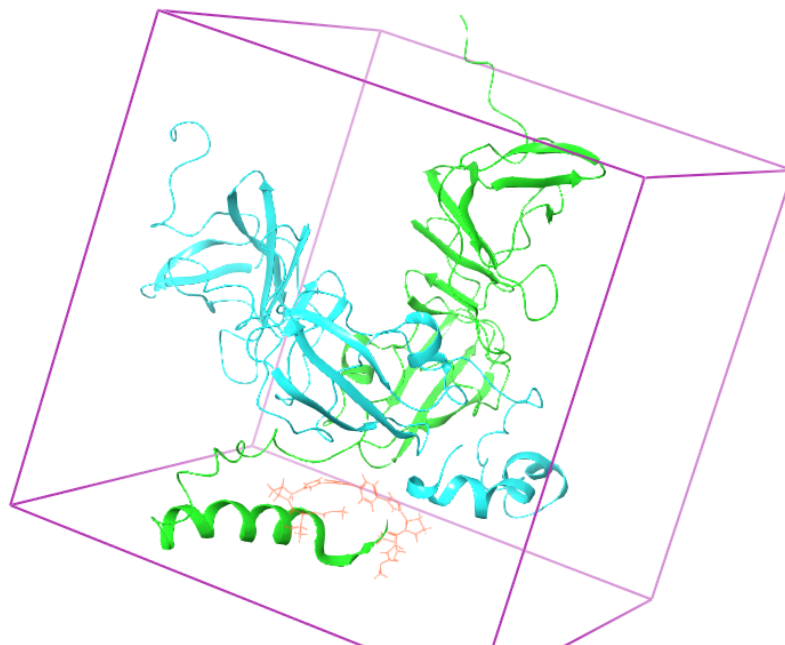


FIGURE 12.6: P32A

Representative snapshot of mutation at P32A, where we observe DCV in contact with AH. AH loses loop structure. Additional changes in DI-DII linker of NS5A structure, as described. Each monomer is shown in cyan and green. DCV in orange. MD total time was 300ns.

12.1.5 P32G

In this section we have the sequence of snapshots which describe the molecular dynamics for the system containing NS5A, DCV and P32G mutation on AH-DI linker of NS5A structure. Figure 12.7 shows a representative snapshot. Molecular dynamics video is described in the following steps.

- Step 1: beginning, DCV in the space between linker and AH.
- Step 2: 15ns, DCV structure is in contact with the AH-DI linker, into an extended position where it interacts with the interdomain space.
- Step 3: 30ns, DCV is located in the interdomain region where it interacts with AH-DI linker. There is no contact with AH.
- Step 4: 80ns, DCV is in close proximity with AH-DI linker located in the interdomain region, this opens DI structure on both subunits of NS5A. The AH-DI linker is in a complete extension in an open conformation.

- Step 5: 98ns, AH loops can change conformation and open into an extended conformation, this changes the location of DCV core which is interacting with AH-DI linker and the interdomain region.
- Step 6: 142ns, DCV remains in contact with AH-linker and in the interdomain region.
- Step 7: 168ns, DCV structure plane turns into a vertical position and interacts with AH, the last loops of the AH are in a twisted position. DCV side chains are located in the interdomain region.
- Step 8: 214ns, DCV returns to its starting position in between the AH-DI linker and the AH. The last loop of AH loses its starting conformation.
- Step 9: 240ns, DCV interacts with the AH-DI linker, while the AH and the interdomain region are all conforming the binding site for DCV. DCV in U-like conformation, allowing interaction with all the key components of the binding site.
- Step 10: 286ns, DCV remains in same position. AH twisted towards membrane location.

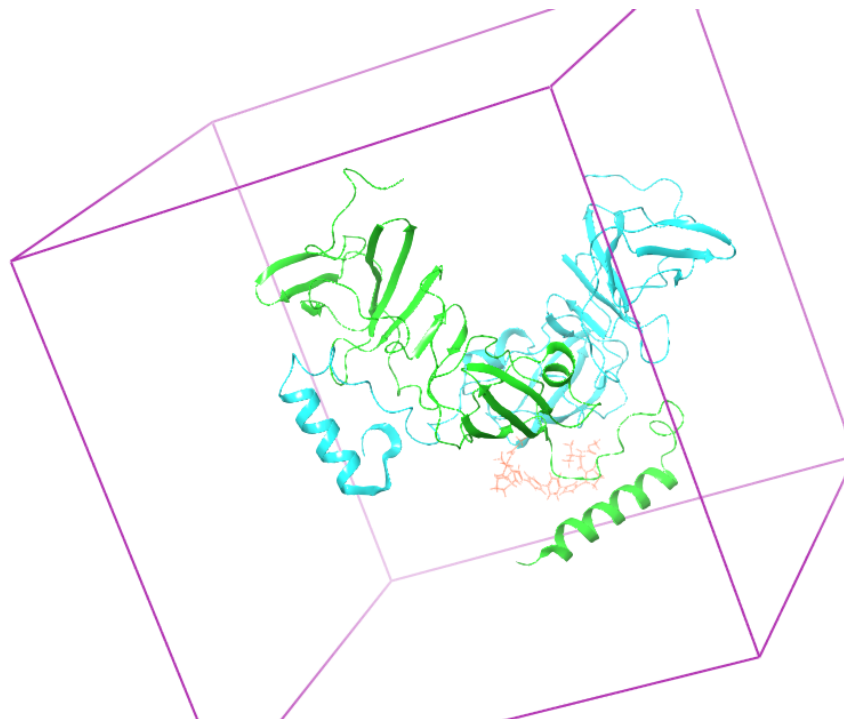


FIGURE 12.7: P32G

Representative snapshot of mutation at P32G, showing the open conformation of AH-DI linker, which can change the interacting points in the binding site of DCV. Each monomer is shown in cyan and green. DCV in orange. MD total time was 300ns.

Molecular Dynamics on P32G showed a rotational change on the AH which brings DCV in close proximity to the interdomain region. This results in a opening of the AH-DI linker. All together, this results correlate to the experimental results, see Figure 11.2, because we can observe no HCV replication or infection due to the structure change of NS5A or might be related to the overall mutation on the 32 position, as we observed similar pattern with P32A mutation.

12.1.6 P32V

To continue, the following sequence of snapshots describe the molecular dynamics for the system containing NS5A, DCV and P32V mutation on AH-DI linker of NS5A structure. Figure 12.8 shows a representative snapshot. Molecular dynamics video is described in the following steps.

- Step 1: beginning, DCV is located at the starting position.
- Step 2: 14ns, DCV structure moves into the interdomain region. The AH-DI linker is in an extended configuration and the AH is interacting with DCV.
- Step 3: 34ns, DCV interacts with AH-DI linker in an open conformation, DCV is located under the interdomain region, in the binding site.
- Step 4: 51ns, DCV remains in same position. AH loses the last loop on its structure.
- Step 5: 72ns, DCV turns core structure into a vertical position and it shifts configuration to interact with AH-DI linker, AH and the interdomain region, making contact with all the key components on the binding site.
- Step 6: 100ns, DCV is in a cross position from AH where it remains through the MD. The AH is in a twisted position interacting with the AH-DI linker and it is located close to the interdomain region.
- Step 7: 120ns, DCV is closer to the AH. The AH-DI linker is in close position to DCV, which remains close to the interdomain region.
- Step 8: 152ns, DCV is around the AH interacting with the AH-DI linker.
- Step 9: 213ns, AH-DI linker in U-like shape, this movement brings it closer to the interdomain region where DCV locates in a crossed position.
- Step 10: an interesting insertion of AH into the interdomain region by AH-DI linker movement. DVC interacts with AH-DI linker and remains located in the interdomain region.

Notably the AH-DI linker conformation is in an open or closed conformation, this movement regulates the shift in the position of DCV. Additionally, both domains from dimers are brought closer together or further apart from this movement. Together these movements might influence the position of the AH in relation to the membrane location. The MD showed that this movement of both AH-DI linkers is important for stabilizing NS5A structure. Thus P32V mutation, as seen in the experimental data, has an impact in HCV replication and HCV infection, which can be explained by the importance of the dynamics in stabilizing NS5A protein.

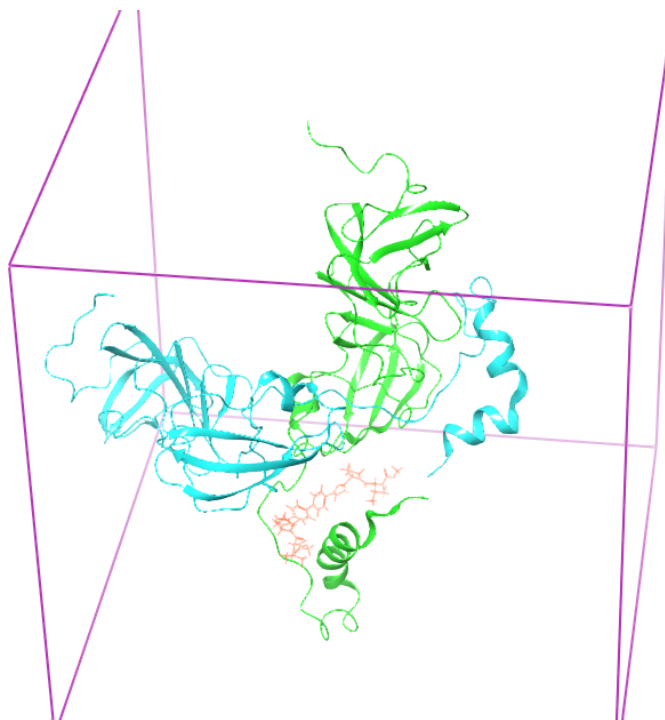


FIGURE 12.8: P32V

Representative snapshot of mutation at P32V, open position of AH-DI linker, shifting DCV position, as described. Each monomer is shown in cyan and green. DCV in orange. MD total time was 300ns.

Overall what we observed with mutations on Proline 32, is that there is a direct impact on HCV replication and infection as observed in experimental results. In addition, there are extensive structure rearrangements which could be key to the mode of action of DCV. This can be explained by the MD, as the binding pocket is located in close relation to each of the key components in the system, the AH, inter domain region and AH-DI linker positions respectively. Therefore, Proline 32 mutation is shown essential for HCV NS5A protein.

12.1.7 P35A

The following sequence of snapshots describe the molecular dynamics for the system containing NS5A, DCV and P35A mutation on AH-DI linker of NS5A structure. Figure 12.9 shows a representative snapshot. Molecular dynamics video is described in the following steps.

- Step 1: beginning, DCV is located in the binding pocket making contact with the key elements of the pocket: the AH-DI linker, AH, and the interdomain region.
- Step 2: 30ns, DCV moves into a closer contact position with to AH.
- Step 3: 51ns, there is a side chain on DCV which is inserted into the interdomain region, the rest remains in contact with AH and linker.
- Step 4: 92ns, DCV remains in a stable configuration in the binding pocket between DI of each NS5A subunits.
- Step 5: 139ns, very stable configuration of key components, DCV remains in the same position, in contact with all the key elements in the binding and affinity pocket.
- Step 6: 185ns, slight movement of DCV structure which brings closer together the side chains and the core.
- Step 7: 196ns, DCV moves accordingly to AH-DI linker in a closed position which brings DCV to a compact configuration, retaining the contact with the AH, AH-DI linker and the interdomain region.
- Step 8: 200ns, DCV core changes plane to horizontal, the contact with the 3 key elements remains.
- Step 9: 244ns, DCV remains in a horizontal position, DCV overall structure maintains contact with key elements.
- Step 10: 279ns, AH-DI linker shifts into an extended position away from AH in a horizontal manner, into a slightly more vertical position maintaining interaction with the key elements of the binding pocket.

This mutation does not show drastic changes in the conformation, and more importantly shows that DCV maintains a stable position in the binding pocket which allows a continuous interaction and/or contact with the key elements of the system. This fact is what keeps DCV in the key position for its activity efficacy. Therefore, this mutation could have an impact in the replication of the virus as on the efficiency of DCV activity. This MD observations correlate to the experimental data seen in Figure 11.2.

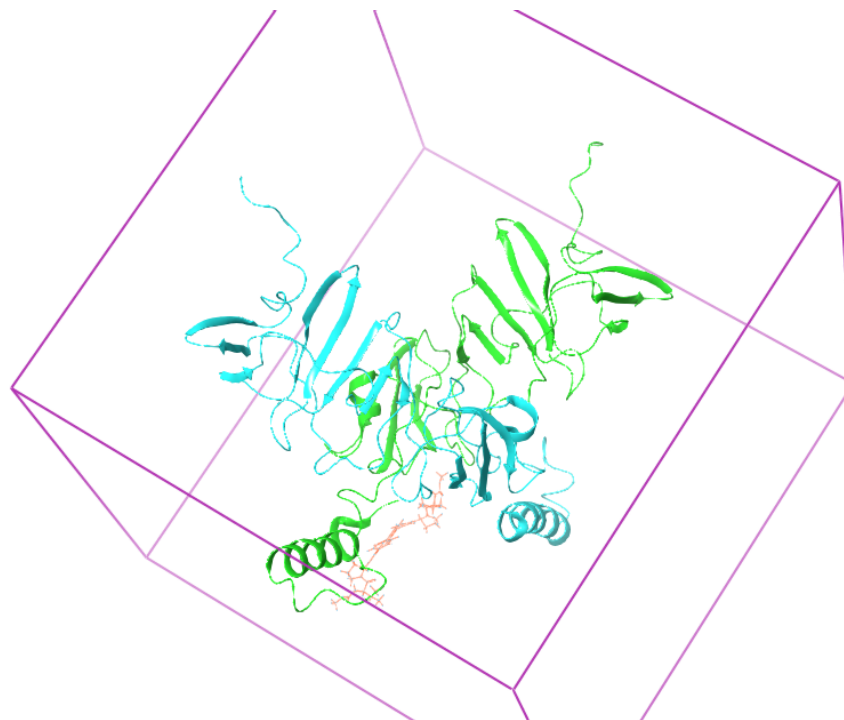


FIGURE 12.9: P35A

Representative snapshot of mutation at P35A, showing DCV in the precise binding site, making connections to the key elements in the pocket, as described. Each monomer is shown in cyan and green. DCV in orange. MD total time was 300ns.

12.1.8 P35G

The following sequence of snapshots describe the molecular dynamics for the system containing NS5A, DCV and P35A mutation on AH-DI linker of NS5A structure. Figure 12.10 shows a representative snapshot. Molecular dynamics video is described in the following steps.

- Step 1: beginning, DCV and key elements of the system remain in beginning position.
- Step 2: 46ns, DCV remains in close contact to key elements in the binding pocket.
- Step 3: 74ns, movement of AH towards DI on one of the dimers shifts location of DCV closer to interdomain region.
- Step 4: 123ns, key elements maintain the structure, DCV moves towards the AH-DI linker.
- Step 5: 141ns, DCV side chains and core do not undergo major changes and key components are stable. DI shifts location according to AH.

- Step 6: 186ns, DCV moves slightly closer to the interdomain region maintaining contact with AH.
- Step 7: 202ns, key components maintain DCV structure in binding site.
- Step 8: 230ns, DCV does not shift plane and remains in binding pocket. AH-DI linker moves into an extended position.
- Step 9: 267ns, AH remains horizontal to the cellular membrane position, keeping DCV in line. AH-DI linker extension provokes movement of DI of NS5A.
- Step 10: 284ns, AH-DI returns to a less extended position, where key elements maintain the binding site where DCV is located.

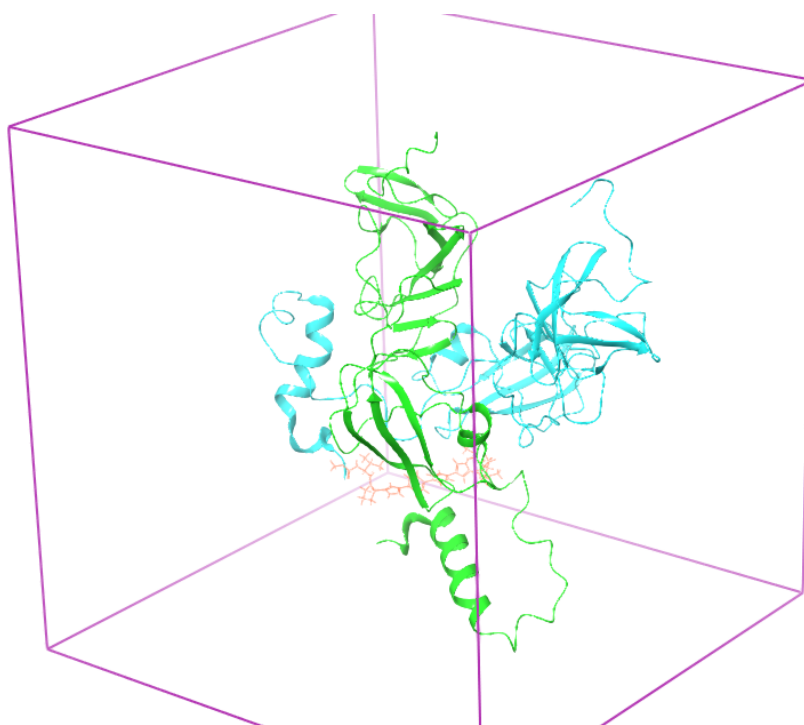


FIGURE 12.10: P35G

Representative snapshot of mutation at P35G, a slight opening of the AH-DI linker. DCV remains in binding pocket making contact with key elements, as described. Each monomer is shown in cyan and green. DCV in orange. MD total time was 300ns.

P35G mutation did not show major NS5A structure rearrangements, maintaining stable the binding pocket of DCV, which correlates to the stability of the mutation on experimental results. When P35G is mutated there is a decreased in normal (wt) HCV replication and infection, but the virus can still have a detectable level of HCV replication and infection. Molecular Dynamics on this mutation show that Proline 35 might not have an essential role on HCV life cycle, but it is essential for the maintenance of DCV's binding pocket.

Snapshots on mutation P35V are not shown due to problems in the re-docking process of DCV into the NS5A structure. Furthermore, the molecular dynamics could not be performed. Improvements on some amino acid interactions can be done to perform a re-docking of DCV.

To conclude we have observe that: mutations on P29X: showed stability in DCV structure. Although no major changes on the conformation of NS5A DI subdomains was seen. P29G, showed that the AH loses the conformation of the AH loops. Additionally, DCV was not in contact with the interdomain region which is the key component of the binding pocket. Mutations on P32X: This mutation showed more drastic conformational changes that would challenge the conformation of the DI subunits in the dimer formation. The AH showed drastic changes in conformation that could suggest the insertion of this into the cellular membrane. Finally, mutations on P35X: This mutation does not alter the structure of NS5A, this might be due to the stability of DCV into its binding pocket and the stability through the dynamics in the contact with the key elements which maintain the molecule in the correct position for its activity.

Altogether, this experiments show that Proline mutations significantly change the position of DCV as seen by molecular dynamics, implicating a different binding site of the drug to the protein, which can have a direct effect on the efficiency and efficacy of the binding of the drug. Interestingly, some of this mutations have a higher impact than others, as already mentioned this might be due to the steric clashes of the amino acid itself or other interactions.

Ultimately, with this experiments we want to show the potential mutations on essential Proline residues that might not only change the position of DCV in its binding pocket, but that might also change its properties. Therefore, we studied DCV essential properties and its impact on the overall structure of NS5A protein.

12.2 DCV structural properties

The following studies are focused on the inhibitor, DCV, and its interactions with Proline residues in NS5A protein. DCV structure ligand interactions showing close proximity and key role of identified Proline residues. These observations show that the effects on essential Proline residues 29, 32 and 35 can potentially change the binding pocket. As our previous results show, this mutations not only change the position of DCV in the binding pocket but its further interactions with the amino acids in the binding pocket. As seen in Figure 12.11, P29, P32 and P35 have a receptor exposure to the interacting zone of DCV. Additionally as previously shown, this Proline residues, showed also a

reduction in HCV replication when mutated, which might be due to its essential role in the stability of the binding pocket.

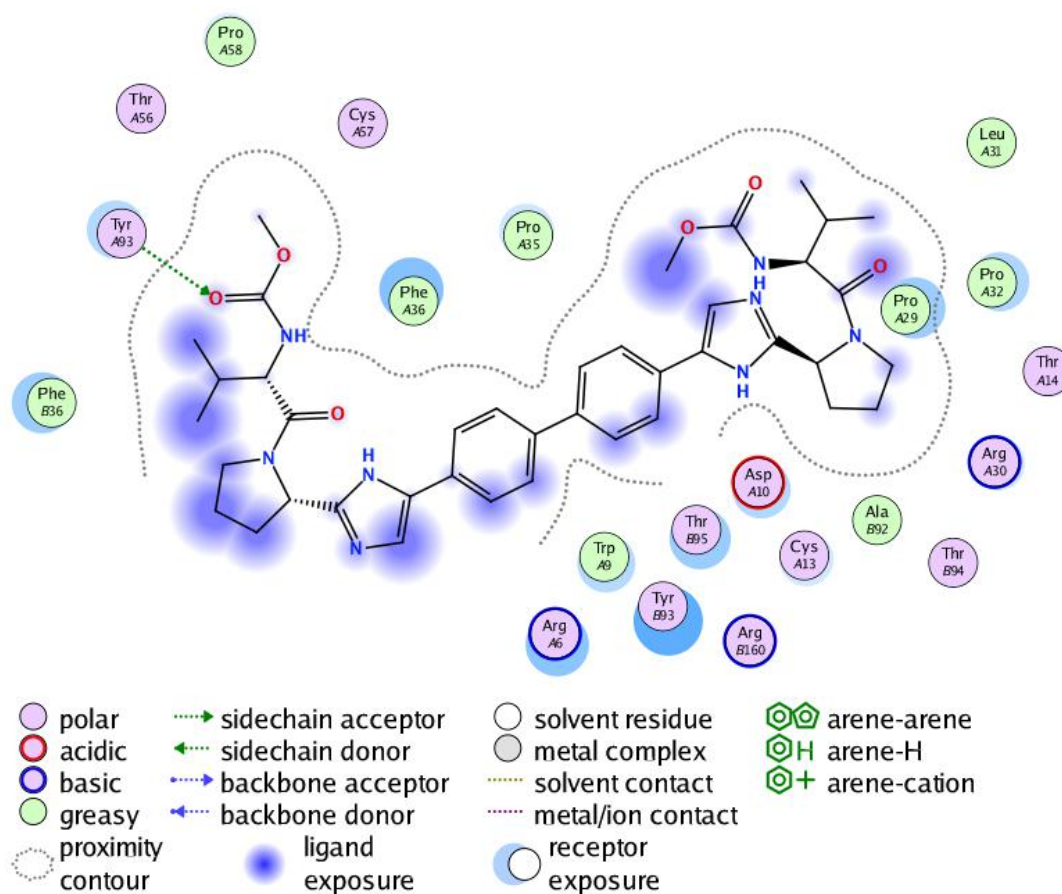


FIGURE 12.11: Daclatasvir interaction map generated in MOE[®], showing important interacting residues. Symbols are characterizing the properties of the amino acids in the proximity of DCV.

12.2.1 DCV binding pocket

Linker AH-DI is the anchoring region which is involved not only in the membrane association but apparently also in the proper docking of DCV. The studies on Proline mutations suggest that AH-DI linker structure is key to ensure the binding pocket of DCV as well as its interaction with the cellular membrane. Our Molecular Dynamics studies were limited, but we did not observe a major conformation change when studying the NS5A dimer or the amphipatic helix alone with the cellular membrane. Re-ensuring that the AH is the main anchor to the cellular membrane giving NS5A stability and DCV a binding pocket. Together with the data on previous experiments in this study (Section 11.1), we can suggest that Daclatasvir binding pocket is stabilized by the proper membrane association. Thus, the AH has a key role in the mode of action of NS5A inhibitors. Therefore, we analyzed the conformation of Daclatasvir binding pocket in

NS5A structure via visual inspection of the interacting amino acids and close contacts in NS5A dimer. In Figure 12.12, we observe the position of docked DCV in relation to the Proline mutations positions.

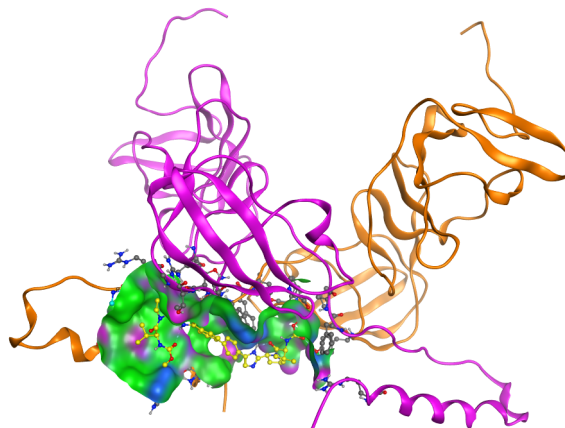


FIGURE 12.12: NS5A dimer plus DCV binding pocket. A. DCV molecule is in yellow, its binding site is in green and NS5A dimer in magenta and orange. Proline mutations are marked in cyan.

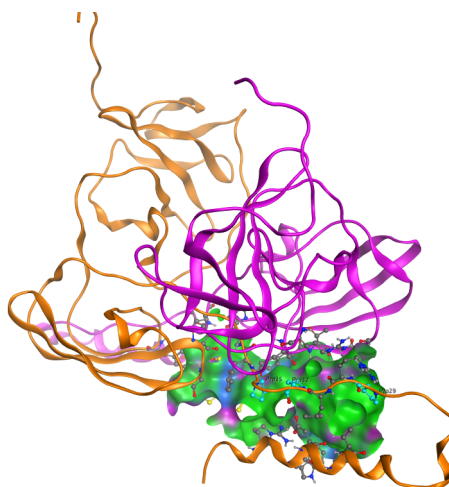


FIGURE 12.13: NS5A dimer plus DCV binding pocket. B. Different angle, DCV molecule is in yellow, its binding site is in green and NS5A dimer in magenta and orange. Proline mutations are marked in cyan.

Although together all the results we gathered in the Proline mutation studies, are strongly suggesting that this Prolines have an essential role in the stability of the binding pocket and in the structure of the linker connecting the amphipatic helix with NS5A; the cellular membrane in this whole picture is not taken into account. And regarding the importance of NS5A functions, the cellular membrane must be a point of study to complete the overview of the effects on NS5A inhibitors. Therefore, we studied the NS5A protein in a dimer form together with the cellular membrane. For this purpose we use

computational methods to predict and formulate the structure of NS5A on the cellular membrane. By visual inspection we observed that NS5A dimer is positioned on top of the cellular membrane being the AH the anchor to it. The Molecular Dynamics studies showed that the dimer moves through but does not detach from the cellular membrane. The linkers give flexibility to the whole protein providing a bridge-like structure which could be useful for the DCV molecule to access the binding pocket.

Unfortunately, this system is too unstable to analyse via MD, and it is too big to predict further interactions and conformational changes. For this reason, we decided to reduce the system into the analysis of just the AH in presence of the cellular membrane.

12.3 Amphipatic helix and membrane simulations

As computational tools can be powerful enough to get big systems to be studied by molecular dynamics, it has its limitations. The bigger the system the more powerful the computational tools and so the more time the studies take. For the purpose of the present analysis in here, we narrow our study to focus on the interaction of the amphipatic helix containing the Proline rich linker, which is the main anchoring part of NS5A to the ER-like membrane, taken from <https://www.ucalgary.ca/tieleman/publications>.

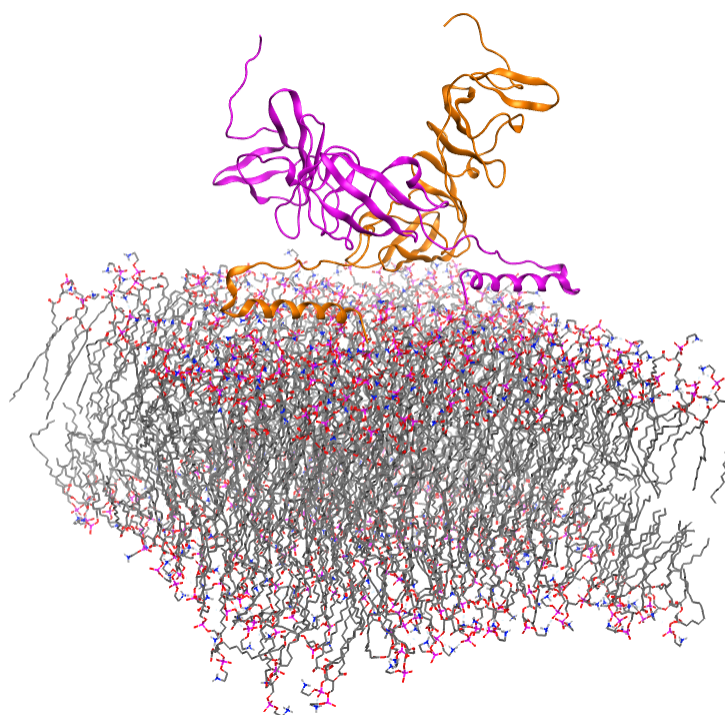


FIGURE 12.14: NS5A dimer containing AH and linker on cellular membrane. NS5A dimer built with AH and Proline-rich linker on top of POPE cellular ER membrane-like. Solvent water.

12.3.1 Amphipathic helix orientation in cellular membrane

NS5A is tightly associated with the ER membrane and behaves as an integral membrane protein, with a few more contacts besides the amphipathic helix. Likewise, the hydrophobic and basic residues following the NS5A amphipathic alpha-helix could participate in membrane association. Moreover, residues located downstream of amino acids 1 to 31 were determined to interact with the cellular membrane [175]. The amphipathic helix is the main anchor, yet the region can be extended to ensure the membrane association, creating a platform with hydrophilic residues and asymmetric distribution of charged residues on the cytosolic side of the N- terminal [33].

As mentioned before in section 2.7.5.2, at the N-terminal region of NS5A contains 30 amino acid residues which serve as a membrane anchor for NS5A, forming an in-plane amphipathic helix embedded into the cytosolic leaflet of the cellular membrane bilayer. Previous studies [15, 175] on NMR data showed that the anchoring helix is five residues from the N- terminus of the D1 structure which suggests it is close to the membrane, where it can possibly interact with RNA. In the same study [175], it is suggested that the interaction might be through the D1 dimer groove which is facing away from the cellular membrane. Interestingly, this groove can act as an RNA-binding pocket because it is a highly basic region, making an electrostatic contact with the basic region of the groove [37].

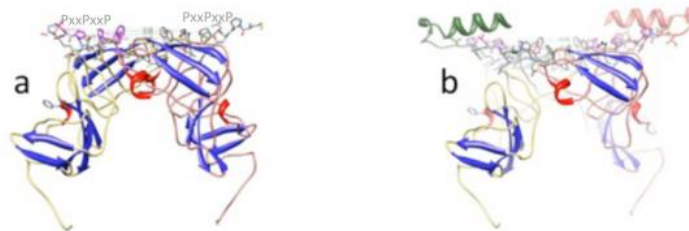


FIGURE 12.15: NS5A dimer with Proline-rich linker. AH-linker homology based on PxxPxxP. Taken from Nettles et al 2014, [1].

So for our studies we decided to have the amphipathic helix together with the Proline-rich linker together with the cellular membrane for the molecular dynamics. As shown in Figure 12.16, orientation of AH could be vertical or horizontal, although previous data have shown that the AH is in-plane from the cellular membrane, we explore both structures on molecular dynamics to determine the system's limitations. As predicted before, the amphipathic helix structure lies on top of the cellular membrane, we ruled out the vertical position because the molecular dynamics showed no systematical pattern that would make sense with previous and experimental data. Thus, we continue with the horizontal model of AH and cellular membrane.

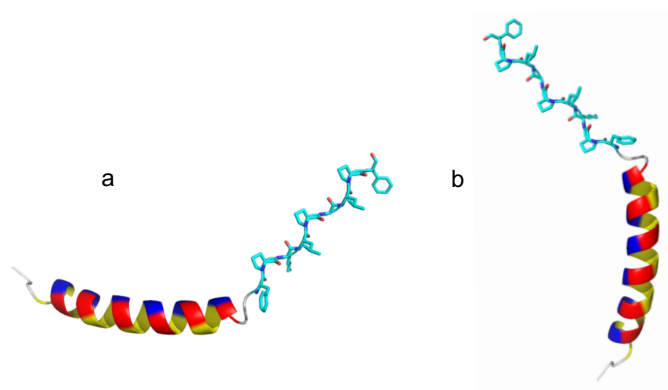


FIGURE 12.16: Amphipatic helix orientation
AH orientation with Proline-rich linker. a. Horizontal orientation and b. Vertical orientation. Taken from [176].

12.3.2 Amphipatic helix and membrane association

The model was constructed manually including the AH in a horizontal position together with the POPE cellular membrane (as described in 10.11.3). We ran molecular dynamics with established conditions as shown in Methods section 10.11.3. The system looks like in Figure 12.17, where the conditions were the same as set up for all the molecular dynamics, to keep consistency.

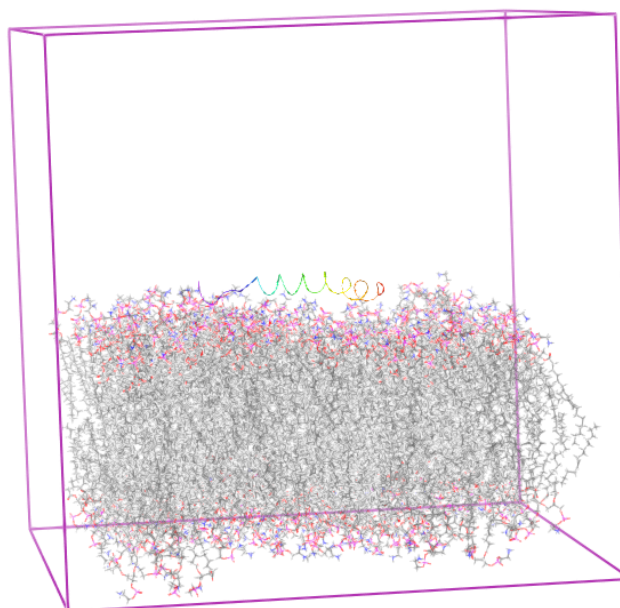


FIGURE 12.17: Amphipatic helix and membrane
AH construct including Proline rich linker in starting position of built-up model in a horizontal orientation from the POPE cellular membrane. This system was used as set-up for Molecular Dynamics.

The molecular dynamics run by Desmond showed what others and us have predicted, the amphipatic helix besides being the major anchor to the membrane it is flexible and changes conformation during the 500ns of MD, Figures 12.17, 12.18, 12.19, and 12.20, where we can see that the AH-membrane association, undergoes several structure changes. This changes are the basis to fulfill NS5A main functions, as the protein can move to allow interactions and thus, open and close conformations that also allow the binding of NS5A inhibitors, including DCV. Because of systems limitations we studied only the association of AH to the membrane, but we can predict that the AH has a flexibility that the linker provides, which can be crucial for the binding of DCV as seen in the Proline-mutations molecular dynamics, following Figures. .

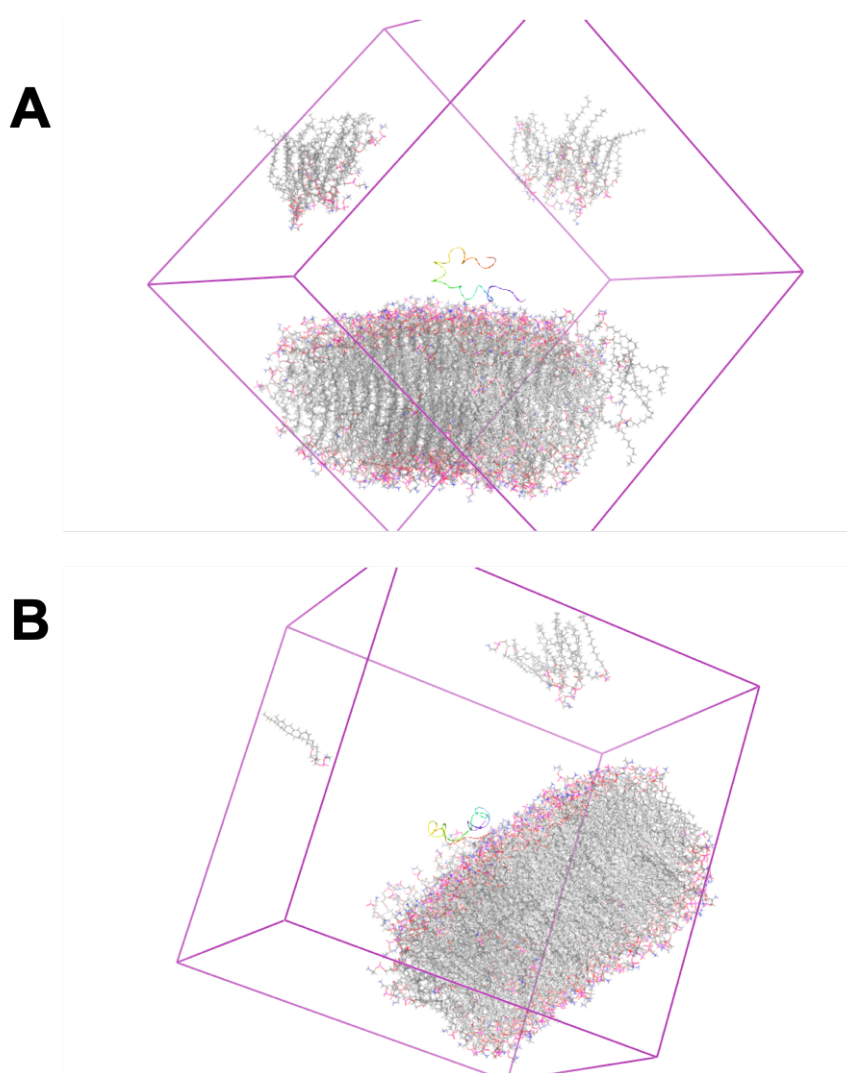


FIGURE 12.18: Molecular Dynamics of AH-Proline rich linker (AH-DI linker)

A. Snapshot taken at 72ns, showing AH on top of POPE cellular membrane. As described in the text, AH is in close contact with the cellular membrane, amino acids in loop are shown interacting with hydrophobic lipid groups on cellular membrane. B. Snapshot taken at 244ns, where AH-DI linker (Proline-rich linker), is inserting in cellular membrane.

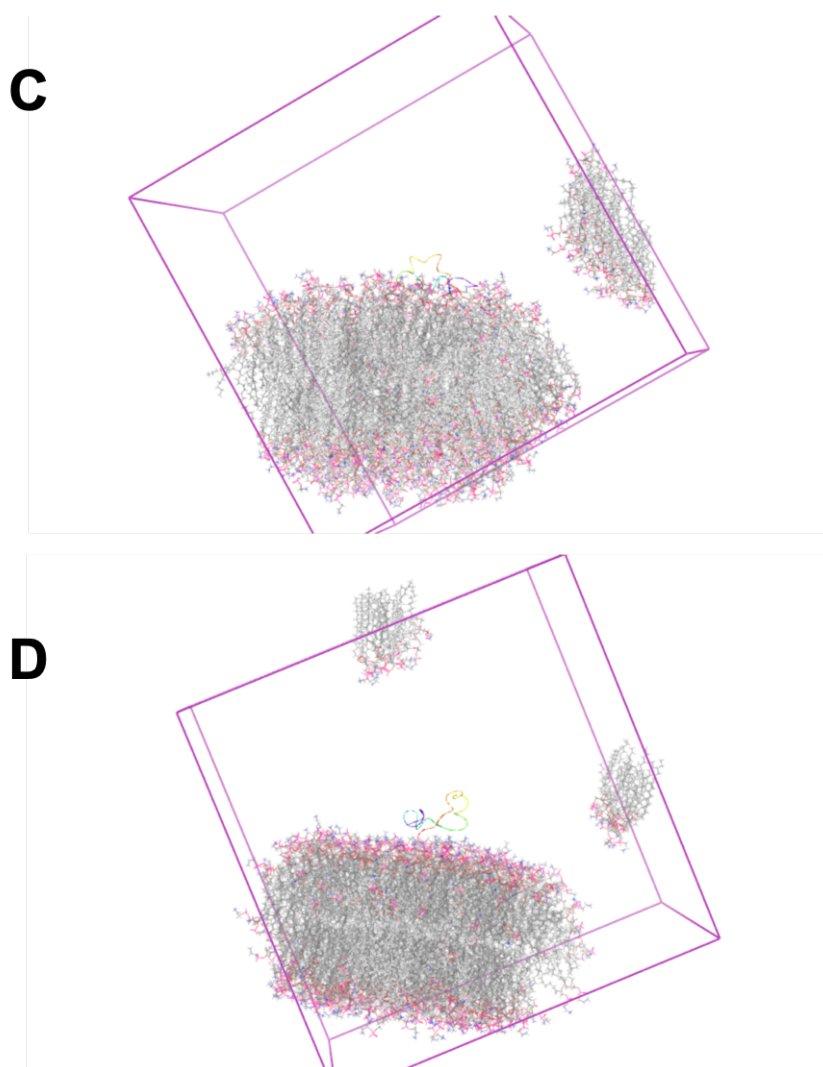


FIGURE 12.19: Molecular Dynamics of AH-Proline rich linker (AH-DI)

- C. Representative snapshot taken at 331ns, where the majority of the AH is inserted in the cellular membrane. D. Snapshot taken at 443ns, where AH is in contact with cellular membrane via the Proline-rich linker (AH-DI), through the dynamics we observe this movement of the AH.

However, molecular dynamics can just predict and model what we include in the system and it might be that the whole protein undergoes several other conformational changes which might also be the reason for the proteins functions. Regardless, our MD showed that the linker plays a major role in maintaining the protein attached to the cellular membrane via the AH. As mentioned previously, resistance mutations arise in this important part of the protein, the molecular dynamics show its relevant role in keeping the membrane association, which has not been studied before. This results show that the protein's association to the membrane might be essential to the mode of action of the inhibitor Daclatasvir.

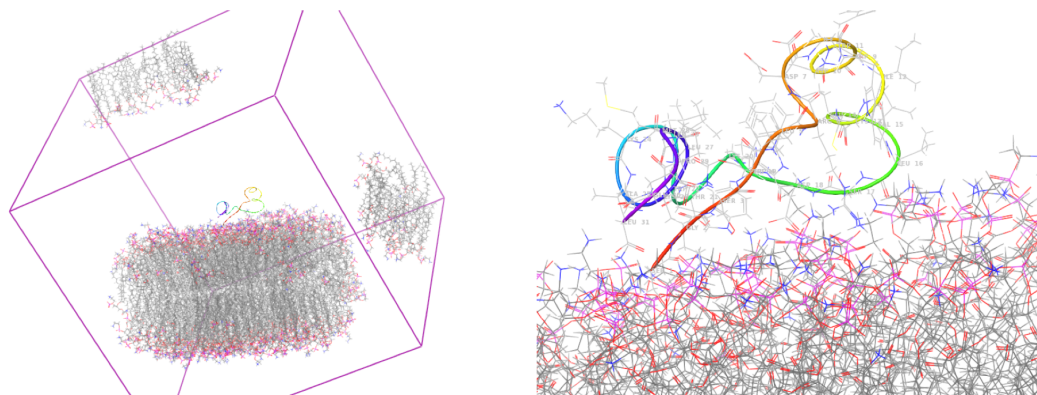


FIGURE 12.20: Molecular Dynamics of AH-Proline rich linker (AH-DI)
 Representative snapshot taken at 481ns of molecular dynamics, where the amphipatic helix sits on top of the membrane on a horizontal manner making contact with the cellular membrane mostly via the Proline-rich linker (AH-DI).

Our studies generated a more precise model for the mechanism of action of NS5A inhibitor, Daclatasvir, where importantly Proline mutations showed an impact in HCV life cycle. We could prove this by molecular dynamics where we followed each mutation and by looking at HCV replication and infection. The correlation of these observations suggest that some of the mutations might have an effect on HCV life cycle due to a conformational change of the AH-DI linker. The mechanism behind this involves the attachment of the AH to the cellular membrane, as seen from the AH and membrane association results. Furthermore, we could follow this AH-membrane association via molecular dynamics, where we could predict the importance of the Proline-rich linker not only in the maintenance of NS5A structure but additionally in the binding of DCV inhibitor, which can be use for the improvement of future antiviral development. Moreover, to our understanding and already proven by others [117], we observed the inhibitory effect of DCV on the envelopment of HCV viral particles. In addition to the already know efficacy of NS5A inhibitor, DCV, we could explain its high potency is due to the major conformational changes that NS5A undergoes which are crucial for its mode of action. Particularly, we reveal the importance of key elements (amphipatic helix, AH-DI linker and the interdomain region) in the binding site, that could be target of future antivirals against HCV. Altogether the present studies, result in a better understanding of the mechanism of action of NS5A inhibitor DCV, plus expanding the knowledge on the infection dynamics.

Chapter 13

Discussion

13.1 HCV assembly impaired by DCV activity

Chronic hepatitis C infection remains a major public health threat, requiring research and development of more specific and effective inhibitors. The emergence of resistance mutations and the divergence in HCV variant genotypes, makes this task significantly difficult [60, 127, 177]. However, cell-based HCV replicon, and the discovery of highly potent direct acting antivirals are now the best antiviral therapy for HCV infection [82]. The pico-molar activity of NS5A inhibitors was discovered in 2009, since then several underlying mechanisms of action had been proposed. Mainly two hypothesis have now been confirmed: first, the antiviral mechanism targets NS5A activities regarding HCV replication [41, 127, 131], second, the mode of action targets only assembly of HCV virus [118, 126]. Soon, the confirmation of the impairment of HCV replication by NS5A inhibitors led to one open question: what is the effect of NS5A inhibitors on HCV assembly of viral particles. Our group and other [117] tried to target this question and elucidate the mechanism of action of NS5A inhibitor, DCV.

Therefore, we wanted to study the impact of DCV on HCV assembly process, whether the effect of NS5A inhibitors was affecting only the assembly process. For this purpose we use SOF as positive control on our titrations studies to make the effect of DCV evident, since as already known, SOF is a drug targeting NS5B, thus, only inhibiting HCV replication. We confirmed that SOF had an effect in HCV replication and does not interfere with HCV viral particles assembly process. Furthermore, we established EC_{50} values for SOF and DCV in our HCV electroporation protocol, which we used to prove that DCV does not only inhibit replication but also affects assembly of viral particles by blocking their envelopment, which was confirmed at the same time by Boson *et al*, in

2017. In addition, our titration experiments, showed that DCV and SOF achieved the optimal concentrations that can be use in combination therapy [178, 179].

Additionally we showed that there is an evident peak of DCV inhibition at 24hrs post transfection, where we can detect a decline on HCV replication and infection, coherent to what described in literature [126, 131]. Finally, we showed that NS5A assembly functions are blocked by DCV using several biochemical assays which confirmed that DCV had an effect on HCV assembly, specifically on the envelopment of HCV viral particles. Altogether, these experiments showed and support what others also proved [117], DCV has a dual mode of action targeting NS5A protein activities. The mechanism of action behind this dual mode of action was also described by Boson *et al* [117], where DCV was shown to be inhibiting the envelopment of viral particles by blocking the transfer of the viral genome to the assembly sites. The outcome of inhibiting both replication and assembly of viral particles results in the clustering of HCV proteins because they cannot exit. Therefore, this dual mode of action of DCV explains the efficacy of the drug.

The efficacy of DCV as an antiviral agent has been observed when using a single ascending-dose in viral load 24h after drug administration in patients receiving a 100-mg dose [36, 126]. This studies show that after *in vivo* administration of DCV, HCV RNA declines with extreme rapidity, falling approximately 2 logs within the first 6h post dosing, followed by a slower phase of decline [131]. These can be now explained by our observations, since DCV can effectively block replication of viral HCV RNA and virion assembly [127]. Likewise, we observed that time of drug addition affects DCV inhibition of HCV infection. The envelopment of viral particles was disrupted already at 24 hpi, were we see a slight decline of DCV effect. Hence, when virus assembly is not blocked efficiently, there is a continued release of new viral particles, which is why we see a delay after treatment. A more precise time of drug addition could target both processes, replication and assembly, which can improve the dual action of the inhibitor. Therapy using other DAA inhibitors can also be improved by the time of dosing DCV in combination therapy.

A big remaining question regarding NS5A is its oligomerization state, as reported by others [37, 38, 127], evidence of a higher oligomer formation of NS5A protein has been hypothesized, however no prove of this oligomer has been made. Our results showed evidence of the formation of high molecular weight oligomer of NS5A protein under PFA treatment. We found that the optimal concentration of PFA is around 2% when treating HCV wt genotype construct and 3% for the resistant mutant Y93H. The smear detected in the experiments is an indication of oligomer formation, which are present in both constructs at different PFA% concentrations. Moreover, when using 99 °C, the smear disappeared into more defined bands, this suggested that there are several molecular

weight NS5A protein detection [40, 48]. There were no evident features that the resistant mutation on Y93H could affect the oligomer formation. However, the experiments were not entirely conclusive and for future experiments PFA different concentrations and temperatures can be used to define the molecular weight of the oligomer. Moreover, addition of DCV treatment could answer whether or not NS5A forms an oligomer that could be targeted by NS5A inhibitors. To achieve this, we propose biochemical BRET assay, to determine the oligomerization state of NS5A and the effects of DCV on the oligomer formation. In the present study we designed, improved and constructed the necessary tools to perform such experiments in the future.

Another question that could be answer by using BRET assay as a tool, would be the mode of action of synergistic compounds proposed by Sun *et al*, [62], where the formation of a high oligomer has been supported by using additional drugs [62, 180], which can enhance and restore the inhibition. This theory, is supported by the hypothesis that this cooperative interaction between the compounds is due to NS5A protein communication with each other, meaning, that one inhibitor binds to a resistant NS5A, which leads to a conformational change that is transmitted to adjacent NS5As, resensitizing resistant NS5A. This leads to restore the inhibition by the second inhibitor bound to the next NS5A, which are together forming an oligomer [62]. Important to realize that the drug sensitivity-determining residues are located away from dimerization which shows that DCV does not interfere with dimerization, this does not rule out if the compound affects other forms of oligomerization [181]. As future perspective, the baseline of our studies can provide initial studies to elucidate the mechanism behind the synergistic effect.

The novel features discovered in our results together with recent research on NS5A inhibitor, DCV [26, 117, 162, 182], can improve specific development of new inhibitors by exploiting the dual mode of action. In addition to the understanding of the mechanism of action of the synergistic compounds.

13.2 Proline mutations impact on HCV replication, infection and DCV binding

Furthermore, deciphering the MOA of NS5A inhibitors is important to understand how antiviral therapy works, but improving the structural model of NS5A, can be used to improve and develop new antivirals. Moreover, fortunately, amphipatic helix structure is known by NMR studies [33] and domain I has been previously crystallized [37–39], their functions are very well studied, as reviewed in the Introduction section I. Information on the structure of NS5A components is key to fulfill gaps in the understanding how

the virus-inhibitors work [1, 158]. Few studies focused on the analysis of the linker connecting the AH to the domain I of NS5A protein. Hence, this information is crucial since most of the resistant mutations are clustering in this area, located on the surface of domain Ia and the unstructured linker region (amino acids 2635) that connects the N-terminal AH with the core of DI [45, 62].

Additionally, exploring the structure of NS5A in detail, would explain recent experimental data about DCV and synergistic compounds [62, 180], as already mentioned. Some hypothesis include the involvement of conformational changes and/or the binding of DCV to folding intermediate(s), for example, between AH and DI.

For this purpose we looked into AH-DI linker to find conserved residues that could be involved in the stability of NS5A structure, thus important for DCV binding pocket. Our collaborators (Cristoph Combet, Lyon) found very conserved Proline residues, which are also present in the linker regions connecting DI subdomain a and b, and the linker connecting DI-DII[183, 184], which were subjected to site-directed mutagenesis to study the impact on HCV life cycle, experiments were performed *in vitro* and then studied using Molecular Dynamics, to merge both branches of science and corroborate the results. The ultimate goal was to obtain a model *in silico*, which can be use to predict new NS5A conformations in relation to new mutations when DCV is present.

In fact, *in silico* models have predicted conformations of full-length NS5A DI protein receptor which were suitable for docking [1, 158]. Then, we integrated this model into our studies were we mutated each Proline and docked DCV molecule. As observed in the Molecular Dynamics, each mutation introduced a different arrangement which led to a conformational change that could make the mutation as wildtype (such as: P35A, P35G, P100V, P102G, P102V, P103A, P103G, P103V, P189A, P189G, P189V, P192A, P192G, P192V and P194G) or inhibiting HCV replication and infection (such as: P29A, P29V, P32A, P32G, P32V, P100A, P100G, P102A, P194A and P194V). Accordingly, the MD showed why and how each Proline mutation impacted on NS5A conformation and thus, on HCV life cycle. Additionally, we observed that the Prolines which behaved as the wildtype HCV virus JCR2a, Prolines 29A, P29V, P32A, P32G and P32V on AH-DI linker, P100A, 100G and 102A on DIa-DIb linker and P194A and 194V on linker DI-DII, showed complete RNA replication inhibition, thus these residues showed also a critical conformational changes on the binding site of DCV. The importance of the amino acid substitution (Proline to Alanine, Glycine or Valine) could be due to clashes or amino acid interactions, which made each mutation have a different effect on NS5A structure, therefore changing the nature of DCV binding site. Key elements (AH, AH-DI linker and the interdomain region) in the binding site showed different rearrangements when conserved Proline residues were mutated.

Notably, P29G, showed major changes in the AH conformation, which provokes lost contact between DCV and the interdomain region of the binding pocket. Mutations on Proline 32, to any other amino acid also showed drastic conformational changes that led to the lost of contact between DCV and key elements in the binding pocket. In addition to the slight change in AH conformation that showed an insertion into the cellular membrane location, this changes led to a change in the binding site of DCV. Coherent to our results, this year it was reported that deletion of Proline 32 results in the virological failure in patients receiving NS5A inhibitors, glecaprevir and pibrentasvir [185], which can be explained using our MD model, that shows this Proline mutations having an impact in binding DCV. Finally, mutations on Proline 35, to any amino acid did not alter the structure of NS5A, which gives the binding site the stability to maintain DCV in its binding pocket. Importantly, we and others [182] recently showed that P35A retained the ability to replicate but showed defects in virus assembly. P35A exhibited a modest reduction in infectivity which explained why this mutation could be crucial for HCV life cycle and DCV binding [182]. The binding pocket described for DAAs has been suggested to contain residues located in the flexible linker region and the amphipathic alpha-helix at the N-terminal to the structured cytosolic portion of domain DI, in different computational models [1, 39, 158, 177]. In addition, several of these conserved Proline residues have been found to be essential through the different HCV genotypes [183, 184, 186].

Altogether, these results suggest that NS5A conserved Proline residues are important for the conformation and/or self-interaction of NS5A protein. Importantly, the correlation of the experimental results with our computational model, showed how each substitution is changing the interaction partners and key elements on the activities of NS5A DI and the binding pocket of DCV, plus as discussed in the next section, these Proline residues also have an impact on membrane association and DCV binding.

Interestingly, it is known that Proline residues can undergo *cis-trans* isomerization, which has been found to be very important for protein folding, cell signaling, auto-inhibition and other cellular processes. In contrast to covalent modifications performed by post-translational processes, Proline isomerization is an intrinsic conformational exchange process that has the potential to control protein activity without altering the covalent structure of the protein [187]. It has been described that the isomerization process has two distinct features, one is to introduce dramatic effects on protein structure due to the difference between *cis* and *trans* conformations states of the dihedral angle (ω) of the prolyl bond (X-P) that is large (180°); the second one is, that the process can be modulated by both intramolecular and intermolecular interactions [187]. At this end, this could explain the MD observations on Proline mutations and the effects of these mutations in the overall NS5A structure and therefore in DCV binding. Several

other studies are looking to develop a new inhibitors using this approach; for example, cyclophilins, a family of host peptidyl-prolyl *cis-trans* isomerases (PPIases), play a pivotal role in the life cycles of many viruses and therefore represent an attractive target for broad-spectrum antiviral development such as: small-molecule cyclophilin inhibitor (SMCypI), DEB025/Debio 025 (Alisporivir) [188, 189]. In our studies we observe that when mutating Proline residues, *cis-trans* isomerization can be important for the mechanism of action of NS5A inhibitors [159], as this modification introduces drastic conformational changes that promote or not the binding to DCV. Our computational model can be use in the future to predict the importance of Proline residues inside the binding pocket.

Another interesting point is when we looked at residues 24, 30, and 35 all lie inside or close to a potential double SH3 domain-binding motif P29-xx-P-xx-P35, (referred in the present study as the AH-DI linker). Although interaction with host factors containing SH3 domains has been reported for NS5A [190, 191], there has been no evidence reported yet that this particular motif takes part in such interactions. On the other hand, a P-xx-P-xx-P motif has been identified and structurally resolved in the sorting nexin 5 [1, 62, 192], where it plays a role in specific lipid binding. In NS5A, mutation P35A has been shown to slightly reduce virus infectivity, induce defects of virus assembly and not to have much effect on viral RNA replication, as already mentioned [182]. Taken together, the present experiments together with the recent reports, support the existence of this conserved and potentially functional motif, as well as the presence of compensating mutations in and around it, suggest that these regions of NS5A plays a role in specific interactions with lipids or host factors. [186]

These results are merely limited by the absence of the cellular membrane which might play a key role in NS5A and in DCV binding. This led us to study in detail then how is the AH associated to the membrane and whether this is important for DCV binding.

13.3 AH and membrane dynamics

NS5A is tightly associated with the ER membrane and behaves as an integral membrane protein. In fact, based on targeted mutagenesis and RNA replication analyses of polar residues at the membrane surface, it has been define as a unique platform that is involved in specific protein-protein interactions essential for the assembly of a functional HCV replication complex [13, 45]. The amphipatic helix of NS5A exhibits a hydrophobic, tryptophan-rich side embedded in the cytosolic leaflet of the membrane bilayer, whereas the polar, charged side is exposed to the cytosol which is found to be highly conserved among 280 HCV isolates of various genotypes [175]. Molecular dynamic studies have

shown that when restraining the two α helices by the membrane lipid bilayer in the close conformation, results in the stability of the homodimer interactions and reduction of its flexibility [158]. Very clear differences were also observed by superimposing the two models (claw-like and back-to-back), the differences rely on the hinge region connecting the alpha-helix to the core of D1 for each monomer. This hinge region is important for resistance mutations emergence to DCV treatment [158]. Importantly, the hydrophobic and basic residues following the NS5A amphipathic alpha-helix could participate in membrane association [33, 131]. Other residues or segments located downstream of amino acids 131 were determined to interact with the membrane. Even though the N-terminal amphipathic helix is the main anchor, the region can be extended to ensure the membrane association, creating a platform with hydrophilic residues and asymmetric distribution of charge residues on the cytosolic side of the N-terminal [33].

There is no consensus orientation of the α helix in the computational model attempts, sometimes it can be modelled in parallel to each other in the two monomers with its N-terminus pointing to the centre of the dimer [1], sometimes away from the dimer, and in other analysis kinked and pointing sideways [158, 193]. Multiple models reported the amphipathic helix, differing in their bending, based on the NMR data (PDB IDs 1R7C through 1R7G) [175, 176]. For this reason in our studies we wanted to determine which is the optimal AH position and to build-up a model that could be use in the future to study resistance mutations, NS5A inhibitors positioning and mode of action of NS5A inhibitors. For this purpose first, we decided to perform MD on the position of the AH on cellular membranes. Therefore, we included the Proline rich linker, and the amphipathic helix structure (PDB: 1R7G) together with POPE cellular membrane. Our results show that from the two potential conformations (horizontal or vertical) of the AH in relation to the cellular membrane, it is very likely to be sitting horizontally on top of the membrane and keeps associated with NS5A, which is consistent to previous reports [175]. Moreover, our studies reveal that NS5A protein is linked to the membrane using the AH in its horizontal position, and that this interaction changes through time (MD: 500ns). This conformational changes are important for the protein dynamics in relation to the cellular membrane and play key role in the binding site of DCV.

Second, we studied in detail the conformation of the AH-DI, Proline rich linker in association with the cellular membrane, and we observed that the linker does not change drastically its conformation staying in close proximity to the cellular membrane. This could explain why NS5A remains attached to the cellular membrane via the AH, plus the additional interactions from the AH-DI linker promote NS5A-membrane association. Reports have described that HCV RNA replication is not impaired by membrane association of NS5A but of additional functions of the N-terminal [33], which is consistent to our experimental and computational data. In addition to the fact that AH-DI linker has

been suggested to affect the association of NS5A to membranes and/or host proteins, which can also be disrupted by NS5A inhibitor (DCV) binding [118].

The MD performed in the present study reveal the mechanism behind it, where the AH-DI linker contains important residues (for example: Prolines to Alanine, Valine or Glycine) that can insert or delete amino acid interactions which are critical for the maintenance of NS5A functions. Berger *et al*, also hypothesized that NS5A inhibitors (DCV and other BMS compounds) docked into the cleft at the dimer interface, suggesting that the segment connecting AH and D1 might compete for the same binding site as inhibitors. In our data, we can observe that the conformational changes might induce drastic changes in AH-DI which can result in a modification of its interaction with the cellular membrane, this could be totally explained when using the re-docking DCV molecule on the system. Consistent to our data, DCV and NS5A showed mainly hydrophobic interactions without possibilities for water molecules to mediate those interactions [193]. Additional changes in DI-DII linkers were also observed this could further explain differences in RNA binding or in the interaction with different host proteins. However, molecular dynamics studies have certain limitations in the number of atoms to study, which is why our aim was to build a model that can be use in the future to study amino acid substitutions during inhibitors presence in relation to the cellular membrane.

Furthermore, our results indicated that AH of HCV NS5A protein can spontaneously bind and penetrate to an endoplasmic reticulum complex membrane containing (POPE). We observed that the AH shows its anchoring role in keeping the protein on the membrane surface. Proper orientation of the AH at membrane surface was identified through MD analysis. Remarkably, AH-DI linker was observed to be important to maintain the protein structure stable. Simulated results provide us with a detailed characterization of insertion, orientation and AH-interaction of NS5A amphipatic helix at membrane environment, thus enhancing our understanding of structural functions and mechanism for the association of HCV NS5A protein with respect to ER membranes. In conclusion, Proline mutations seem to affect the conformation of AH or the AH-DI linker which can possibly have an effect not only in the binding to DCV (as previously described) but also on the cellular membrane interaction. Thus, our *in silico* model predictions can be used to: elucidate interactions within DCV binding site key components; predict mutations on the Proline rich linker that can affect DCV binding, and ultimately as a build-up model to study protein-membrane association via an amphipatic helix.

Lastly, it has also been reported that the presence of amphipatic helices are one of the most important classes of membrane curvature sensors found in a wide range of proteins, including trafficking proteins, where they regulate, for example, protein coat assembly. This fact was of interest in our study since our molecular dynamics showed an

indication of membrane curvature when the amphipathic helix was present together with the cellular membrane. The mechanism by which AHs can achieve membrane curvature involves the AHs fold upon contact to membranes and insert their hydrophobic face in the lipid bilayer often with the help of positively charged residues situated on the polar face of the helix. The insertion process is thought to be facilitated by curvature-induced defects in lipid packing that result in a higher affinity of AHs for positively curved membranes [194]. In fact other viruses such as Influenza virus has been shown to use membrane curvature process to promote assembly of the virus [195]. In addition, experimental results by Schley *et al*, confirmed that viral protein is associated with increased membrane curvature, where they used a mathematical model to show that localized increases in curvature alone are sufficient to generate viral buds. The magnitude of the protein-induced curvature is calculated from the size of the amphipathic region hypothetically removed from the inner membrane as a result of translation, with a change in membrane stiffness estimated from observed differences in virion deformation as a result of protein depletion [196]. However more detailed studies and research on this aspect using our model could elucidate the mechanism by which HCV is using membrane curvature during infection.

In summary, our results showed that DCV inhibits envelopment of HCV viral particles, thus, showing a dual mechanism of action. Furthermore, studies on Proline mutations, showed that some of these residues are critical not only in stabilizing NS5A conformation and self-interaction, but also in DCV binding process, shown by computational tools. Additionally, we showed the importance of the cellular membrane when studying NS5A, NS5A inhibitors and resistant mutations. Altogether we build-up a model which can be use the future to study NS5A protein- membrane association, in presence of NS5A inhibitors. Although there are many groups contributing to the studying of HCV life cycle, there are still open questions that can be targeted by computational tools, working together with experimental data, which can extend and clarify our understanding of NS5A inhibitors and apply this knowledge to the improvement of antiviral development.

Appendix A

Appendix

A.1 Proline mutations impact on HCV replication, infection and DCV binding

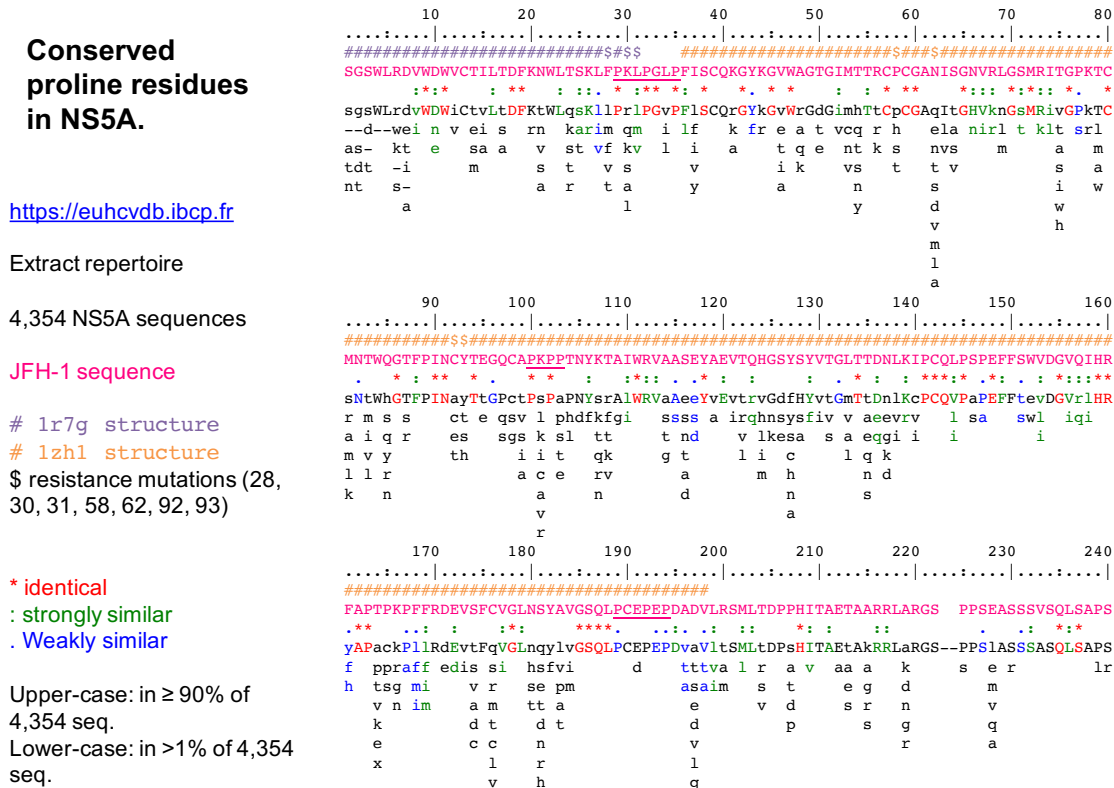


FIGURE A.1: Conserved Proline residues

Analysis of conserved Proline residues in HCV genotype JFH-1, using Amphipatic helix PDB: 1R7G and using NS5A PDB: 1ZH1.

A.2 HCV assembly impaired by DCV activity

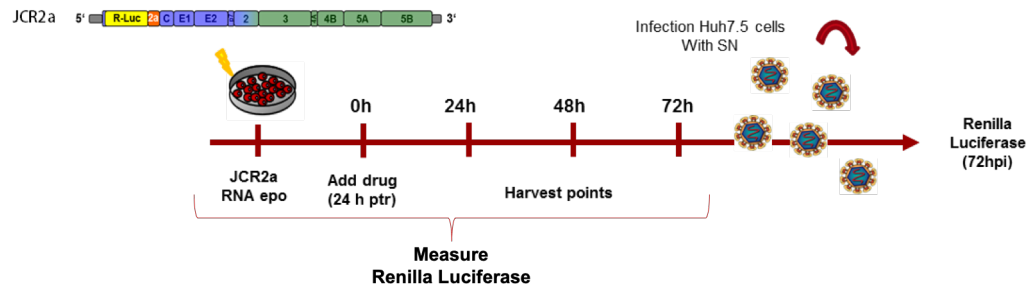


FIGURE A.2: Diagram of experimental design

This diagram represents the experimental design of all the experiments using SOF and DCV. Details are also described in the Methods section 10.

A.3 Drug titration

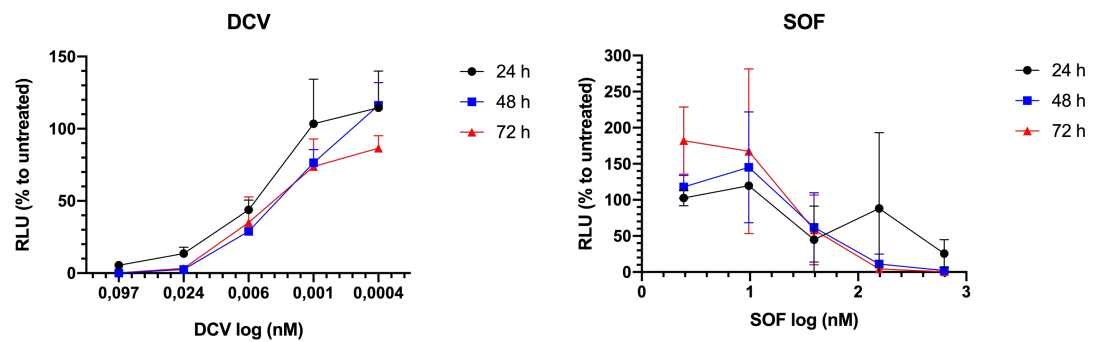


FIGURE A.3: DCV and SOF titration

DCV and SOF titration data, replication and reinfection $n=3$. Details are also described in the Methods section 10.

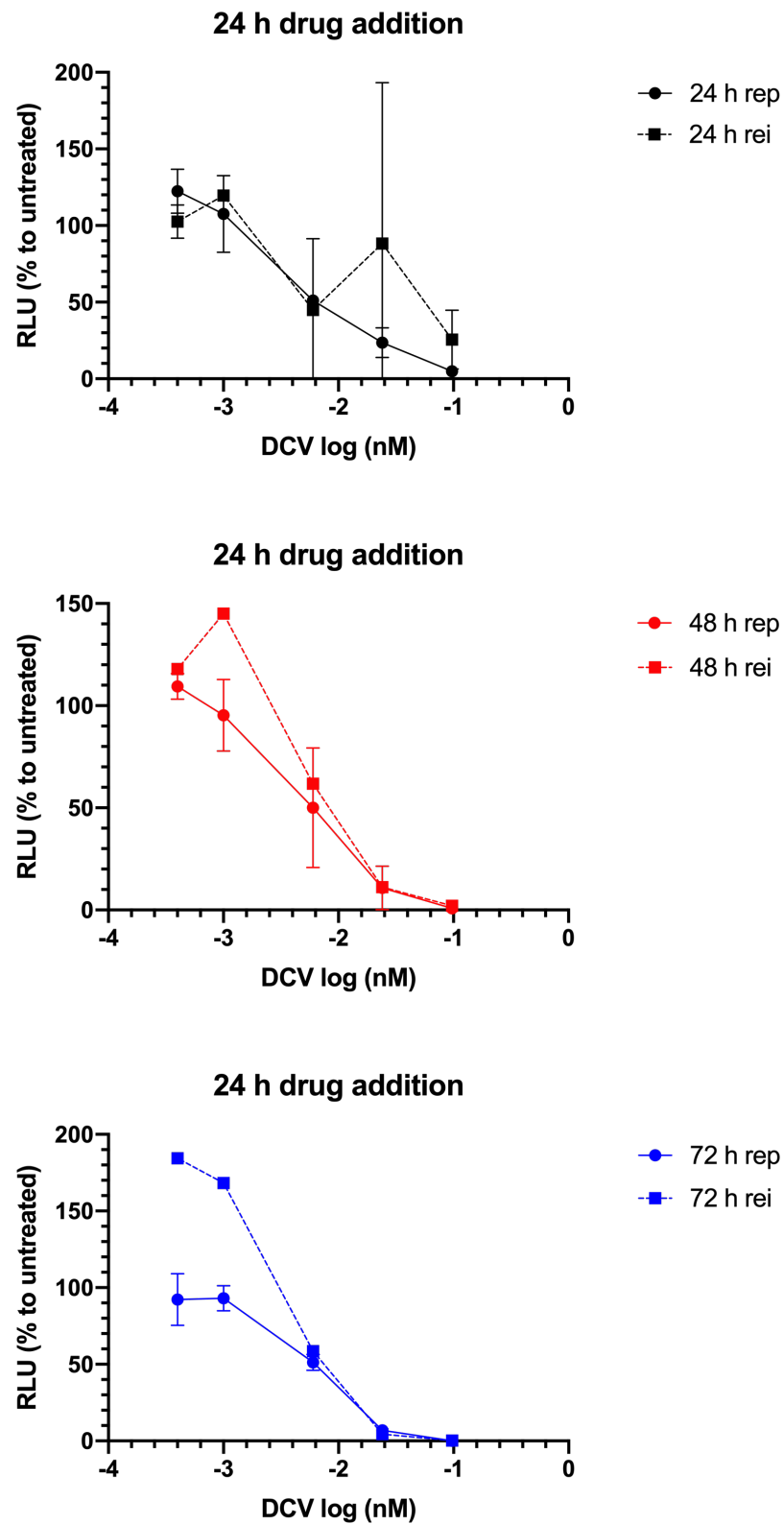


FIGURE A.4: DCV titration

DCV titration data, replication and reinfection $n=3$. Details are also described in the Methods section 10.

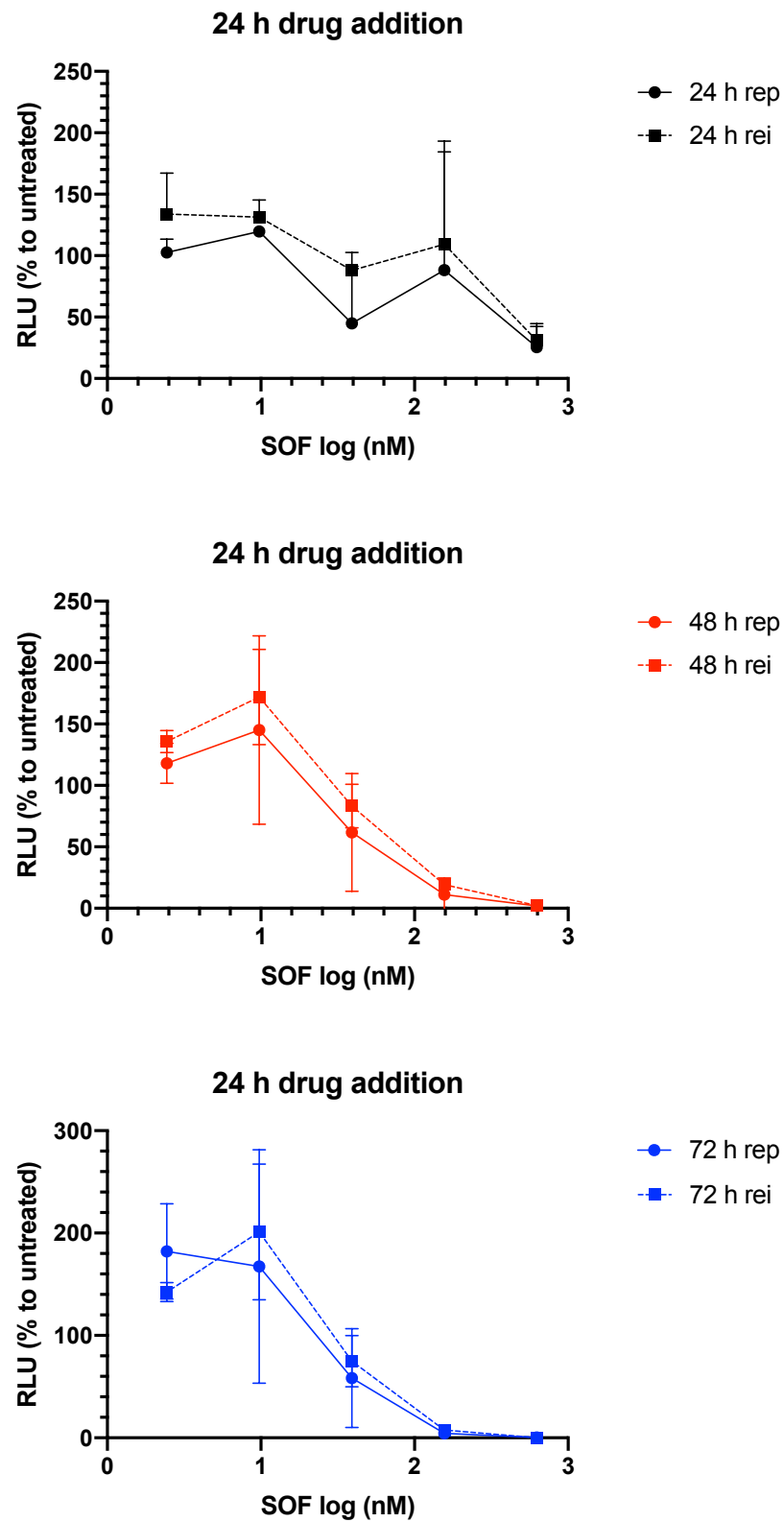


FIGURE A.5: SOF titration

DCV titration data, replication and reinfection $n=3$. Details are also described in the Methods section 10.

Bibliography

- [1] James H Nettles, Richard A Stanton, Joshua Broyde, Franck Amblard, Hongwang Zhang, Longhu Zhou, Junxing Shi, Tamara R McBrayer, Tony Whitaker, Steven J Coats, et al. Asymmetric binding to ns5a by daclatasvir (bms-790052) and analogs suggests two novel modes of hcv inhibition. *J. Med. Chem.*, 57(23):10031–10043, 2014.
- [2] World Health Organization. Hepatitis c. Technical report, Genf, Schweiz, 2017. URL <http://www.who.int/mediacentre/factsheets/fs164/en/>.
- [3] Doris B. Strader and Leonard B. Seeff. A brief history of the treatment of viral hepatitis c. *Clinical Liver Disease*, 1(1):6–11, 2012. ISSN 2046-2484. doi: 10.1002/cld.1. URL <http://dx.doi.org/10.1002/cld.1>.
- [4] Rachel H. Westbrook and Geoffrey Dusheiko. Natural history of hepatitis c. *Journal of Hepatology*, 61(1, Supplement):S58 – S68, 2014. ISSN 0168-8278. doi: <https://doi.org/10.1016/j.jhep.2014.07.012>. URL <http://www.sciencedirect.com/science/article/pii/S0168827814004814>.
- [5] Brett D. Lindenbach and Charles M. Rice. Molecular biology of flaviviruses. volume 59 of *Advances in Virus Research*, pages 23 – 61. Academic Press, 2003. doi: [https://doi.org/10.1016/S0065-3527\(03\)59002-9](https://doi.org/10.1016/S0065-3527(03)59002-9). URL <http://www.sciencedirect.com/science/article/pii/S0065352703590029>.
- [6] Peter Simmonds, Paul Becher, Jens Bukh, Ernest A. Gould, Gregor Meyers, Tom Monath, Scott Muerhoff, Alexander Pletnev, Rebecca Rico-Hesse, Donald B. Smith, Jack T. Stapleton, and ICTV Report Consortium. Ictv virus taxonomy profile: Flaviviridae. *Journal of General Virology*, 98(1):2–3, 2017. URL <http://jgv.microbiologyresearch.org/content/journal/jgv/10.1099/jgv.0.000672>.
- [7] Caroline Thurner, Christina Witwer, Ivo L. Hofacker, and Peter F. Stadler. Conserved rna secondary structures in flaviviridae genomes. *Journal of General Virology*, 85(5):1113–1124, 2004. URL <http://jgv.microbiologyresearch.org/content/journal/jgv/10.1099/vir.0.19462-0>.

- [8] Jane P. Messina, Isla Humphreys, Abraham Flaxman, Anthony Brown, Graham S. Cooke, Oliver G. Pybus, and Eleanor Barnes. Global distribution and prevalence of hepatitis c virus genotypes. *Hepatology*, 61(1):77–87, 2015. ISSN 1527-3350. doi: 10.1002/hep.27259. URL <http://dx.doi.org/10.1002/hep.27259>.
- [9] Behzad Hajarizadeh, Jason Grebely, and Gregory J Dore. Epidemiology and natural history of hcv infection. *Nature Reviews Gastroenterology and Hepatology*, 10(9):553, 2013.
- [10] Seng-Lai Tan. *Hepatitis C Viruses: Genomes and molecular biology*. Horizon Scientific Press, 2006.
- [11] Daniel M. Forton, Peter Karayiannis, Nadiya Mahmud, Simon D. Taylor-Robinson, and Howard C. Thomas. Identification of unique hepatitis c virus quasispecies in the central nervous system and comparative analysis of internal translational efficiency of brain, liver, and serum variants. *Journal of Virology*, 78(10):5170–5183, 2004. doi: 10.1128/JVI.78.10.5170-5183.2004. URL <http://jvi.asm.org/content/78/10/5170.abstract>.
- [12] Ping LH Lemon SM. Brown EA, Zhang H. Secondary structure of the 5' non-translated regions of hepatitis c virus and pestivirus genomic rnas. *Nucleic Acids Res*, 20:5041–5045, 1992.
- [13] Ralf Bartenschlager, Francois-Loic Cosset, and Volker Lohmann. Hepatitis c virus replication cycle. *Journal of Hepatology*, 53(3):583 – 585, 2010. ISSN 0168-8278. doi: <https://doi.org/10.1016/j.jhep.2010.04.015>. URL <http://www.sciencedirect.com/science/article/pii/S0168827810004745>.
- [14] Vanesa Madan and Ralf Bartenschlager. Structural and functional properties of the hepatitis c virus p7 viroporin. *Viruses*, 7(8):4461–4481, 2015. ISSN 1999-4915. doi: 10.3390/v7082826. URL <http://www.mdpi.com/1999-4915/7/8/2826>.
- [15] R Bartenschlager, L Ahlborn-Laake, J Mous, and H Jacobsen. Kinetic and structural analyses of hepatitis c virus polyprotein processing. *Journal of Virology*, 68(8):5045–5055, 1994. URL <http://jvi.asm.org/content/68/8/5045.abstract>.
- [16] John McLauchlan, Marius K. Lemberg, Graham Hope, and Bruno Martoglio. Intramembrane proteolysis promotes trafficking of hepatitis c virus core protein to lipid droplets. *The EMBO Journal*, 21(15):3980–3988, 2002. ISSN 0261-4189. doi: 10.1093/emboj/cdf414. URL <http://emboj.embopress.org/content/21/15/3980>.

- [17] R. Graham Hope and John McLauchlan. Sequence motifs required for lipid droplet association and protein stability are unique to the hepatitis c virus core protein. *Journal of General Virology*, 81(8):1913–1925, 2000. URL <http://jgv.microbiologyresearch.org/content/journal/jgv/10.1099/0022-1317-81-8-1913>.
- [18] Francois Penin, Jean Dubuisson, Felix A. Rey, Darius Moradpour, and Jean-Michel Pawlotsky. Structural biology of hepatitis c virus. *Hepatology*, 39(1):5–19, 2004. ISSN 1527-3350. doi: 10.1002/hep.20032. URL <http://dx.doi.org/10.1002/hep.20032>.
- [19] Anne Op De Beeck, Laurence Cocquerel, and Jean Dubuisson. Biogenesis of hepatitis c virus envelope glycoproteins. *Journal of General Virology*, 82(11):2589–2595, 2001. URL <http://jgv.microbiologyresearch.org/content/journal/jgv/10.1099/0022-1317-82-11-2589>.
- [20] Wei Cun, Jieyun Jiang, and Guangxiang Luo. The c-terminal -helix domain of apolipoprotein e is required for interaction with nonstructural protein 5a and assembly of hepatitis c virus. *Journal of Virology*, 84(21):11532–11541, 2010. doi: 10.1128/JVI.01021-10. URL <http://jvi.asm.org/content/84/21/11532.abstract>.
- [21] Luis Carrasco. Modification of membrane permeability by animal viruses. volume 45 of *Advances in Virus Research*, pages 61 – 112. Academic Press, 1995. doi: [https://doi.org/10.1016/S0065-3527\(08\)60058-5](https://doi.org/10.1016/S0065-3527(08)60058-5). URL <http://www.sciencedirect.com/science/article/pii/S0065352708600585>.
- [22] Vlastimil Jirasko, Roland Montserret, Nicole Appel, Anne Janvier, Leah Eustachi, Christiane Brohm, Eike Steinmann, Thomas Pietschmann, Francois Penin, and Ralf Bartenschlager. Structural and functional characterization of nonstructural protein 2 for its role in hepatitis c virus assembly. *Journal of Biological Chemistry*, 283(42):28546–28562, 2008. doi: 10.1074/jbc.M803981200. URL <http://www.jbc.org/content/283/42/28546.abstract>.
- [23] Christopher T. Jones, Catherine L. Murray, Dawnnica K. Eastman, Jodie Tassello, and Charles M. Rice. Hepatitis c virus p7 and ns2 proteins are essential for production of infectious virus. *Journal of Virology*, 81(16):8374–8383, 2007. doi: 10.1128/JVI.00690-07. URL <http://jvi.asm.org/content/81/16/8374.abstract>.
- [24] P.K.R. Kumar, Keigo Machida, Petri T. Urvil, Nobuko Kakiuchi, Daesety Vishnuvardhan, Kunitada Shimotohno, Kazunari Taira, and Satoshi Nishikawa. Isolation of rna aptamers specific to the ns3 protein of hepatitis c virus from a pool of

- completely random rna. *Virology*, 237(2):270 – 282, 1997. ISSN 0042-6822. doi: <https://doi.org/10.1006/viro.1997.8773>. URL <http://www.sciencedirect.com/science/article/pii/S0042682297987730>.
- [25] Satoshi Ishido, Tsunenori Fujita, and Hak Hotta. Complex formation of ns5b with ns3 and ns4a proteins of hepatitis c virus. *Biochemical and Biophysical Research Communications*, 244(1):35 – 40, 1998. ISSN 0006-291X. doi: <https://doi.org/10.1006/bbrc.1998.8202>. URL <http://www.sciencedirect.com/science/article/pii/S0006291X9898202X>.
- [26] Nicole Appel, Torsten Schaller, Francois Penin, and Ralf Bartenschlager. From structure to function: New insights into hepatitis c virus rna replication. *Journal of Biological Chemistry*, 281(15):9833–9836, 2006. doi: 10.1074/jbc.R500026200. URL <http://www.jbc.org/content/281/15/9833.short>.
- [27] Etienne Meylan, Joseph Curran, Kay Hofmann, Darius Moradpour, Marco Binder, Ralf Bartenschlager, and Jrg Tschopp. Cardif is an adaptor protein in the rig-i antiviral pathway and is targeted by hepatitis c virus. 437:1167–72, 11 2005.
- [28] Kui Li, Eileen Foy, Josephine C. Ferreon, Mitsuyasu Nakamura, Allan C. M. Ferreon, Masanori Ikeda, Stuart C. Ray, Michael Gale, and Stanley M. Lemon. Immune evasion by hepatitis c virus ns3/4a protease-mediated cleavage of the toll-like receptor 3 adaptor protein trif. *Proceedings of the National Academy of Sciences*, 102(8):2992–2997, 2005. ISSN 0027-8424. doi: 10.1073/pnas.0408824102. URL <http://www.pnas.org/content/102/8/2992>.
- [29] Erika A. Eksioglu, Haizhen Zhu, Lilly Bayouth, Jennifer Bess, Hong-yan Liu, David R. Nelson, and Chen Liu. Characterization of hcv interactions with toll-like receptors and rig-i in liver cells. *PLOS ONE*, 6(6):1–12, 06 2011. doi: 10.1371/journal.pone.0021186. URL <https://doi.org/10.1371/journal.pone.0021186>.
- [30] Marika Lundin, Magnus Monn, Anders Widell, Gunnar von Heijne, and Mats A. A. Persson. Topology of the membrane-associated hepatitis c virus protein ns4b. *Journal of Virology*, 77(9):5428–5438, 2003. doi: 10.1128/JVI.77.9.5428-5438.2003. URL <http://jvi.asm.org/content/77/9/5428.abstract>.
- [31] Daniel M. Jones, Arvind H. Patel, Paul Targett-Adams, and John McLauchlan. The hepatitis c virus ns4b protein can trans-complement viral rna replication and modulates production of infectious virus. *Journal of Virology*, 83(5):2163–2177, 2009. doi: 10.1128/JVI.01885-08. URL <http://jvi.asm.org/content/83/5/2163.abstract>.

- [32] Shirin Einav, Menashe Elazar, Tsafi Danieli, and Jeffrey S Glenn. A nucleotide binding motif in hepatitis c virus (hcv) ns4b mediates hcv rna replication. *Journal of virology*, 78(20):11288–11295, 2004.
- [33] Francois Penin, Volker Brass, Nicole Appel, Stephanie Ramboarina, Roland Montserret, Damien Ficheux, Hubert E. Blum, Ralf Bartenschlager, and Darius Moradpour. Structure and function of the membrane anchor domain of hepatitis c virus nonstructural protein 5a. *Journal of Biological Chemistry*, 279(39):40835–40843, 2004. doi: 10.1074/jbc.M404761200. URL <http://www.jbc.org/content/279/39/40835.abstract>.
- [34] Timothy L. Tellinghuisen, Katie L. Foss, Jason C. Treadaway, and Charles M. Rice. Identification of residues required for rna replication in domains ii and iii of the hepatitis c virus ns5a protein. *Journal of Virology*, 82(3):1073–1083, 2008. doi: 10.1128/JVI.00328-07. URL <http://jvi.asm.org/content/82/3/1073.abstract>.
- [35] Volker Brass, Elke Bieck, Roland Montserret, Benno Wlk, Jan Albert Hellings, Hubert E. Blum, Francois Penin, and Darius Moradpour. An amino-terminal amphipathic α -helix mediates membrane association of the hepatitis c virus nonstructural protein 5a. *Journal of Biological Chemistry*, 277(10):8130–8139, 2002. doi: 10.1074/jbc.M111289200. URL <http://www.jbc.org/content/277/10/8130.abstract>.
- [36] Min Gao, Richard E Nettles, Makonen Belema, Lawrence B Snyder, Van N Nguyen, Robert A Fridell, Michael H Serrano-Wu, David R Langley, Jin-Hua Sun, Donald R OBoyle II, et al. Chemical genetics strategy identifies an hcv ns5a inhibitor with a potent clinical effect. *Nature*, 465(7294):96, 2010.
- [37] Timothy L Tellinghuisen, Joseph Marcotrigiano, and Charles M Rice. Structure of the zinc-binding domain of an essential component of the hepatitis c virus replicase. *Nature*, 435(7040):374, 2005.
- [38] Robert A. Love, Oleg Brodsky, Michael J. Hickey, Peter A. Wells, and Ciarn N. Cronin. Crystal structure of a novel dimeric form of ns5a domain i protein from hepatitis c virus. *Journal of Virology*, 83(9):4395–4403, 2009. doi: 10.1128/JVI.02352-08. URL <http://jvi.asm.org/content/83/9/4395.abstract>.
- [39] Sebastian M Lambert, David R Langley, James A Garnett, Richard Angell, Katy Hedgethorpe, Nicholas A Meanwell, and Steve J Matthews. The crystal structure of ns5a domain 1 from genotype 1a reveals new clues to the mechanism of action for dimeric hcv inhibitors. *Protein Science*, 23(6):723–734, 2014.

- [40] Luyun Huang, Elena V Sineva, Michele RS Hargittai, Suresh D Sharma, Mehul Suthar, Kevin D Raney, and Craig E Cameron. Purification and characterization of hepatitis c virus non-structural protein 5a expressed in escherichia coli. *Protein expression and purification*, 37(1):144–153, 2004.
- [41] Min Gao. Antiviral activity and resistance of hcv ns5a replication complex inhibitors. *Current opinion in virology*, 3(5):514–520, 2013.
- [42] Chunhong Yin, Niluka Goonawardane, Hazel Stewart, and Mark Harris. A role for domain i of the hepatitis c virus ns5a protein in virus assembly. *PLOS Pathogens*, 14(1):1–32, 01 2018. doi: 10.1371/journal.ppat.1006834. URL <https://doi.org/10.1371/journal.ppat.1006834>.
- [43] Matthew J. Evans, Charles M. Rice, and Stephen P. Goff. Phosphorylation of hepatitis c virus nonstructural protein 5a modulates its protein interactions and viral rna replication. *Proceedings of the National Academy of Sciences*, 101(35):13038–13043, 2004. ISSN 0027-8424. doi: 10.1073/pnas.0405152101. URL <http://www.pnas.org/content/101/35/13038>.
- [44] B De Chasse, V Navratil, Lionel Tafforeau, MS Hiet, A Aublin-Gex, S Agaugue, G Meiffren, F Pradezynski, BF Faria, T Chantier, et al. Hepatitis c virus infection protein network. *Molecular systems biology*, 4(1):230, 2008.
- [45] Kristi L Berger, Sean M Kelly, Tristan X Jordan, Michael A Tartell, and Glenn Randall. Hepatitis c virus stimulates the phosphatidylinositol 4-kinase iii alpha-dependent phosphatidylinositol 4-phosphate production that is essential for its replication. *Journal of virology*, 85(17):8870–8883, 2011.
- [46] Simon Reiss, Ilka Rebhan, Perdita Backes, Ines Romero-Brey, Holger Erfle, Petr Matula, Lars Kaderali, Marion Poenisch, Hagen Blankenburg, Marie-Sophie Hiet, et al. Recruitment and activation of a lipid kinase by hepatitis c virus ns5a is essential for integrity of the membranous replication compartment. *Cell host & microbe*, 9(1):32–45, 2011.
- [47] Hengli Tang. Cyclophilin inhibitors as a novel hcv therapy. *Viruses*, 2(8):1621–1634, 2010.
- [48] Takashi Kaneko, Yasunori Tanji, Shinya Satoh, Makoto Hijikata, Shinichi Asabe, Koichi Kimura, and Kunitada Shimotohno. Production of two phosphoproteins from the ns5a region of the hepatitis c viral genome. *Biochemical and biophysical research communications*, 205(1):320–326, 1994.

- [49] Karen E. Reed and Charles M. Rice. Identification of the major phosphorylation site of the hepatitis c virus h strain ns5a protein as serine 2321. *Journal of Biological Chemistry*, 274(39):28011–28018, 1999. doi: 10.1074/jbc.274.39.28011. URL <http://www.jbc.org/content/274/39/28011.abstract>.
- [50] Manuela Quintavalle, Sonia Sambucini, Vincenzo Summa, Laura Orsatti, Fabio Talamo, Raffaele De Francesco, and Petra Neddermann. Hepatitis c virus ns5a is a direct substrate of casein kinase i- α , a cellular kinase identified by inhibitor affinity chromatography using specific ns5a hyperphosphorylation inhibitors. *Journal of Biological Chemistry*, 282(8):5536–5544, 2007.
- [51] Timothy L Tellinghuisen, Katie L Foss, and Jason Treadaway. Regulation of hepatitis c virion production via phosphorylation of the ns5a protein. *PLoS pathogens*, 4(3):e1000032, 2008.
- [52] Petra Neddermann, Manuela Quintavalle, Chiara Di Pietro, Angelica Clementi, Mauro Cerretani, Sergio Altamura, Linda Bartholomew, and Raffaele De Francesco. Reduction of hepatitis c virus ns5a hyperphosphorylation by selective inhibition of cellular kinases activates viral rna replication in cell culture. *Journal of Virology*, 78(23):13306–13314, 2004. doi: 10.1128/JVI.78.23.13306-13314. 2004. URL <http://jvi.asm.org/content/78/23/13306.abstract>.
- [53] K E Reed, J Xu, and C M Rice. Phosphorylation of the hepatitis c virus ns5a protein in vitro and in vivo: properties of the ns5a-associated kinase. *Journal of Virology*, 71(10):7187–97, 1997. URL <http://jvi.asm.org/content/71/10/7187.abstract>.
- [54] Yung-Chia Chen, Wen-Chi Su, Jing-Ying Huang, Ti-Chun Chao, King-Song Jeng, Keigo Machida, and Michael M. C. Lai. Polo-like kinase 1 is involved in hepatitis c virus replication by hyperphosphorylating ns5a. *Journal of Virology*, 84(16):7983–7993, 2010. doi: 10.1128/JVI.00068-10. URL <http://jvi.asm.org/content/84/16/7983.abstract>.
- [55] Luyun Huang, Jungwook Hwang, Suresh D Sharma, Michele RS Hargittai, Yingfeng Chen, Jamie J Arnold, Kevin D Raney, and Craig E Cameron. Hepatitis c virus nonstructural protein 5a (ns5a) is an rna-binding protein. *Journal of Biological Chemistry*, 280(43):36417–36428, 2005.
- [56] Holly R Ramage, G Renuka Kumar, Erik Verschueren, Jeffrey R Johnson, John Von Dollen, Tasha Johnson, Billy Newton, Priya Shah, Julie Horner, Nevan J Krogan, et al. A combined proteomics/genomics approach links hepatitis c virus infection with nonsense-mediated mrna decay. *Molecular cell*, 57(2):329–340, 2015.

- [57] Asish K. Ghosh, Mainak Majumder, Robert Steele, Peter Yaciuk, John Chrivia, Ranjit Ray, and Ratna B. Ray. Hepatitis c virus ns5a protein modulates transcription through a novel cellular transcription factor srcap. *Journal of Biological Chemistry*, 275(10):7184–7188, 2000. doi: 10.1074/jbc.275.10.7184. URL <http://www.jbc.org/content/275/10/7184.abstract>.
- [58] Motoyuki Otsuka, Naoya Kato, Keng-Hsin Lan, Hideo Yoshida, Jun Kato, Tadashi Goto, Yasushi Shiratori, and Masao Omata. Hepatitis c virus core protein enhances p53 function through augmentation of dna binding affinity and transcriptional ability. *Journal of Biological Chemistry*, 275(44):34122–34130, 2000.
- [59] Michael Gale, Collin M Blakely, Bart Kwieciszewski, Seng-Lai Tan, Michelle Dosssett, Norina M Tang, Marcus J Korth, Stephen J Polyak, David R Gretch, and Michael G Katze. Control of pkr protein kinase by hepatitis c virus nonstructural 5a protein: molecular mechanisms of kinase regulation. *Molecular and cellular biology*, 18(9):5208–5218, 1998.
- [60] Lu Gao, Hideki Aizaki, Jian-Wen He, and Michael MC Lai. Interactions between viral nonstructural proteins and host protein hvap-33 mediate the formation of hepatitis c virus rna replication complex on lipid raft. *Journal of virology*, 78(7):3480–3488, 2004.
- [61] Precious J Lim, Udayan Chatterji, Daniel Cordek, Suresh D Sharma, Jose A Garcia-Rivera, Craig E Cameron, Kai Lin, Paul Targett-Adams, and Philippe A Gallay. Correlation between ns5a dimerization and hepatitis c virus replication. *Journal of Biological Chemistry*, 287(36):30861–30873, 2012.
- [62] Jin-Hua Sun, Donald R OBoyle II, Robert A Fridell, David R Langley, Chunfu Wang, Susan B Roberts, Peter Nower, Benjamin M Johnson, Frederic Moulin, Michelle J Nophsker, et al. Resensitizing daclatasvir-resistant hepatitis c variants by allosteric modulation of ns5a. *Nature*, 527(7577):245, 2015.
- [63] Sven-Erik Behrens, L Tomei, and R De Francesco. Identification and properties of the rna-dependent rna polymerase of hepatitis c virus. *The EMBO journal*, 15(1):12–22, 1996.
- [64] Volker Lohmann, F Körner, Ulrike Herian, and Ralf Bartenschlager. Biochemical properties of hepatitis c virus ns5b rna-dependent rna polymerase and identification of amino acid sequence motifs essential for enzymatic activity. *Journal of virology*, 71(11):8416–8428, 1997.

- [65] Darius Moradpour, Volker Brass, Elke Bieck, Peter Friebe, Rainer Gosert, Hubert E Blum, Ralf Bartenschlager, François Penin, and Volker Lohmann. Membrane association of the rna-dependent rna polymerase is essential for hepatitis c virus rna replication. *Journal of virology*, 78(23):13278–13284, 2004.
- [66] Patrice André, Gabriel Perlemuter, Agata Budkowska, Christian Bréchet, and Vincent Lotteau. Hepatitis c virus particles and lipoprotein metabolism. In *Seminars in liver disease*, volume 25, pages 93–104. Copyright© 2005 by Thieme Medical Publishers, Inc., 333 Seventh Avenue, New York, NY 10001, USA., 2005.
- [67] Hua Huang, Fang Sun, David M Owen, Weiping Li, Yan Chen, Michael Gale, and Jin Ye. Hepatitis c virus production by human hepatocytes dependent on assembly and secretion of very low-density lipoproteins. *Proceedings of the National Academy of Sciences*, 104(14):5848–5853, 2007.
- [68] Elisa Scarselli, Helenia Ansuini, Raffaele Cerino, Rosa Maria Roccasecca, Stefano Acali, Gessica Filocamo, Cinzia Traboni, Alfredo Nicosia, Riccardo Cortese, and Alessandra Vitelli. The human scavenger receptor class b type i is a novel candidate receptor for the hepatitis c virus. *The EMBO journal*, 21(19):5017–5025, 2002.
- [69] Piero Pileri, Yasushi Uematsu, Susanna Campagnoli, Giuliano Galli, Fabiana Falugi, Roberto Petracca, Amy J Weiner, Michael Houghton, Domenico Rosa, Guido Grandi, et al. Binding of hepatitis c virus to cd81. *Science*, 282(5390):938–941, 1998.
- [70] Matthew J Evans, Thomas von Hahn, Donna M Tscherne, Andrew J Syder, Maryline Panis, Benno Wölk, Theodora Hatziiioannou, Jane A McKeating, Paul D Bieniasz, and Charles M Rice. Claudin-1 is a hepatitis c virus co-receptor required for a late step in entry. *Nature*, 446(7137):801, 2007.
- [71] Shufeng Liu, Wei Yang, Le Shen, Jerrold R Turner, Carolyn B Coyne, and Tianyi Wang. Tight junction proteins claudin-1 and occludin control hepatitis c virus entry and are downregulated during infection to prevent superinfection. *Journal of virology*, 83(4):2011–2014, 2009.
- [72] Alexander Ploss, Matthew J Evans, Valeriya A Gaysinskaya, Maryline Panis, Hana You, Ype P de Jong, and Charles M Rice. Human occludin is a hepatitis c virus entry factor required for infection of mouse cells. *Nature*, 457(7231):882, 2009.
- [73] Donna M Tscherne, Christopher T Jones, Matthew J Evans, Brett D Lindenbach, Jane A McKeating, and Charles M Rice. Time-and temperature-dependent activation of hepatitis c virus for low-ph-triggered entry. *Journal of virology*, 80(4):1734–1741, 2006.

- [74] Gualtiero Alvisi, Vanesa Madan, and Ralf Bartenschlager. Hepatitis c virus and host cell lipids: an intimate connection. *RNA biology*, 8(2):258–269, 2011.
- [75] Emmanuelle Blanchard, Sandrine Belouzard, Lucie Goueslain, Takaji Wakita, Jean Dubuisson, Czeslaw Wychowski, and Yves Rouillé. Hepatitis c virus entry depends on clathrin-mediated endocytosis. *Journal of virology*, 80(14):6964–6972, 2006.
- [76] Chang Kyong-Mi Kim Chang Wook. Hepatitis c virus: virology and life cycle. *Clin Mol Hepatol*, 19(1):17–25, 2013. doi: 10.3350/cmh.2013.19.1.17. URL <http://www.e-cmh.org/journal/view.php?number=1025>.
- [77] David Paul, Vanesa Madan, and Ralf Bartenschlager. Hepatitis c virus rna replication and assembly: Living on the fat of the land. *Cell Host & Microbe*, 16(5):569 – 579, 2014. ISSN 1931-3128. doi: <https://doi.org/10.1016/j.chom.2014.10.008>. URL <http://www.sciencedirect.com/science/article/pii/S1931312814003862>.
- [78] David Paul and Ralf Bartenschlager. Architecture and biogenesis of plus-strand rna virus replication factories. *World journal of virology*, 2(2):32, 2013.
- [79] Artur Kaul, Sarah Stauffer, Carola Berger, Thomas Pertel, Jennifer Schmitt, Stephanie Kallis, Margarita Zayas Lopez, Volker Lohmann, Jeremy Luban, and Ralf Bartenschlager. Essential role of cyclophilin a for hepatitis c virus replication and virus production and possible link to polyprotein cleavage kinetics. *PLoS pathogens*, 5(8):e1000546, 2009.
- [80] Volker Lohmann. Hepatitis c virus rna replication. In *Hepatitis C virus: from molecular virology to antiviral therapy*, pages 167–198. Springer, 2013.
- [81] Maria Teresa Catanese, Kunihiro Uryu, Martina Kopp, Thomas J Edwards, Linda Andrus, William J Rice, Mariena Silvestry, Richard J Kuhn, and Charles M Rice. Ultrastructural analysis of hepatitis c virus particles. *Proceedings of the National Academy of Sciences*, 110(23):9505–9510, 2013.
- [82] V Lohmann, F Körner, J-O Koch, U Herian, L Theilmann, and R Bartenschlager. Replication of subgenomic hepatitis c virus rnas in a hepatoma cell line. *Science*, 285(5424):110–113, 1999.
- [83] Keril J Blight, Jane A McKeating, and Charles M Rice. Highly permissive cell lines for subgenomic and genomic hepatitis c virus rna replication. *Journal of virology*, 76(24):13001–13014, 2002.
- [84] Peter Friebe, Julien Boudet, Jean-Pierre Simorre, and Ralf Bartenschlager. Kissing-loop interaction in the 3 end of the hepatitis c virus genome essential for rna replication. *Journal of virology*, 79(1):380–392, 2005.

- [85] Torsten Schaller, Nicole Appel, George Koutsoudakis, Stephanie Kallis, Volker Lohmann, Thomas Pietschmann, and Ralf Bartenschlager. Analysis of hepatitis c virus superinfection exclusion by using novel fluorochrome gene-tagged viral genomes. *Journal of virology*, 81(9):4591–4603, 2007.
- [86] George Koutsoudakis, Artur Kaul, Eike Steinmann, Stephanie Kallis, Volker Lohmann, Thomas Pietschmann, and Ralf Bartenschlager. Characterization of the early steps of hepatitis c virus infection by using luciferase reporter viruses. *Journal of virology*, 80(11):5308–5320, 2006.
- [87] Tomoko Date, Takanobu Kato, Michiko Miyamoto, Zijiang Zhao, Kotaro Yasui, Masashi Mizokami, and Takaji Wakita. Genotype 2a hepatitis c virus subgenomic replicon can replicate in hepg2 and imy-n9 cells. *Journal of Biological Chemistry*, 279(21):22371–22376, 2004.
- [88] Takaji Wakita, Thomas Pietschmann, Takanobu Kato, Tomoko Date, Michiko Miyamoto, Zijiang Zhao, Krishna Murthy, Anja Habermann, Hans-Georg Kräusslich, Masashi Mizokami, et al. Production of infectious hepatitis c virus in tissue culture from a cloned viral genome. *Nature medicine*, 11(7):791, 2005.
- [89] Birke Bartosch, Alessandra Vitelli, Christelle Granier, Caroline Goujon, Jean Dubuisson, Simona Pascale, Elisa Scarselli, Riccardo Cortese, Alfredo Nicosia, and François-Loïc Cosset. Cell entry of hepatitis c virus requires a set of co-receptors that include the cd81 tetraspanin and the sr-b1 scavenger receptor. *Journal of Biological Chemistry*, 278(43):41624–41630, 2003.
- [90] Mayla Hsu, Jie Zhang, Mike Flint, Carine Logvinoff, Cecilia Cheng-Mayer, Charles M Rice, and Jane A McKeating. Hepatitis c virus glycoproteins mediate ph-dependent cell entry of pseudotyped retroviral particles. *Proceedings of the National Academy of Sciences*, 100(12):7271–7276, 2003.
- [91] Jens Bukh. Animal models for the study of hepatitis c virus infection and related liver disease. *Gastroenterology*, 142(6):1279–1287, 2012.
- [92] Rani Burm, Laura Collignon, Ahmed Atef Mesalam, and Philip Meuleman. Animal models to study hepatitis c virus infection. *Frontiers in immunology*, 9, 2018.
- [93] Rani Burm, Laura Collignon, Ahmed Atef Mesalam, and Philip Meuleman. Animal models to study hepatitis c virus infection. *Frontiers in Immunology*, 9:1032, 2018. ISSN 1664-3224. doi: 10.3389/fimmu.2018.01032. URL <https://www.frontiersin.org/article/10.3389/fimmu.2018.01032>.
- [94] David G Bowen and Christopher M Walker. Adaptive immune responses in acute and chronic hepatitis c virus infection. *Nature*, 436(7053):946, 2005.

- [95] Courtney Wilkins and Michael Gale Jr. Recognition of viruses by cytoplasmic sensors. *Current opinion in immunology*, 22(1):41–47, 2010.
- [96] Markus H Heim and Robert Thimme. Innate and adaptive immune responses in hcv infections. *Journal of hepatology*, 61(1):S14–S25, 2014.
- [97] Su-Hyung Park and Barbara Rehermann. Immune responses to hcv and other hepatitis viruses. *Immunity*, 40(1):13–24, 2014.
- [98] Stacy M Horner and Michael Gale Jr. Regulation of hepatic innate immunity by hepatitis c virus. *Nature medicine*, 19(7):879, 2013.
- [99] Robert Thimme, Marco Binder, and Ralf Bartenschlager. Failure of innate and adaptive immune responses in controlling hepatitis c virus infection. *FEMS microbiology reviews*, 36(3):663–683, 2012.
- [100] Nandan S Gokhale, Christine Vazquez, and Stacy M Horner. Hepatitis c virus: strategies to evade antiviral responses. *Future virology*, 9(12):1061–1075, 2014.
- [101] Eileen Foy, Kui Li, Rhea Sumpter, Yueh-Ming Loo, Cynthia L Johnson, Chunfu Wang, Penny Mar Fish, Mitsutoshi Yoneyama, Takashi Fujita, Stanley M Lemon, et al. Control of antiviral defenses through hepatitis c virus disruption of retinoic acid-inducible gene-1 signaling. *Proceedings of the National Academy of Sciences of the United States of America*, 102(8):2986–2991, 2005.
- [102] Martin Baril, Marie-Eve Racine, François Penin, and Daniel Lamarre. Mavs dimer is a crucial signaling component of innate immunity and the target of hepatitis c virus ns3/4a protease. *Journal of virology*, 83(3):1299–1311, 2009.
- [103] Guangdi Li and Erik De Clercq. Current therapy for chronic hepatitis c: The role of direct-acting antivirals. *Antiviral research*, 142:83–122, 2017.
- [104] Christian Steinkühler, Gabriella Biasiol, Mirko Brunetti, Andrea Urbani, Uwe Koch, Riccardo Cortese, Antonello Pessi, and Raffaele De Francesco. Product inhibition of the hepatitis c virus ns3 protease. *Biochemistry*, 37(25):8899–8905, 1998.
- [105] Montse Llinas-Brunet, Murray Bailey, Gulrez Fazal, Sylvie Goulet, Ted Halmos, Steven Laplante, Roger Maurice, Martin Poirier, Marc-André Poupart, Diane Thibeault, et al. Peptide-based inhibitors of the hepatitis c virus serine protease. *Bioorganic & Medicinal Chemistry Letters*, 8(13):1713–1718, 1998.

- [106] Daniel Lamarre, Paul C Anderson, Murray Bailey, Pierre Beaulieu, Gordon Bolger, Pierre Bonneau, Michael Bös, Dale R Cameron, Mireille Cartier, Michael G Cordingley, et al. An ns3 protease inhibitor with antiviral effects in humans infected with hepatitis c virus. *Nature*, 426(6963):186, 2003.
- [107] Alexander J Thompson, Stephen A Locarnini, and Michael R Beard. Resistance to anti-hcv protease inhibitors. *Current opinion in virology*, 1(6):599–606, 2011.
- [108] Vincenzo Summa, Steven W Ludmerer, John A McCauley, Christine Fandozzi, Christine Burlein, Giuliano Claudio, Paul J Coleman, Jillian M DiMuzio, Marco Ferrara, Marcello Di Filippo, et al. Mk-5172, a selective inhibitor of hepatitis c virus ns3/4a protease with broad activity across genotypes and resistant variants. *Antimicrobial agents and chemotherapy*, pages AAC-00324, 2012.
- [109] Mingjun Huang, Steven Podos, Dharaben Patel, Guangwei Yang, Joanne L Fabrycki, Yongsen Zhao, Christopher Marlor, Preeti Kapoor, Xiangzhu Wang, Akihiro Hashimoto, et al. Ach-2684: Hcv ns3 protease inhibitor with potent activity against multiple genotypes and known resistant variants. *Hepatology*, 52:1204A, 2010.
- [110] Åsa Rosenquist, Bertil Samuelsson, Per-Ola Johansson, Maxwell D Cummings, Oliver Lenz, Pierre Raboisson, Kenny Simmen, Sandrine Vendeville, Herman de Kock, Magnus Nilsson, et al. Discovery and development of simeprevir (tmc435), a hcv ns3/4a protease inhibitor. *Journal of medicinal chemistry*, 57(5):1673–1693, 2014.
- [111] Guangdi Li and Erik De Clercq. Current therapy for chronic hepatitis c: The role of direct-acting antivirals. *Antiviral Research*, 142:83 – 122, 2017. ISSN 0166-3542. doi: <https://doi.org/10.1016/j.antiviral.2017.02.014>. URL <http://www.sciencedirect.com/science/article/pii/S0166354216307525>.
- [112] Karolina Madela and Christopher McGuigan. Progress in the development of anti-hepatitis c virus nucleoside and nucleotide prodrugs. *Future medicinal chemistry*, 4(5):625–650, 2012.
- [113] Michael J Sofia, Donghui Bao, Wonsuk Chang, Jinfa Du, Dhanapalan Nagarathnam, Suguna Rachakonda, P Ganapati Reddy, Bruce S Ross, Peiyuan Wang, Hai-Ren Zhang, et al. Discovery of a β -d-2-deoxy-2- α -fluoro-2- β -c-methyluridine nucleotide prodrug (psi-7977) for the treatment of hepatitis c virus. *Journal of medicinal chemistry*, 53(19):7202–7218, 2010.

- [114] Jaehoon Shim, Gabry Larson, Vicky Lai, Suhaila Naim, and Jim Zhen Wu. Canonical 3-deoxyribonucleotides as a chain terminator for hcv ns5b rna-dependent rna polymerase. *Antiviral research*, 58(3):243–251, 2003.
- [115] George Kukolj, Graham A McGibbon, Ginette McKercher, Martin Marquis, Sylvain Lefèbvre, Louise Thauvette, Jean Gauthier, Sylvie Goulet, Marc-André Poupart, and Pierre L Beaulieu. Binding site characterization and resistance to a class of non-nucleoside inhibitors of the hepatitis c virus ns5b polymerase. *Journal of Biological Chemistry*, 280(47):39260–39267, 2005.
- [116] Edward J Gane, Catherine A Stedman, Robert H Hyland, Xiao Ding, Evguenia Svarovskaia, William T Symonds, Robert G Hindes, and M Michelle Berrey. Nucleotide polymerase inhibitor sofosbuvir plus ribavirin for hepatitis c. *New England Journal of Medicine*, 368(1):34–44, 2013.
- [117] Bertrand Boson, Solène Denolly, Fanny Turlure, Christophe Chamot, Marlène Dreux, and François-Loïc Cosset. Daclatasvir prevents hepatitis c virus infectivity by blocking transfer of the viral genome to assembly sites. *Gastroenterology*, 152(4):895–907, 2017.
- [118] Carola Berger, Inés Romero-Brey, Danijela Radujkovic, Raphael Terreux, Margarita Zayas, David Paul, Christian Harak, Simone Hoppe, Min Gao, Francois Penin, et al. Daclatasvir-like inhibitors of ns5a block early biogenesis of hepatitis c virus-induced membranous replication factories, independent of rna replication. *Gastroenterology*, 147(5):1094–1105, 2014.
- [119] David R McGivern, Takahiro Masaki, Sara Williford, Paul Ingravallo, Zongdi Feng, Frederick Lahser, Ernest Asante-Appiah, Petra Neddermann, Raffaele De Francesco, Anita Y Howe, et al. Kinetic analyses reveal potent and early blockade of hepatitis c virus assembly by ns5a inhibitors. *Gastroenterology*, 147(2):453–462, 2014.
- [120] Stefan Zeuzem, Christophe Hézode, Jean-Pierre Bronowicki, Veronique Loustaud-Ratti, Francisco Gea, Maria Buti, Antonio Olveira, Tivadar Banyai, M Tarek Al-Assi, Joerg Petersen, et al. Daclatasvir plus simeprevir with or without ribavirin for the treatment of chronic hepatitis c virus genotype 1 infection. *Journal of hepatology*, 64(2):292–300, 2016.
- [121] Robert J Fontana, Robert S Brown, Ana Moreno-Zamora, Martin Prieto, Shobha Joshi, Maria-Carlota Londoño, Kerstin Herzer, Kristina R Chacko, Rudolf E Stauber, Viola Knop, et al. Daclatasvir combined with sofosbuvir or simeprevir in liver transplant recipients with severe recurrent hepatitis c infection. *Liver Transplantation*, 22(4):446–458, 2016.

- [122] Lenore A Pelosi, Stacey Voss, Mengping Liu, Min Gao, and Julie A Lemm. Effect on hepatitis c virus replication of combinations of direct-acting antivirals, including ns5a inhibitor daclatasvir. *Antimicrobial agents and chemotherapy*, 56(10):5230–5239, 2012.
- [123] Vincent Leroy, Peter Angus, Jean-Pierre Bronowicki, Gregory J Dore, Christophe Hezode, Stephen Pianko, Stanislas Pol, Katherine Stuart, Edmund Tse, Fiona McPhee, et al. Daclatasvir, sofosbuvir, and ribavirin for hepatitis c virus genotype 3 and advanced liver disease: A randomized phase iii study (ally-3+). *Hepatology*, 63(5):1430–1441, 2016.
- [124] Anna S Lok, David F Gardiner, Christophe Hézode, Eric J Lawitz, Marc Bourlière, Gregory T Everson, Patrick Marcellin, Maribel Rodriguez-Torres, Stanislas Pol, Lawrence Serfaty, et al. Randomized trial of daclatasvir and asunaprevir with or without pegifn/rbv for hepatitis c virus genotype 1 null responders. *Journal of hepatology*, 60(3):490–499, 2014.
- [125] Teresa I Ng, Preethi Krishnan, Tami Pilot-Matias, Warren Kati, Gretja Schnell, Jill Beyer, Thomas Reisch, Liangjun Lu, Tatyana Dekhtyar, Michelle Irvin, et al. In vitro antiviral activity and resistance profile of the next-generation hepatitis c virus ns5a inhibitor pibrentasvir. *Antimicrobial agents and chemotherapy*, 61(5):e02558–16, 2017.
- [126] Jeremie Guedj, Harel Dahari, Libin Rong, Natasha D Sansone, Richard E Nettles, Scott J Cotler, Thomas J Layden, Susan L Uprichard, and Alan S Perelson. Modeling shows that the ns5a inhibitor daclatasvir has two modes of action and yields a shorter estimate of the hepatitis c virus half-life. *Proceedings of the National Academy of Sciences*, 110(10):3991–3996, 2013.
- [127] Julie A Lemm, Donald O’Boyle, Mengping Liu, Peter T Nower, Richard Colonno, Milind S Deshpande, Lawrence B Snyder, Scott W Martin, Denis R St Laurent, Michael H Serrano-Wu, et al. Identification of hepatitis c virus ns5a inhibitors. *Journal of virology*, 84(1):482–491, 2010.
- [128] Makonen Belema and Nicholas A Meanwell. Discovery of daclatasvir, a pan-genotypic hepatitis c virus ns5a replication complex inhibitor with potent clinical effect, 2014.
- [129] Jean-Michel Pawlotsky. Ns5a inhibitors in the treatment of hepatitis c. *Journal of Hepatology*, 59(2):375 – 382, 2013. ISSN 0168-8278. doi: <https://doi.org/10.1016/j.jhep.2013.03.030>. URL <http://www.sciencedirect.com/science/article/pii/S0168827813002092>.

- [130] Cristina Simona Strahotin and Michael Babich. Hepatitis c variability, patterns of resistance, and impact on therapy. *Advances in Virology*, 2012, 2012.
- [131] Paul Targett-Adams, Emily JS Graham, Jenny Middleton, Amy Palmer, Stephen M Shaw, Helen Lavender, Philip Brain, Thien Duc Tran, Lyn H Jones, Florian Wakenhut, et al. Small molecules targeting hepatitis c virus-encoded ns5a cause subcellular redistribution of their target: insights into compound modes of action. *Journal of virology*, 85(13):6353–6368, 2011.
- [132] Christopher J Neufeldt, Mirko Cortese, Eliana G Acosta, and Ralf Bartenschlager. Rewiring cellular networks by members of the flaviviridae family. *Nature Reviews Microbiology*, 16(3):125, 2018.
- [133] David Paul, Vanesa Madan, Omar Ramirez, Maja Bencun, Ina Karen Stoeck, Vlastimil Jirasko, and Ralf Bartenschlager. Glycine zipper motifs in hepatitis c virus nonstructural protein 4b are required for the establishment of viral replication organelles. *Journal of virology*, 92(4):e01890–17, 2018.
- [134] Esther L Ashworth Briggs, Rafael GB Gomes, Malaz Elhussein, William Collier, I Stuart Findlow, Syma Khalid, Chris J McCormick, and Philip TF Williamson. Interaction between the ns4b amphipathic helix, ah2, and charged lipid headgroups alters membrane morphology and ah2 oligomeric state implications for the hepatitis c virus life cycle. *Biochimica et Biophysica Acta (BBA)-Biomembranes*, 1848(8):1671–1677, 2015.
- [135] Menashe Elazar, Ping Liu, Charles M Rice, and Jeffrey S Glenn. An n-terminal amphipathic helix in hepatitis c virus (hcv) ns4b mediates membrane association, correct localization of replication complex proteins, and hcv rna replication. *Journal of virology*, 78(20):11393–11400, 2004.
- [136] Chao Lin, Jun-Wei Wu, Kathy Hsiao, and MS Su. The hepatitis c virus ns4a protein: interactions with the ns4b and ns5a proteins. *Journal of virology*, 71(9):6465–6471, 1997.
- [137] Huynh Minh Hung, Tran Dieu Hang, and Minh Tho Nguyen. Molecular details of spontaneous insertion and interaction of hcv non-structure 3 protease protein domain with pip2-containing membrane. *Proteins: Structure, Function, and Bioinformatics*, 2018.
- [138] Nam-Joon Cho, Kwang Ho Cheong, ChoongHo Lee, Curtis W Frank, and Jeffrey S Glenn. Binding dynamics of hepatitis c virus' ns5a amphipathic peptide to cell and model membranes. *Journal of virology*, 81(12):6682–6689, 2007.

- [139] Meirav Matto, Charles M Rice, Benjamin Aroeti, and Jeffrey S Glenn. Hepatitis c virus core protein associates with detergent-resistant membranes distinct from classical plasma membrane rafts. *Journal of virology*, 78(21):12047–12053, 2004.
- [140] Stephanie T Shi, Stephen J Polyak, Hong Tu, Deborah R Taylor, David R Gretch, and Michael MC Lai. Hepatitis c virus ns5a colocalizes with the core protein on lipid droplets and interacts with apolipoproteins. *Virology*, 292(2):198–210, 2002.
- [141] J-E Kim, WK Song, KM Chung, SH Back, and SK Jang. Subcellular localization of hepatitis c viral proteins in mammalian cells. *Archives of virology*, 144(2):329–343, 1999.
- [142] Menashe Elazar, Kwang Ho Cheong, Ping Liu, Harry B Greenberg, Charles M Rice, and Jeffrey S Glenn. Amphipathic helix-dependent localization of ns5a mediates hepatitis c virus rna replication. *Journal of virology*, 77(10):6055–6061, 2003.
- [143] Phillip J Stansfeld and Mark SP Sansom. Molecular simulation approaches to membrane proteins. *Structure*, 19(11):1562–1572, 2011.
- [144] Matthieu Chavent, Anna L Duncan, and Mark SP Sansom. Molecular dynamics simulations of membrane proteins and their interactions: from nanoscale to mesoscale. *Current opinion in structural biology*, 40:8–16, 2016.
- [145] Phillip J Stansfeld. Computational studies of membrane proteins: from sequence to structure to simulation. *Current opinion in structural biology*, 45:133–141, 2017.
- [146] Eric H Lee, Jen Hsin, Marcos Sotomayor, Gemma Comellas, and Klaus Schulten. Discovery through the computational microscope. *Structure*, 17(10):1295–1306, 2009.
- [147] Frank L Graham, J Smiley, WC Russell, and R Nairn. Characteristics of a human cell line transformed by dna from human adenovirus type 5. *Journal of General Virology*, 36(1):59–72, 1977.
- [148] Hidekazu Nakabayashi, Kazuhisa Taketa, Keiko Miyano, Takashi Yamane, and Jiro Sato. Growth of human hepatoma cell lines with differentiated functions in chemically defined medium. *Cancer research*, 42(9):3858–3863, 1982.
- [149] Thomas Pietschmann, Volker Lohmann, Artur Kaul, Nicole Krieger, Gabriele Rinck, Gabriel Rutter, Dennis Strand, and Ralf Bartenschlager. Persistent and transient replication of full-length hepatitis c virus genomes in cell culture. *Journal of virology*, 76(8):4008–4021, 2002.

- [150] Jens Bukh, Thomas Pietschmann, Volker Lohmann, Nicole Krieger, Kristina Faulk, Ronald E Engle, Sugantha Govindarajan, Max Shapiro, Marisa St Claire, and Ralf Bartenschlager. Mutations that permit efficient replication of hepatitis c virus rna in huh-7 cells prevent productive replication in chimpanzees. *Proceedings of the National Academy of Sciences*, 99(22):14416–14421, 2002.
- [151] Nicole Krieger, Volker Lohmann, and Ralf Bartenschlager. Enhancement of hepatitis c virus rna replication by cell culture-adaptive mutations. *Journal of virology*, 75(10):4614–4624, 2001.
- [152] Thomas Pietschmann, Artur Kaul, George Koutsoudakis, Anna Shavinskaya, Stephanie Kallis, Eike Steinmann, Karim Abid, Francesco Negro, Marlene Dreux, Francois-Loic Cosset, et al. Construction and characterization of infectious intragenotypic and intergenotypic hepatitis c virus chimeras. *Proceedings of the National Academy of Sciences*, 103(19):7408–7413, 2006.
- [153] Li-Shuang Ai, Yu-Wen Lee, and Steve S-L Chen. Characterization of hepatitis c virus core protein multimerization and membrane envelopment: revelation of a cascade of core-membrane interactions. *Journal of virology*, 83(19):9923–9939, 2009.
- [154] Khaled Alsaleh, Pierre-Yves Delavalle, André Pillez, Gilles Duverlie, Véronique Descamps, Yves Rouillé, Jean Dubuisson, and Czeslaw Wychowski. Identification of basic amino acids at the n-terminal end of the core protein that are crucial for hepatitis c virus infectivity. *Journal of virology*, 84(24):12515–12528, 2010.
- [155] Juliane Gentsch, Christiane Brohm, Eike Steinmann, Martina Friesland, Nicolas Menzel, Gabrielle Vieyres, Paula Monteiro Perin, Anne Frentzen, Lars Kaderali, and Thomas Pietschmann. Hepatitis c virus p7 is critical for capsid assembly and envelopment. *PLoS pathogens*, 9(5):e1003355, 2013.
- [156] Cordula Klockenbusch and Juergen Kast. Optimization of formaldehyde cross-linking for protein interaction analysis of non-tagged integrin 1. *BioMed Research International*, 2010, 2010.
- [157] Johan Bacart, Caroline Corbel, Ralf Jockers, Stéphane Bach, and Cyril Couturier. The bret technology and its application to screening assays. *Biotechnology Journal: Healthcare Nutrition Technology*, 3(3):311–324, 2008.
- [158] Khaled H Barakat, Anwar Anwar-Mohamed, Jack A Tuszynski, Morris J Robins, D Lorne Tyrrell, and Michael Houghton. A refined model of the hcv ns5a protein

- bound to daclatasvir explains drug-resistant mutations and activity against divergent genotypes. *Journal of chemical information and modeling*, 55(2):362–373, 2014.
- [159] Xavier Hanouille, Aurélie Badillo, Jean-Michel Wieruszkeski, Dries Verdegem, Isabelle Landrieu, Ralf Bartenschlager, François Penin, and Guy Lippens. Hepatitis c virus ns5a protein is a substrate for the peptidyl-prolyl cis/trans isomerase activity of cyclophilins a and b. *Journal of Biological Chemistry*, 284(20):13589–13601, 2009.
- [160] Toshana L. Foster, Philippe Gallay, Nicola J. Stonehouse, and Mark Harris. Cyclophilin a interacts with domain ii of hepatitis c virus ns5a and stimulates rna binding in an isomerase-dependent manner. *Journal of Virology*, 85(14):7460–7464, 2011. ISSN 0022-538X. doi: 10.1128/JVI.00393-11. URL <https://jvi.asm.org/content/85/14/7460>.
- [161] Vineela Chukkapalli, Kristi L Berger, Sean M Kelly, Meryl Thomas, Alexander Deiters, and Glenn Randall. Daclatasvir inhibits hepatitis c virus ns5a motility and hyper-accumulation of phosphoinositides. *Virology*, 476:168–179, 2015.
- [162] Margarita Zayas, Gang Long, Vanesa Madan, and Ralf Bartenschlager. Coordination of hepatitis c virus assembly by distinct regulatory regions in nonstructural protein 5a. *PLoS pathogens*, 12(1):e1005376, 2016.
- [163] Ralf Bartenschlager, François Penin, Volker Lohmann, and Patrice André. Assembly of infectious hepatitis c virus particles. *Trends in microbiology*, 19(2):95–103, 2011.
- [164] Brett D Lindenbach. Virion assembly and release. In *Hepatitis C Virus: From Molecular Virology to Antiviral Therapy*, pages 199–218. Springer, 2013.
- [165] Takahiro Masaki, Ryosuke Suzuki, Kyoko Murakami, Hideki Aizaki, Koji Ishii, Asako Murayama, Tomoko Date, Yoshiharu Matsuura, Tatsuo Miyamura, Takaji Wakita, et al. Interaction of hepatitis c virus nonstructural protein 5a with core protein is critical for the production of infectious virus particles. *Journal of virology*, 82(16):7964–7976, 2008.
- [166] Yusuke Miyanari, Kimie Atsuzawa, Nobuteru Usuda, Koichi Watashi, Takayuki Hishiki, Margarita Zayas, Ralf Bartenschlager, Takaji Wakita, Makoto Hijikata, and Kunitada Shimotohno. The lipid droplet is an important organelle for hepatitis c virus production. *Nature cell biology*, 9(9):1089, 2007.
- [167] Vlastimil Jirasko, Roland Montserret, Ji Young Lee, Jérôme Gouttenoire, Darius Moradpour, François Penin, and Ralf Bartenschlager. Structural and functional

- studies of nonstructural protein 2 of the hepatitis c virus reveal its key role as organizer of virion assembly. *PLoS pathogens*, 6(12):e1001233, 2010.
- [168] Andreas Merz, Gang Long, Marie-Sophie Hiet, Britta Brügger, Petr Chlanda, Patrice Andre, Felix Wieland, Jacomine Krijnse-Locker, and Ralf Bartenschlager. Biochemical and morphological properties of hepatitis c virus particles and determination of their lipidome. *Journal of Biological Chemistry*, 286(4):3018–3032, 2011.
- [169] Perdita Backes, Doris Quinkert, Simon Reiss, Marco Binder, Margarita Zayas, Ursula Rescher, Volker Gerke, Ralf Bartenschlager, and Volker Lohmann. Role of annexin a2 in the production of infectious hepatitis c virus particles. *Journal of virology*, 84(11):5775–5789, 2010.
- [170] Ji-Young Lee, Eliana G. Acosta, Ina Karen Stoeck, Gang Long, Marie-Sophie Hiet, Birthe Mueller, Oliver T. Fackler, Stephanie Kallis, and Ralf Bartenschlager. Apolipoprotein e likely contributes to a maturation step of infectious hepatitis c virus particles and interacts with viral envelope glycoproteins. *Journal of Virology*, 88(21):12422–12437, 2014. ISSN 0022-538X. doi: 10.1128/JVI.01660-14. URL <https://jvi.asm.org/content/88/21/12422>.
- [171] Wagane J. A. Benga, Sophie E. Krieger, Maria Dimitrova, Mirjam B. Zeisel, Marie Parnot, Joachim Lupberger, Eberhard Hildt, Guangxiang Luo, John McLauchlan, Thomas F. Baumert, and Catherine Schuster. Apolipoprotein e interacts with hepatitis c virus nonstructural protein 5a and determines assembly of infectious particles. *Hepatology*, 51(1):43–53, 2010. doi: 10.1002/hep.23278. URL <https://aasldpubs.onlinelibrary.wiley.com/doi/abs/10.1002/hep.23278>.
- [172] Nicole Appel, Ulrike Herian, and Ralf Bartenschlager. Efficient rescue of hepatitis c virus rna replication by trans-complementation with nonstructural protein 5a. *Journal of virology*, 79(2):896–909, 2005.
- [173] Teymur Kazakov, Feng Yang, Harish N Ramanathan, Andrew Kohlway, Michael S Diamond, and Brett D Lindenbach. Hepatitis c virus rna replication depends on specific cis-and trans-acting activities of viral nonstructural proteins. *PLoS pathogens*, 11(4):e1004817, 2015.
- [174] Xiao Tong and Bruce A Malcolm. Trans-complementation of hcv replication by non-structural protein 5a. *Virus research*, 115(2):122–130, 2006.
- [175] François Penin, Volker Brass, Nicole Appel, Stephanie Ramboarina, Roland Montserret, Damien Ficheux, Hubert E Blum, Ralf Bartenschlager, and Darius

- Moradpour. Structure and function of the membrane anchor domain of hepatitis c virus nonstructural protein 5a. *Journal of Biological Chemistry*, 279(39):40835–40843, 2004.
- [176] Hangfei Qi, C. Anders Olson, Nicholas C. Wu, Ruian Ke, Claude Loverdo, Virginia Chu, Shawna Truong, Roland Remenyi, Zugen Chen, Yushen Du, Sheng-Yao Su, Laith Q. Al-Mawsawi, Ting-Ting Wu, Shu-Hua Chen, Chung-Yen Lin, Weidong Zhong, James O. Lloyd-Smith, and Ren Sun. A quantitative high-resolution genetic profile rapidly identifies sequence determinants of hepatitis c viral fitness and drug sensitivity. *PLOS Pathogens*, 10(4):1–12, 04 2014. doi: 10.1371/journal.ppat.1004064. URL <https://doi.org/10.1371/journal.ppat.1004064>.
- [177] Richard Colonna, Julie Lemm, Donald O’boyle, Min Gao, Jeffrey Romine, Scott Martin, Lawrence Snyder, Michael Serrano-Wu, Milind Deshpande, Darren Whitehouse, et al. Combination pharmaceutical agents as inhibitors of hcv replication, March 31 2005. US Patent App. 10/637,156.
- [178] Tania M Welzel, Jörg Petersen, Kerstin Herzer, Peter Ferenci, Michael Gschwantler, Heiner Wedemeyer, Thomas Berg, Ulrich Spengler, Ola Weiland, Marc van der Valk, et al. Daclatasvir plus sofosbuvir, with or without ribavirin, achieved high sustained virological response rates in patients with hcv infection and advanced liver disease in a real-world cohort. *Gut*, pages gutjul–2016, 2016.
- [179] Tarik Asselah. Daclatasvir plus sofosbuvir for hcv infection: an oral combination therapy with high antiviral efficacy. *Journal of hepatology*, 61(2):435–438, 2014.
- [180] Seung-Hoon Lee, Jae-Su Moon, Bo-Yeong Pak, Geon-Woo Kim, Wooseong Lee, Hee Cho, SangKyu Kim, Seong-Jun Kim, and Jong-Won Oh. Ha1077 displays synergistic activity with daclatasvir against hepatitis c virus and suppresses the emergence of ns5a resistance-associated substitutions in mice. *Scientific reports*, 8(1):12469, 2018.
- [181] Choongho Lee, Han Ma, Julie Qi Hang, Vincent Leveque, Ella H Sklan, Menashe Elazar, Klaus Klumpp, and Jeffrey S Glenn. The hepatitis c virus ns5a inhibitor (bms-790052) alters the subcellular localization of the ns5a non-structural viral protein. *Virology*, 414(1):10–18, 2011.
- [182] Chunhong Yin, Niluka Goonawardane, Hazel Stewart, and Mark Harris. A role for domain i of the hepatitis c virus ns5a protein in virus assembly. *PLoS pathogens*, 14(1):e1006834, 2018.
- [183] Mair Hughes, Sarah Gretton, Holly Shelton, David D Brown, Christopher J McCormick, Allan GN Angus, Arvind H Patel, Stephen Griffin, and Mark Harris. A

- conserved proline between domains ii and iii of hepatitis c virus ns5a influences both rna replication and virus assembly. *Journal of virology*, 83(20):10788–10796, 2009.
- [184] Marie Dujardin, Vanesa Madan, Roland Montserret, Puneet Ahuja, Isabelle Huvent, Helene Launay, Arnaud Leroy, Ralf Bartenschlager, François Penin, Guy Lippens, et al. A proline-tryptophan turn in the intrinsically disordered domain 2 of ns5a protein is essential for hepatitis c virus rna replication. *Journal of Biological Chemistry*, pages jbc–M115, 2015.
- [185] Hayato Uemura, Yoshihito Uchida, Jun-ichi Kouyama, Kayoko Naiki, Shohei Tsuji, Kayoko Sugawara, Masamitsu Nakao, Daisuke Motoya, Nobuaki Nakayama, Yukinori Imai, et al. Ns5a-p32 deletion as a factor involved in virologic failure in patients receiving glecaprevir and pibrentasvir. *Journal of gastroenterology*, pages 1–12, 2019.
- [186] Elena Knops, Saleta Sierra, Prabhav Kalaghatgi, Eva Heger, Rolf Kaiser, and Olga Kalinina. Epistatic interactions in ns5a of hepatitis c virus suggest drug resistance mechanisms. *Genes*, 9(7):343, 2018.
- [187] Paramita Sarkar, Charles Reichman, Tamjeed Saleh, Raymond B Birge, and Charalampos G Kalodimos. Proline cis-trans isomerization controls autoinhibition of a signaling protein. *Molecular cell*, 25(3):413–426, 2007.
- [188] Quentin Nevers, Isaac Ruiz, Nazim Ahnou, Flora Donati, Rozenn Brillet, Laurent Softic, Maxime Chazal, Nolwenn Jouvenet, Slim Fourati, Camille Baudesson, et al. Characterization of the anti-hepatitis c virus activity of new nonpeptidic small-molecule cyclophilin inhibitors with the potential for broad anti-flaviviridae activity. *Antimicrobial agents and chemotherapy*, 62(7):e00126–18, 2018.
- [189] Lotte Coelmont, Xavier Hanouille, Udayan Chatterji, Carola Berger, Joke Snoeck, Michael Bobardt, Precious Lim, Inge Vliegen, Jan Paeshuyse, Grégoire Vuagniaux, et al. Deb025 (alisporivir) inhibits hepatitis c virus replication by preventing a cyclophilin a induced cis-trans isomerisation in domain ii of ns5a. *PloS one*, 5(10): e13687, 2010.
- [190] Andrew Macdonald, Sabine Mazaleyrat, Christopher McCormick, Andrew Street, Nicholas J Burgoyne, Richard M Jackson, Virginie Cazeaux, Holly Shelton, Kalle Saksela, and Mark Harris. Further studies on hepatitis c virus ns5a–sh3 domain interactions: identification of residues critical for binding and implications for viral rna replication and modulation of cell signalling. *Journal of General Virology*, 86(4):1035–1044, 2005.

- [191] Andrew Macdonald, Katherine Crowder, Andrew Street, Christopher McCormick, and Mark Harris. The hepatitis c virus ns5a protein binds to members of the src family of tyrosine kinases and regulates kinase activity. *Journal of General Virology*, 85(3):721–729, 2004.
- [192] Leonardus MI Koharudin, William Furey, Hao Liu, Yong-Jian Liu, and Angela M Gronenborn. The phox domain of sorting nexin 5 lacks phosphatidylinositol 3-phosphate (ptdins (3) p) specificity and preferentially binds to phosphatidylinositol 4, 5-bisphosphate (ptdins (4, 5) p2). *Journal of Biological Chemistry*, 284(35):23697–23707, 2009.
- [193] Marawan Ahmed, Abhishek Pal, Michael Houghton, and Khaled Barakat. A comprehensive computational analysis for the binding modes of hepatitis c virus ns5a inhibitors: the question of symmetry. *ACS infectious diseases*, 2(11):872–881, 2016.
- [194] Nikos S Hatzakis, Vikram K Bhatia, Jannik Larsen, Kenneth L Madsen, Pierre-Yves Bolinger, Andreas H Kunding, John Castillo, Ulrik Gether, Per Hedegård, and Dimitrios Stamou. How curved membranes recruit amphipathic helices and protein anchoring motifs. *Nature chemical biology*, 5(11):835, 2009.
- [195] Nathan W Schmidt, Abhijit Mishra, Jun Wang, William F DeGrado, and Gerard CL Wong. Influenza virus a m2 protein generates negative gaussian membrane curvature necessary for budding and scission. *Journal of the American Chemical Society*, 135(37):13710–13719, 2013.
- [196] David Schley, Robert J Whittaker, and Benjamin W Neuman. Arenavirus budding resulting from viral-protein-associated cell membrane curvature. *Journal of The Royal Society Interface*, 10(86):20130403, 2013.